

WALL - FLOOR SLAB JOINT BEHAVIOUR IN BRICKWORK

A Thesis submitted for the Degree of

Doctor of Philosophy

of the

UNIVERSITY OF EDINBURGH

by

August Henri Paul MAURENBRECHER, B.Sc.



Department of Civil Engineering and Building Science

August 1972

to my parents

CONTENTS

	page
Acknowledgements	vii
Abstract	viii
Principal Notations	ix
Conversion Factors	xi
CHAPTER 1 INTRODUCTION	
1.1 Problems and Assumptions in Joint Design	
1.1.1 Introduction	1
1.1.2 The Unrestrained Slab	1
1.1.3 The Restrained Slab	2
1.2 Experimental Investigation	4
CHAPTER 2 EXPERIMENTAL ARRANGEMENT AND PROCEDURE FOR THE MODEL JOINT TESTS AND WALLS	
2.1 Introduction	7
2.2 Brickwork Properties	
2.2.1 Brick	7
2.2.2 Mortar	8
2.3 Workmanship	8
2.4 Construction Procedure	9
2.5 Small Walls	
2.5.1 Test Arrangement	9
2.5.2 Test Procedure	10
2.6 Joint Models	
2.6.1 Test Arrangement	12
2.6.2 Testing Procedure	13
CHAPTER 3 SINGLE LEAF BRICKWORK UNDER AXIAL COMPRESSION	
3.1 Introduction	17
3.2 Single Leaf Brickwork Loaded to Failure	
3.2.1 Stress-Strain Relationship	17
3.2.2 Ultimate Strength	18

3.3	Cycled Loading	
3.3.1	Tests and Results	21
3.3.2	Analysis and Discussion	21
3.4	Central Gaps in the Mortar Joint	
3.4.1	Load Transfer Across the Mortar Joint	29
3.4.2	Theoretical Analysis	30
3.5	Conclusions	33
CHAPTER 4	THE RELATION BETWEEN THE EXPERIMENTAL STRAINS IN THE WALL AND THE APPLIED SLAB FORCES	
4.1	Introduction	34
4.2	Experimental Strain Results	34
4.3	Linear Stress-Strain Analysis	40
4.4	Correlation Between the Experimental Strains and the Applied Slab Moment and Load Using the Linear Stress-Strain Theory	
4.4.1	Forces Acting on the Experimental Model	43
4.4.2	Constants Needed for the Linear Theory	44
4.4.3	Results	45
4.5	Tension in Brickwork	
4.5.1	Eccentricity Causing Zero Stress on One Face of the Wall	50
4.5.2	Experimental Results	51
4.6	Conclusions	53
CHAPTER 5	FLOOR SLAB ROTATION AT ITS JUNCTION WITH THE WALL	
5.1	Introduction	54
5.2	Floor Slab Rotation	
5.2.1	Results	54
5.2.2	Discussion	54
5.3	Slab Rotation in a Wall with No Tensile Cracks and a Linear Stress-Strain Curve	
5.3.1	Theory and Results	59
5.3.2	Discussion	60

5.4	End Fixity of Walls	62
5.5	Lateral Deflection of the Wall-Slab Test Model	63
5.6	Conclusions	67
CHAPTER 6 FAILURE AT THE WALL-FLOOR SLAB JUNCTION		
6.1	Introduction	68
6.2	Forces Acting at the Joint	
6.2.1	No Tension Cracks	69
6.2.2	Moment Distribution in the Test Models when Tensile Cracking Occurs	70
6.2.3	Moment Distribution at the Joint when the Slab is Supported on More than One Side	75
6.3	Equilibrium Failure	
6.3.1	Experimental Results	77
6.3.2	Other Experimental Results	77
6.3.3	Discussion	78
6.4	Wall Failure	
6.4.1	Experimental Results	82
6.4.2	Failure of the Walls	82
6.4.3	Strength of Walls under Axial Load and Moment	86
6.4.4	Discussion	87
6.5	Floor Slab Failure	
6.5.1	Introduction	92
6.5.2	Shear Failure Round the End Reinforcement	92
6.5.3	Shear Failure Across the Reinforcement	93
6.5.4	Tensile Failure	93
6.6	Conclusions	96
CHAPTER 7 FLOOR SLAB - WALL INTERACTION IN A FULL SCALE BUILDING		
7.1	Introduction	97
7.2	Materials	
7.2.1	Brick	97
7.2.2	Mortar	98
7.2.3	Concrete	98
7.2.4	Brickwork	98
7.2.5	Floor Slabs	98

7.3	Precautions and Technique in Outdoor Testing	103
7.4	Slab Loading Tests	
7.4.1	Experimental Measurements	104
7.4.2	Experimental Procedure	105
7.4.3	Experimental Results	105
7.5	Analysis of Results	
7.5.1	Introduction	109
7.5.2	Precompression	109
7.5.3	Rotation of the Walls at the Junction with the Slab	110
7.5.4	Rotation and Deflection of the Floor Slab	112
7.5.5	Interaction of the Floor and the Wall	113
7.6	Discussion	116
7.7	Conclusions	117
CHAPTER 8	GENERAL CONCLUSIONS AND SUGGESTIONS FOR FURTHER RESEARCH	
8.1	General Conclusions	118
8.2	Suggestions for Further Research	121
REFERENCES		122
APPENDIX 1		
A1.1	Review - Sahlin	
A1.1.1	Introduction	126
A1.1.2	Theory	126
A1.1.3	Experimental	130
A1.2	Review - National Institute for Materials Testing	133
A1.3	Review - Watstein and Johnson	135
A1.4	Review - Carlsen	136
A1.5	Review - Maurenbrecher and Hendry	137

APPENDIX 2

A2.1	Experimental Equipment	
A2.1.1	The Demec Gauge	138
A2.1.2	Vibrating Strain Gauge	139
A2.1.3	Dial Gauge	139
A2.1.4	Clinometer	140
A2.1.5	Load Cells	141
A2.1.6	Digital Voltmeter	141

APPENDIX 3

A3.1	Effect of Gauge Length on the Measurement of Vertical Strains	
A3.1.1	Choice of Gauge Length	142
A3.1.2	Relationship between the Gauge Length and the Brickwork Modulus	143
A3.2	Effect of a Gap in the Mortar Joint - Finite Element Analysis	
A3.2.1	Finite Element Program	144
A3.2.2	Analysis	145

APPENDIX 4

	Linear Stress-Strain Theory	
A4.1	Introduction	147
A4.2	Central Gap in the Wall $a_e/t \leq 1 - 2v/t$	
A4.2.1	Moment	148
A4.2.2	Increasing Axial Load	149
A4.2.3	No Increase in Axial Load	149
A4.3	Central Gap in the Wall $a_e/t \geq 1 - 2v/t$	
A4.3.1	Moment	150
A4.3.2	Increasing Axial Load	150
A4.3.3	No Increase in Axial Load	151
A4.4	Moment and Axial Load Predicted From Strains	
A4.4.1	Effect of a_e and k on the Moment Predicted from Strains	151
A4.4.2	Effect of a_e and k on the Axial Load Predicted from Strains	152

A4.5	Stress Distribution due to Eccentric Loading in a Solid, Linearly Elastic Wall with No Tensile Strength	153
A4.6	Moment Causing Tension in the Wall	153

APPENDIX 5

A5.1	Equations Governing the Behaviour of a Solid, Linearly Elastic Wall with No Tensile Strength	
A5.1.1	Wall with No Tensile Cracks	158
A5.1.2	Wall with Tensile Cracks	158
A5.2	Equations for Wall Deflection and Rotation	
A5.2.1	Wall with No Tensile Cracks	159
A5.2.2	Wall with Tensile Cracks	160

APPENDIX 6

A6.1	The Axial Load-Moment Interaction Diagram	
A6.1.1	Linear Stress-Strain	162
A6.1.2	Experimental Stress-Strain	163
A6.2	Relation Between Ultimate Moment and Precompression in the Joint Test Models	165
A6.3	Design of the Six Inch Slab	
A6.3.1	Specifications	166
A6.3.2	Ultimate Moment	167
A6.3.3	Ultimate Shear	167
A6.3.4	Bond	168
A6.4	Slab for Test Model No. 1	
A6.4.1	Slab Properties	168
A6.5	Slab for Test Model No. 3	
A6.5.1	Slab Properties	169
A6.5.2	Ultimate Moment	169

APPENDIX 7

A7.1	Finite Element Analysis of the Floor Slab Deflection	170
A7.2	Finite Difference Analysis of the Floor Slab Deflection	171

ACKNOWLEDGEMENTS

I would like to thank Professor A. W. Hendry for the opportunity of working under his personal supervision.

The Science Research Council awarded me a three year Research Studentship for which I am grateful.

My thanks to the Technical Staff for all the help they have given me.

ABSTRACT

This thesis concentrates on the immediate area of the joint between a single leaf, loadbearing, brickwork wall and a reinforced concrete floor slab.

An experimental investigation is conducted on nine full scale models of a single leaf wall with a cantilevering floor slab bearing fully into the wall. The wall is first loaded to a set load and then an increasing slab load is applied to failure. The effect of the following two variables on the rotation of the floor slab and the strains in the wall is investigated :

1. Does the magnitude of the load in the wall above the wall-slab junction affect the rotation of the slab ? Three different loads were compared. The load had little effect on the rotation of the slab unless tensile cracks developed in the joint; then an increase in load reduced slab rotation.

2. What is the relation between slab rotation at the joint and the applied slab moment for three different walls made from the same brick but using different mortars - $1:\frac{1}{2}:3$, $1:1:6$ and $1:2:9$ cement:lime:sand mixes ? The moment-rotation curves had an approximately linear slope until tensile cracking developed in the joint. The weaker the wall the smaller the slope.

Tests on axially loaded walls were necessary to obtain the stress-strain relationship of brickwork under increasing and decreasing load. The effect of a central gap in the mortar joint on the vertical strain distribution was investigated using the finite element technique. Using the results a theory is developed to explain the elastic and ultimate properties of single leaf brickwork under flexural loading.

As a complement to the model tests, similar joints were tested in a full scale, five storey, brickwork structure. The slab restraining moments at the joints are significant - up to 30% of full fixity. The tests confirm that precompression has little effect on slab rotation if no tensile cracks develop in the joint.

PRINCIPAL NOTATIONS

a	width of gap in the mortar joint
a_e	gap width of equivalent hollow wall
A	cross-sectional area of a wall = bt or $b(t - a_e)$
b	length of wall; bearing length of slab into wall
c	coefficient taking into account the reduced stiffness of the wall due to tensile cracking (see fig A5.1)
d	overall depth of floor slab
e	eccentricity of load
E	compression modulus
E_b, E_m	brick and mortar compression moduli
E_{exp}	experimental compression modulus based on a solid section
E_s	true brickwork compression modulus
f'_c	concrete cylinder strength
$g =$	$1/(1 + d/2h)$
h	height of wall
I	second moment of area = $bt^3/12$ or $b(t^3 - a_e^3)/12$
k	ratio of unloading to loading modulus
l	moment arm about the centre line of the wall of the slab load, V, applied to the test models
M	moment
M_p, M_1	moment at slab level applied to the wall with constant pre-compression
M_{p+v}, M_2	moment at slab level applied to the wall with increasing load
M'	moment induced at the far ends of the walls in the test models
M_s	slab restraining moment
P	precompressive load on the walls in the test models
R	see equations A4.20 and A4.21
t	wall thickness

- v distance to the neutral axis of the flexural stresses
measured from the tensile side of the wall
- V slab load in the test models
- V_b proportion of brick covered by a gauge length on brickwork
- z depth of tensile crack
- ϵ strain
- σ stress
- ϕ rotation of slab or wall at the joint

CONVERSION FACTORS

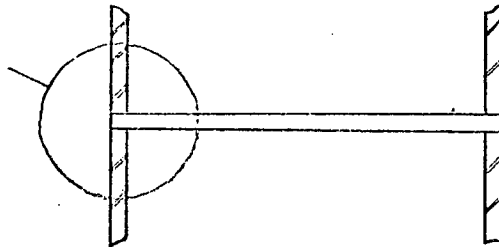
	Imperial Units	SI Units
Length	1 ft	0.3048 m
	1 in	25.4 mm
Area	1 in ²	645.2 mm ²
	1 ft ²	0.0929 m ²
Section Modulus	1 in ³	16.39 x10 ⁻⁶ m ³
Second Moment of Area	1 in ⁴	0.4162 x10 ⁻⁶ m ⁴
Density	1 lb/ft ³	16.02 kg/m ³
Force	1 lbf	4.448 N
	1 tonf	9.964 kN
Force/unit length	1 lbf/ft	14.59 N/m
	1 tonf/ft	32.69 kN/m
Pressure	1 lbf/in ²	6.895 kPa (kN/m ²)
	1 lbf/ft ²	47.88 Pa (N/m ²)
Moment of Force	1 lbf in	0.1130 N m
	1 lbf in/ft	0.3707 N m/m
<hr/>		
Angle	1 mrad	206 sec

1.1 PROBLEMS AND ASSUMPTIONS IN JOINT DESIGN

1.1.1 Introduction

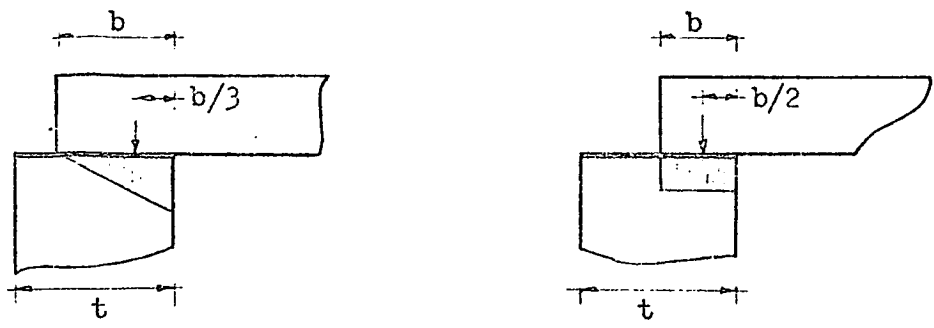
The primary purpose of the junction between a loadbearing wall and a floor is the transfer of load from the floor to the wall. The floor load may be transferred eccentrically inducing a moment in the wall. In addition the end rotation of the floor may be restrained by the wall causing a transfer of moment to the wall equal to the slab restraining moment. Difficulty occurs in the analysis of the junction since the wall and the wall to slab joint can take little tensile stress.

Factors affecting the behaviour of the joint are briefly discussed in the next two sections. This thesis concentrates on the immediate area of the joint (see section 1.2), investigating the behaviour of full scale models of a single leaf wall with a cantilevering concrete slab bearing fully into it. The effect of two variables - the load in the wall due to upper storeys (precompression) and brickwork strength - on the rotation of the floor slab and the strains in the wall is investigated.



1.1.2 The Unrestrained Slab

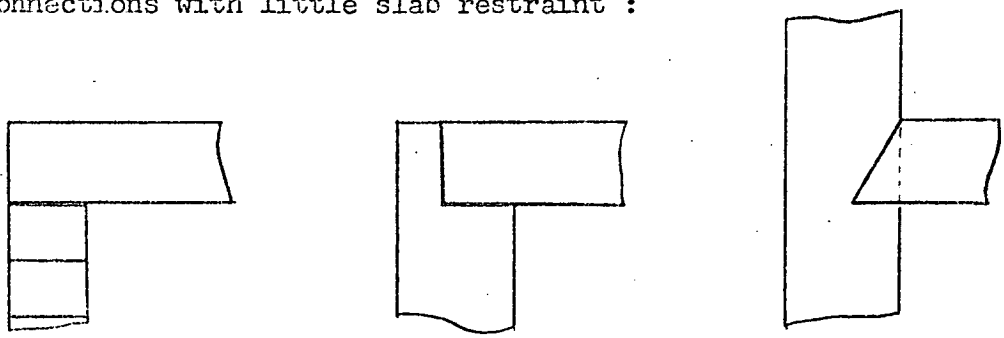
If the slab rotation is not restrained, the moment applied to the wall will be due to the eccentric application of the slab load. This occurs with roof slabs and is assumed to occur in many cases at intermediate floors (6). The slab load is assumed to cause a triangular stress distribution under the bearing area of the slab (4,6,35). If the slab is of moderate span a uniform stress distribution is sometimes assumed (6).



The assumption of a triangular stress distribution has some confirmation by experiment (39) at low slab rotations. With increasing loads and for more slender slabs the eccentricity at the joint increases to a limit (approaching $t/2$, local deformation reducing the eccentricity). The eccentricity may decrease at high loads as local crushing occurs in the mortar joint and/or possible large end rotations of the wall develop if the moment is high enough to cause tensile cracking in the wall, causing the wall to rotate more than the slab (near buckling loads). The maximum eccentricity in the wall may also occur at or near the point of maximum lateral deflection as will happen in the latter case.

The eccentricity may be reduced by providing a hinge about the centre line of the wall or a rubber packing in the joint between the wall and the slab (39). With mortar mixes of $1:\frac{1}{2}:4\frac{1}{2}$ or weaker, local deformation of the mortar joint is assumed to reduce the eccentricity (4). More effective would be a weaker mortar joint near the slab in comparison with the other joints in the wall.

Typical connections with little slab restraint :



1.1.3 The Restrained Slab

At intermediate floors restraint to slab rotation occurs at the wall-slab joint. When there are no tensile cracks at the joint, the walls resist a moment equal to the slab restraining moment while the slab load is transferred to the centre of the wall cross-section. Moments can then be found using a moment distribution method. The moment distribution at the joint will depend on the end moment-rotation characteristics of

the floors and walls. The more the slab end is allowed to rotate (slab not cantilevering) the smaller the slab restraining moment. The stiffness of the uncracked walls is calculated by usual methods but if tensile cracks occur this reduces the stiffness of the wall.

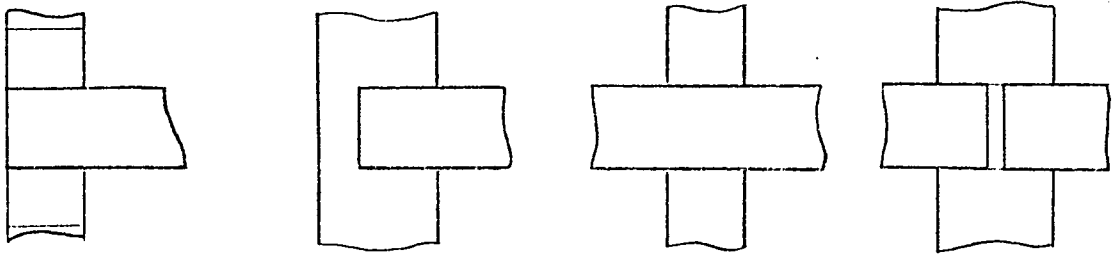
Reference 4 assumes a fixed connection when the average stress in the wall is greater than 100 lbf/in^2 and a $1:\frac{1}{2}:3$ mortar mix is used. But weaker mortars should also be able to give this fixity at that stress while the stress over which fixity occurs is dependent on the slab moment. The magnitude of the slab restraining moment is dependent on factors such as the length of bearing of the slab, the strength and stiffness of the wall, the load in the wall above the slab and the maximum moment the slab can resist.

The effect of axial load and tensile cracking on a solid, linearly elastic wall has been investigated by Sahlin (30,32) based on theory developed by Angervo and Putkonen (2). Tensile cracking at the joint imposes a limiting slab restraining moment dependent on the load in the wall above the slab - failure may occur earlier in the slab, or compressive or buckling failure may occur in the wall though buckling is not likely with usual storey height walls (32).

The sequence of construction also affects the fixity of the slab. A precast slab may be considered to be hinged when considering moments due to slab dead loads since the slab is allowed to deflect and rotate when it is positioned (35). With an in-situ slab there is a different result since the slab is cast onto the top course of the wall below. If the supports are withdrawn from the slab before the next storey walls are built, the slab ends will rotate - this rotation is opposed by the supporting wall thus imposing a restraining moment on the slab unless tensile cracking occurs. If cracking occurs, a moment is applied to the wall only, due to an eccentrically applied slab dead load. With increasing load from subsequently built walls above the slab, the moment applied to the wall below the slab may be considerable (see section 7.5.5). Reference 4 neglects this and assumes the in-situ slab behaves as the precast slab.

If the in-situ or precast slab is supported while the next storey is built, the dead load slab restraining moments will be distributed between the top and bottom walls.

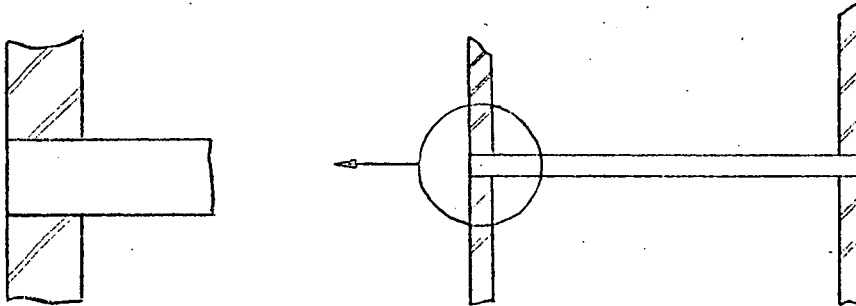
Typical connections causing slab restraint :



1.2 EXPERIMENTAL INVESTIGATION

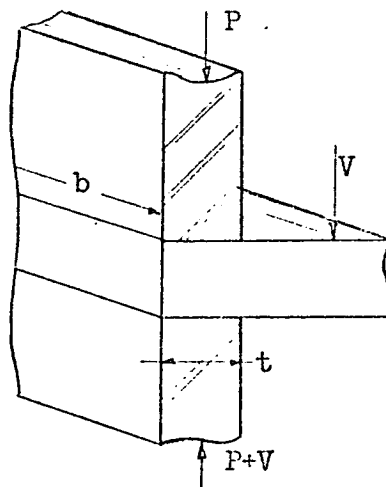
The previous sections have given a brief review of the problems facing the designer when considering the floor-wall junction. Appendix 1 gives a review of previous experimental work on the floor-wall junction. Apart from Sahlin's work (30,31,32) there has been little experimental or theoretical investigation into the behaviour of joints which do not resist tension.

The experimental work in this thesis is confined to a simple joint between a single leaf brick wall and a reinforced concrete slab bearing fully into it. No work had previously been conducted on this type of joint although this joint is now becoming more common.



Two variables were investigated making use of a full scale model of the joint :

1. The effect of the load in the wall above the slab (precompression). Does the magnitude of the precompressive stress affect the fixity of the slab ? Three different precompressions were compared - 200, 400 and 600 lbf/in² (P/bt). These were held constant while the slab load, V , was increased from zero to failure.



2. The effect of brickwork strength. Walls with lower strength mortars are likely to allow more rotation of the floor for a given moment - thus a lower slab restraining moment. How much more rotation is allowed? A comparison is made between walls made from the same brick but with three differing mortars - $1:\frac{1}{4}:3$, $1:1:6$ and $1:2:9$ cement:lime:sand mixes by volume.

A combination of each of the above variables was tested giving a total of nine 'joint tests'. There were also two preliminary tests. For each test, slab rotation was measured as well as the lateral deflection of the wall. In addition flexural strains were measured in the walls - this has not been done before but is considered necessary if the slab and wall rotations are to be properly understood. The assumption of a solid, linearly elastic material must be checked. These measurements are considered more useful and accurate than a measurement of the relative rotation between the floor slab and the wall at the joint as Sahlin (30) has done.

Tests on axially loaded walls were necessary to obtain the stress-strain relationship of brickwork under increasing and decreasing load. The effect of a central gap in the mortar joint on the vertical strain distribution was investigated using the finite element technique. Making use of the results from axially loaded walls, the elastic and ultimate properties of single leaf brickwork under flexural loading were considered.

As a complement to the model tests, similar joints were tested in a full scale five storey brickwork structure. A floor bearing into an outside wall was loaded up to 40 lbf/ft^2 to see how the wall-floor joint behaved. This was repeated for each floor level.

The following chapters explain the tests and results in detail. Each chapter, except Chapter 8, has an appendix given the same number as the chapter but prefixed by the letter A.

CHAPTER 2 - EXPERIMENTAL ARRANGEMENT AND PROCEDURE FOR THE
MODEL JOINT TESTS AND WALLS

2.1 INTRODUCTION

This chapter gives the material properties, the construction procedure, the experimental arrangement and the experimental procedure for the model wall-floor joint tests and associated tests on small walls.

2.2 BRICKWORK PROPERTIES

2.2.1 Brick

Double frogged Blairadam bricks were used (fig 2.1).

Compressive Strength : 5345 lbf/in²

Standard deviation : 595 lbf/in²

Tested in accordance with CP 3921:1965 (10)

Size : $2\frac{7}{8}$ in x $4\frac{1}{8}$ in x $8\frac{5}{8}$ in exact
 $3\frac{1}{4}$ in x $4\frac{1}{2}$ in x 9 in nominal

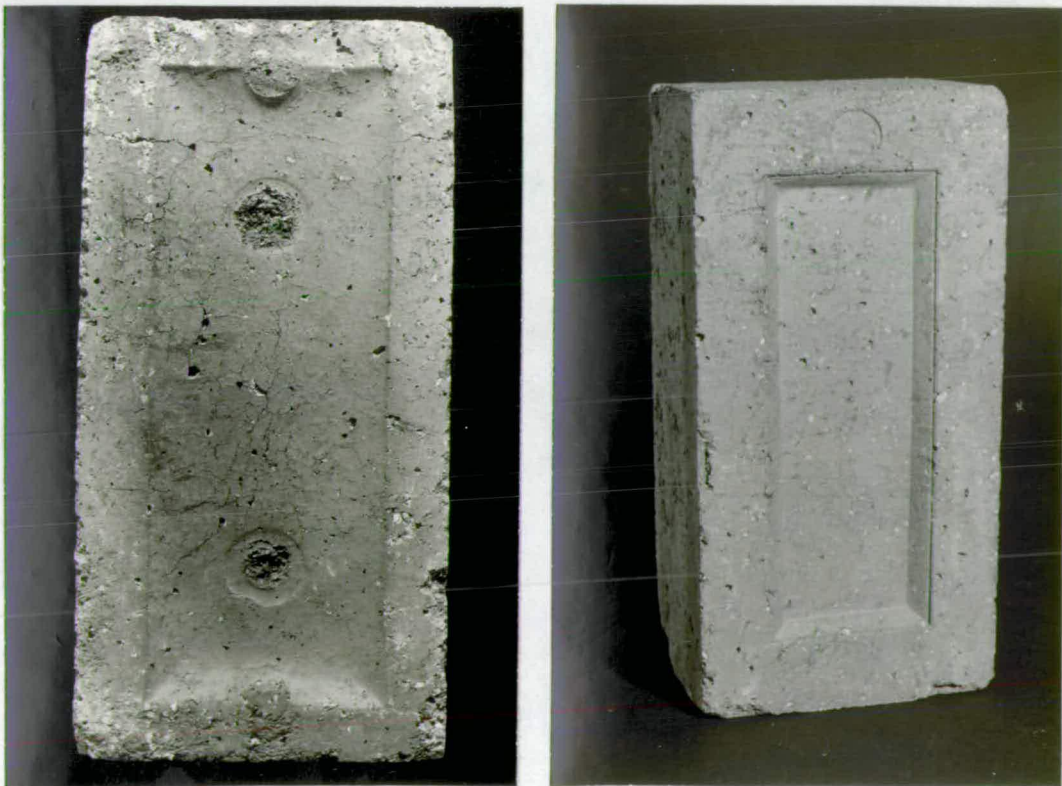


Figure 2.1 Blairadam Brick

2.2.2 Mortar

A building sand together with a rapid-hardening Portland cement and a hydrated lime were used for all mortars.

Compressive Strength : 4 inch cubes tested in accordance with the BCRA Model Specification (5).

Average strength at 14 or more days :

1:2:9 245 lbf/in²

1:1:6 510 lbf/in²

1: $\frac{1}{4}$:3 2345 lbf/in²

Individual results in Table 3.1 .

Mix : The mix proportions are cement:lime:sand by volume. The components are batched by weight based on the following bulk densities :

Sand	90 - 100 lb/ft ³
Lime	40 lb/ft ³
Cement	90 lb/ft ³

The water content was left to the bricklayer. In practice this varied from $w/c = 2$ for the 1:2:9 mortar to $w/c = 1$ for the 1: $\frac{1}{4}$:3 mortar.

2.3 WORKMANSHIP

The walls were built to a standard expected of supervised brickwork in practice.

A course rod ensured uniform mortar joints and overall height. Except for two preliminary tests, all the walls were built by the same bricklayer.

Mortar was laid with a furrow down the centre - this meant that gaps existed along the middle of the bed after the bricks were laid. This was further aggravated by incomplete filling of the shallow downward facing frog. This commonly happens in practice and as it is difficult to control it was decided to allow this extra variable. The effect of it is discussed in Chapter 3. The only certain way of avoiding this is to build with bricks without a downward facing frog.

2.4 CONSTRUCTION PROCEDURE

Seven course walls were built onto 1 inch thick steel plates. For the joint tests, the slab was then bedded into position, its free end supported by a dexion frame. Seven more courses were built onto the slab. The same slab was used in all the tests.

Walls were air cured in the laboratory with occasional moistening by a spray during the first few days. The top of the wall was later capped by either a 6 in x 3 in steel channel or a 1 inch steel plate using a 1:3 alumina cement:sand mix by volume.

2.5 SMALL WALLS

2.5.1 Test Arrangement

All walls were tested in a fixed head 100 ton Avery. The wall and loading beams were accurately positioned along the axis of the Avery with the help of two theodolites. Plywood packing, rubber sheets and/or thin metal sheets were inserted at some points of the loading beams to produce a more even distribution of load (figs 2.2 & 2.3).



Figure 2.2 Wall Type A

2.5.2 Test Procedure

Instrumentation :

Demec gauges : 2 in and 8 in gauge lengths.

Test :

Load was applied in stages. At each stage strain readings were taken while the load was held constant (fig 2.3). In most cases the load was increased to failure (no previous loading) but in a few walls the load was cycled. Tests lasted a long time due to the many strain readings taken - it also approximated the time taken in the joint tests reducing differences due to creep.

Some individual cases are now discussed :

1. 1:2:9 mortar wall No. 5 - Type A

In this test the load was cycled. In the first cycle the load in terms of stress was increased in stages from 0 to 280 lbf/in² and then unloaded in stages back to zero. This was repeated for 480 and 680 lbf/in². The wall was then loaded to failure. After reaching each load stage the load was held constant for 5 minutes before strain readings commenced. This reduced strain variations, due to creep, between the first and last strain readings at each stage. Total time spent on this test was approximately 18 hours (about 5 hours/cycle and 3 hours for the test to failure).

2. 1: $\frac{1}{2}$:3 mortar wall No. 6 - Type B

Load was cycled. At each load stage strain readings lasted for 20 minutes for the first cycle and 10 minutes for later cycles. Readings were taken as soon as the load stage was reached as there was negligible creep except when nearing failure loads. Total time spent on this test was 9 hours.

3. 1: $\frac{1}{2}$:3 mortar wall No. 4 - Type A

This wall was loaded to failure with the load applied in stages. Total time was 4 hours.

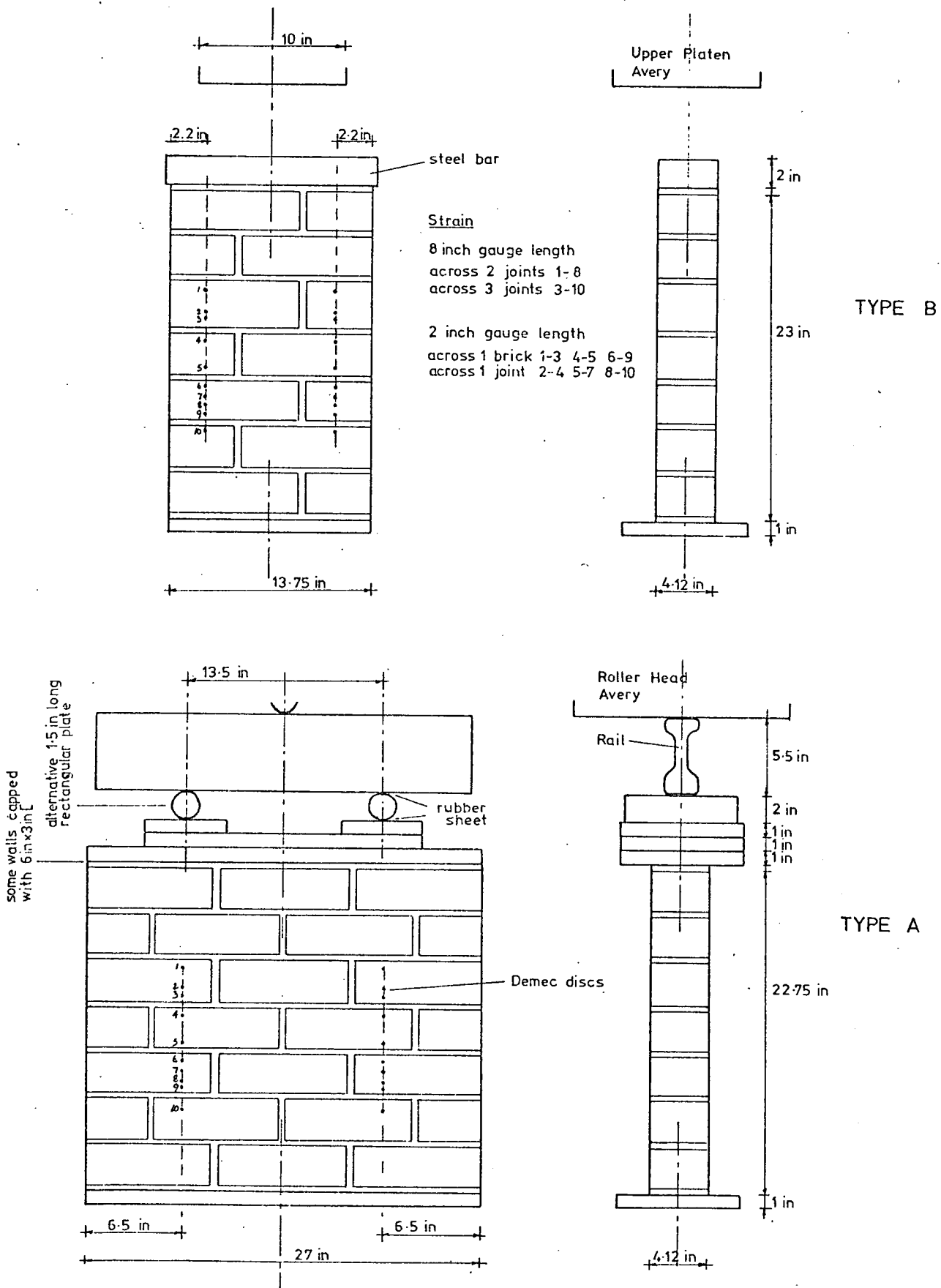


Fig. 2.3

AXIALLY LOADED WALLS

2.6 JOINT MODELS

2.6.1 Test Arrangement

Photographs and a diagram of the model and test arrangement can be seen in figures 2.4 to 2.7 .

Two types of loading are applied to the model - a vertical precompressive load applied to the walls and a vertical load applied to the free end of the slab.

The precompressive wall load was applied by a 100 ton Avery hydraulic testing rig.

Three small 6 ton hydraulic jacks applied an upward force to the free end of the slab - the loading was inverted compared to practice. This makes the application of the load easier and it avoids complete collapse of the model at failure. To measure the jack load a 3 ton load cell with a self-aligning cap was placed under each jack. A stabilised power supply provided 10 volts DC to the load cells while the output was given by a digital voltmeter. Hydraulic pressure to the jacks was supplied by a hand pump and in later experiments by an electric pump. The pressure when using the hand pump had to be adjusted frequently. With the electric pump, an Enerpac adjustable relief valve provided a constant pressure setting but at certain pressures tended to resonate causing sudden drops in pressure - again pressure would have to be manually controlled. In future tests a connection should be made to a more stable hydraulic unit such as the Avery.

The models were built near to the Avery. Their size made handling reasonably easy. The wall sections were high enough to allow an even distribution of the precompressive stress near the joint (load at the top was applied over part of the wall only). The slab length was the maximum allowed by the test equipment thus providing the maximum possible moment for a given jacking load. The model supported by a dexion frame was built onto a steel plate with castor wheels at each corner.

The day before a test, the model was rolled into the Avery leaving the rollers clear of the bottom loading platen. When the platen was raised it bore directly onto the plate lifting the wheels from the surrounding floor. After positioning the model two channels were inserted under the slab and bolted back to back. Onto these were placed the load cells, the jacks and the loading bars. Onto the top wall were

placed a steel plate, a steel bar, plywood sheets and thin metal sheets, the latter filling any small gaps between the bar and the top platen. The steel bar and the wall were lined up in the Avery with a theodolite.

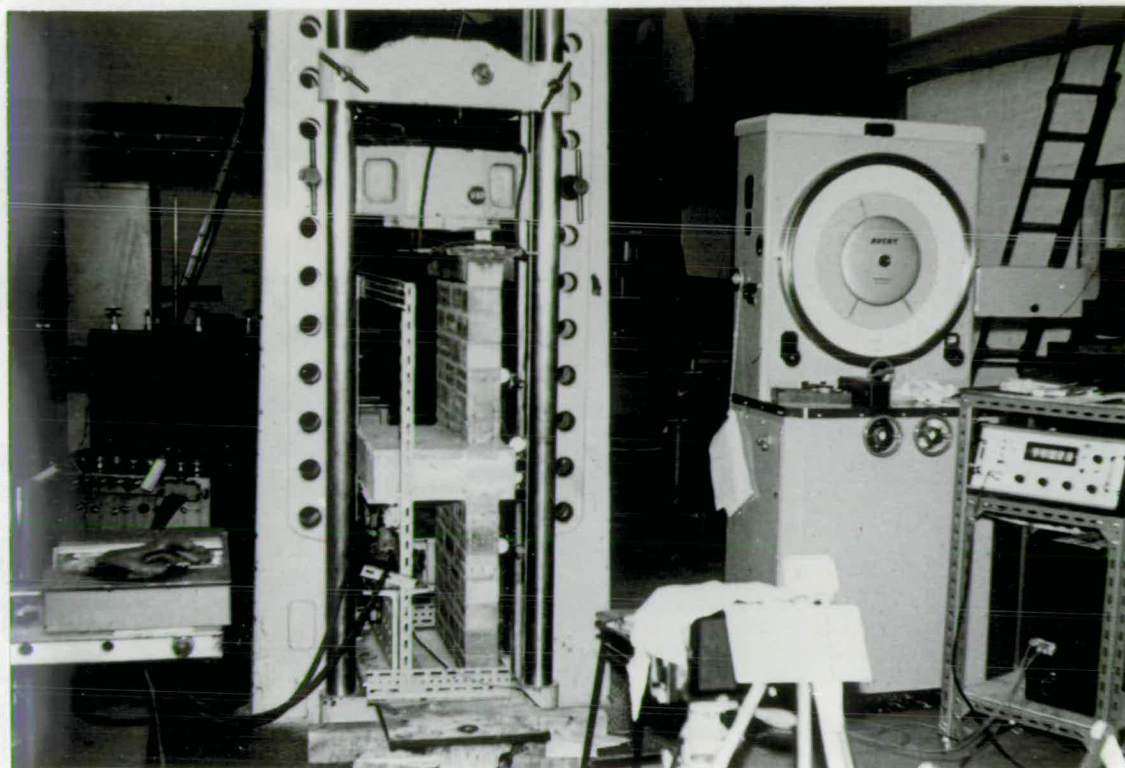


Figure 2.4 Test Arrangement - Model Joint Test

2.6.2 Testing Procedure

Instrumentation :

2 in and 8 in gauge length demec gauges.

0.0001 in dial gauges.

The 8 inch demec gauges measured the strain due to compression and bending in the wall above and below the slab. The 2 inch gauges measured deformation across the mortar joints - slab to wall and the course immediately following.

The dial gauges measured lateral deflection of the wall, rotation of the slab and on some occasions rotation of the loaded ends of the wall. The gauges were held in position by magnetic bases attached to the Avery frame.

Figure 2.5 shows the position of the dial gauges and the layout of the strain measurements.

Test :

Initial readings were taken. The wall was then loaded in stages up to a set precompression. The strains obtained for this part of the test gave the stress-strain curve in compression.

Next jacking loads were applied to the slab in stages while keeping the precompression in the bottom section of the wall constant. This meant increasing the Avery load by the same amount as the jacking load. Strain and deflection readings were taken giving bending strains, rotations and lateral deflection. Dial gauges were read at the beginning and end of each load stage. All tests were completed without a break. Time for a test was on average $5\frac{1}{2}$ hours (range 3 to 10 hours).

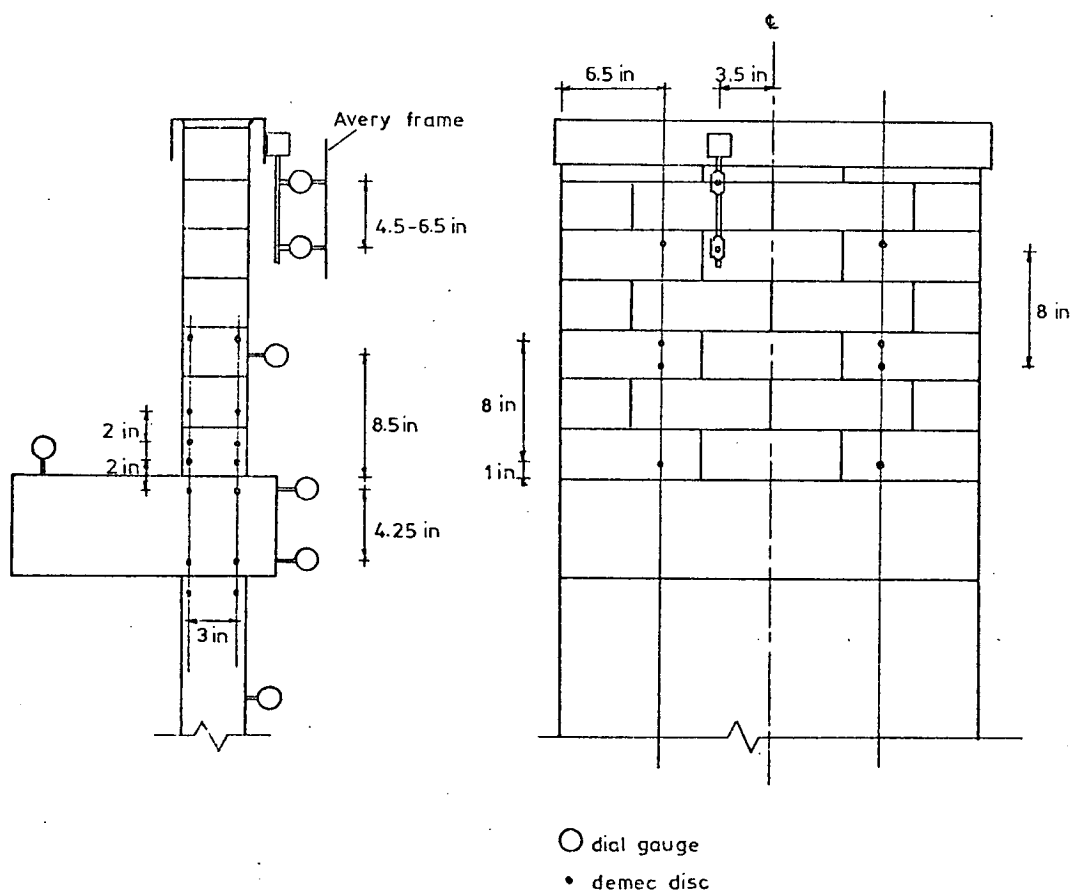


Fig. 2.5 DIAL GAUGE AND DEMEC POSITIONS

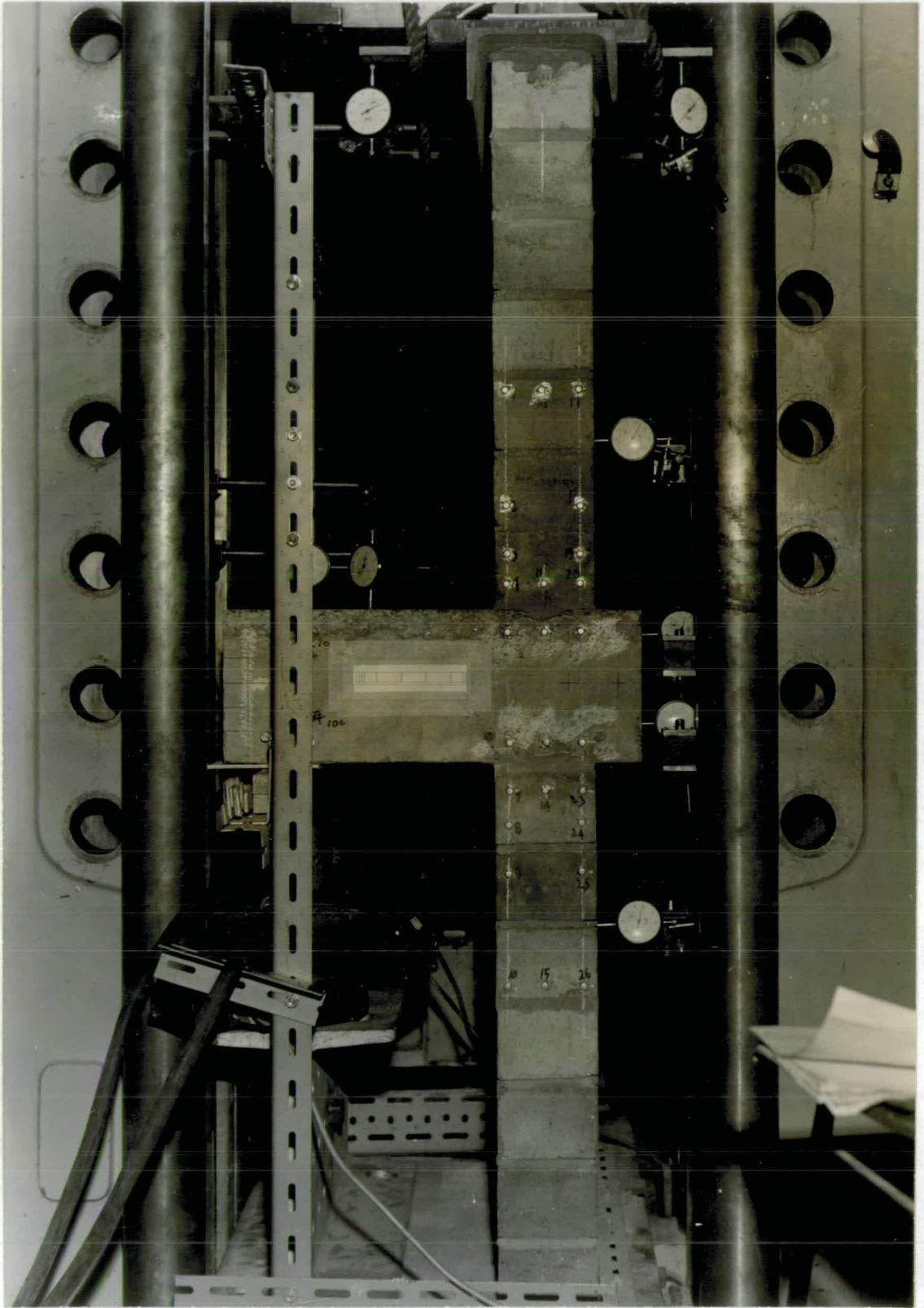
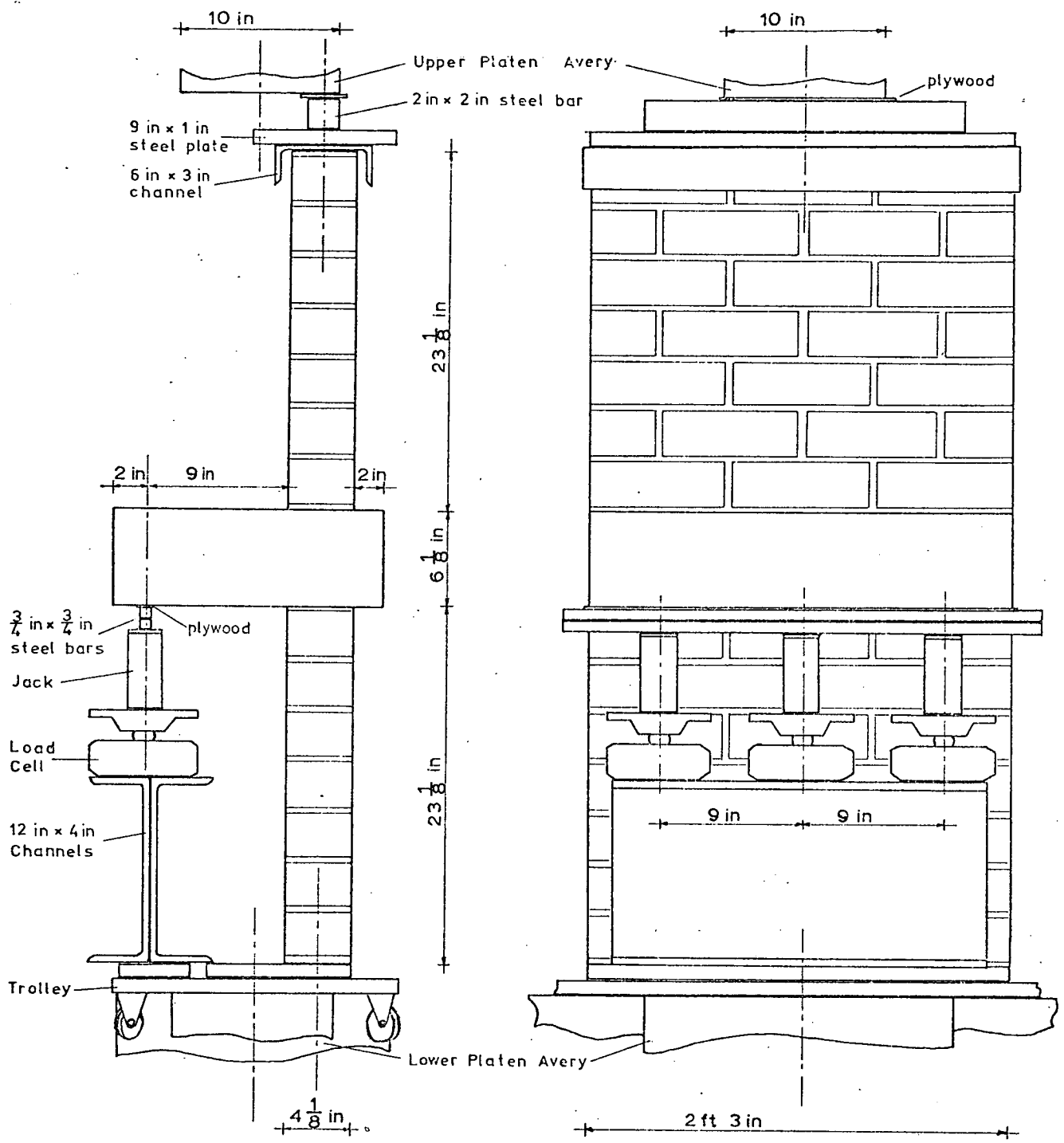


Figure 2.6 Wall - Floor Joint Model



1/10 Scale

Fig. 2.7 MODEL LOADING ARRANGEMENT

3.1 INTRODUCTION

Brickwork is a composite material composed of two phases - brick and mortar. The phases are in parallel, implying equal vertical stress in the brick and mortar. The mortar provides a bedding for the brick allowing a more uniform transfer of load from one brick to another.

An investigation into the deformation of this two phase material under axial compression is the purpose of this chapter.

The stress-strain relationship was experimentally investigated for three different strengths of brickwork - the same bricks were used throughout with three different mortars - 1:2:9, 1:1:6 and 1: $\frac{1}{4}$:3 mixes - as used in the joint tests. Two loadings are considered :

1. Loading up to failure giving the stress-strain curve for a wall loaded for the first time.
2. Cycled loading to see the effect of unloading and reloading on the stress-strain curve.

The latter aspect is necessary for the analysis of axially loaded brickwork subjected to flexural stresses.

The latter part of the chapter deals with the transfer of load across the mortar joint. The effect of a central gap in the mortar joint on the overall vertical strain distribution is considered. To simplify calculations, the solid brick wall is replaced by an equivalent hollow wall. This is done with the help of a finite element analysis.

3.2 SINGLE LEAF BRICKWORK LOADED TO FAILURE

3.2.1 Stress-Strain Relationship

Typical stress-strain curves for walls of three different strengths are shown in figure 3.3 .

The 1: $\frac{1}{4}$:3 mortar wall has an initial linear curve while the 1:1:6 and 1:2:9 mortar walls usually have a non-linear curve throughout. The non-linearity at the start is due to the mortar, the brick having an initial linear stress-strain curve. The curves are representative, there being variations in strain on different sections of the wall as well as on different walls. Variations are caused by differences between indi-

vidual bricks (eg. cracks), differing mortar batches, workmanship and uniformity of load application. To reduce positional variations the strains were always measured at the same positions, these being symmetrical about the centre of the wall and identical on both sides of the wall thus reducing the effect of load eccentricity. To reduce variations due to non-uniform brickwork properties, the final results were at least an average of four gauge positions (sometimes as many as twelve). Notes on the effect of gauge length are given in Appendix 3.

3.2.2 Ultimate Strength

Near failure continuous light cracking noises are heard - vertical hair-line cracks develop at the ends (down centre and near the edge of the bricks) and through the bricks and collar joints at the side (figs 3.1 & 3.2). Soon after small bits of mortar and brick, near to the mortar joints, spall off. With increasing loads cracks widen, finally causing the cracked sections to shear and buckle off causing failure. The failure process is slow, the ultimate load varying by a few tons depending on the rate of loading.

For comparison, two brick sections after failure are shown in figure 3.7*.
Table 3.1 gives the mortar strength and the ultimate strength for the walls tested.

* Three rectangular sections cut from the brick were tested. The nominal dimensions were 1 in x 3 in x 9 in . The specimens were capped with a dental plaster. Two 2.5 inch vibrating wire strain gauges were attached to the sides. The brick properties are assumed to be isotropic for this test as the load is applied along a different axis from that in practice. Their average compressive strength was 3650 lbf/in² (2500, 3300 & 5145 lbf/in²).



Figure 3.1 Failure of a 1:1/4:3 Mortar Wall - No WS9b

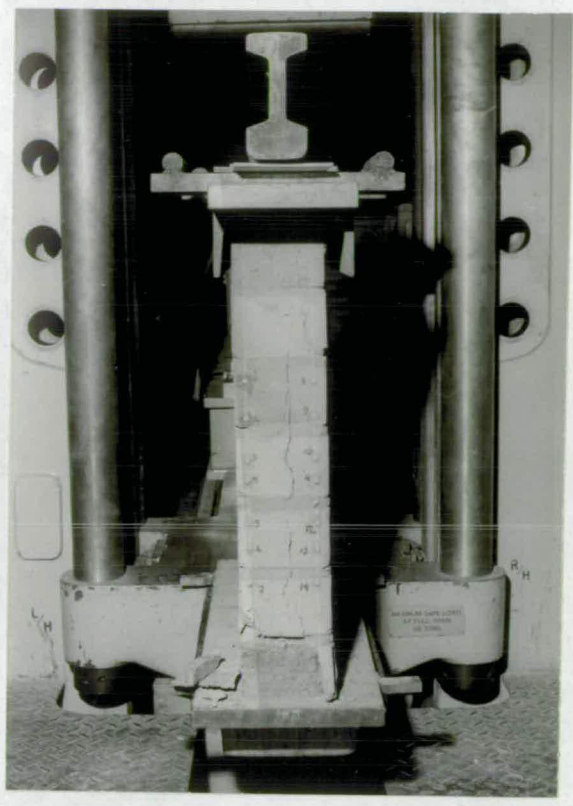


Figure 3.2 Vertical Cracks at Failure of a 1:1/4:3 Mortar Wall - No 4

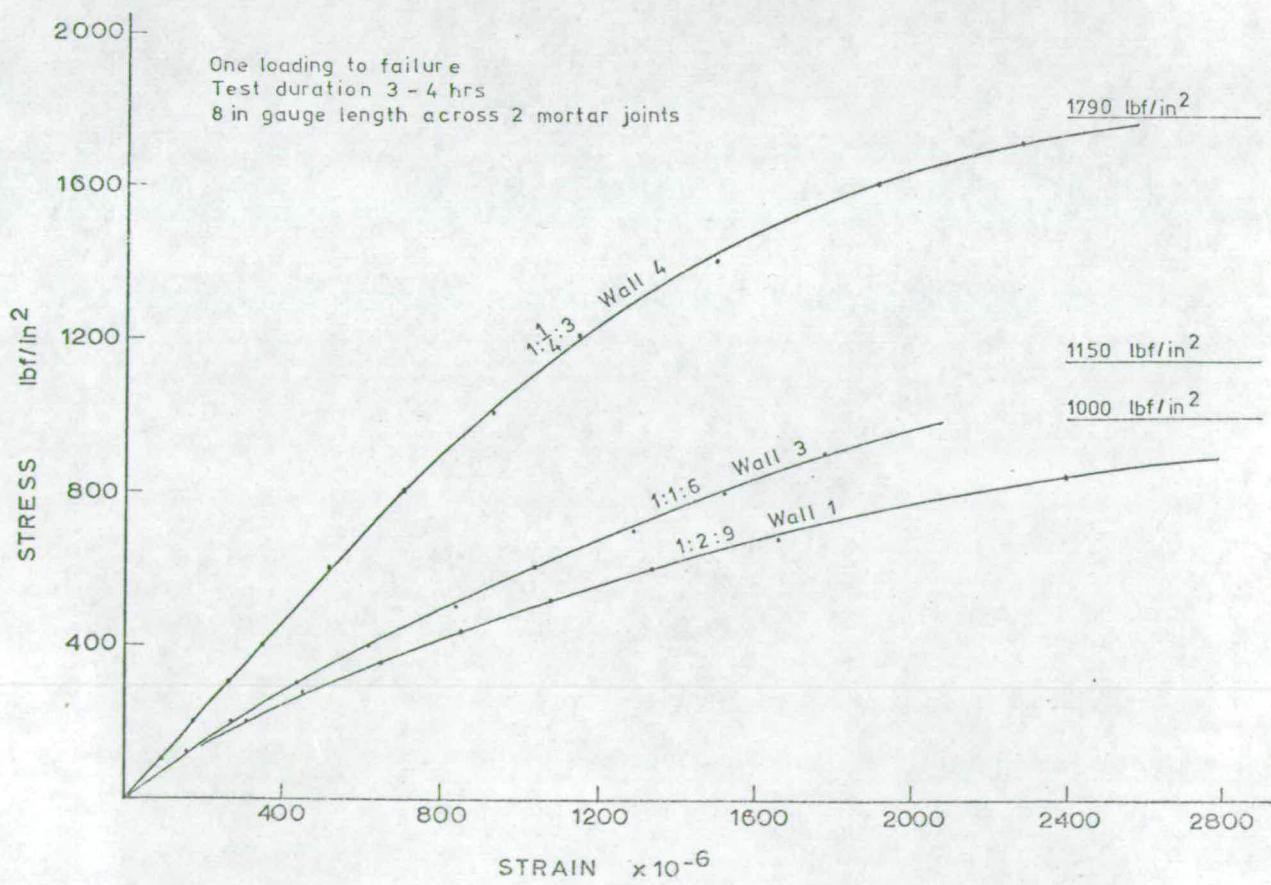


Fig. 3.3 Typical Stress - Strain Curves Axial Compression

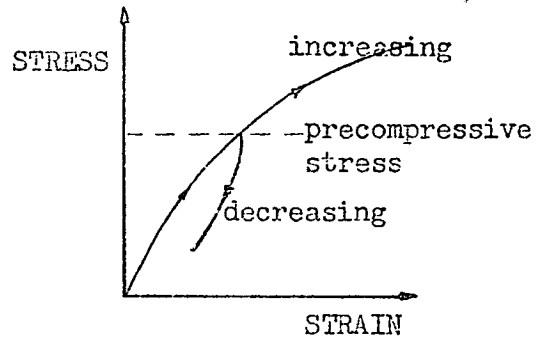
TABLE 3.1 - WALL PROPERTIES

Mortar Mix by Volume	Wall No.	Type	Age at Test days	4 in mortar cube strength lbf/in ²	Ultimate Strength lbf/in ²	Notes
1:2:9	1	A	21	180	1005	WS - wall slab joint model b - bottom section t - top section * 2.78 inch mortar cubes
	5	A	40	310	1185	
	WS11b	A	60		965	
	WS1		112	325		
	WS3		15	145		
	WS4		15	110		
	WS11		20	270		
	WS12		32	360		
1:1:6	2	A	15	295	885	
	3	A	26	585	1150	
	7	B	51	670	1340	
	WS5b	A	54		990	
	WS6t	A	135		1225	
	WS7b	A	61		1315	
	WS5		14	385		
	WS6		15	575		
	WS7		28	545		
1:½:3	4	A	107	2340	1790	
	6	B	42	3200	1420	
	WS9b	A	35		1585	
	WS8		17	1365		
	WS9		32	2510*		
	WS10		84	2385		

3.3 CYCLED LOADING

3.3.1 Tests and Results

Take a wall with a constant precompressive stress situated above a junction with a floor slab. When the slab is loaded it applies a moment to the wall causing a simultaneous increase and decrease of the strain on opposite sides of the wall. Thus from a point on the stress-strain curve given by the precompressive stress, the stress-strain relationship with decreasing stress must be known.



The load on three walls was cycled to various stress levels before final loading to failure while three brick samples were loaded over one cycle. Figures 3.4 to 3.6 show the stress-strain behaviour for brickwork under cycled loading. The figures show the behaviour over 8 inch gauge lengths covering two mortar joints and over 2 inch gauge lengths on brick only. The difference in strain magnitudes shows the effect of the mortar on the strain.

Figure 3.8 shows the stress-strain behaviour for brick over one cycle. Table 3.2 gives the tangent modulus of the initial linear portion of the loading path for each cycle and the ratio of the unloading to loading chord moduli about the maximum stress for each cycle.

3.3.2 Analysis and Discussion

The walls follow similar patterns. During the first load cycle, the stress-strain curve follows the usual path but on unloading a very different path is observed. The curve is non-linear and of opposite shape to that of the loading curve (convex looking upwards). A permanent set occurs at zero stress, this being greatest for the 1:2:9 mortar wall. Reloading causes an initial convex upward portion which becomes approximately linear up to the previously attained stress level after which the curve takes up the shape of the initial loading path. If the previously attained stress level is not reached the unloading curve will show much reduced hysteresis with little set at zero stress. This is shown by the 1:½:3 mortar wall.

The reloading curves for a given wall have similar slopes and can be considered to be equivalent to the initial tangent modulus. Table 3.2 shows that cycling the load on the two weaker walls makes the reloading curve considerably more linear except at low stresses.

The unloading curves for the walls have a much steeper slope than the loading curves, the ratio being greater for the weaker walls and with increasing stress levels. The difference in the slope of the unloading curves for the walls is not large. Figure 3.9 shows the unloading curves, taking the origin as the point on the curve at which unloading started (maximum stress for a particular cycle).

The tests on three brick samples show hysteresis and illustrate the possible variation between the bricks.

Both brick and mortar exhibit hysteresis. In an elastic material hysteresis occurs when more work is done during loading than unloading, the strain returning to zero but by a different path. Brickwork approximately follows this pattern when the load is cycled below a previously attained stress level.

For an initial load cycle or a cycle above a previously attained stress, the strain does not return to zero and larger hysteresis loops are observed mainly due to the non-linearity of the loading path. Some of the residual strain will be recovered in time but the greater proportion is due to local failure within the brick and mortar. The $1:\frac{1}{4}:3$ mortar brickwork shows relatively small residual strain as is to be expected as the loading curve is linear over the range tested. Looking at the loading paths for the $1:1:6$ and $1:2:9$ mortar walls, the tangent modulus decreases with increasing stress mainly due to the breakdown of the cement-aggregate bond. Khoo (20) found this to occur for $1:1:6$ and $1:\frac{1}{2}:3$ mortars under triaxial compression. The brick also exhibits increasing residual strain with increasing stress. The bricks used contain many shrinkage cracks, and compaction and breakdown along these cracks is the most likely cause for the residual strain.

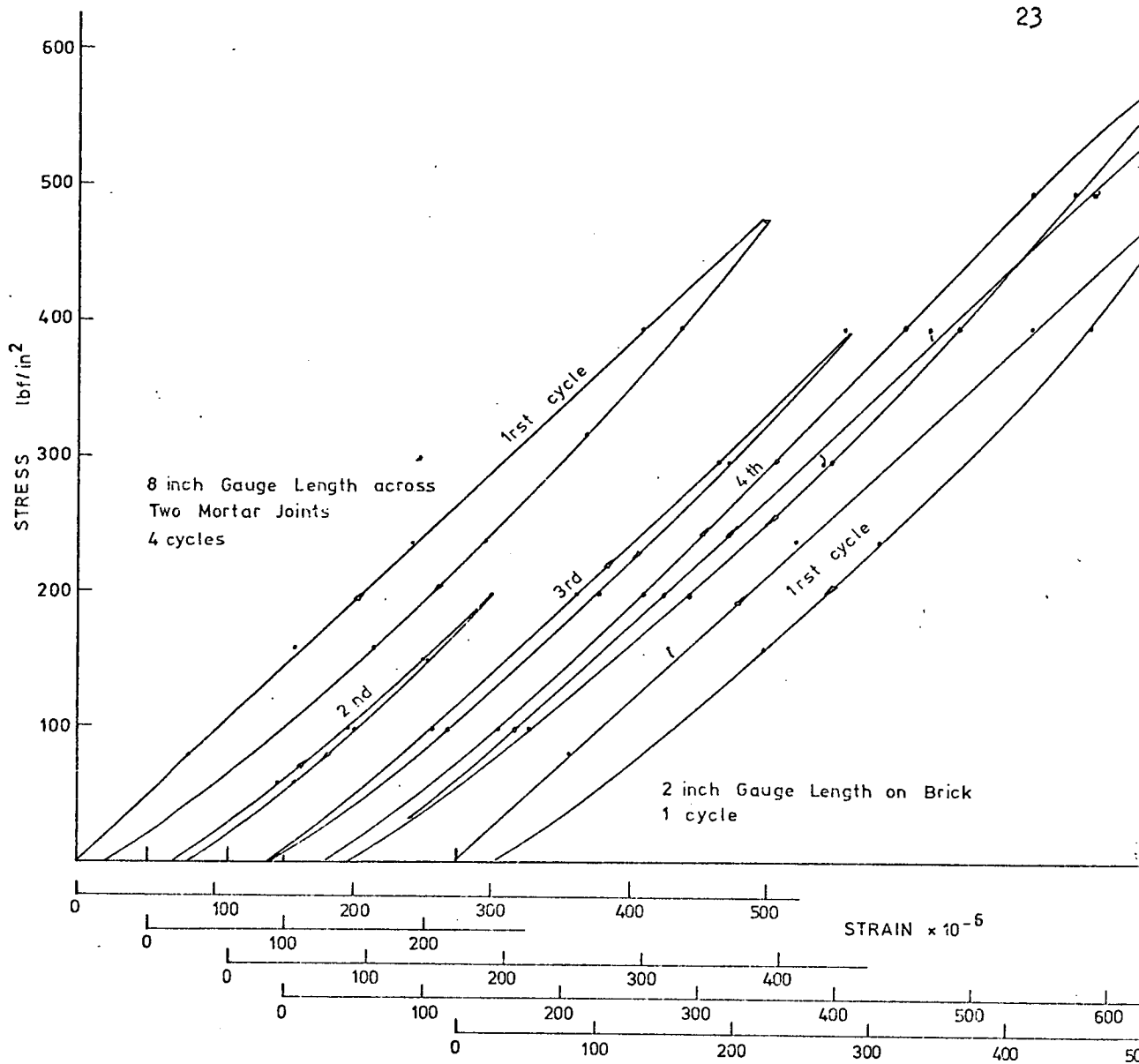


Fig. 3.4 Cyclic Stress-Strain Curves for a $1:\frac{1}{4}:3$ Mortar Wall (No. 6)

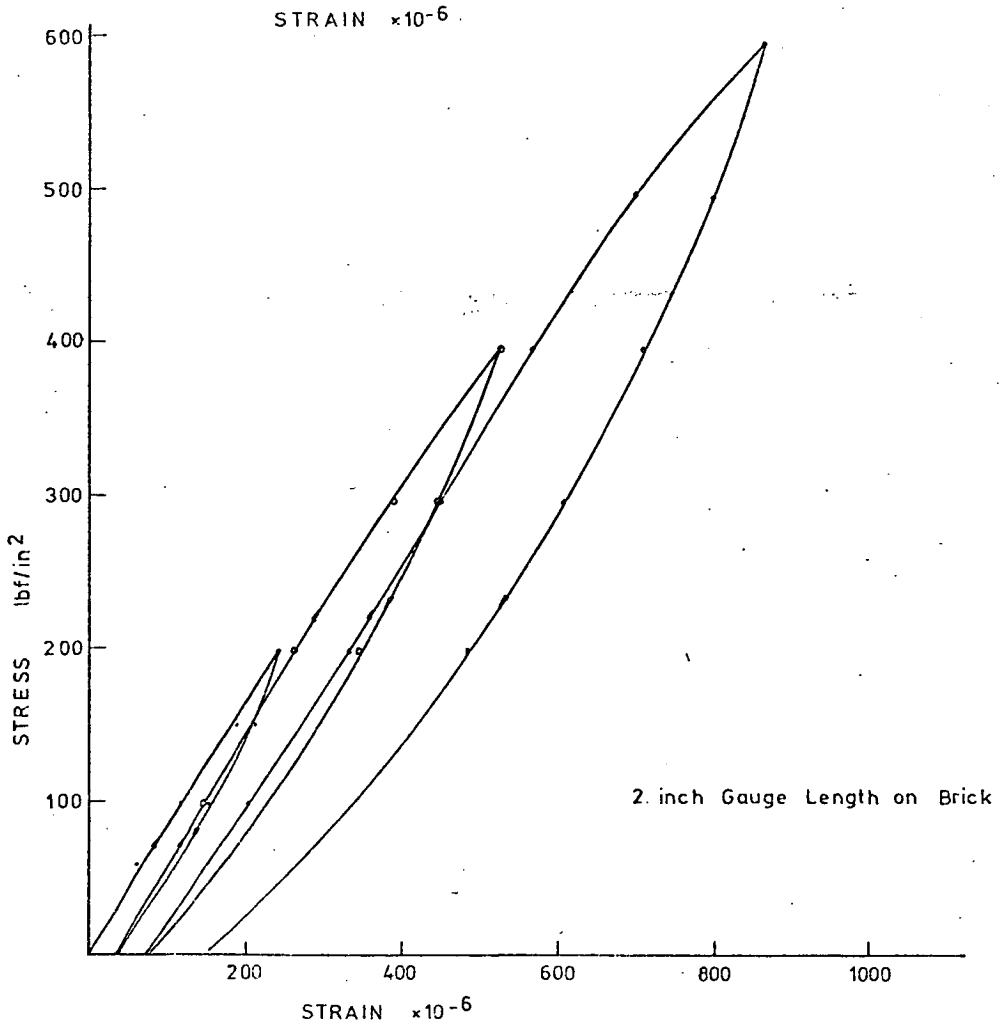
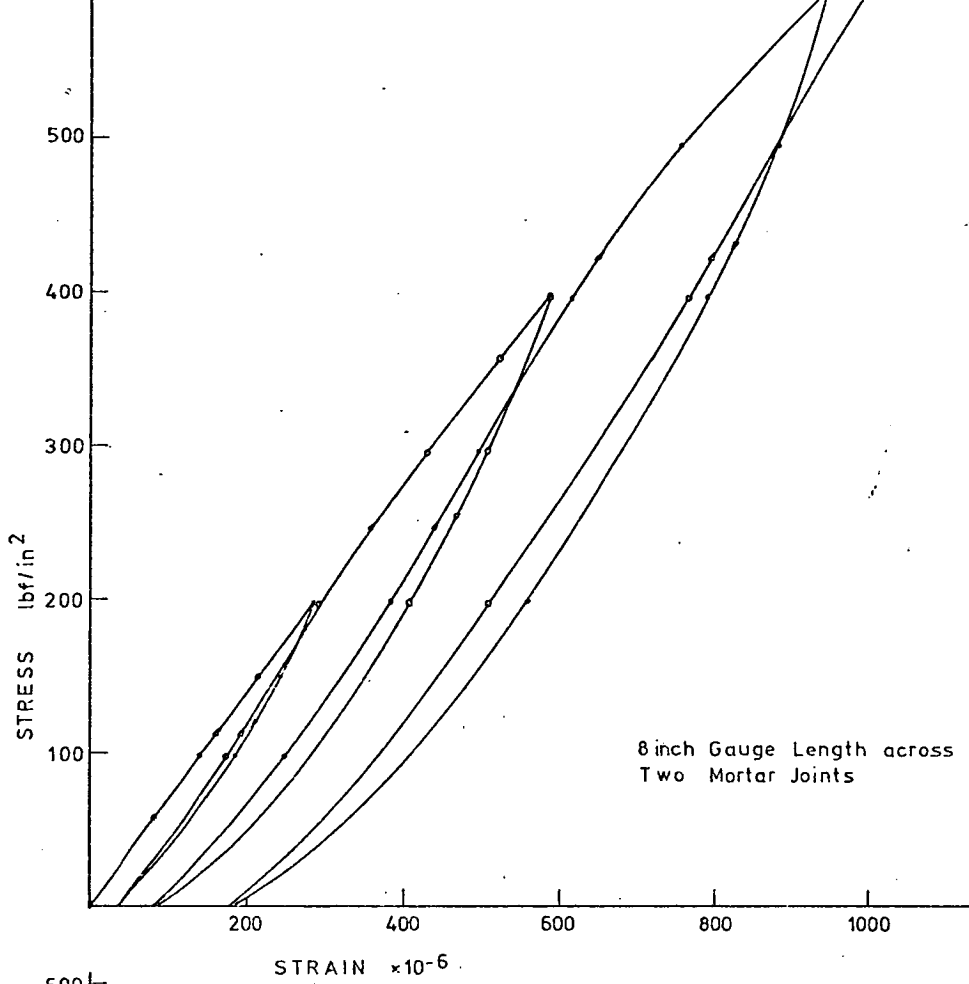


Fig. 3.5 Cyclic Stress-Strain Curves for a 1:1:6 Mortar Wall (No.7)

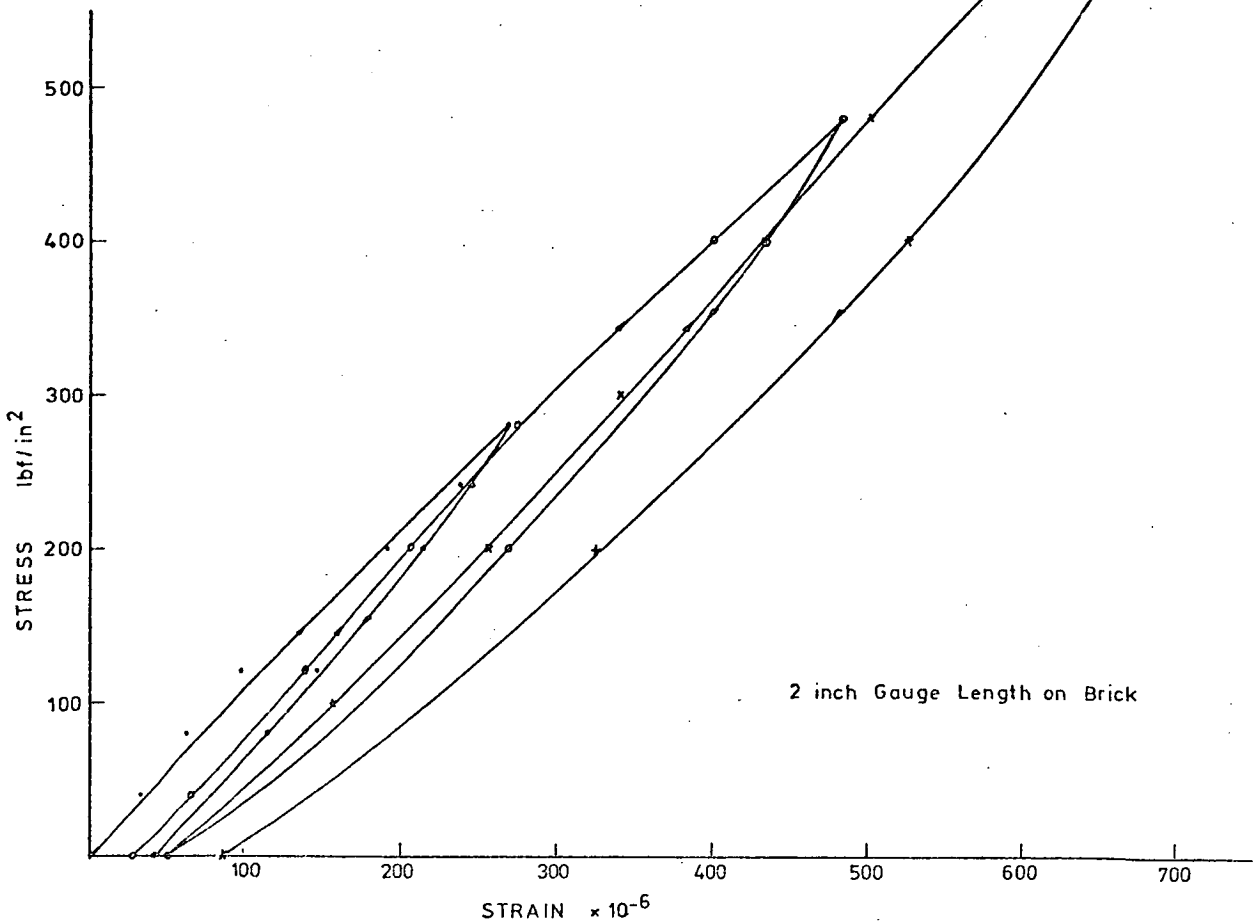
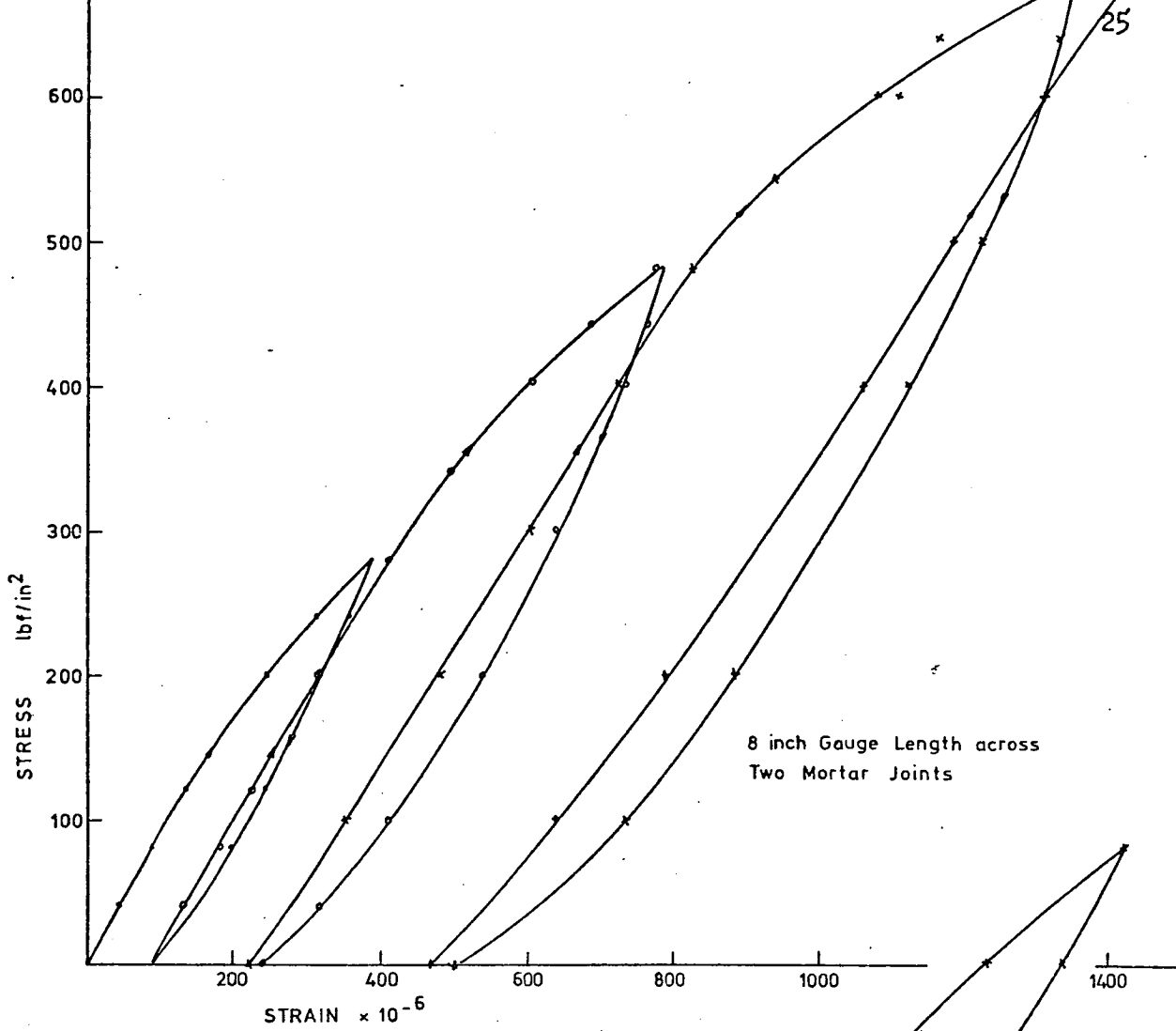


Fig. 3.6 Cyclic Stress-Strain Curves for a 1:2:9 Mortar Wall (No. 5)

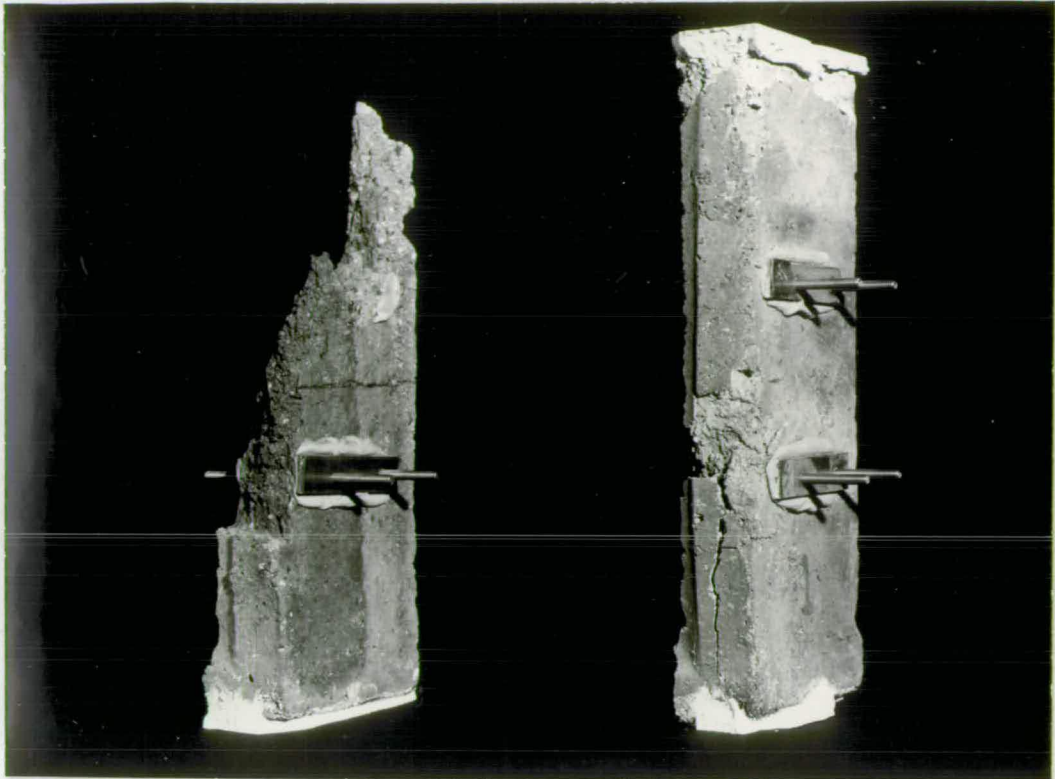


Figure 3.7 Brick Sections after Failure

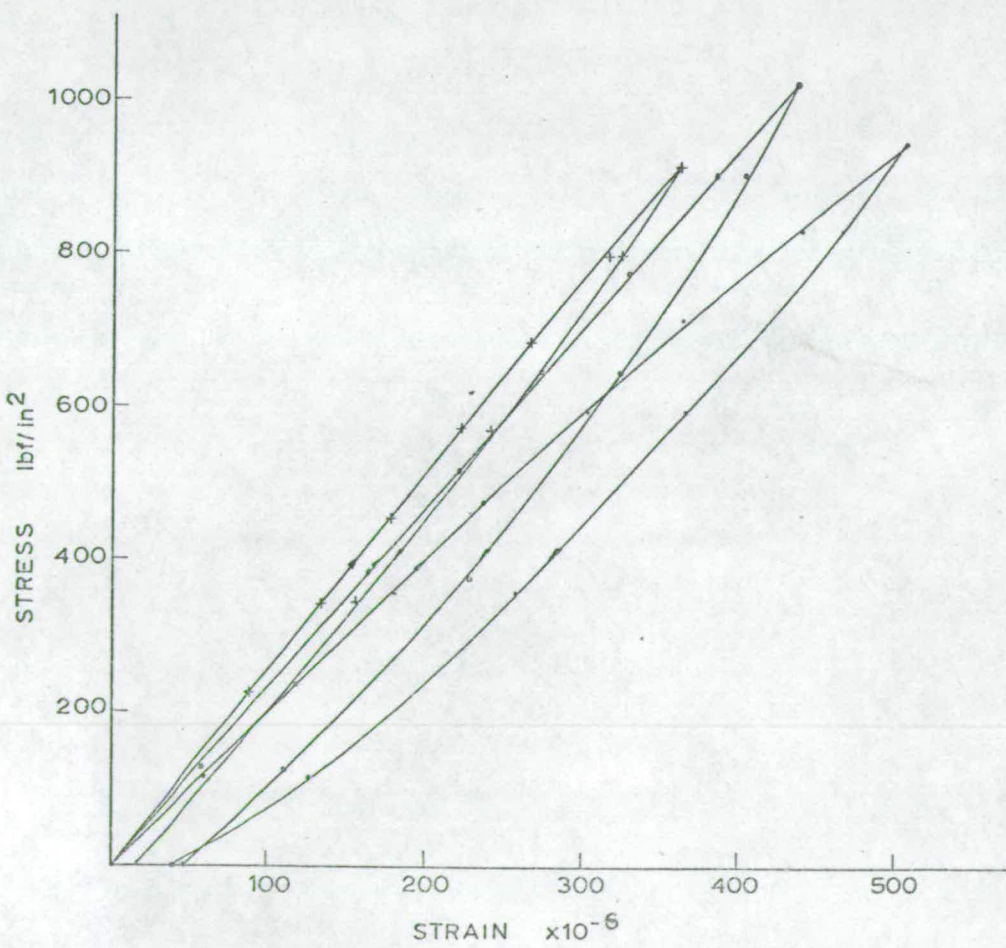


Fig. 3.8 One Load Cycle on Three Brick Sections

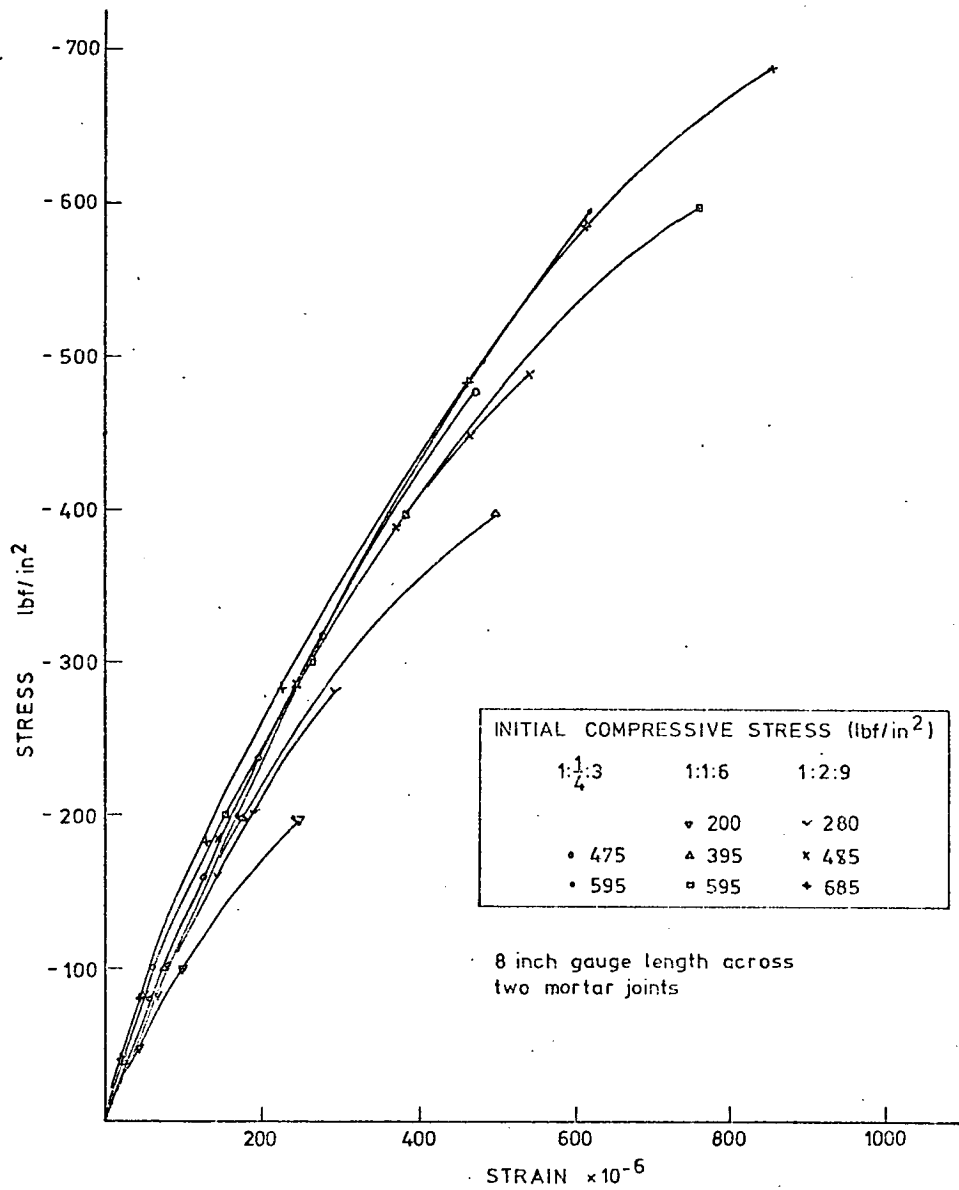


Fig. 3.9 Unloading Stress-Strain Curves for Brickwork
-stress reduced to zero from given stress levels

TABLE 3.2 - EFFECT OF LOAD CYCLING ON BRICKWORK MODULI

Mortar Mix by Volume	Cycle No.	Tangent Modulus Loading 1,2	Chord Modulus					Max Stress in Cycle
			Stress Interval	Average Stress	Loading Modulus	Unloading Modulus	Ratio	
1:2:9 Wall No. 5	1	0.95	180-280	230	0.57	1.1	1.9	280
	2	0.88	385-485	435	0.48	1.4	3.0	485
	3	0.82	585-685	635	0.32	1.8	5.6	685
	failure	0.81						
1:1:6 Wall No. 7	1	0.70	100-200	150	0.70	1.0	1.4	200
	2	0.87	295-395	345	0.64	1.25	2.0	395
	3	0.86	495-595	545	0.54	1.65	3.0	595
	failure	0.82						
1:½:3 Wall No. 6	1	0.96	375-475	425	0.96	1.3	1.4	475
	2	0.95						200
	3	0.96	295-395	345	0.96	1.1	1.1	395
	4 ³ failure	1.04 0.95	495-595	545	0.87	1.2	1.4	595
Brick Sections								
1	1	2.00	850-950	900	1.65	2.95	1.8	950
2	1	2.58	810-910	860	2.4	3.1	1.3	910
3	1	2.35	930-1030	980	2.35	3.7	1.6	1030

Notes :

Units - stresses in lb/in^2 and moduli in $\times 10^6 \text{ lb}/\text{in}^2$

1. In cycle 1, the tangent modulus is the initial tangent modulus.
2. In cycles other than the first, the tangent modulus represents the best tangent in the initial portion of the curve before the previous load level is reached. At the start of loading the curve is usually of a convex upwards shape - this is neglected.
3. In cycle 4 of the 1:½:3 mortar wall the loading and unloading moduli may be too low. The values depend on the strain reading at maximum stress level. $0.87 \times 10^6 \text{ lb}/\text{in}^2$ is likely to be too low based on previous experience.

3.4 CENTRAL GAPS IN THE MORTAR JOINT

3.4.1 Load Transfer Across the Mortar Joint

In brickwork the mortar ensures a more uniform transfer of load across the joint. This aspect is now discussed with regard to the walls used in the experiments.

The mortar joint is often assumed to be solid but in practice the mortar is laid with a furrow down the centre - in effect introducing a central gap transferring no load. With solid bricks this gap may be small. With bricks having frogs facing downwards, the frog is often not properly filled and with shallow frogs often unfilled. This will produce an even larger gap limited by the width of the frog (fig 3.10). At the mortar joints the load is therefore concentrated at the edges of the brick.



Figure 3.10 - Central Gap in the Mortar Joint (Wall No. 6)

The gap affects the vertical strain on the sides of the wall. If the stresses are based on the full cross-section, the calculated value for the compression modulus will be too small. Now if this modulus is used theoretically it will give the correct values for axial strains but not for flexural strains which will be overestimated.

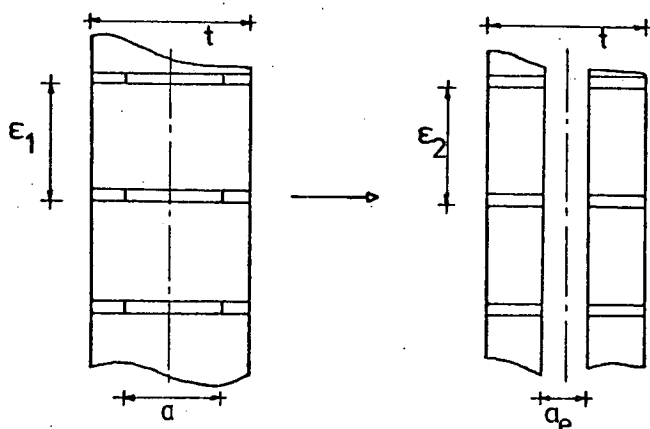
To obtain a better value for the compression modulus is difficult since the stresses are not uniform. An analysis based on the finite element technique is used to find the effect of the gap on the surface strains of the wall.

3.4.2 Theoretical Analysis

To simplify calculations the following assumptions are made :

1. The gap in the joint extends throughout the length of the mortar course (neglecting the end sections of the brick in contact with the mortar).
2. The gap width is uniform.

The purpose of this analysis is to replace the wall by an equivalent hollow section giving the same external strains (fig 3.11).



For the same axial load, P

$$\epsilon_1 = \epsilon_2$$

$$E_{\text{exp}} = \frac{P/bt}{\epsilon_2} = \frac{P/bt}{\epsilon_1}$$

Figure 3.11 - Wall with Gaps in the Mortar Joint replaced by an Equivalent Hollow Wall

- Notation :
- a = width of gap in the mortar joint
 - a_e = gap width of equivalent hollow wall
 - E_{exp} = compression modulus of brickwork assuming a solid section.
 - E_s = true compressive modulus of brickwork (ie. if the section had been solid).

- E_b = true brick modulus
 E_m = true mortar modulus
 V_b = proportion of brick covered by gauge length

E_{exp} and E_s are related by the following equation :

$$E_s = E_{\text{exp}} \left(\frac{t}{t - a_e} \right) \quad \text{--- (3.1)}$$

1. Axial Loading

The first wall section in figure 3.11 was analysed using a finite element program (section A3.2). The analysis was carried out for differing values of gap width, a , and ratios of brick to mortar modulus, E_b/E_m .

The results of the analysis gave the vertical strain over the height of one mortar joint plus one brick. From this a value of E_{exp} was obtained assuming a solid section. The value of E_s is given by :

$$E_s = \frac{E_b}{V_b + (E_b/E_m)(1 - V_b)} \quad \text{--- (3.2)}$$

The derivation of this equation is given in the appendix (section A3.1.2).

Using the values of E_{exp} and E_s , the effective gap is found from equation 3.1. Results are shown graphically in figure 3.12.

As an example, for a mortar gap width of 2.62 inches and a ratio of $E_b/E_m = 1$, the effective gap width becomes 2.11 inches.

2. Eccentric Loading

The object of replacing the brick wall by an equivalent hollow one is its use in predicting experimental flexural strains in walls subjected to eccentric loading.

Using the calculated values of a_e and E_s , the strains under eccentric loading can be predicted by simple theory.

$$\epsilon = \frac{M\bar{y}}{E_s I} \quad \text{--- (3.3)}$$

where M = moment

$$\bar{y} = t/2$$

$$I = b(t^3 - a_e^3)/12$$

The results from this equation compare well with those obtained from the finite element analysis (Table A3.1, Appendix 3) - the difference only a few percent.

3. Application to Experimental Analysis

From experiment a value of E_{exp} is obtained. Assuming a value for the gap width in the mortar joint and a ratio of brick to mortar modulus (only a rough value is necessary), a value for the effective gap width is found using figure 3.12. Equation 3.1 gives a value for E_s . The flexural strains can then be calculated.

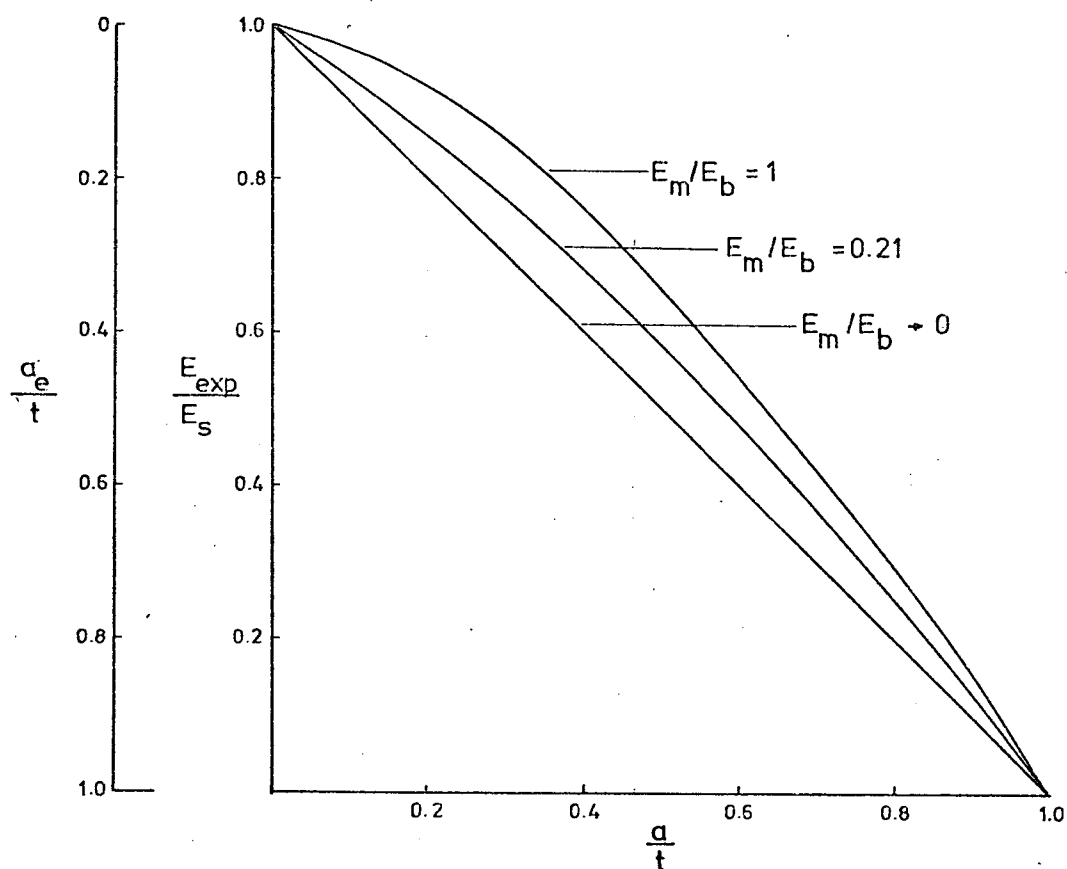


Figure 3.12 Effective Gap versus Actual Gap for varying values of E_b/E_m

3.5 CONCLUSIONS

1. The loading and unloading paths of the brick and brickwork stress-strain curves are different. A permanent strain occurs on unloading. The difference in the loading and unloading paths and the magnitude of the permanent strain, increase with increasing stresses and with decreasing strength of brickwork (increasing curvature of the stress-strain curve)(figs 3.4 - 3.6).
2. Walls under axial load subjected to flexural stresses have different moduli for increasing and decreasing stress. In the first load cycle the ratio of the unloading to the loading modulus varied from 1.4 to 5.6 (Table 3.2).
3. Cycling the load produces a more linear stress-strain curve on reloading up to the point of the maximum previously attained stress. This will reduce the ratio of the unloading to loading modulus to values approaching unity. More tests are needed to obtain these values.
4. Central gaps in the mortar joint will cause an incorrect experimental value for the brickwork compression modulus if this is based on the full cross-section.
5. Substituting an equivalent hollow wall with an increased compression modulus gives good results for both axial and flexural strains when compared with the theoretical results obtained from an analysis of a wall with gaps in the mortar joint only.

CHAPTER 4 - THE RELATION BETWEEN THE EXPERIMENTAL STRAINS IN THE WALL AND THE APPLIED SLAB FORCES

4.1 INTRODUCTION

The experimental stress-strain behaviour of brickwork under axial load was shown in Chapter 3. The results are used to explain the behaviour of precompressed brickwork subjected to bending moment.

Nine brick wall - floor models as described in Chapter 2 were tested. The walls were precompressed to given loads and then the free end of the slab was loaded, superimposing a bending moment in both wall sections and an increasing axial load in one wall section. The vertical strains due to slab loading were measured in the walls above and below the slab. The strains were used to predict the applied slab loading. Simple bending theory, assuming a solid cross-section and an experimental compression modulus, underestimated the applied moment while the slab load was either correctly predicted or overestimated. The result for moment was surprising since the predicted moment if different from the applied moment would be expected to be larger because of possible stress concentrations near the joint inducing larger strains.

Two possible reasons are suggested for this :

1. Gaps along the centre line of the mortar joints due to unfilled frogs and furrowing of the mortar. This causes an underestimation of the experimental compression modulus if based on a solid cross-section (section 3.4).
2. An unloading modulus (decreasing stress) different from the loading modulus (increasing stress).

The effect of the two factors on the flexural behaviour of brickwork is investigated.

4.2 EXPERIMENTAL STRAIN RESULTS

Vertical strain readings were obtained on opposite faces of the walls above and below the slab. Figures 4.1 to 4.3 show the strains resulting from the increasing moment and load due to the slab, starting from the three initial precompressions for the three types of wall tested.

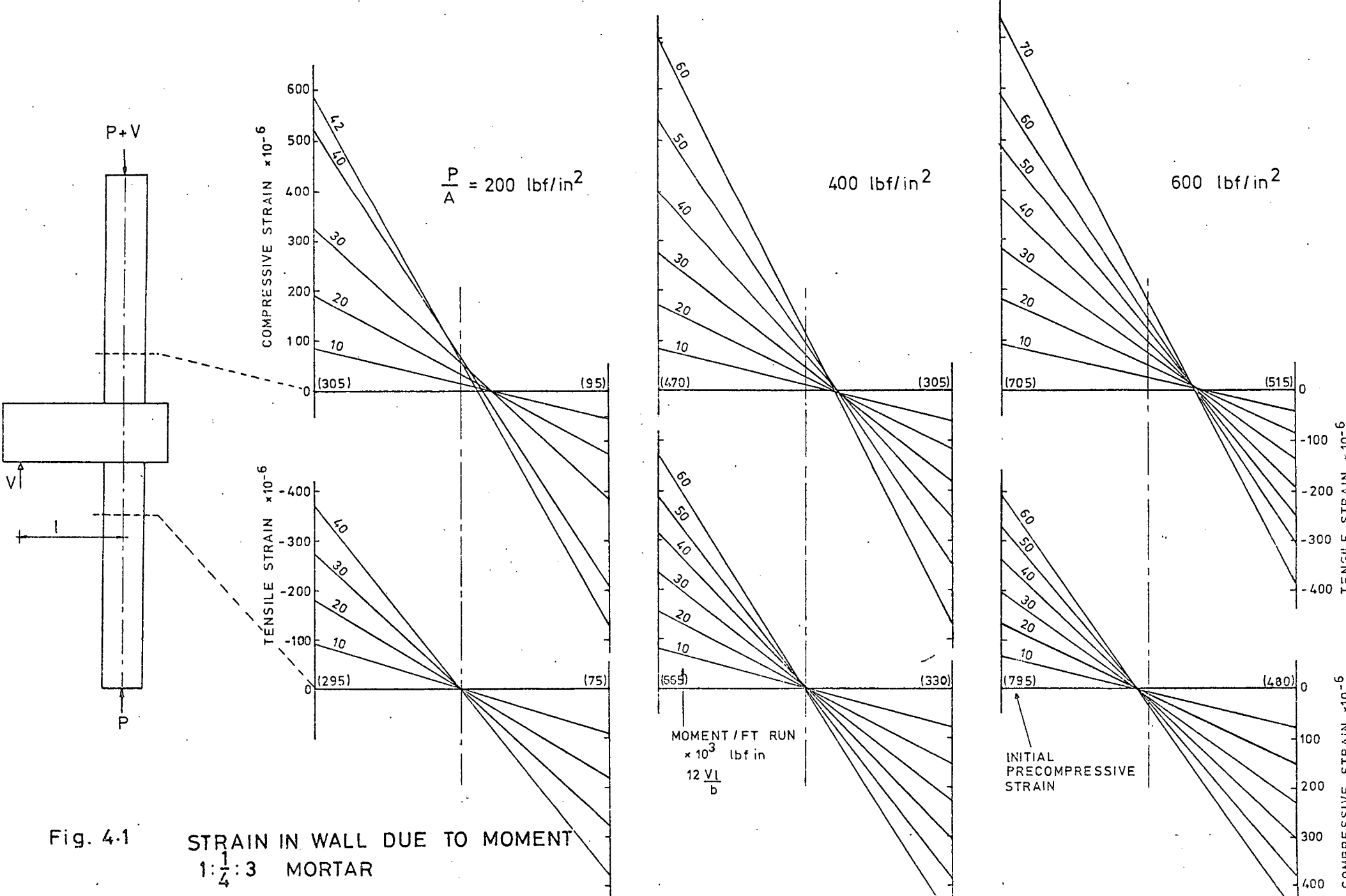
The strain planes have a common point of intersection and provide an experimental basis for the assumption that a cross-section remains plane under flexural deformation. Haller (17) had come to this conclusion after testing a series of brick piers under vertical load at various eccentricities (fig 4.4).

The position of the intersection of the strain planes is determined by the applied load eccentricity, the stress-strain relationship (loading and unloading), tensile cracking in the cross-section and to a lesser extent any effective gaps in the wall. If these factors remain constant, the intersection point will be in a fixed position.

In eccentrically loaded walls - increasing moment with increasing load - the position of the strain plane intersection point is determined by the load eccentricity, tensile cracks and the loading stress-strain curve. In Haller's tests* (17), assuming a linear stress-strain curve and no tensile strength, the load eccentricity is predicted quite accurately by the intersection point of the strain planes (fig 4.4). The predicted eccentricities are slightly larger than the applied eccentricities. The difference can be reduced by taking the experimental stress-strain curve and the lateral deflection of the pier into account.

In tests described in this thesis the slab moment to slab load ratio is a constant in all the experiments - thus constant load eccentricity for the strains due to slab forces. The eccentricity of the existing axial wall load increases with increase in slab moment. There is a major difference between these results and those of Haller - the moment is applied after the wall has been loaded. The effect of the unloading stress-strain relationship must be taken into account. Thus loading history is important.

* In this reference, the figure illustrating the strain planes contains incorrect values for the eccentricity due to elastic strains (compare to ref. 16). In both references one of the eccentricities due to total strain is incorrect.



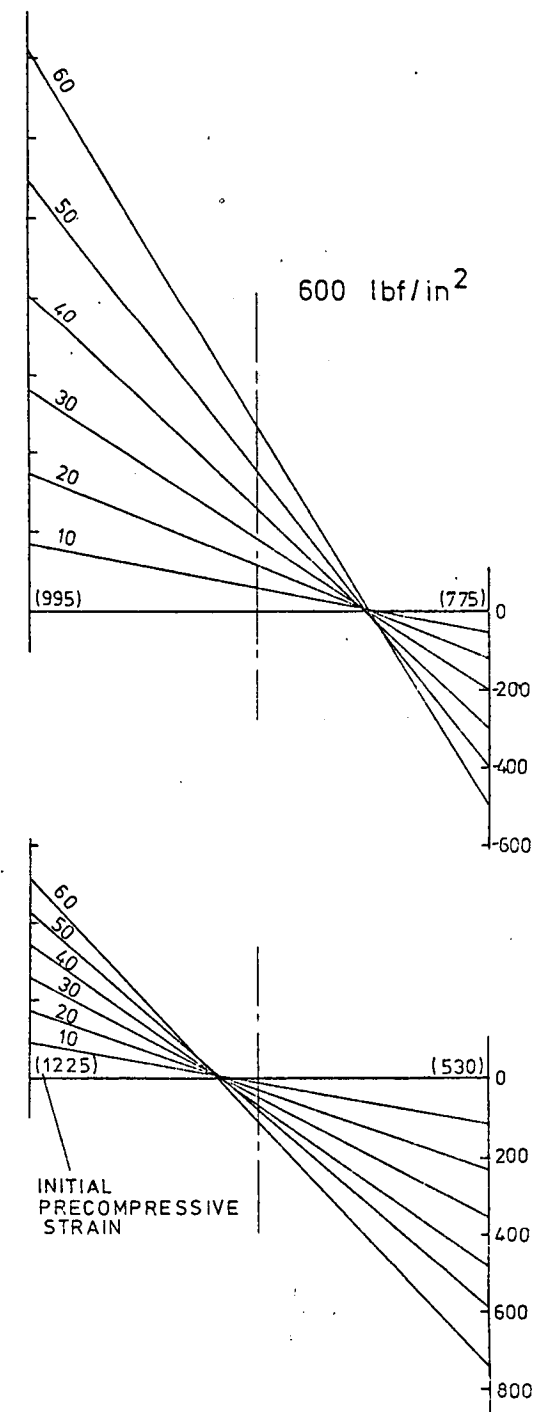
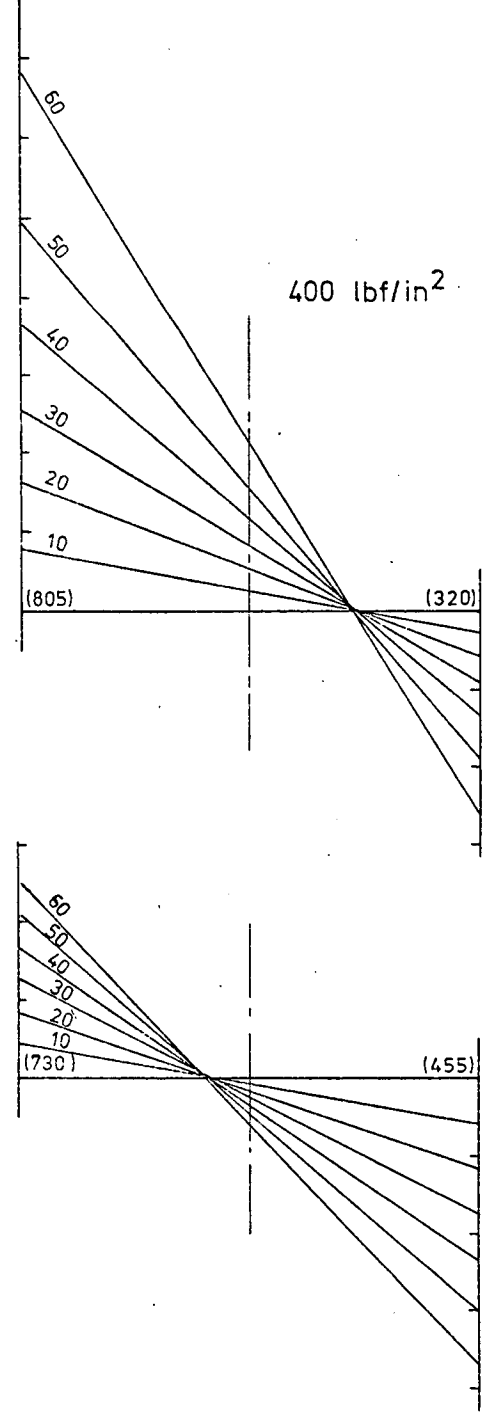
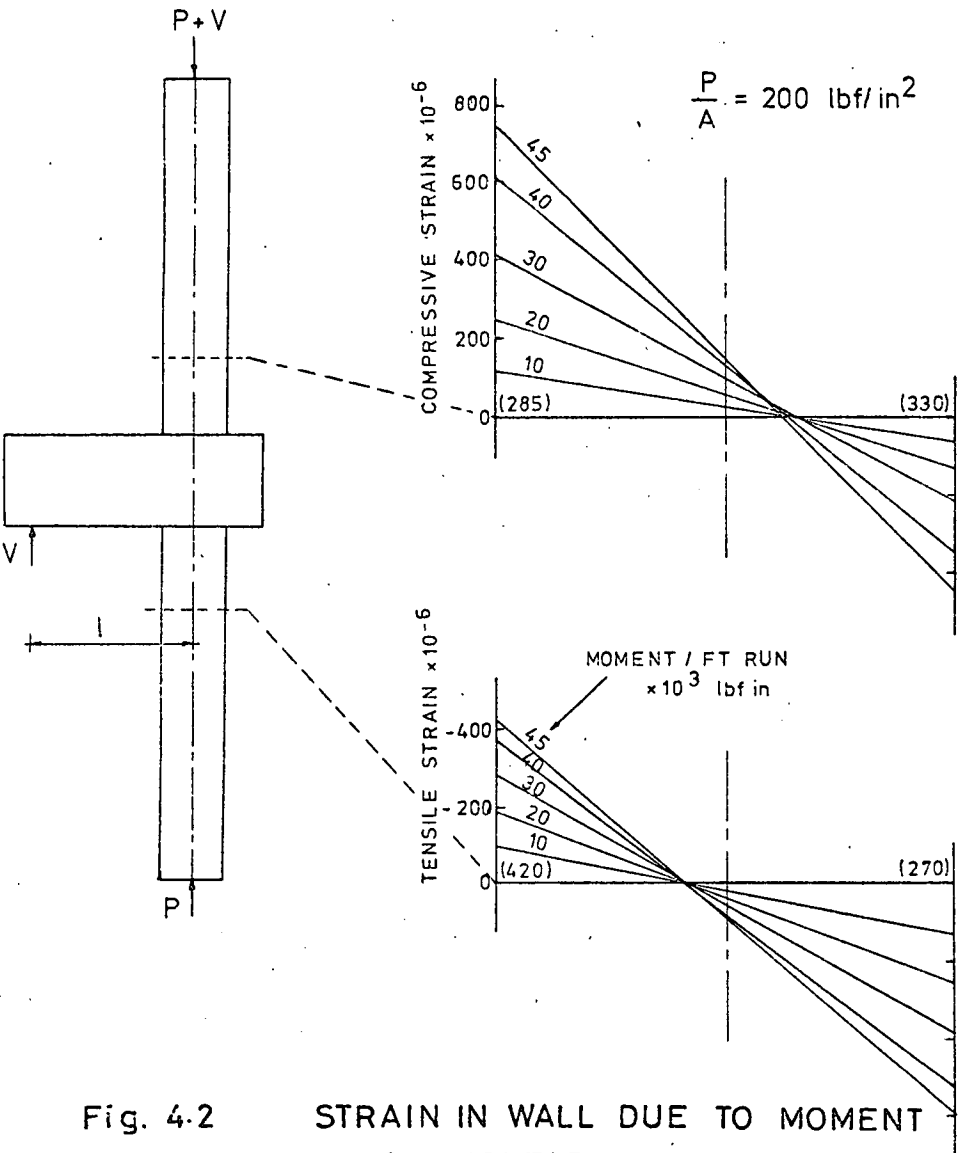


Fig. 4.2 STRAIN IN WALL DUE TO MOMENT
1:1:6 MORTAR

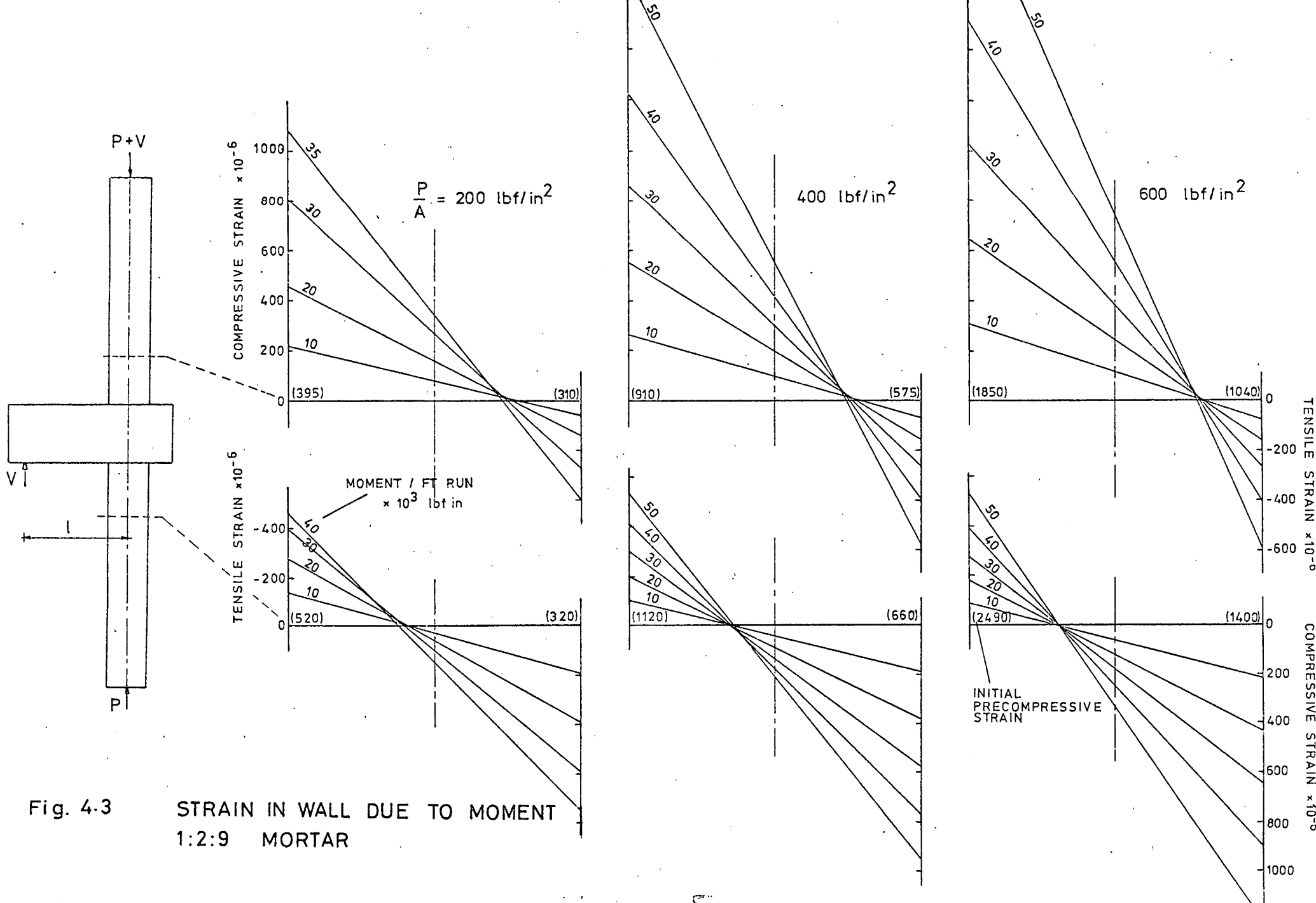
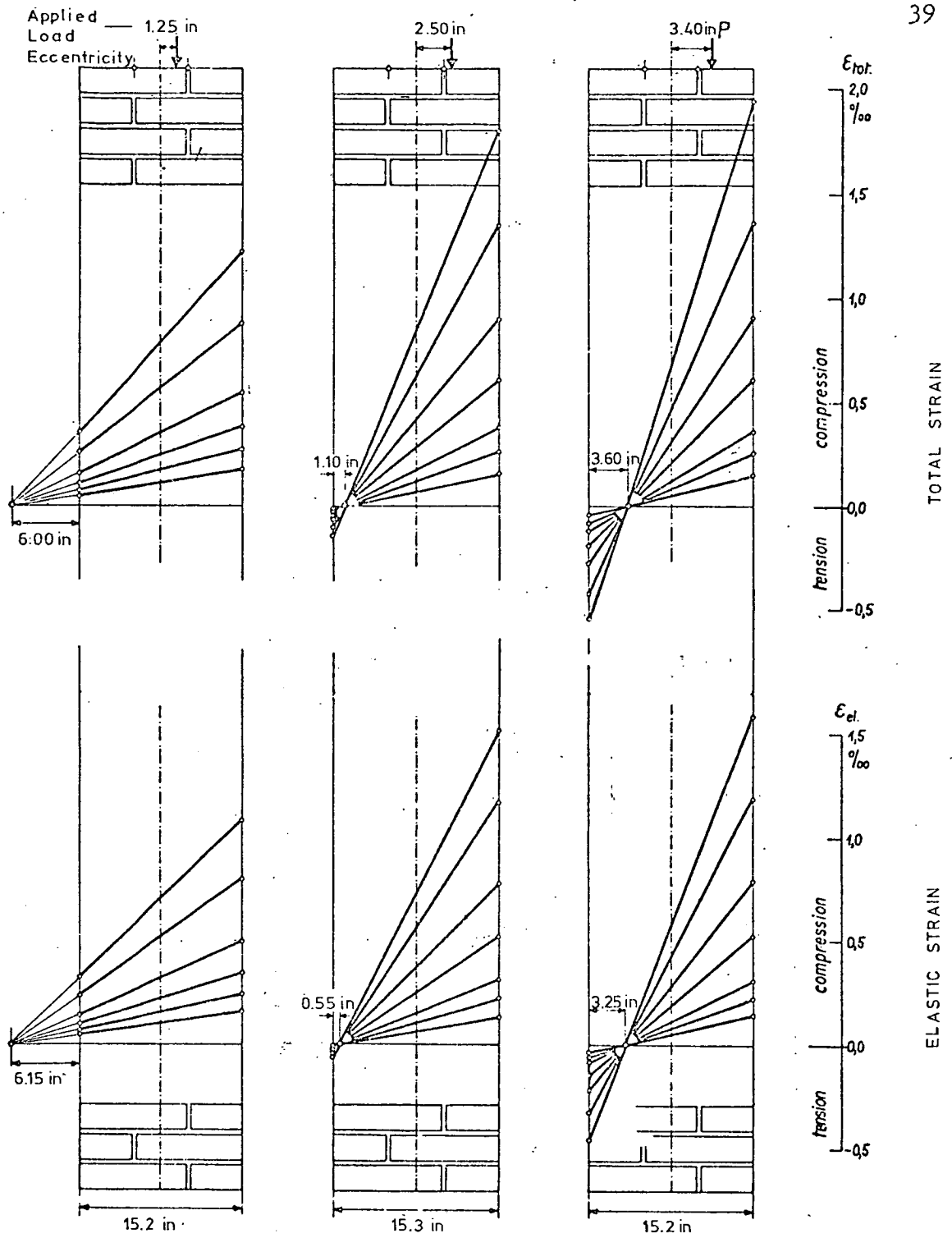


Fig. 4-3 STRAIN IN WALL DUE TO MOMENT
 1:2:9 MORTAR



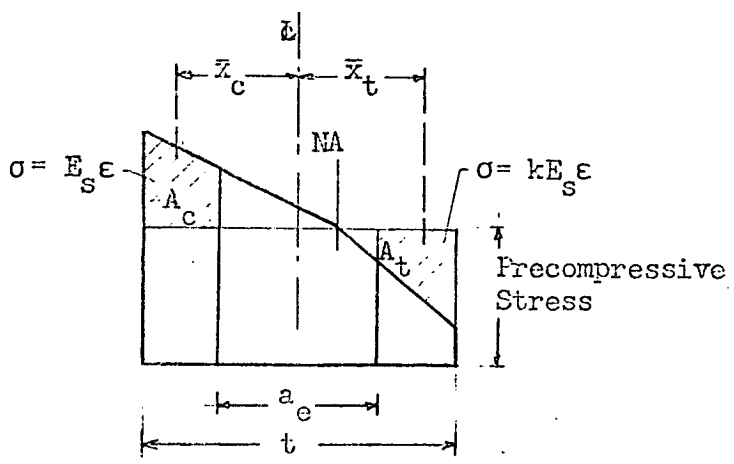
Predicted Eccentricity of the Load from :

Total Strain	1.40 in	2.90 in	3.80 in
Elastic Strain	1.40 in	2.75 in	3.60 in

Figure 4.4 Strain Planes in 11 ft 2 in high Brick Piers with Knife Edge Supports (by Haller, Ref. 17)

4.3 LINEAR STRESS-STRAIN ANALYSIS

A linear stress-strain theory, developed in Appendix 4, takes into account the effects of a gap in the mortar joint and a differing loading from unloading modulus. The basic parameters are illustrated in the following sketch showing a typical stress distribution :



$$\text{Moment} = \bar{x}_c A_c + \bar{x}_t A_t$$

$$\begin{aligned} \text{Increase in Axial Load} \\ = A_c - A_t \end{aligned}$$

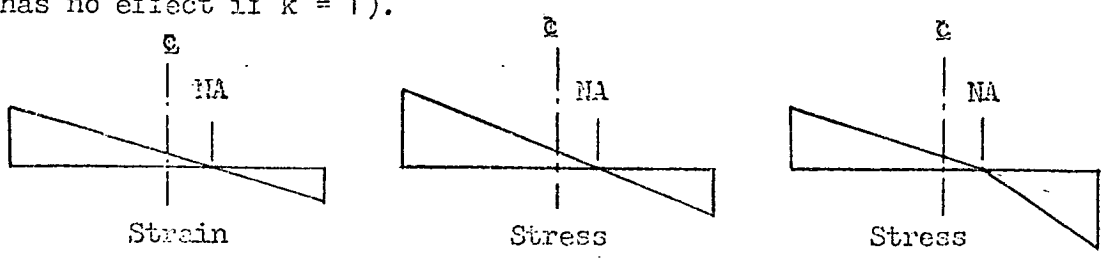
k = ratio of unloading to loading modulus

a_e = effective gap

The effects of the ratio of the unloading to the loading modulus, k , and the gap in the mortar joint represented by an effective gap, a_e , are illustrated graphically.

Figure 4.6 shows, for a wall subjected to a pure bending moment, that a visible effect of k on the stress diagram is the displacement of the neutral axis from the centre line of the wall. This is shown for all values of a_e (section A4.4.1, part 4).

This displacement could also be due to an increasing axial load. When axial load is present and $k > 1$, one of the difficulties in experimental analysis is differentiating the effects of the two. In figure 4.7 the effect of changing the value of k , by an amount Δk , on the magnitude of the axial load is shown (section A4.4.2). The effect is greatest when the neutral axis is displaced a small amount. Varying k has a greater effect on the magnitude of the axial load than varying a_e (a_e has no effect if $k = 1$).



Displacement of the neutral axis due to :
Increasing Axial Load $k > 1$

Figure 4.5 shows the effect of k on the magnitude of the moment for various values of a_e (section A4.4.1). Here as opposed to the axial load, the effect of changing a_e is greater than that of changing k especially with higher values of k . The graph shows the ratio of the moment for a given value of k and a_e to the moment for a solid section with $k = 1$ (in both cases the same value of flexural compressive strain, ϵ_c).

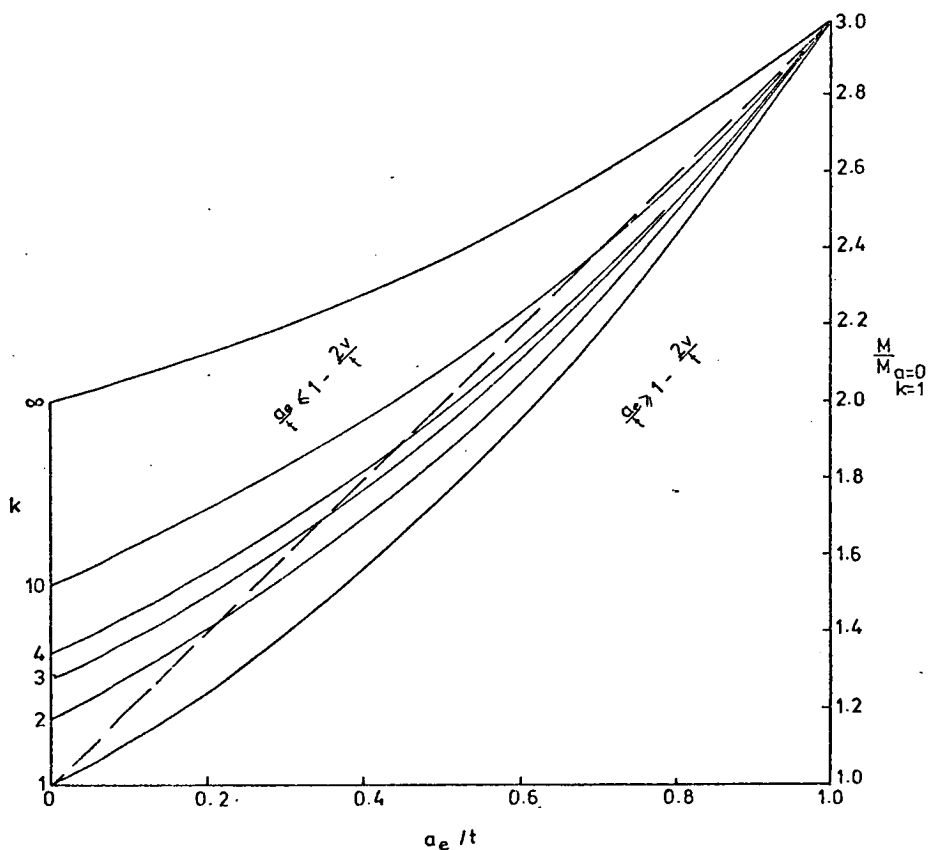


Fig. 4.5 Effect of k and a_e on moment predicted from strains

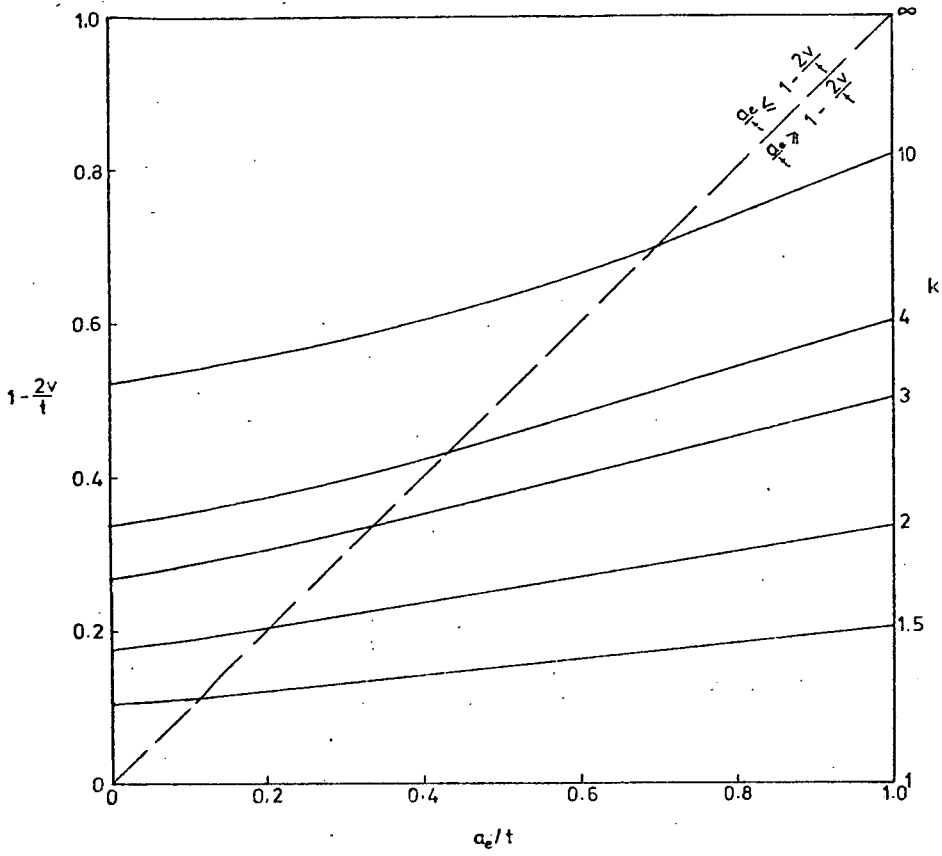


Fig. 4.6 Effect of k and a_e on the position of the neutral axis

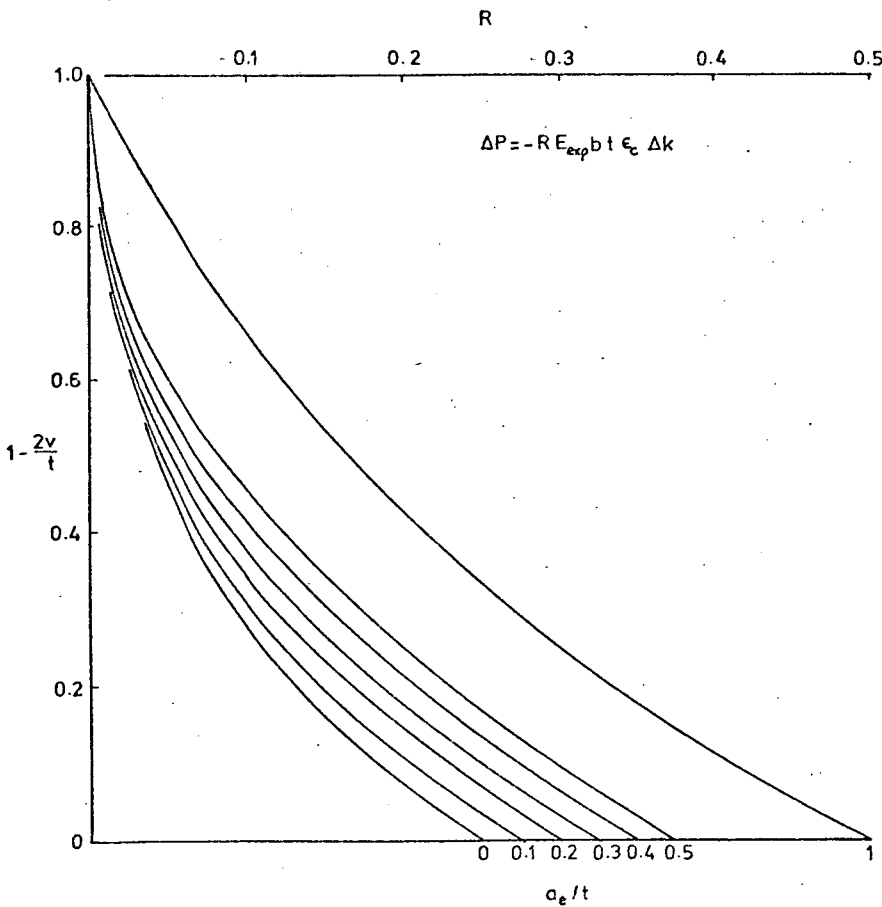
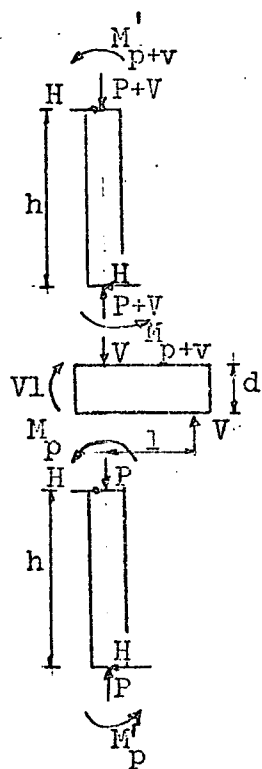


Fig. 4.7 Effect of a change in k on axial load predicted from strains

4.4 CORRELATION BETWEEN THE EXPERIMENTAL STRAINS AND THE APPLIED SLAB MOMENT AND LOAD USING THE LINEAR STRESS-STRAIN THEORY

4.4.1 Forces Acting on the Experimental Model

The following sketch shows the forces acting on the wall-floor test model (section 6.2 does this in detail).



$$M_s = Vl$$

$$H = \frac{M'_p + M'_{p+v} + Vl}{2h + d}$$

If the ends of the wall are fully fixed :

$$M'_p = M_p/2$$

$$M'_{p+v} = M_{p+v}/2$$

If hinged :

$$M'_p = M'_{p+v} = 0$$

The top and bottom of the model are partially fixed. The possible range of moment along the wall is shown in the sketch below. Strain results show that the end restraining moments are very approximately 20% of the full fixing moment (section 5.4). That amount of fixity does not affect the moment much at the position where strain was measured.

full

fixity

hinge

$$\frac{M_{p+v}}{2}$$

Range of moment at the centre line
of the 8 inch strain gauge :

$$0.56M - 0.69M$$

5 in

$$M_{p+v}$$

$M (= M_s/2$ if the top and bottom
walls have the same properties)

4.4.2 Constants needed for the Linear Theory

To use the linear theory, values of k , a_e and E_{exp} have to be found for each test model.

1. Ratio of the Unloading to the Loading Modulus, k

Assuming there is no change in axial load due to slab forces in the lower wall section of the test models (only a moment is applied), any displacement of the point of intersection of the strain planes from the centre line of the wall is assumed to be caused by the differing moduli under increasing and decreasing load. Knowing the displacement, the ratio of the unloading to the loading modulus, k , can be found using equation 4.1 (Table 4.1).

$$k = \frac{1 + a_e/t + 4(0.5 - v/t)}{1 + a_e/t - 4(0.5 - v/t)} \quad \text{--- (4.1)}$$

$$a_e/t \geq 1 - 2v/t$$

$t(0.5 - v/t)$ = displacement from the centre line of the wall.

Derivation in section A4.3 .

TABLE 4.1 - RATIO OF THE UNLOADING TO THE LOADING MODULUS FROM EXPERIMENTAL STRAINS

Precompressive Stress lb/in ²	Type of Brickwork					
	1:2:9 Mortar		1:1:6 Mortar		1:1/4:3 Mortar	
	0.5t - v in	k	0.5t - v in	k	0.5t - v in	k
200	0.41	1.8 (1.8)	0.34	1.6 (1.4)	0	1.0 (-)
400	0.62	2.6 (2.7)	0.34	1.6 (2.3)	-0.07	0.9 (-)
600	0.82	3.8 (5.0)	0.41	1.8 (3.3)	0.21	1.4 (1.4)

- Notes :
1. Displacement v taken from figures 4.1 to 4.3
 2. $t = 4.12$ in
 3. In calculations k taken to be ≥ 1
 4. In brackets are the values (some interpolated) obtained from the tests on axially loaded walls (Table 3.2)
 5. Values of a_e 1:2:9 = 1.5 in ; 1:1:6 = 1.5 in ; 1:1/4:3 = 1.2 in

2. Values of Effective Gap Width - a_e

The 1: $\frac{1}{4}$:3 mortar walls at precompressions of 200 and 400 lbf/in² are assumed to have values of $k = 1$ since their strain planes in the wall subjected to moment only, pass through the centre line of the wall (fig 4.1). Using the results for the 400 lbf/in² test, a value of a_e was chosen to give results for moment equivalent to those in a model with hinged ends. This value of a_e was used to obtain values for the other walls.

The experimental value of a_e was 1.2 inches ($a_e/t = 0.3$). From figure 3.12, the actual gap width of the mortar joint is 1.9 inches. Taking this value, values of a_e for the other walls are obtained from figure 3.12 - dependent on the ratio of the brick to mortar modulus. The results are given in Table 4.2 .

3. Values of the Experimental Compression Modulus, E_{exp}

The values for the moduli are obtained from the stress-strain relationships of the wall sections obtained when loaded to their set precompression.

These can be determined fairly accurately for the 1: $\frac{1}{4}$:3 mortar walls - a linear stress-strain curve over the precompressions tested.

So that the linear theory could be applied to the 1:1:6 and 1:2:9 mortar walls, both having non-linear curves, the tangent modulus at the set precompression is used. The estimation here is more approximate than the 1: $\frac{1}{4}$:3 mortar walls. As the weaker walls vary more in their properties, using strains to predict moments and loads can only be used with any accuracy if the experimental stress-strain curve is known.

4.4.3 Results

1. Moment Predicted from Strains

Table 4.2 gives predicted moments in the upper and lower wall sections and compares their sum to the applied moment assuming a moment distribution based on walls with one end hinged. Figure 4.8 shows the results graphically for the 1: $\frac{1}{4}$:3 mortar walls and compares them to the results obtained assuming a solid section with $k = 1$.

The overall results are good. For the weaker walls, the compression moduli are estimated to the nearest 50×10^3 lbf/in² from their individual stress-strain curves at the point of the set precompression. Thus

the possible error increases with decreasing modulus explaining the increasing variation with the weaker walls and the low result for the 1:2:9 mortar wall at 600 lbf/in^2 precompression. See also the discussion in Chapter 5 on lateral deflection (section 5.5).

The values of k are based on the bottom wall and assumed to be the same for the top wall - another source of error. In addition the gap in the mortar joint is assumed to be constant.

The weaker walls show increasing difference between predicted and applied moment with increasing moment - probably due to a decreasing tangent modulus.

The $1:\frac{1}{2}:3$ mortar walls give good results (to be expected for the 400 lbf/in^2 wall) except for the 200 lbf/in^2 wall. The large difference at higher moments may be explained by tensile cracking which will occur at approximately a slab moment of $30 \times 10^3 \text{ lbf in/ft}$ (Table 4.4). A possibility at lower moments is an incorrect modulus for the wall, the modulus based on a curve extending to only 200 lbf/in^2 .

2. Increasing Axial Load Predicted from Strains

Table 4.3 gives the predicted increasing axial load in the wall section with increasing precompression. Figure 4.8 shows the results graphically for the $1:\frac{1}{2}:3$ mortar walls and compares them to the results obtained assuming a solid wall with $k = 1$.

The increasing axial load should be equivalent to the increase in slab jacking load. The only accurate results are those for the $1:\frac{1}{2}:3$ mortar walls which have a linear stress-strain curve. The 1:2:9 mortar wall at 600 lbf/in^2 precompression gives good results too but this may be more luck when compared to the other results.

Apart from the latter result, the results for the 1:1:6 and 1:2:9 mortar walls are far out in magnitude but not in proportion (i.e. twice the jacking load produces approximately twice the predicted load). Changing the value of k would correct most of the results without affecting the moment results very much. The necessary changes in k range from 0.5 to 1.5 .

3. Conclusions

The experimental results were carefully analysed - curves for strain versus moment were drawn through the experimental points to get better estimates and spot obvious errors including zero errors.

The results cannot be improved very much as they depend on too many variables. Many more tests are needed to evaluate the effect of these variables.

With an increasing number of tests better average results will be obtained but nevertheless it will always be difficult to apply these to individual walls except for the 1:1/4:3 mortar walls which can be expected to give consistent results.

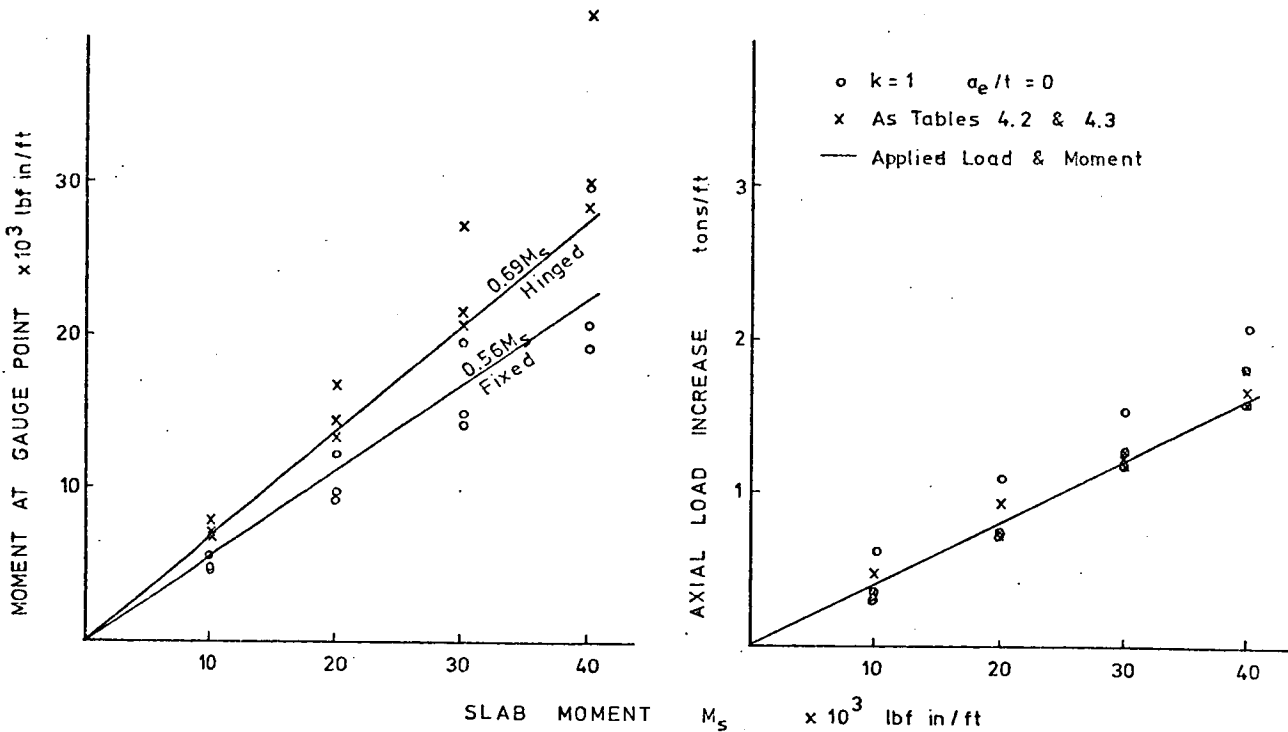


Figure 4.8 Moment and Axial Load Predicted from Experimental Strains
 - 1:1/4:3 mortar Test Models

TABLE 4.2 - MOMENT PREDICTED FROM EXPERIMENTAL STRAIN RESULTS

Precompression 200					400			600 lbf/in ²			Notes
M _s	0.69M _s	M _{p+v}	M _p	$\frac{M_t}{0.69M_s}$	M _{p+v}	M _p	$\frac{M_t}{0.69M_s}$	M _{p+v}	M _p	$\frac{M_t}{0.69M_s}$	
1:¼:3 mortar											
10	6.9	3.5	4.4	1.14	3.6	3.1	0.97	3.4	3.8	1.04	a/t = 0.45
20	13.8	7.8	8.9	1.21	7.2	6.1	0.96	6.9	7.5	1.04	1:¼:3
30	20.7	13.4	13.6	1.30	11.5	9.1	1.00	10.8	11.3	1.04	a _e /t = 0.30
40	27.6	22.6	18.4	1.48	16.4	12.1	1.03	15.0	15.0	1.09	1:1:6 &
E _{exp}		1.06	1.06		1.07	0.85		1.0	0.96		1:2:9
k		1	1		1	1		1.4	1.4		a _e /t = 0.37
t/2 - v		0.41	0		0.41	0		0.62	0.21		M _t = M _{p+v} + M _p
1:1:6 mortar											Units :
10	6.9	3.3	3.4	0.97	3.9	3.4	1.06	3.1	3.8	1.00	Moment
20	13.8	6.8	6.9	0.99	8.2	6.9	1.09	6.8	7.5	1.04	x10 ³ lbf in/ft
30	20.7	11.4	10.4	1.05	13.5	10.5	1.16	11.1	11.3	1.08	t/2 - v
40	27.6	17.5	13.9	1.14	18.4	13.9	1.17	16.3	15.0	1.13	inch
E _{exp}		0.6	0.5		0.65	0.55		0.5	0.55		E _{exp}
k		1.6	1.6		1.6	1.6		1.8	1.8		x10 ⁶ lbf/in ²
t/2 - v		0.62	0.34		0.96	0.34		0.96	0.41		
1:2:9 mortar											
10	6.9	3.4	3.8	1.04	4.0	3.7	1.12	2.5	2.3	0.70	
20	13.8	7.8	7.6	1.12	8.8	7.5	1.18	5.4	4.9	0.75	
30	20.7	14.1	11.3	1.23	14.4	11.4	1.25	8.8	7.6	0.79	
40	27.6				21.0	15.5	1.32	13.3	10.6	0.87	
E _{exp}		0.45	0.35		0.40	0.35		0.20	0.20		
k		1.8	1.8		2.6	2.6		3.8	3.8		
t/2 - v		0.96	0.41		1.03	0.62		1.17	0.82		

Note : The sum of the moments at gauge points in terms of slab moment should be $0.69M_s$ if the far ends of the walls are hinged
 $0.56M_s$ if the far ends of the walls are fixed

TABLE 4.3 - AXIAL LOAD INCREASE PREDICTED BY EXPERIMENTAL STRAINS

Precompression		200		400		600 lbf/in ²	
M_s $\times 10^3$ lbf in/ft	V tonf	V_{p+v} tonf	V_{p+v}/V	V_{p+v} tonf	V_{p+v}/V	V_{p+v} tonf	V_{p+v}/V
<u>1:1/2:3</u> mortar							
10	0.41	0.35	0.86	0.30	0.72	0.48	1.17
20	0.81	0.76	0.94	0.71	0.87	0.94	1.16
30	1.22	1.29	1.05	1.18	0.97	1.25	1.02
40	1.63	1.58	0.97	1.83	1.12	1.68	1.03
<u>1:1:6</u> mortar							
10	0.41	0.19	0.46	0.66	1.60	0.58	1.42
20	0.81	0.48	0.59	1.34	1.65	1.05	1.30
30	1.22	0.78	0.64	1.99	1.64	1.62	1.33
40	1.63	0.93	0.57	2.89	1.77	2.25	1.38
<u>1:2:9</u> mortar							
10	0.41*	0.66	1.83	0.67	1.64	0.38	0.92
20	0.81	1.32	1.86	1.32	1.63	0.77	0.95
30	1.22	2.26	2.11	1.88	1.54	1.13	0.92
40	1.63			2.47	1.51	1.60	0.98
<p>Notes : M_s is the applied slab moment $a/t = 0.45$ (other values see Table 4.2) *for the 1:2:9 mortar test model at 200 lbf/in² precompression, the values of V are reduced by 10%. V applied slab load V_{p+v} load obtained from strains</p>							

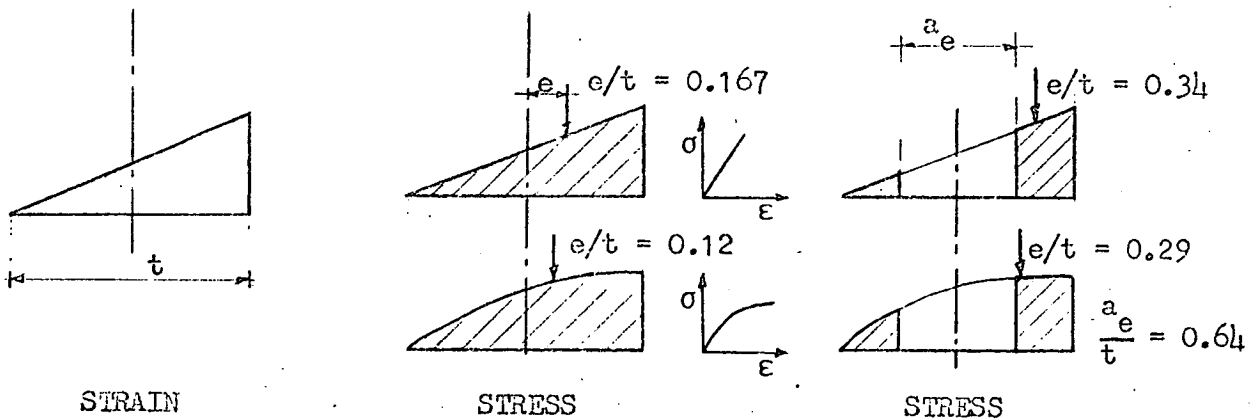
4.5 TENSION IN BRICKWORK

4.5.1 Eccentricity Causing Zero Stress on One Face of the Wall

When tensile strains occur, brickwork is assumed to take no tensile stresses although it has resisted stresses up to 135 lbf/in^2 in laboratory tests (34)*.

The point at which the strains become tensile is thus of interest. This is usually taken to occur when the load eccentricity exceeds one sixth of the wall thickness. This value is based on the assumption that the stress-strain relation is linear and the cross-section is solid and rectangular.

A rectangular cross-section with a central gap increases the eccentricity necessary to cause tension while a non-linear stress-strain relation (reducing tangent modulus) reduces the eccentricity. This is illustrated in the following sketches based on results from Chapter 6.



Section A4.6 in the Appendix gives the basic theory for walls with a linear stress-strain relation, a gap in the centre and an unloading modulus greater than the loading modulus. The results are shown graphically in figure 4.9 .

* Six brick high, two brick length wallettes were eccentrically loaded (10 in from centre line of wall - top and bottom). Using one brick ($11\,770 \text{ lbf/in}^2$ compressive strength, $10.6 \text{ g/min}/30 \text{ in}^2$ suction rate), mortars similar to those in this thesis were tested - 1:2:9, 1:1:6 and $1:\frac{1}{4}:3$ mixes giving flexural strengths of 85, 96 and 135 lbf/in^2 respectively (average of 5 samples).

4.5.2 Experimental Results

Tensile cracks develop in the mortar joints, the bricks being able to take considerably more tension.

The moment at which tension occurs is predicted using the linear theory and compared to the experimental results (Table 4.4).

The following values for effective gap and k (unloading/loading modulus) give an eccentricity of $0.23t$ necessary to cause tension (fig 4.9).

$$a_e/t = 0.30 \quad k = 1 \quad 1:\frac{1}{4}:3 \text{ mortar}$$

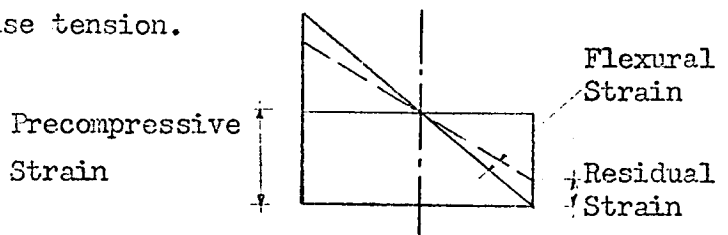
$$a_e/t = 0.37 \quad k = 2^* \quad 1:1:6 \text{ \& } 1:2:9 \text{ mortars}$$

The experimental strains were measured at two levels :

1. A 2 inch gauge length across the mortar joint between the slab and the first brick in the wall.
2. An 8 inch gauge length covering two mortar joints and brick (centre line 5 inches from the slab surface).

The necessary moment in terms of the applied slab moment for tension to occur at these points is given by slab moments equal to $2.3M_c$ and $2.9M_c$ respectively where moments larger than M_c cause tension (derived assuming the far ends of the wall are hinged - any fixity will increase the slab moment necessary to cause tension).

The experimental slab moments produce a flexural tensile strain equalling the average precompressive strain. The effect of permanent residual strains is also considered for the 8 inch gauge length - this reduces the moment necessary to cause tension.



The theory developed gives better results than the usual assumption of a solid section and a single modulus (values in brackets in Table 4.4).

*Here a linear unloading modulus depends on the residual strain at zero stress (see section A4.6, part 3).



TABLE 4.4 - SLAB MOMENT CAUSING TENSION IN THE WALL SUBJECTED TO MOMENT ONLY

Precompression: M_c lbf/in ²	M_c $\times 10^3$ lbf in/ft	Moment in terms of Applied Slab Moment $\times 10^3$ lbf in/ft				
		2 in gauge		8 in gauge		
		Theory	Exp. ¹	Theory	Exp. ¹	Exp. ²
200	9.5	22	22	27	21	-
	(6.8) ⁴	(16)	31	(20)	38	33
			-		34	25
400	18.5	42	45	54	60	-
	(13.6)	(31)	44	(39)	71	62
			60		73	60
600	28	64	69	81	96	93
	(20.4)	(47)	68	(59)	84	84
			-		70	70

Notes :

1. When the tensile strain exceeds the average precompressive strain for the 1: $\frac{1}{4}$:3, 1:1:6 & 1:2:9 mortar walls respectively.
2. Residual strain at zero stress taken into account using values from figures 3.4 to 3.6 .
3. $M_c = Pe$ where P = precompressive force/ft
 e = eccentricity at start of tension (0.23t)
4. Values in brackets for $e = 0.167t$ (solid section)

4.6 CONCLUSIONS

1. The relation between moment and the resulting flexural strains is affected by the following parameters :
 1. Stress-strain relationship - loading and unloading.
 2. Central gaps in the mortar joint.
2. The strain planes due to slab moment have a common point of intersection, large deviations only occurring when tensile cracks develop (figs 4.1 - 4.3).
3. A linear stress-strain theory is proposed taking into account an effective central gap in the wall and an unloading modulus different from the loading modulus. This gives better results for moment than for axial load and in both cases better results than those obtained by assuming a solid section with a single modulus. The method can be used with accuracy with the $1:\frac{1}{4}:3$ mortar walls having a linear stress-strain relationship over most of the stress range covered. Unless the stress-strain curve is known for the other walls there will be large variations between theory and experiment. With repeated slab loading the modulus for the latter walls will become approximately linear and thus may give better results.
4. The eccentricity at which tension occurs in the wall is increased due to the central gap in the mortar joints. Residual strains on unloading will decrease this eccentricity.

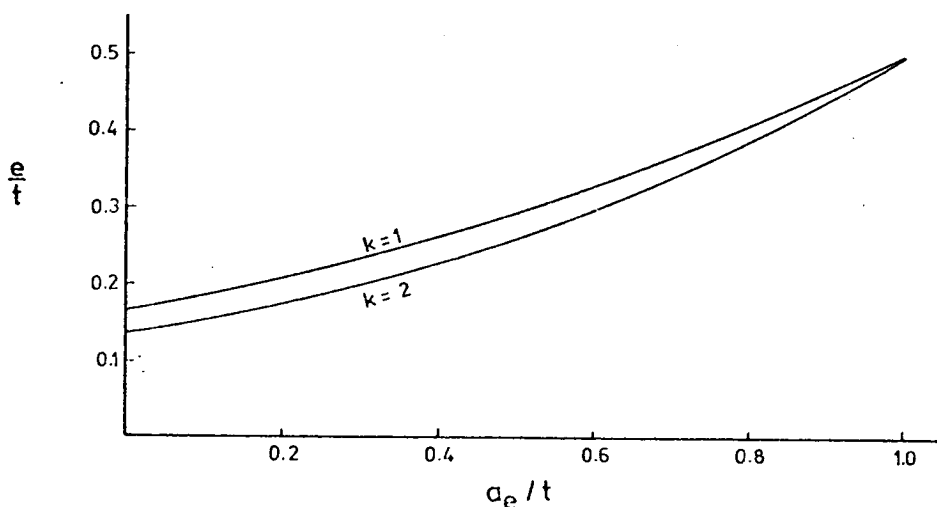


Figure 4.9 Eccentricity Causing Zero Stress on One Face of the Wall

CHAPTER 5 - FLOOR SLAB ROTATION AT ITS JUNCTION WITH THE WALL

5.1 INTRODUCTION

Two factors affecting floor slab rotation at its junction with the wall are the rigidity of the wall and the precompression in the wall. The factors are investigated experimentally and theoretically.

The rigidity of the wall is varied by changing the mortar in the brickwork thereby altering the elastic modulus.

The precompression mainly affects the point at which tensile cracking occurs in the wall while to a lesser degree it may also affect the elastic modulus of the wall if the precompressive stress falls within the non-linear range of the stress-strain curve. Three different precompressive stresses are compared - 200, 400 and 600 lbf/in². The precompressions are high, allowing larger applied slab moments and thus larger strains and rotations before tensile cracking occurs - the effect of precompression is then more clearly seen.

The theory concentrates on slab rotations before tensile cracking occurs giving values for the slope of the initial linear portion of the moment-rotation curve.

A final section discusses the lateral deflection of the walls and the slab.

5.2 FLOOR SLAB ROTATION

5.2.1 Results

In each test, load was applied to the slab thereby producing a moment at the joint. Slab rotation at the joint was measured at regular intervals, the resulting moment-rotation relationships shown in figures 5.1 to 5.3 .

5.2.2 Discussion

The relationship between moment and slab rotation has a definite pattern. There is an initial approximately linear portion which begins to decrease in slope as tensile cracking begins in the wall and rapidly decreases as the ultimate moment is reached. Non-linear stress-strain curves would cause a decrease in slope too, although more gradual than that due to cracking.

For a given strength of brickwork, the initial slope has a fairly constant value for the three precompressions considered. Thus low moments will produce similar rotations at all three precompressions - little effect on fixity. At higher moments curves will be non-linear, the point at which non-linearity occurs being mainly dependent on the precompression. Here, for a given moment, an increase in precompression will cause a decrease in rotation - an increase in fixity.

The slope of the linear portion of the curve decreases with decrease in brickwork strength. Taking values at a precompression of 200 lbf/in², the relative experimental values of rotation for a given moment over the linear portion of the curve are in the ratio of 1:1.2:2.2 for the 1: $\frac{1}{2}$:3, 1:1:6 and 1:2:9 mortar walls respectively.

Another effect for the 1:1:6 and 1:2:9 mortar walls, although not clearly shown, is a reduction in slope with increase in precompression. This is due to their non-linear stress-strain curve - increasing stress causes a decrease in modulus although this is partly offset by the effect of the unloading modulus which is little affected by the precompressive stress and may even slowly increase with increasing stress levels (fig 3.9).

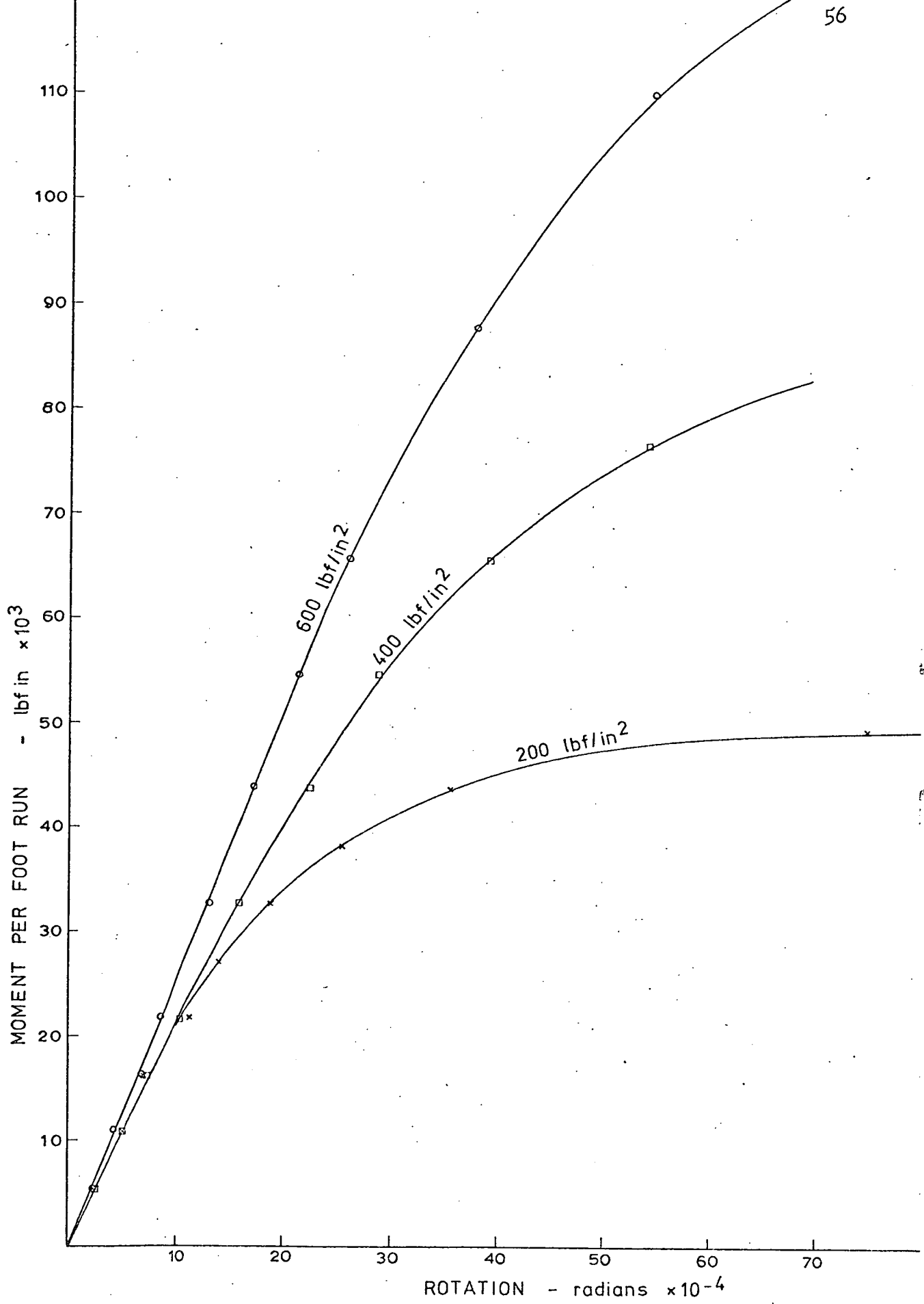


Fig. 5.1 MOMENT VS. SLAB ROTATION 1: $\frac{1}{4}$:3 MORTAR AT THREE PRECOMPRESSIONS

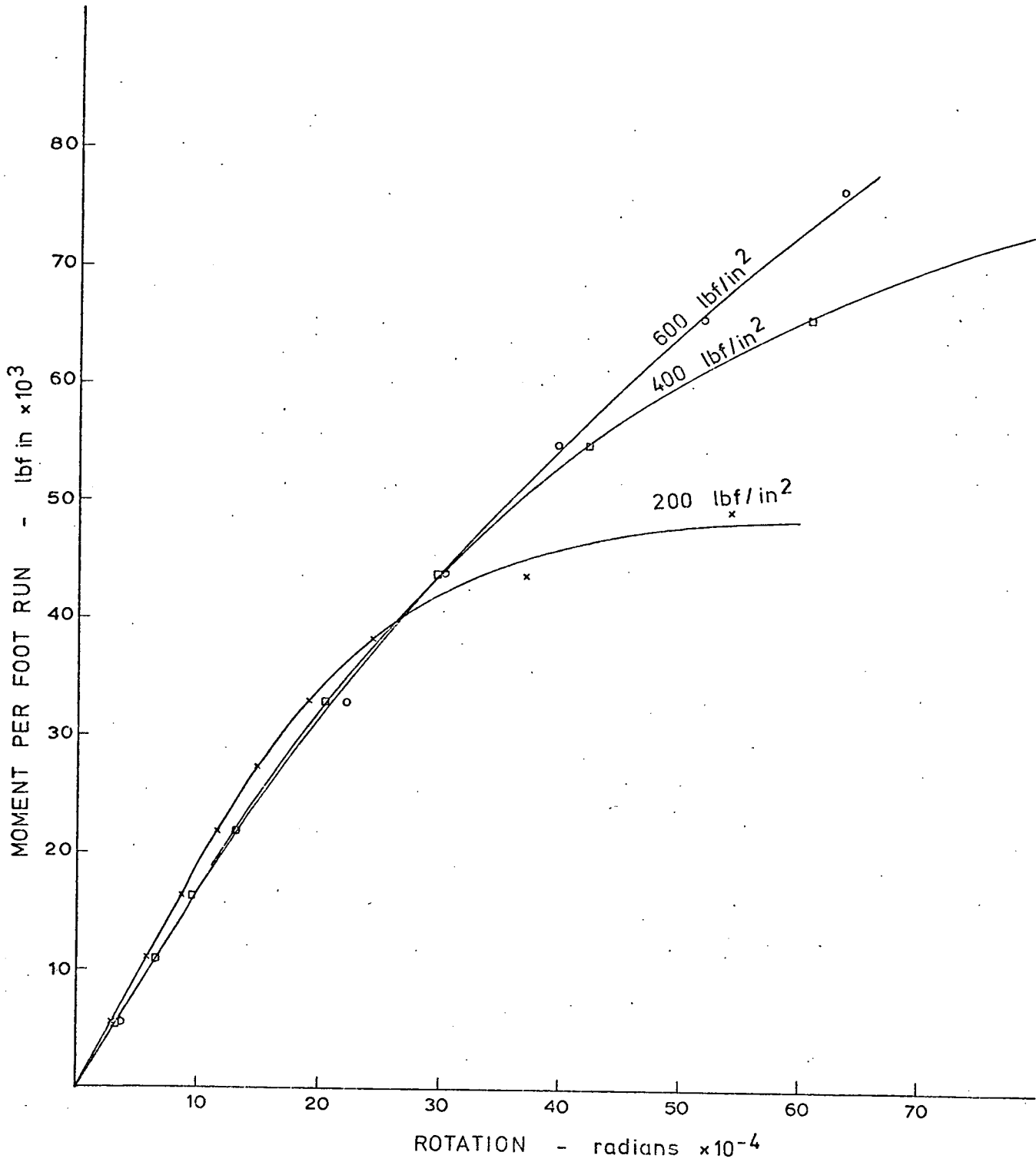


Fig. 5-2 MOMENT VS. SLAB ROTATION 1:1:6 MORTAR
AT THREE PRECOMPRESSIONS

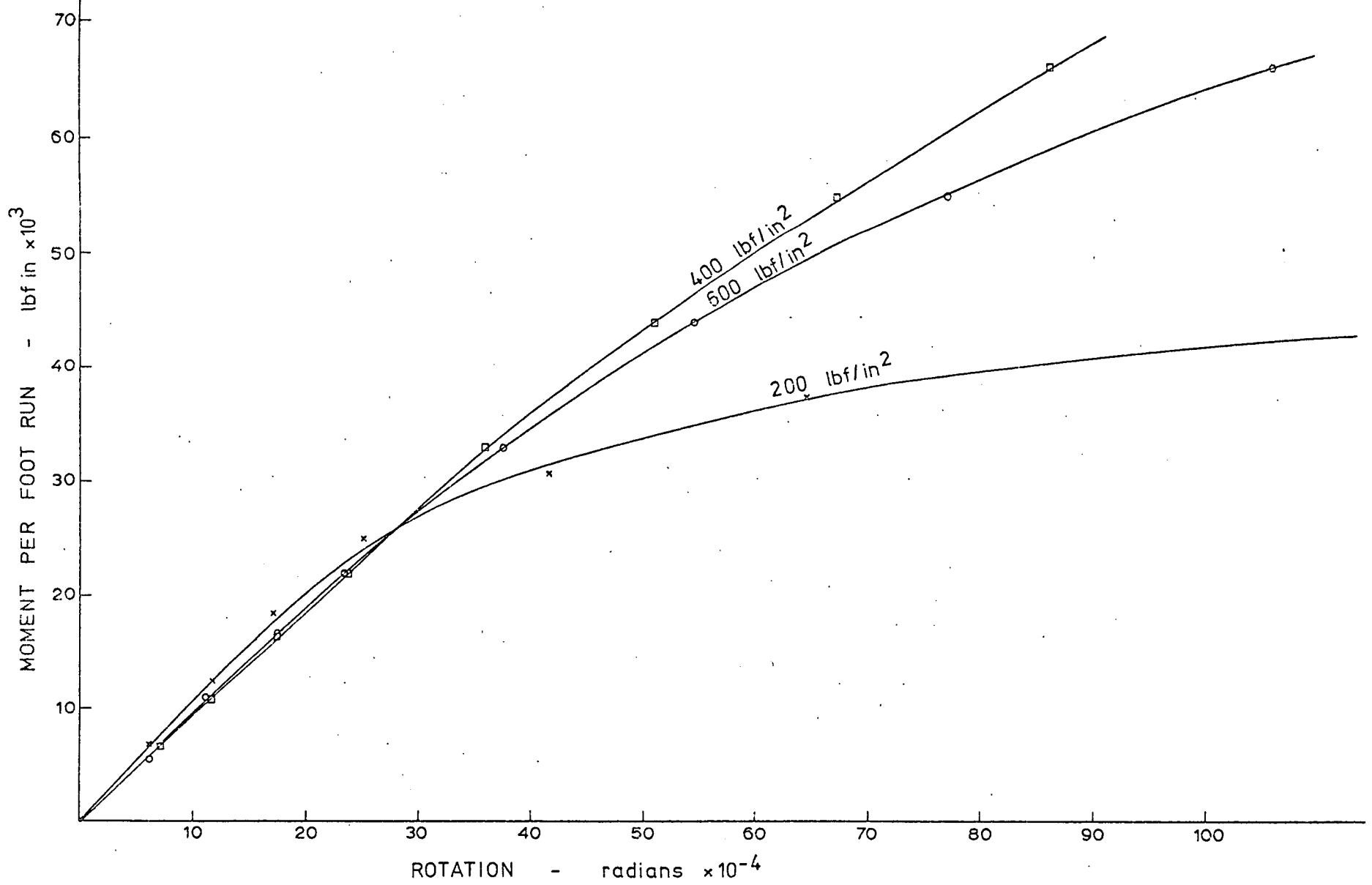
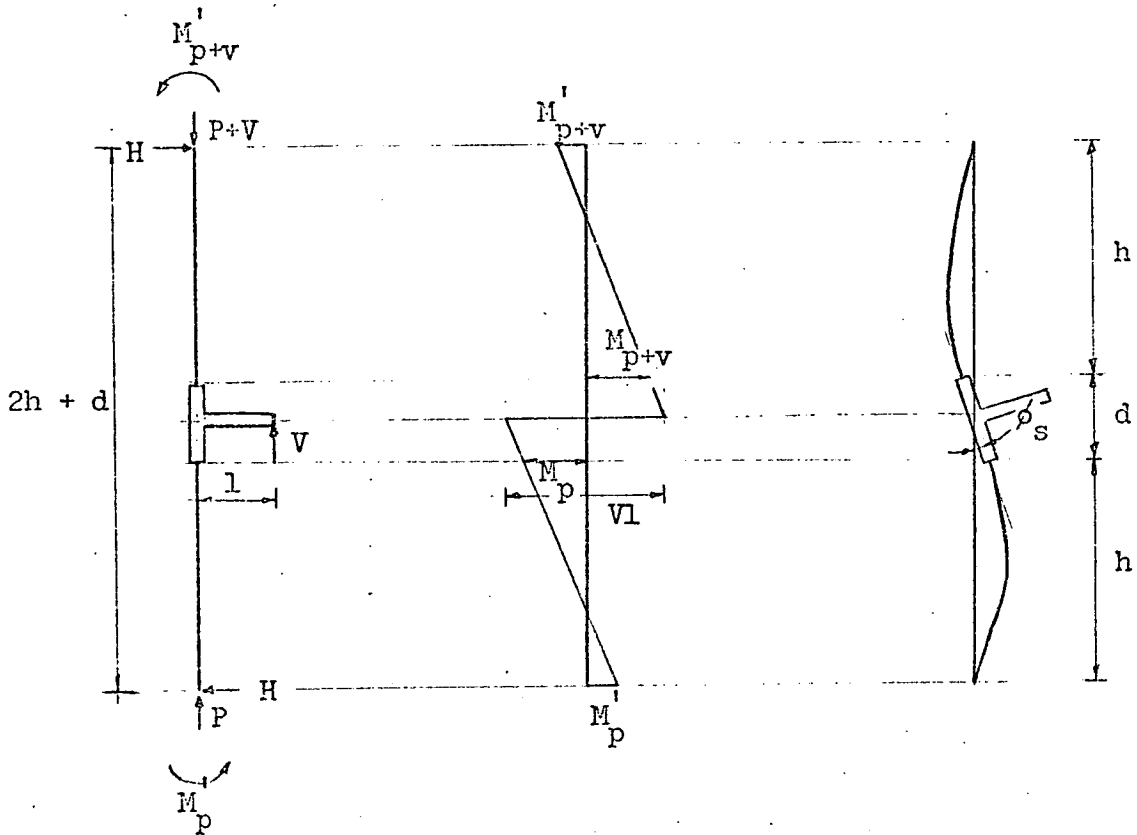


Fig. 5.3

MOMENT VS. SLAB ROTATION AT THREE PRECOMPRESSIONS 1:2:9 MORTAR

5.3 SLAB ROTATION IN A WALL WITH NO TENSILE CRACKS AND A LINEAR STRESS-STRAIN CURVE

5.3.1 Theory and Results



The initial part of the experimental moment-rotation relationship for the slab at the joint is linear. Tensile cracks in the walls do not develop until the latter part of this initial stage.

The angle of rotation at the ends of each wall at slab level are assumed to be the same - slab much stiffer than the wall. The angle of rotation at slab level is obtained using the equation shown (equation A5.7, Appendix 5) :

$$\phi_1 = \frac{2M_1 - M_2}{6} \frac{h}{EI} \quad \text{--- (5.1)}$$

where M_1 & M_2 are wall end moments
 h = height of the wall

The equation is then modified. One wall section is considered whose properties are the average of both sections. Thus moment from the slab is distributed equally to both walls. Assume the fixing moments are zero (this assumption is considered later - section 5.4).

Equation 5.1 becomes :

$$\phi_s = \frac{M_p h}{3E_{\text{exp}} I} \quad \text{--- (5.2)}$$

where $M_p = M_{p+v} = M_s/2.26$
 $M_s = V_l$
 $E_{\text{exp}} = \text{experimental compression modulus}$
 $I = bt^3/12$

In terms of slab moment equation 5.2 becomes :

$$\frac{\phi_s}{M_s} = \frac{h}{6.8E_{\text{exp}} I} \quad \text{--- (5.3)}$$

Equation 5.3 gives values of ϕ_s/M_s for a solid section with an unloading modulus equal to the loading modulus ($k = 1$). The results are shown in Table 5.1 .

The equation is next adjusted to take into account a wall with a central gap and a value of $k > 1$. Equation 5.3 becomes :

$$\frac{\phi_s}{M_s} = \frac{h}{6.8E_{\text{exp}} I} \frac{1}{M_{a_e, k} / M_{a_e=0, k=1}} \quad \text{--- (5.4)}$$

where values for the latter term are obtained from figure 4.5 for given values of a_e/t and k . Results are shown in Table 5.1 together with the experimental values.

5.3.2 Discussion

The theoretical values for rotation based on a solid section and a compressive tangent modulus overestimate the experimental results while values based on a gap in the joint and an unloading modulus in addition to the loading modulus underestimate the results. This underestimation may be due to several factors such as variations in assumed properties and local deformations in the mortar joints next to the slab.

Slab rotation after tensile cracking occurs is not investigated although Appendix 5 gives an equation (A5.10) for the rotation of a short, solid, linearly elastic wall with no tensile strength. A more thorough investigation will need to take into account walls with gaps in the joint, non-linear stress-strain curves, unloading curves different from the loading curve and a variable though small tensile strength. Test models will need lateral restraint at floor level and more accurately defined end conditions.

TABLE 5.1 - SLAB ROTATION AT ITS JUNCTION WITH THE WALL

Mortar Mix	Precompression lbf/in ²	E _{exp} x10 ⁶ lbf/in ²	k	a _e /t	$\frac{M}{M_{a=0, k^e=1}}$	$\frac{\phi_{s, exp}}{H_s}$	$\frac{\phi_s}{H_s}$ a=0 k ^e =1	$\frac{\phi_s}{H_s}$ a _e , k	$\frac{\phi_{s, a_e, k}}{\phi_{s, exp}}$
1:¼:3	200	1.06	1	0.30	1.38	43	46	33	0.77
	400	0.96	1	0.30	1.38	45	50	36	0.80
	600	0.98	1.4	0.30	1.46	38	49	34	0.90
1:1:6	200	0.55	1.6	0.37	1.6	52	88	55	1.06
	400	0.60	1.6	0.37	1.6	59	81	50	0.85
	600	0.58	1.8	0.37	1.6	60	83	52	0.87
1:2:9	200	0.40	1.8	0.37	1.6	95	121	75	0.79
	400	0.38	2.6	0.37	1.69	109	127	75	0.69
	600	0.20	3.8	0.37	1.76	105	242	137	1.30

- Notes :
1. For the 1:1:6 and 1:2:9 mortar walls, the compression modulus, based on 1 brick + 1 mortar joint, is about 6% less than E_{exp}, based on an 8 inch gauge length covering two mortar joints - thus theoretical values shown can be increased by 6%.
 2. The theoretical values of rotation are based on walls with their far ends hinged. An end fixity of 20% full fixity will reduce the ϕ values by 6%.
 3. E_{exp} is the average tangent modulus of the top and bottom walls at the given precompression (see Table 4.2 for individual values).

5.4 END FIXITY OF WALLS

The fixity at the far end of the walls is difficult to estimate. If fully fixed, the fixing moment will be one half the applied moment at the slab end of the wall.

Short walls with a resulting greater stiffness and smaller rotations will have less fixity for a given end condition. Yokel, Mathey and Dijkers (41) have found this to be so for eccentrically loaded concrete masonry walls with a flat ended condition.

To obtain an estimate of the fixity, rotation was measured in some cases at the top wall end but the few results are too erratic though they do show significant rotation.

Another approach is to measure the bending strains at two different levels and then to compare their ratio with the same ratio assuming a fully fixed or hinged joint. The sum of the bending strains (both positive) was taken to be proportional to the moment. Here again the results vary especially for the bottom wall (Table 5.2). From the results the end of the top wall has a fixity of approximately 20% full fixity while the bottom wall up to twice that amount although one result gives hardly any fixity. There is also a tendency for the fixity to increase with increasing moment (increasing rotation) - this increase can be marked if there are large lateral deflections (such as the 1:2:9 mortar wall at 200 lbf/in² precompression - see figure 5.5).

If a fixity of 20% full fixity is assumed, this would reduce the theoretical values of the rotation-moment ratio (ϕ_s/M_s) for a hinged end condition by 6%.

TABLE 5.2 - FIXITY AT THE FAR END OF THE WALLS

Slab Moment x10 ³ lbf in/ft	Percentage Full Fixity							
	Top Wall				Bottom Wall			
	1:2:9		1:1:6		1:2:9		1:1:6	
	200	400	200	400	200	400	200	400
10	4	22	0	22	30	33	0	7
20	15	22	14	22	30	48	0	7
30	22	22	43	19	44	56	0	7
40	-	26	64	22	74	56	7	11

Note : Values are the percentage full fixity in a given mortar wall at a set precompression (lbf/in²).

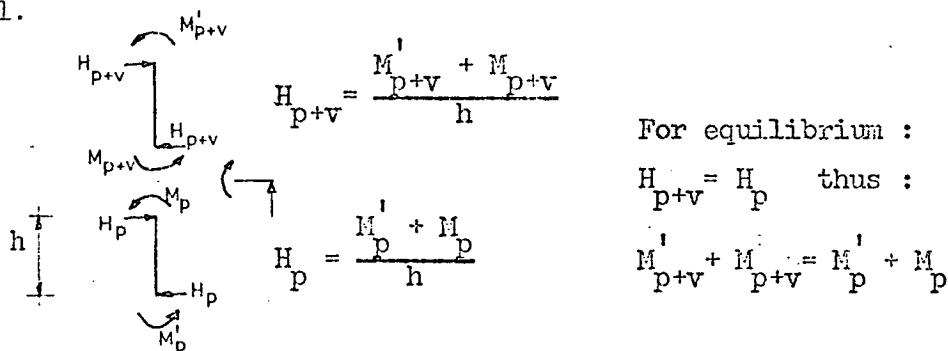
5.5 LATERAL DEFLECTION OF THE WALL-SLAB TEST MODEL

During each test, lateral deflections were measured at three levels. The deflections versus slab moment are shown in figures 5.4 and 5.5. An approximate curve is drawn through the three experimental points assuming the top and bottom of the model have no lateral movement. The maximum recorded lateral deflection at slab level is also shown.

The deflection curves show an effect similar to that of the strain planes - there is a common point of intersection situated along the centre line of the wall. This points towards little change in moduli and a constant ratio of slab moment to slab load over the range shown.

An explanation is needed for the variation in height of the intersection point or in other words the cause of lateral deflection at slab level. One of the differences between the model tests and a wall-slab intersection in practice is the restraint to lateral movement at slab level. In the former, lateral deflection is allowed while in the latter it is restrained.

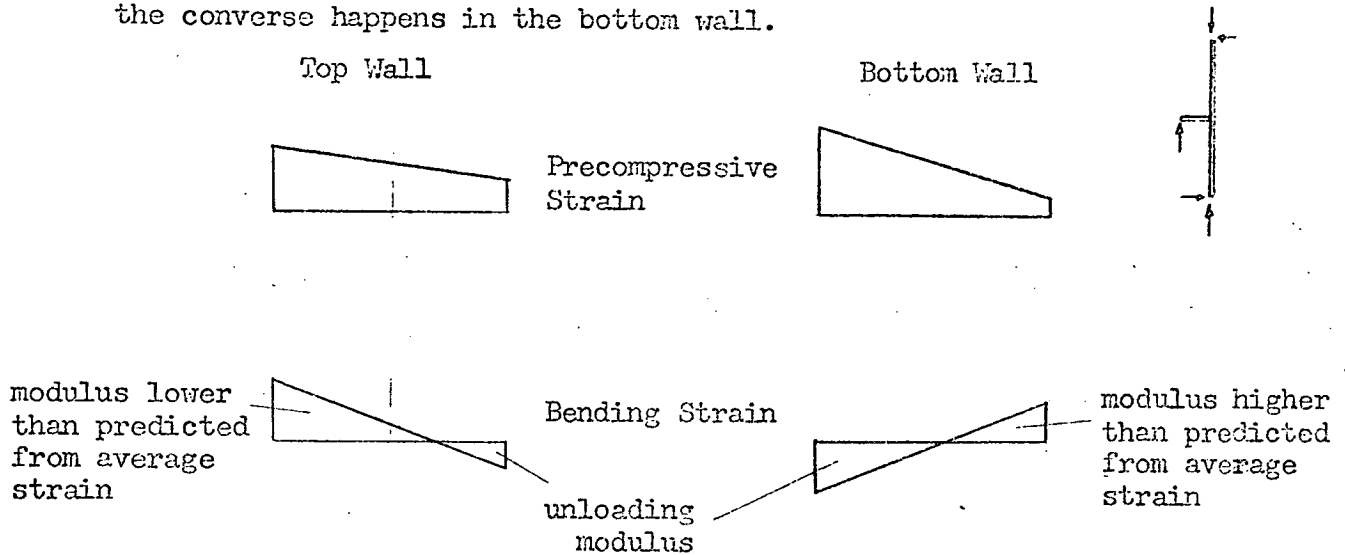
In the tests, if no lateral movement is to occur at slab level, the horizontal forces induced by the applied moments must be balanced at slab level.



If there is a moment difference at slab level due to unequal stiffnesses of the walls, lateral deflection will occur until the sum of the moments at both ends of each wall is equal.

All the models follow this trend except for three cases. The 1:1:6 mortar wall at 400 lbf/in^2 precompression shows an intersection about the centre line of the slab while the measured modulus for the top wall is larger than the bottom wall. An error in the top wall modulus is possible as the moment predictions from strains are too high (Table 4.2) (see also following discussion). The 1:2:9 mortar walls at precompressions of 400 lbf/in^2 and 600 lbf/in^2 show little difference in moduli thus should have no lateral deflection at midheight.

The reason for the discrepancy is probably due to the initial precompression which causes a much larger strain on the slab side of the model than the other, the effect being greater in the bottom wall (fig 4.3). On applying slab moment this difference in strain is further increased in the top wall while reduced in the bottom wall. The effective modulus for the top wall will be lower than predicted from average strains while the converse happens in the bottom wall.



When cracking occurs at the joint, greatly increased lateral deflections occur towards the slab side. This is due to the upper wall resisting an increased moment caused by eccentric application of the slab load (as opposed to moment). Lateral deflection occurs until this extra moment is redistributed between the two walls - for example an increase in fixing moment for the bottom wall and a decrease in top wall fixity. Not much adjustment occurs at slab level as the deflections there are still comparatively small compared to wall width - 0.08 inch (maximum observed) versus a wall thickness of 4.12 inches.

The 1: $\frac{1}{2}$:3 mortar model at 200 lbf/in² precompression deflects in the opposite direction to that expected at failure. This is probably due to tensile cracking occurring in the top wall while none occurs in the bottom wall (excluding the wall-slab joint)(see fig 4.1). The tensile cracking occurs first in the top wall due to the non-uniform precompressive strain (little compressive strain on the tensile face - figure 4.1). The reduced top wall stiffness can cause increased rotation of the wall reducing the tensile crack at the joint, thus reducing the resisting moment. To counteract this effect a movement away from the slab side occurs.

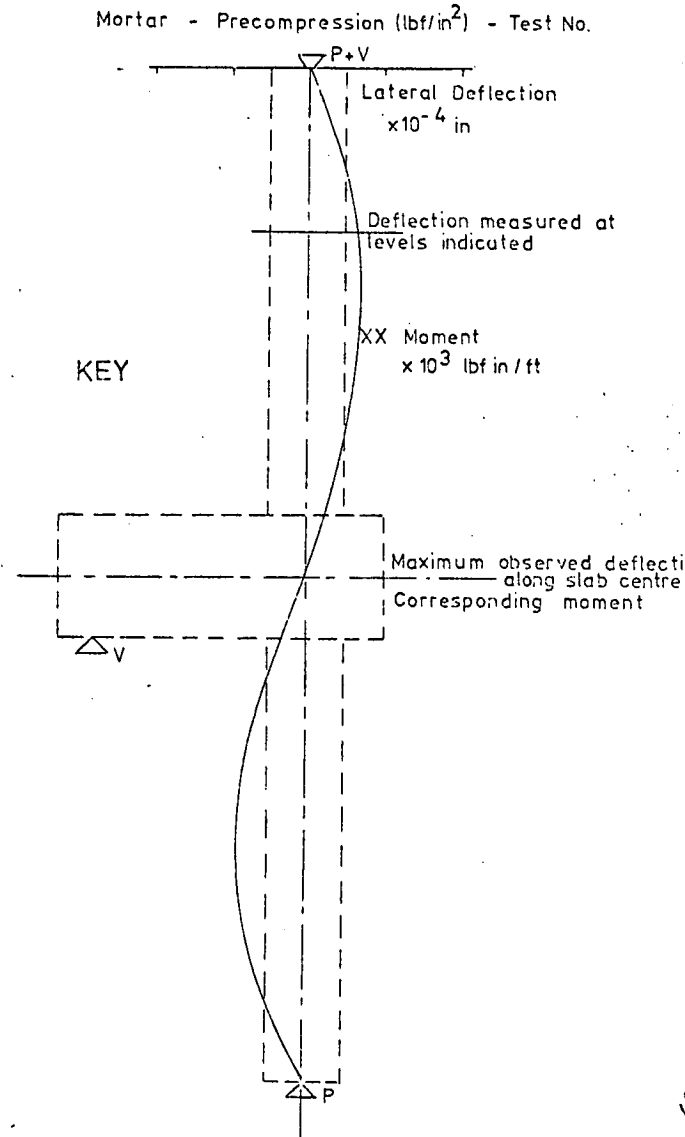
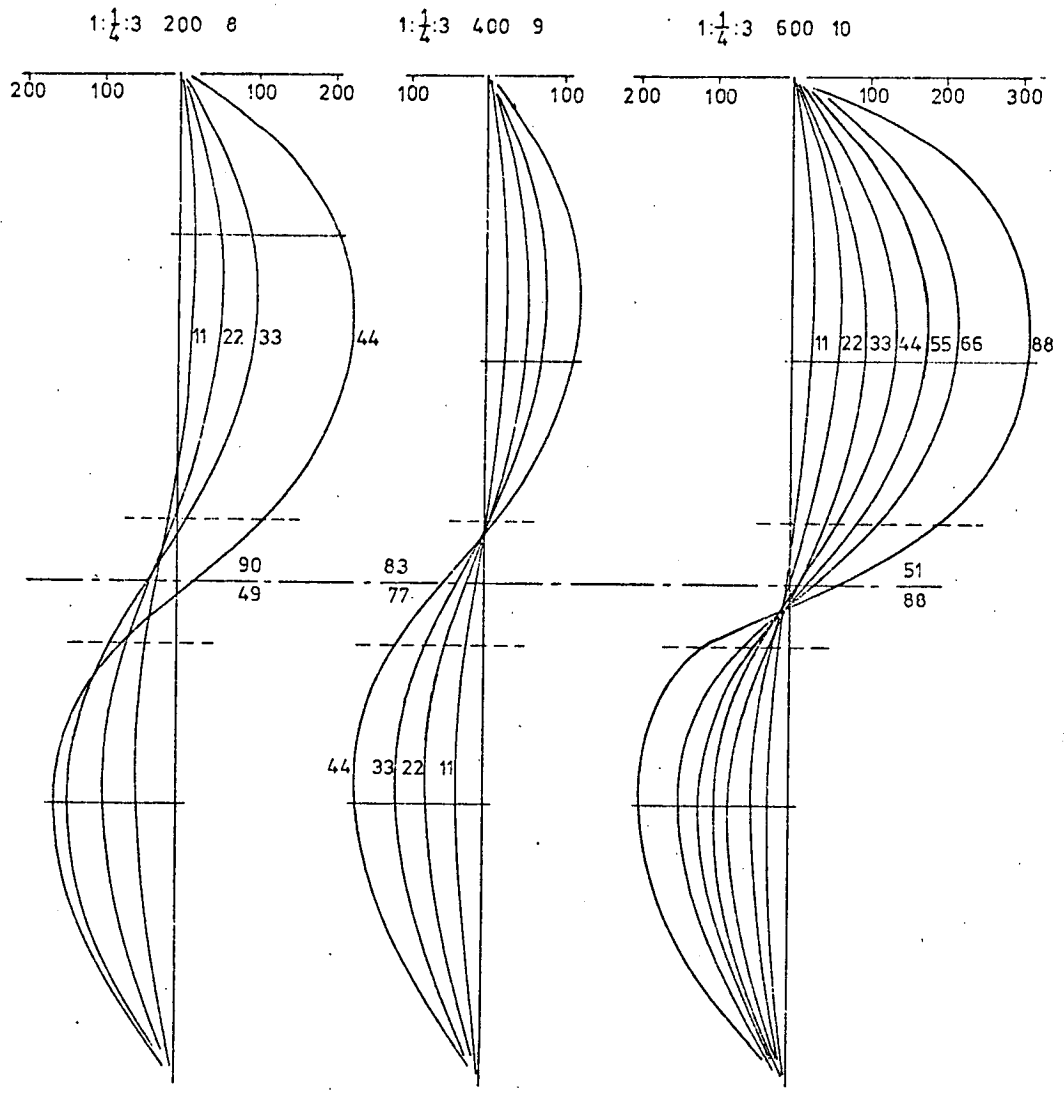
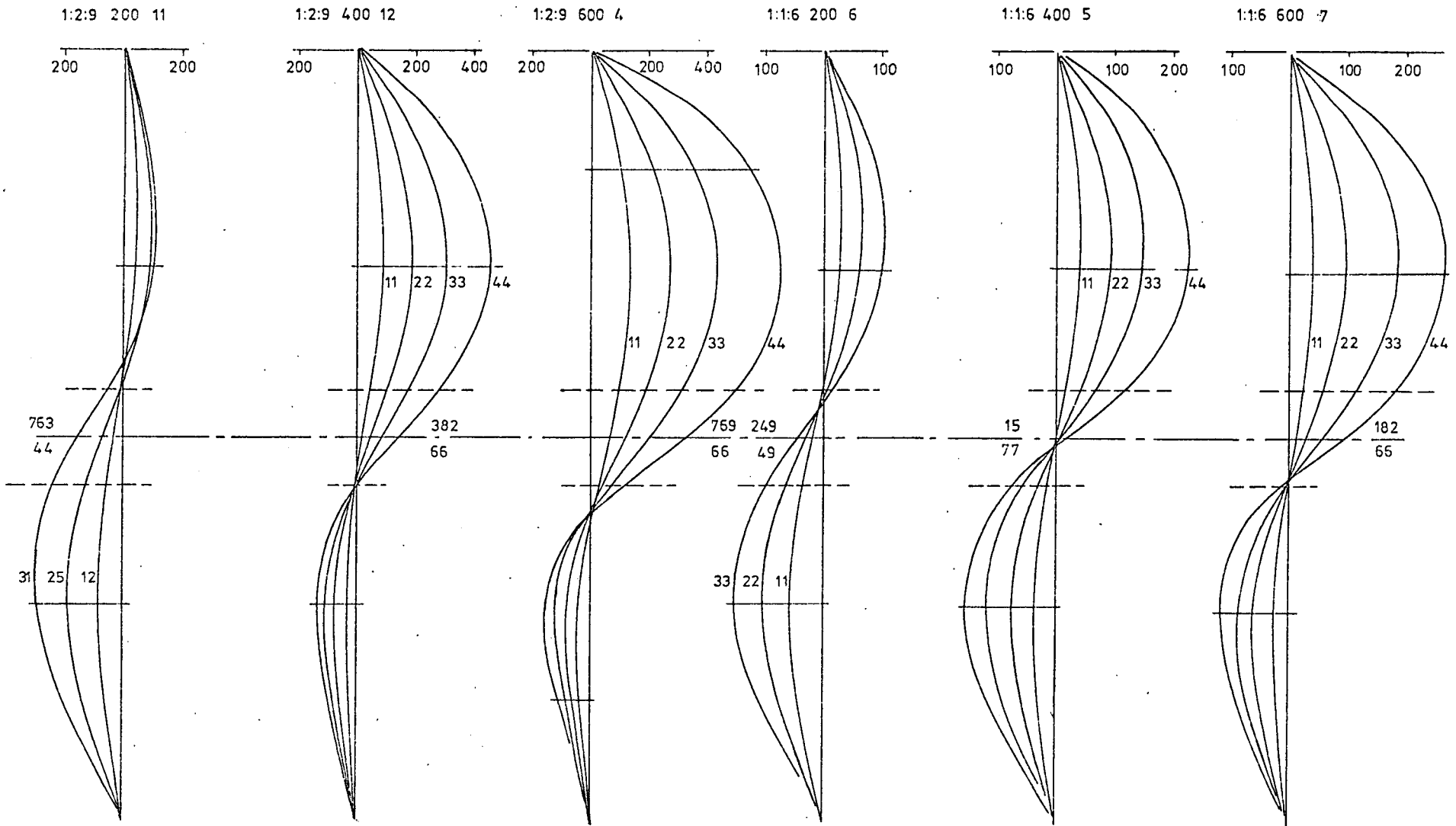


Fig. 5.4 LATERAL DEFLECTION DUE TO SLAB MOMENT



FOR EXPLANATION SEE FIG. 5.4

Fig. 5.5

LATERAL DEFLECTION DUE TO SLAB MOMENT

5.6 CONCLUSIONS

1. The moment-rotation curves all have an initial approximately linear portion. The initial rotation-moment ratio increases with decrease of brickwork strength - an average of 42×10^{-9} rad/lbf in/ft for a 1: $\frac{1}{4}$:3 mortar brickwork, 57×10^{-9} rad/lbf in/ft for a 1:1:6 mortar brickwork and 103×10^{-9} rad/lbf in/ft for a 1:2:9 mortar brickwork (figs 5.1 to 5.3 & Table 5.1).
2. The theoretical values of slope based on a solid section and equal loading and unloading moduli overestimate the experimental results. Theoretical values taking into account a gap in the mortar joint and an unloading modulus larger than the loading modulus tend to underestimate the experimental results. The reasons for this could be variations in the assumed properties and local deformations near to the joint (Table 5.1).
3. Precompression has little effect on the slope of the initial linear portion of the moment-rotation curve. Thus no increase in fixity with increasing precompression. There is the possibility of a decrease in fixity with increasing precompression when it causes a reduction in the tangent compression modulus.
4. When tensile cracking occurs the slope of the moment-rotation curve rapidly decreases becoming zero at the equilibrium moment if wall or slab failure does not occur. In this range increasing precompression does reduce rotation (figs 5.1 to 5.3).
5. The ends of the wall have a variable amount of fixity tending to increase with increasing rotation. Assuming 20% full fixity for both walls reduces the predicted rotation by 6% (Table 5.2).
6. Lateral deflection curves intersect at a common point thus following a pattern similar to that shown by the strain planes (figs 5.4 & 5.5 and 4.1 to 4.3). As opposed to the wall-slab joints in practice, lateral deflection at slab level occurs, this being small in the tests. The deflection is initially due to differences in stiffness between the top and bottom walls and later, with tensile cracking, due to the extra moment resisted by the wall taking the slab load in addition to the precompressive load.

CHAPTER 6 - FAILURE AT THE WALL-FLOOR SLAB JUNCTION

6.1 INTRODUCTION

This chapter investigates the failures in the wall-floor slab joint of the test models.

The first section deals with the behaviour of the floor slab-wall joint. The top wall is under a constant precompression while the applied slab moment is increased. Neither the wall nor the slab fails but as the slab moment increases tensile cracks appear in the joint between the walls and the slab (no tensile strength) until finally the slab levers the walls apart at a constant moment - equilibrium failure.

Equilibrium failure in three test models is then discussed and compared with a simple theoretical analysis.

Wall failure occurs in test models under precompressions of 400 lbf/in² and 600 lbf/in² - spalling of the bricks near the joint. A theory is proposed which takes into account the gap in the mortar joint - this gives better results than the assumption of a solid section.

Three different types of floor slab failure were observed - two shear and one tensile (first two may also be considered as tensile). Two of the failures occurred during preliminary tests after which the slab was designed to be stronger than the wall at failure loads. It enabled the slab to be used for the remaining tests.

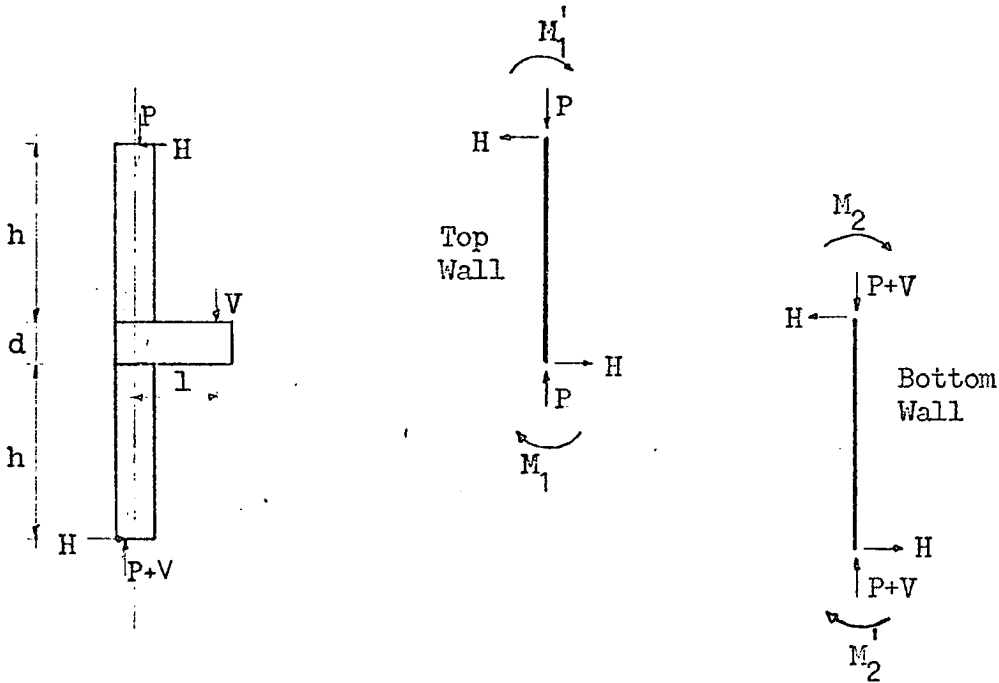
Photographs show the wall-floor slab joint in an inverted position while to avoid confusion in this chapter, the text treats the joints in their correct position.

The notation for the applied wall moments is also changed - M_p becomes M_1 and M_{p+v} becomes M_2 .

6.2 FORCES ACTING AT THE JOINT

6.2.1 No Tension Cracks

The forces acting at the joint are shown in the following sketch :



Moment applied by the slab = M_s

Moment applied to the walls above and below the slab :

$$M_1' = Hh - M_1' \quad \text{--- (6.1)}$$

$$M_2 = Hh - M_2' \quad \text{--- (6.2)}$$

$$\text{where } H = (M_1' + M_2' + M_s)/(2h + d)$$

If the far ends of the wall are hinged $M_1' = M_2' = 0$ and

$$\begin{aligned} M_1 = M_2 &= 0.5M_s/(1 + d/2h) \\ &= 0.5gM_s \quad \text{--- (6.3)} \end{aligned}$$

$$\text{where } 1/g = 1 + d/2h$$

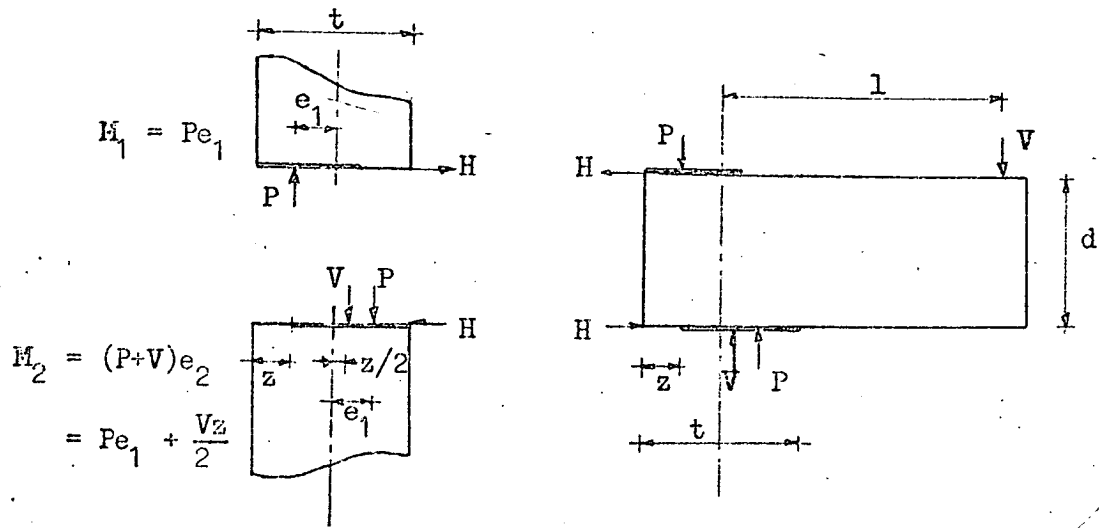
For the test models $g = 0.88$ (hinges assumed at far ends of the wall).

For the full scale test building (Chapter 7) $g \approx 0.96$ (hinges at 0.5 or 0.7 of wall height).

6.2.2 Moment Distribution in the Test Models when Tensile Cracking Occurs

1. Tension Cracks at the Joint

When tensile cracking occurs in the bottom joint, the slab reaction is off-centre transferring a greater proportion of the moment onto the bottom wall.



Moment applied to top wall = M_1

Moment applied to bottom wall = $M_2 = M_1 + Vz/2$ ---- (6.4)

where $z = \text{depth of the tensile crack}$
 $= 3(e_2 - t/6)$ ---- (6.5)

(for a solid, rectangular wall - see figure A4.2)

where $e_2 = M_2 / (P + V)$

where $M_1 = gM_s - M_2$

Substituting the latter three expressions into equation 6.4 :

$M_2 = \frac{P + V}{2P + 0.5V} (gM_s - 0.25Vt)$ ---- (6.6)

For the test models this equation becomes ($M_s = Vl$) :

$M_2 = \frac{4.22Vt}{4P + V}$ ---- (6.7)

The relationship is presented graphically in figure 6.1 in the form M_2/gM_s versus M_s/Pt .

The maximum value of V occurs when $e_2 = t/2$ giving $M_2 = (P + V)t/2$.

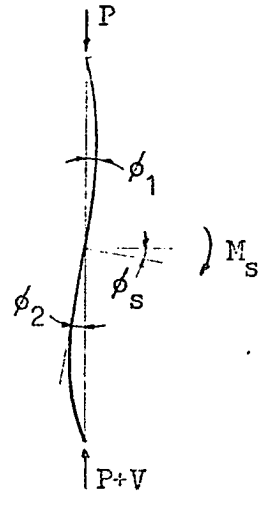
Equation 6.7 then gives $V_{max}/P = 0.54$ (see part 4 of this section).

2. Tension Cracks in the Joint and the Walls

The previous analysis considered a tension crack at the joint. The effect of taking the wall behaviour into account is now investigated.

Assumptions :

1. The far ends of the wall are hinged.
2. The angle of rotation of the walls at the junction is equal throughout the cracking stage.
3. The effect of axial load on lateral deflections is negligible*.
4. Solid, rectangular walls.



If the angles of rotation of the walls are equal at the junction with the floor slab, then $\phi_1 = \phi_2$ or using equation A5.10 :

$$M_1/c_1 = M_2/c_2 \quad \text{where } c \text{ is a coefficient taking into account the reduced stiffness of the wall due to tensile cracking (fig A5.1).}$$

Letting $M_1 + M_2 = gM_s$ ---- (6.8)

$$e_1/t = M_1/Pt \quad e_2/t = M_2/(P + V)t$$

then $gM_s = M_2(1 + c_1/c_2)$ and $Pt = \frac{(c_1/c_2)M_2}{e_1/t}$

$$Vt = M_2 \left(\frac{1}{e_2/t} - \frac{c_1/c_2}{e_1/t} \right) \quad \text{---- (6.9)}$$

Eliminating M_2 between equations 6.8 and 6.9 gives :

$$\frac{e_2}{t} = \frac{gM_s/Vt}{\frac{c_1}{c_2} \left(\frac{gM_s/Vt + e_1/t}{e_1/t} \right) + 1} \quad \text{---- (6.10)}$$

*For the test models at 600 lbf/in² precompression, the load is much less than the buckling load. In terms of h^2/EI the range is 0.24 to 1.2 lbf⁻¹ for the 1:2:9 to 1:1/4:3 mortar walls compared to π^2 for buckling.

Letting $M_s = Vt$ equation 6.10 becomes :

$$\frac{e_2}{t} = \frac{2.35}{\frac{c_1}{c_2} \left(\frac{2.35 + e_1/t}{e_1/t} \right) + 1} \quad \text{--- (6.11)}$$

For a given value of e_1/t the corresponding value of e_2/t can be found by trial and error using figure A5.1 relating e/t to c . The results are presented graphically in figure 6.1 .

3. Approximation to the Moment Distribution in the Cracked Stage

The relationship between M_2/gM_s and M_s/Pt in figure 6.1 is replaced by a linear one. One point is given by the moment needed to start tension in the top wall and the other by the limiting equilibrium moment. In this way lines can be drawn for walls which crack at eccentricities other than $t/6$.

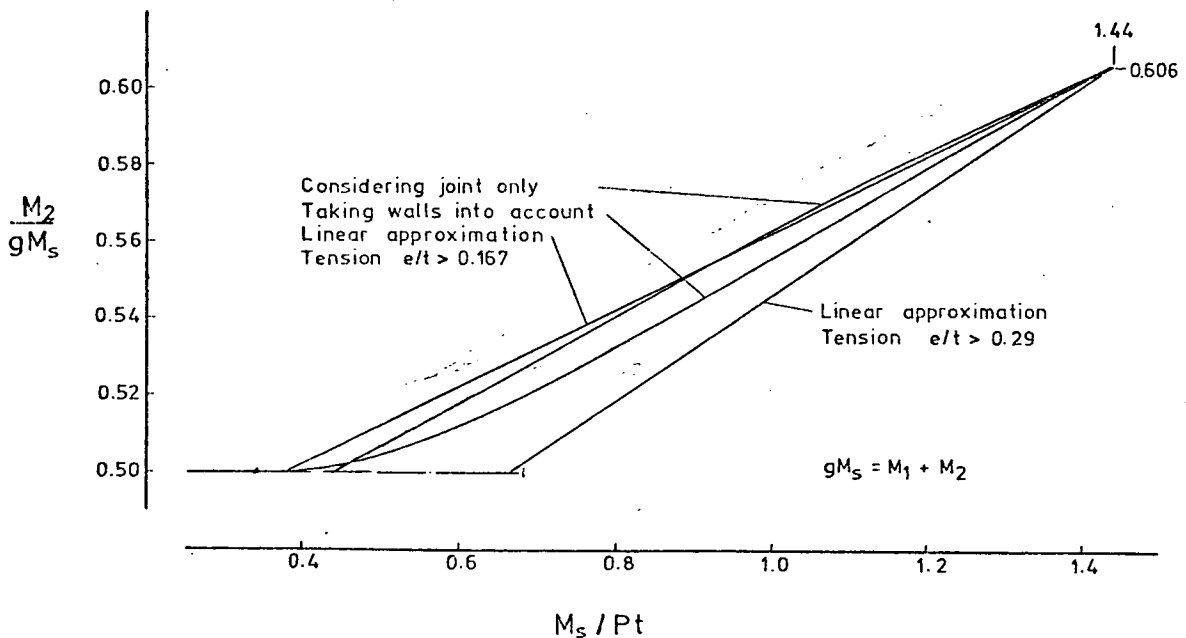


Fig. 6.1 DISTRIBUTION OF SLAB MOMENT TO WALLS AFTER TENSILE CRACKING

For the test models the value for maximum V is $V_{\max}/P = 0.54$.

The maximum slab moment = $M_{s_{\max}} = V_{\max} l = 5.94P$.

The maximum moments applied to the wall are :

$$M_1 = Pt/2 \qquad M_2 = (P + V)t/2$$

and $(M_1 + M_2)/M_{s_{\max}} = 0.88 = g$

In this case the ratio of the sum of the applied wall moments to the slab moment has not changed.

The maximum moment in the slab itself is not M_s but

$$V(1 - t/2) = M_s - Vt/2 \qquad \text{--- (6.13)}$$

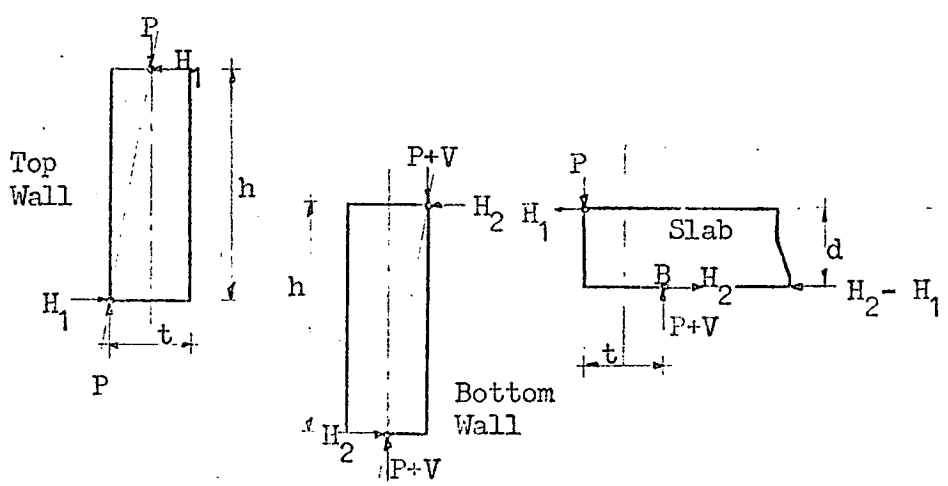
6.2.3 Moment Distribution at the Joint when the Slab is Supported on More than One Side

1. Maximum Slab Moment

One of the joints of a floor slab supported on two sides is considered. There are two important differences with the test models :

1. The moment is statically indeterminate - it is not proportional to the slab load except in a linearly elastic system with no tensile cracking.
2. The floor slab provides restraint against lateral movement at slab level.

The slab moment considered at the joint is the slab restraining moment and not necessarily a moment about the centre line of the walls (the latter will occur before tensile cracking at the joint).



From the sketch, taking moments about B gives :

$$M_s = Pt + H_1 d$$

Assuming pinned ends, the difference in horizontal forces is now resisted by the slab.

$$H_1 = Pt/2h$$

$$M_s = Pt(1 + d/2h) = Pt/g \quad \text{--- (6.14)}$$

The span of the slab is reduced by t/2 which is usually insignificant. The moments applied to the walls are :

$$M_1 = Pt/2 \quad M_2 = (P + V)t/2$$

The top moment is a maximum but the bottom moment can still increase with increasing slab load.

2. Moment Distribution Throughout the Cracking Range

Before cracking occurs the top wall moment is half the slab moment (slightly reduced by the factor g). When cracking occurs throughout the joint, the top wall moment is again half the slab moment. This is assumed to happen throughout the cracking range. Therefore :

$$M_1 = gM_s/2 \quad \text{--- (6.15)}$$

$$M_2 = gM_s/2 + Vz/2 \quad \text{--- (6.16)}$$

The bottom wall resists an extra moment from an eccentrically applied slab load.

For a solid wall the crack depth is given by equation 6.5 :

$$z = 3(e_2 - t/6)$$

For a wall in the full scale test structure (Chapter 7), cracking is assumed to occur when $e/t = 0.22$. Assuming a linear relation for z ,

$$z = 3.57e_2 - 0.786t \quad \text{--- (6.17)}$$

Substituting equation 6.5 into equation 6.16 gives :

$$M_2 = \frac{P+V}{2P-V}(gM_s - 0.5Vt) \quad \text{--- (6.18)}$$

Compare this with equation 6.6 .

Substituting equation 6.17 into equation 6.16 gives :

$$M_2 = \frac{P + V}{2P - 1.75V}(gM_s - 0.786Vt) \quad \text{--- (6.19)}$$

6.3 EQUILIBRIUM FAILURE

6.3.1 Experimental Results

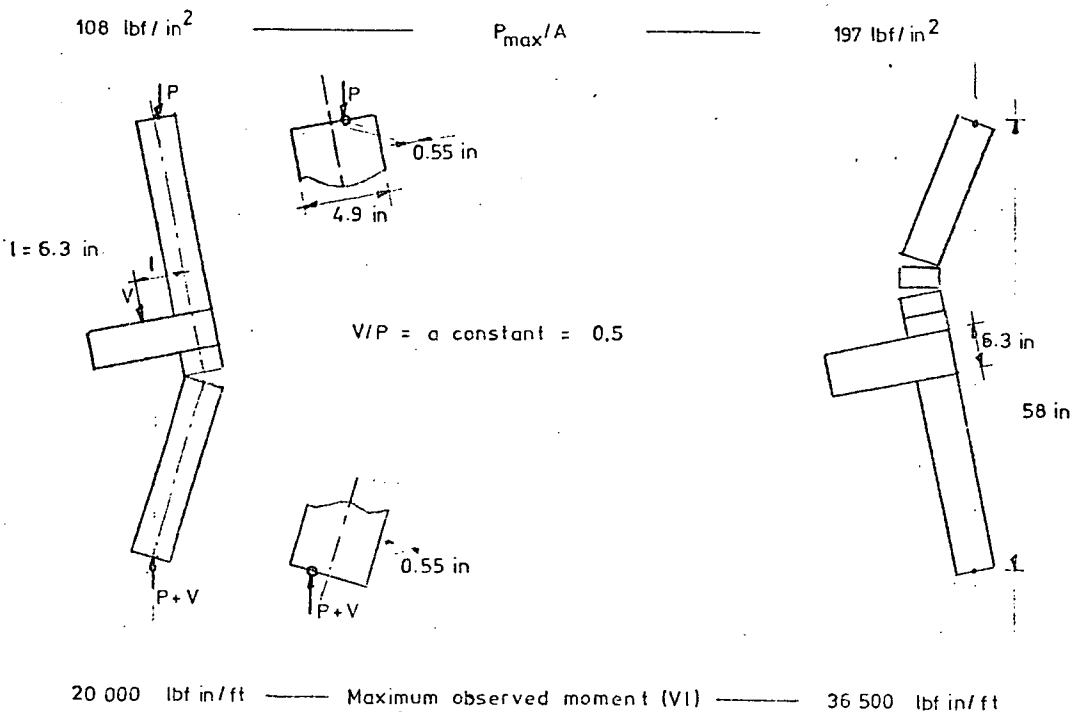
Equilibrium failure occurred in the test models when the precompression was 200 lbf/in^2 . The results are given in Table 6.1, and photographs showing equilibrium failure and local crushing of the mortar joint are shown in figures 6.2 and 6.3.

6.3.2 Other Experimental Results

The National Institute for Materials Testing in Sweden (24, 31 & 32) tested two models similar to the test models. These also seem to have failed without failure of the slab or walls (except for some crushing at the mortar joint), but failure was due to instability as opposed to equilibrium.

The tests have a different loading pattern - the precompression and slab load increase from zero to failure at the same rate and in the same proportion. Instead of having a constant precompression with increasing eccentricity, there is a constant precompressive eccentricity with an increasing precompressive load enabling the relative rotation between the slab and the wall to be investigated.

The walls had hinged ends, the hinges placed off centre to simulate a full length wall with points of inflection half way up the wall. The point of zero moment is thus effectively 53 inches from the centre line of the slab (Appendix 1).



70

The moment from the slab was enough to cause tensile stresses at the joint - eccentricity in the top wall load at slab level was $0.32t$. As the loads increased the two models failed in opposite directions from excessive lateral deflection. This produced two different ultimate moments - one about twice as large as the other.

Having pinned ends off-centre will give a more realistic behaviour of slab-wall interaction, but the slab should also be restrained from moving laterally. Without this restraint, the model is unstable at higher loads and will give neither consistent nor relevant results. If the slab is restrained, failure would occur at much higher moments caused by failure of the slab or wall. Equilibrium failure will not occur as the wall resisting moment is larger than the applied slab moment - a constant ratio throughout the test.

6.3.3 Discussion

The theoretical analysis of joint behaviour assumed small forces, the effects due to lateral deflection, local crushing and non-linear stress-strain being neglected.

Even with low loads, an eccentricity ratio of $e/t = 0.5$ should theoretically cause failure in walls with no tensile strength. Why this does not occur in the tests is due to several factors.

The eccentricity in many cases is a maximum at the joint only.

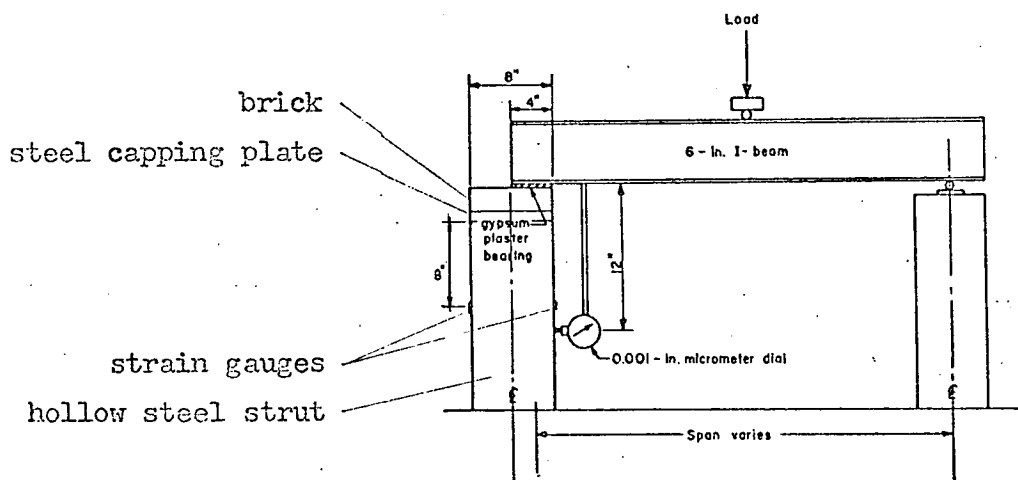
The brickwork can usually resist some tensile stress - one series of tests gave average tensile stresses ranging from 85 to 135 lbf/in² (34, see footnote section 4.5.1). The British Code of Practice for Brickwork (8) allows a value of 10 lbf/in². A solid four inch wall allowed the latter stress would resist a moment of 320 lbf in/ft or a load of 140 lbf/ft at an eccentricity of $0.5t$ (equivalent to a moment of 480 lbf in/ft together with an axial load of 140 lbf/ft).

In many cases the maximum eccentricity will tend to a value slightly lower than $0.5t$. Local deformation and crushing may occur especially in the mortar joint adjacent to the slab (fig 6.3). In the test models no crushing of the brick occurred up to average precompressive stresses of 200 lbf/in² - a stress not often encountered in practice*. In the

*The maximum permissible axial stress for 8 ft high walls supported top and bottom by concrete floors with $1:\frac{1}{2}:3$ mortar and 5000 lbf/in² bricks is 180 lbf/in² (8).

1:2:9 mortar test models spalling of the mortar joint to a depth of $\frac{1}{2}$ inch was observed, representing a limiting eccentricity of $0.44t$. This reduces the ratio V_{\max}/P to 0.46 . Local deformation reduces the limiting eccentricity even more. The limiting eccentricities for the test models failing in equilibrium ranged from $e/t = 0.42$ for the 1:2:9 mortar test models to $e/t = 0.45$ for the 1:1:6 and 1: $\frac{1}{2}$:3 models (average of top and bottom walls).

Watstein and Johnson (39) obtained a limiting eccentricity of $0.4t$ for beam end rotations up to 4×10^{-3} radians, for a simply supported steel joist, one end supported on a brick by a bed of gypsum plaster enclosed by polyethylene sheets (thus no bond). A similar test with bonded plaster (no polyethylene) gave a limiting eccentricity of $0.25t$. This result is surprising - a similar eccentricity to the previous test would be expected or if the bond had not broken a larger eccentricity. A reason for this could be restraint to lateral movement of the strut (see sketch).



Misalignment between the top and bottom walls can increase or decrease the ultimate equilibrium moment. This effect is expected to be small in the test models - misalignment not greater than approximately $1/8$ inch.

The analysis of slender walls under high loads of varying eccentricity is complex. Lateral deflections become significant, the point of maximum eccentricity occurring in the region of maximum lateral deflection. The higher stresses usually mean a reduction in the tangent modulus causing increased deflections.

Sahlin (30) used an analysis for walls without tensile strength taking the lateral deflections into account and assuming a linear stress-strain relation. The analysis shows greatly increased rotations and stresses at loads approaching the buckling load. At high loads the wall end could

rotate more than the slab and would then be restrained by the slab reducing the effective buckling length of the wall. Methods for calculating the buckling curves for walls with no tensile strength having a mathematical non-linear stress-strain equation are reviewed by a French publication (12). More experimental tests on full scale, storey height walls are needed before these factors can be considered in detail.

TABLE 6.1 - SLAB LOADS AND MOMENTS AT FAILURE

Brickwork Mortar by volume	Test Model No.	Precompression		Maximum Slab Load tons	$\frac{V_{\max}}{P}$	Maximum Slab Moment lbf in/ft
		lbf/in ²	tons			
1:½:3	8	200	10	4.7	0.47 ⁵	51 000 ⁴
	9	400	20	8.5	0.42	93 000
	10	600	30	12.5	0.42	137 000
1:1:6	6	200	10	4.9	0.48 ¹	54 000
	5	400	20	7.8	0.39 ²	85 000
	7	600	30	9.0	0.30	99 000
1:2:9	11	200	10	4.0	0.42 ³	44 000
	12	400	20	7.5	0.38	82 000
	4	600	30	6.9	0.23	76 000

- Notes :
- $V_{\max} = 4.9 \text{ t}$ when $P + V = 15 \text{ t}$; $V_{\max}/P = 0.48$
 - $V_{\max} = 7.8 \text{ t}$ when $P + V = 28 \text{ t}$; $V_{\max}/P = 0.39$
 - $V = 4 \text{ t}$ when $P + V = 13.5 \text{ t}$; $V/P = 0.42$. The jack load, V , should have been 3.5 t but the wiring to the load cells incorrect. Estimated $V_{\max} = 4.1 \text{ t}$ - difficult to hold load steady ; $V_{\max}/P = 0.43$.
 - Moments to the nearest thousand - further accuracy not justified. Moments based on a moment arm of 11 inches.
 - The theoretical $V_{\max}/P = 0.54$.

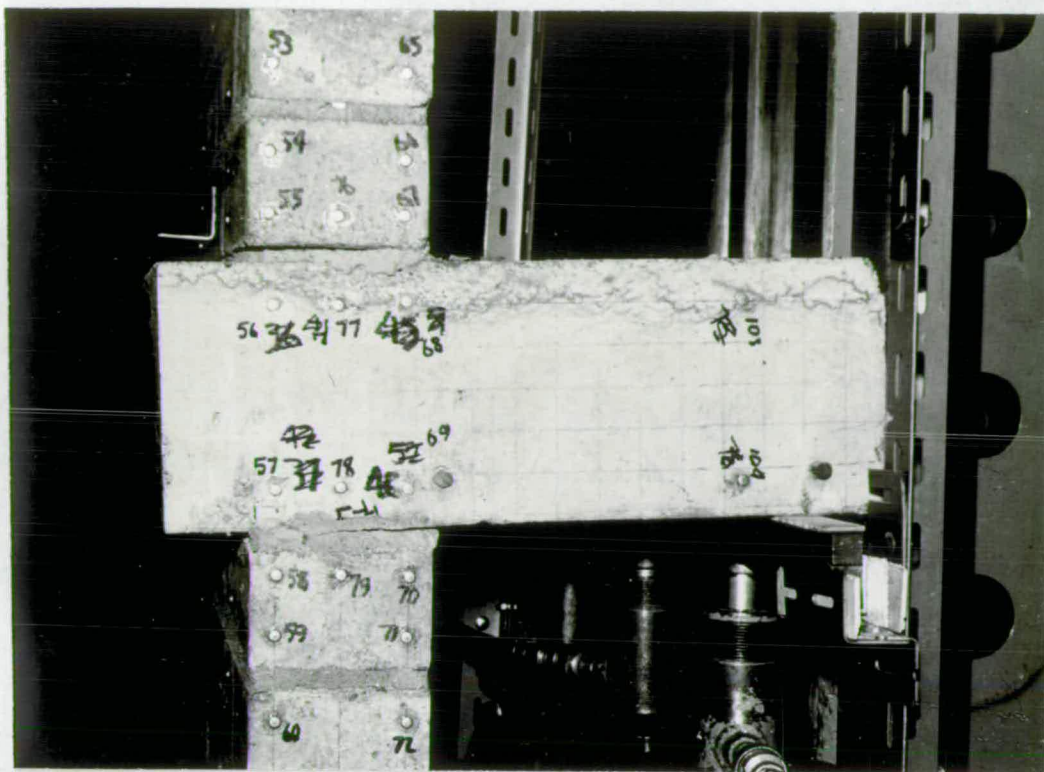


Figure 6.2 - Equilibrium Failure.

1:1:6 Mortar Walls - Precompression 200 lbf/in²

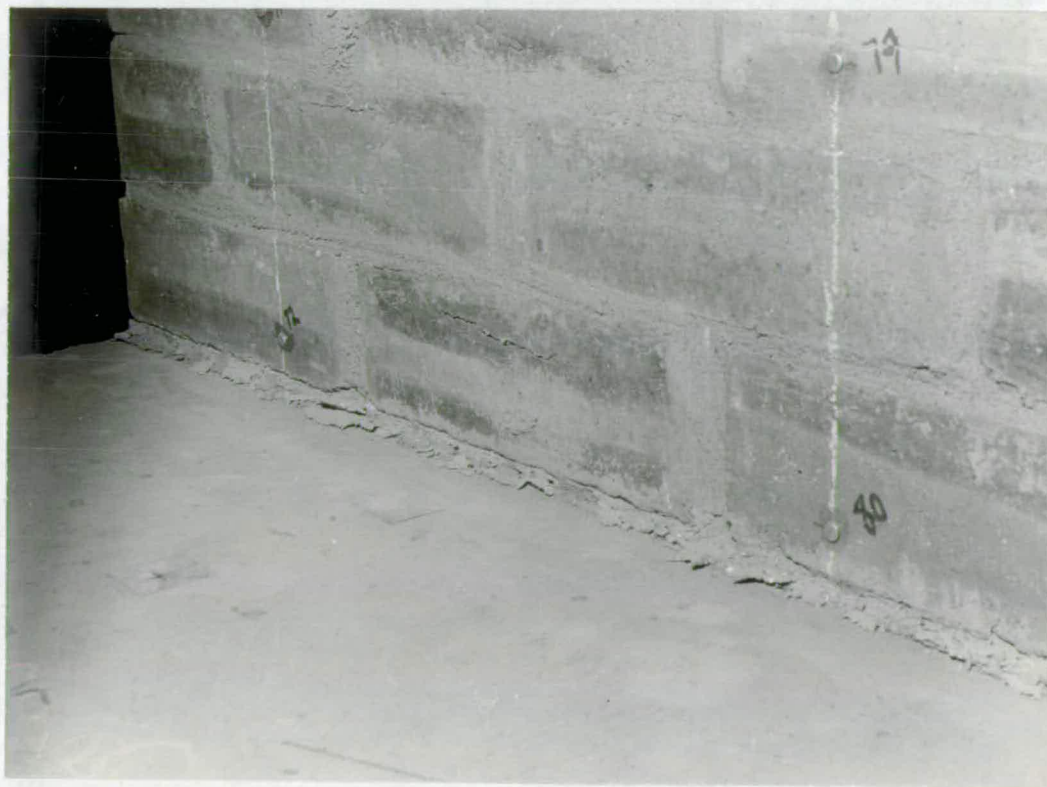


Figure 6.3 - Spalling of the Mortar Joint Adjacent to the Slab .

1:2:9 Mortar Walls - Precompression 200 lbf/in²

6.4 WALL FAILURE

6.4.1 Experimental Results

The ultimate slab loads and moments are shown in Table 6.1 . Failure of the wall is shown in figures 6.4 to 6.8 .

6.4.2 Failure of the Walls

At higher precompressions, wall failure may occur before the equilibrium condition is reached.

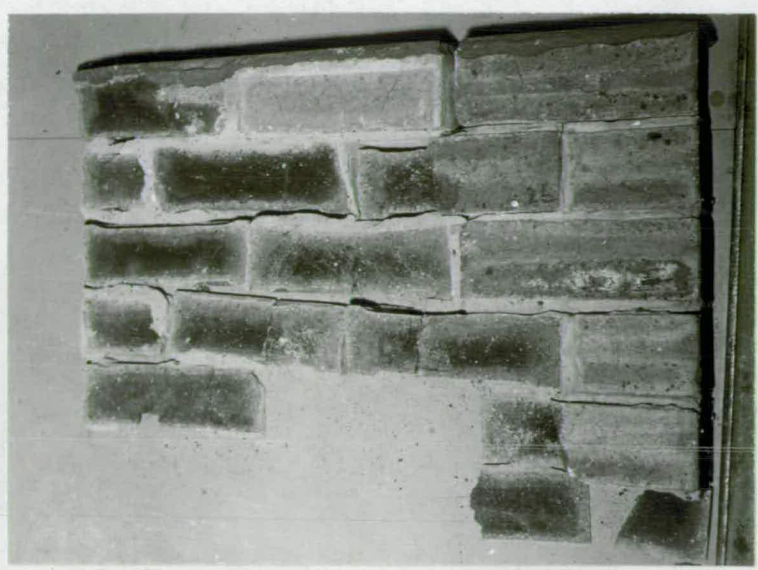
Before failure, the joint tends towards an equilibrium failure - horizontal cracks develop along the mortar joints, usually in the joint between the wall and the slab. In the test models the lower wall resists in addition to the precompression, slab load and a moment up to 50% more than the upper wall (at equilibrium failure). When failure is imminent, spalling occurs from the surface of the mortar joints in the lower wall near the slab. Gradual failure then follows with spalling of the brickwork usually confined to the two or three courses adjacent to the slab although in the case of the 1:2:9 mortar wall at 600 lbf/in² precompression failure extended over most courses (fig 6.5).

Sahlin (30, 31 & 32) has shown failure occurs a few courses away from the slab because of its restraining influence. In his case the slabs were cast in-situ resulting in an excellent bond with the top course of brickwork which may be considered as an extension of the slab. The trend is not shown in the test models, only two cases (figs 6.5 & 6.6) failing a few courses away, but this may be due to variations in brickwork properties and lateral deflections if these are large. Sahlin (30) also tested some precast concrete connections in which the floor bore fully into the wall and there was no insitu connection - the walls failed in areas immediately adjacent to the slab.

With increasing precompression failure will occur without tensile cracks developing. The limiting precompression is the ultimate axial strength of brickwork when no slab moment can be resisted. These aspects are discussed in the next section.



Figure 6.4 - Spalling and Final Failure of a Wall .
 1:1:6 Mortar Wall - Precompression 400 lbf/in²



Back View of Top Wall Reconstructed



Front View of Top Wall After Failure

Figure 6.5 - Wall Failure.
1:2:9 Mortar Wall - Precompression 600 lbf/in²



Figure 6.6
Wall and Slab Failure.
1:1/4:3 Mortar Wall
Precompression 600 lbf/in²



Figure 6.7
Wall Failure.
1:1:6 Mortar Wall
Precompression 600 lbf/in²

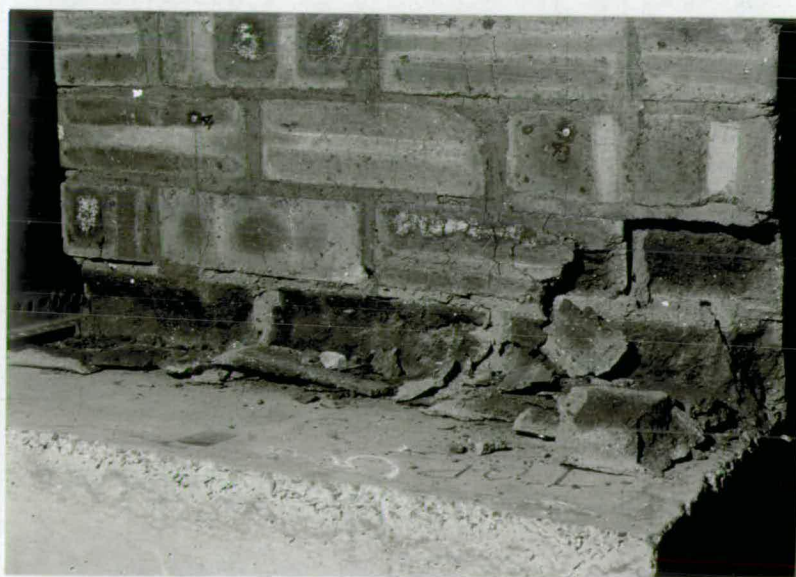


Figure 6.8
Wall Failure.
1:1/4:3 Mortar Wall - Precompression 400 lbf/in²

6.4.3 Strength of Walls Under Axial Load and Moment

The precompressive force, slab load and slab moment may be considered to be equivalent to an axial load and a moment. A wall will resist no moment when there is no load (no tensile strength) nor when the load equals the ultimate compressive load for the wall. In between these values of load the moment capacity varies (fig 6.9), becoming a maximum as half the ultimate load is reached.

An interaction curve based on a solid cross-section and a linear stress-strain curve considerably underestimates the experimental results. Using an experimentally obtained stress-strain curve from a concentric loading test does not explain the difference.

1. Axial Load - Moment Interaction Diagram

An explanation for the difference in the test models may lie in the fact there is a central gap in the mortar joint. The actual ultimate stress at failure is then greater than that based on the full wall cross-section. The area adjacent to the mortar joint is considered and therefore values of actual gap width are used.

Several moment-axial load interaction diagrams are derived for the $1:\frac{1}{4}:3$ mortar walls (fig 6.9 & Appendix 6). The experimental stress-strain curve is used to derive the interaction diagram for gap width to wall width ratios (a/t) of 0.64, 0.45 and 0. The first gap is based on the actual width of the frog while the second is based on strain readings (section 4.4.2). Two further interaction curves assume a linear stress-strain curve and gap width ratios of 0.64 and 0. Curves based on the experimental stress-strain relation and a gap width ratio of 0.64 are drawn for the $1:1:6$ and $1:2:9$ mortar walls (fig 6.9). The curves are similar in shape to the one plotted for the $1:\frac{1}{4}:3$ mortar wall. If the interaction diagram were plotted in a dimensionless form the curves would coincide (load/max load vs. moment/max moment).

2. Load Reduction Factors for Eccentricity

The moment-axial load interaction diagram is also presented in the form of failure load versus eccentricity of the failure load (fig 6.10). The curves are compared with the proposed load reduction factors (slenderness ratio of wall = 6) given in the Draft B.S. Code of Practice for Brickwork (9). The resulting curve is similar except at low eccentricities to a curve for a solid wall and an experimental stress-strain

relation. The code factors greatly underestimate, at higher eccentricities, the failure load for a wall with a central gap.

3. Moment - Axial Load Interaction Curve for the Test Models

A curve is derived relating moment in terms of slab load to precompression for the test models (fig 6.11 & Appendix 6). The curve is the same for the three types of brickwork - dependent on the shape of the axial load-moment interaction curve. At low values of precompression there is an initial slowly decreasing curve representing the increase in moment in the moment-axial load diagram. The suddenly decreasing portion represents the drop in moment with increasing axial load. Most of the experimental results fall within the range covered by the curves for gap width ratios of 0.45 to 0.64. The results follow the general trend of the curve, scatter being caused by the small number of tests and the variability in ultimate stress of the axially loaded specimens.

6.4.4 Discussion

A central gap in the mortar joint increases the predicted moments substantially. Compared to the maximum predicted for a solid wall with a linear stress-strain curve, the non-linear experimental curve with gap ratios of $a/t = 0.64$, 0.45 and 0 gives increases of 110%, 80% and 20% respectively.

Yokel, Mathey and Dijkers (42) have derived the interaction diagram assuming a solid, rectangular cross-section and a linear stress-strain relationship, the wall failing when a limiting stress is reached equal to the ultimate stress under axial load. The theoretical curve considerably underestimates their experimental results on short prisms. Assuming an experimental stress-strain curve from a concentrically loaded prism does not make up the difference nor did they consider it likely to be due to end fixity conditions (eccentric loading at the top of the prism while the bottom has a flat support). Their explanation assumes that the flexural compressive strength of masonry increases with increasing strain gradients - the stress-strain curve for an axially loaded specimen is different from that in the compressive zone of a flexural specimen. But Clark, Gerstle and Tulin (13) who investigated the effects of strain gradient in concrete and mortar specimens concluded 'there is practically no difference in the stress-strain curves up to the point of maximum stress as a result of subjecting either concrete or mortar to a strain

gradient'. The gradient did increase the strain at failure. A similar increase may occur in brickwork (Table A6.1), but the experimental results obtained depend to a large extent on how close to failure the strain was recorded. An increase in ultimate strain beyond that already assumed is not likely to increase the predicted moments much more than the 20% mentioned earlier.

Clark, et al. found that the effect of strain rate is more important. With faster strain rates, the maximum stress increases, the strain corresponding to this stress decreases, and the ultimate strain also decreases. A ratio of strain rates of 25 (0.001 in/in/hr - 0.025 in/in/hr) showed variations between 2 and 10% for the above quantities. Again for the test models this is not likely to explain the large difference in experimental moments (assuming a solid wall).

An investigation into eccentrically loaded short walls similar to that conducted by Yokel, et al. is needed to clarify some of their results as well as those in this thesis and the effects of strain gradient, strain rate and gaps in the mortar joint. The behaviour of the mortar joints will need careful investigation since failure is usually initiated at the joints.

The load reduction factors in the proposed revision of the brickwork code (9) are based on solid walls with a linear stress-strain curve together with a 25% increase in permissible stresses. This in effect takes into account the non-linear behaviour of the stress-strain curve but nevertheless at low eccentricities the factors are too high. Factors based on an experimental curve throughout would be more realistic.

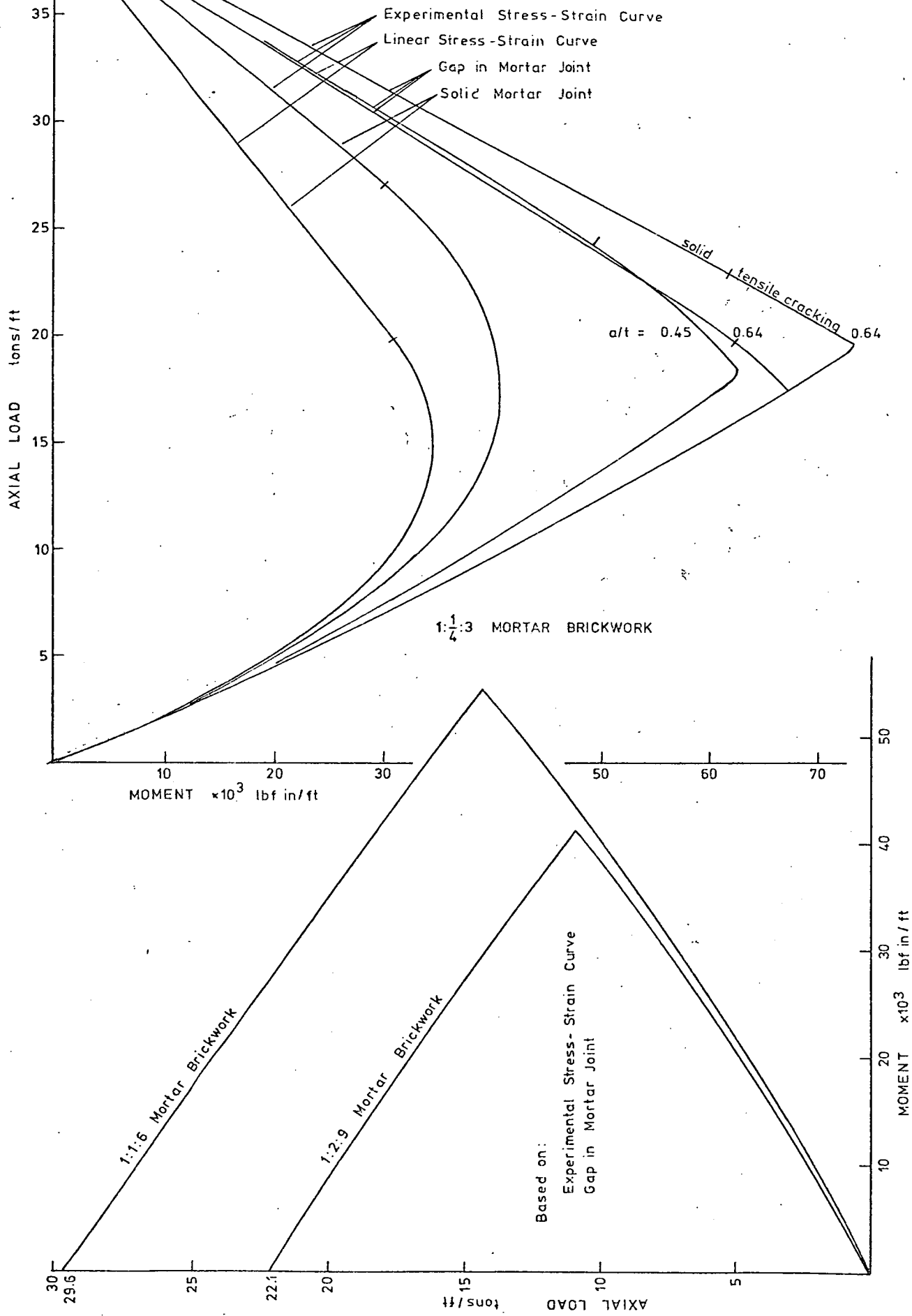


Fig. 6.9 Ultimate Moment - Axial Load Interaction Curve

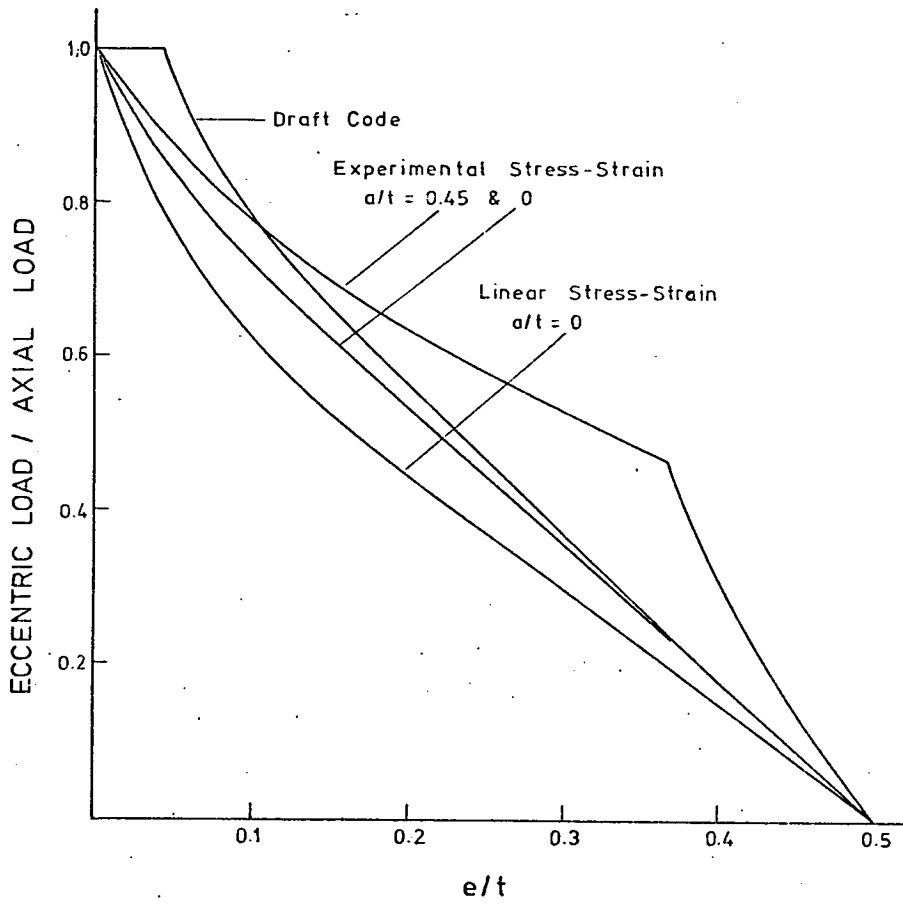


Fig. 6.10 LOAD REDUCTION FACTORS FOR ECCENTRICITY

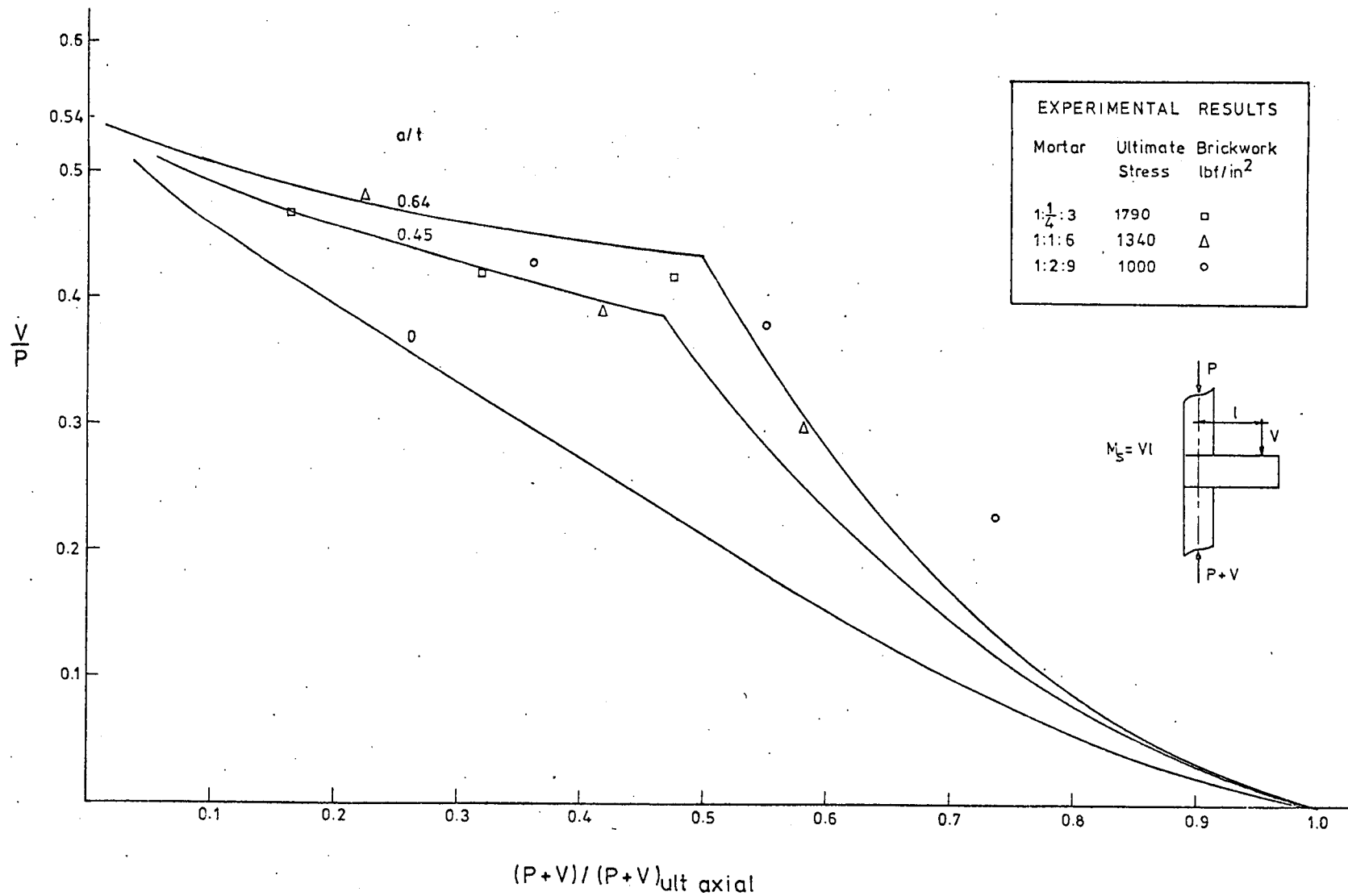


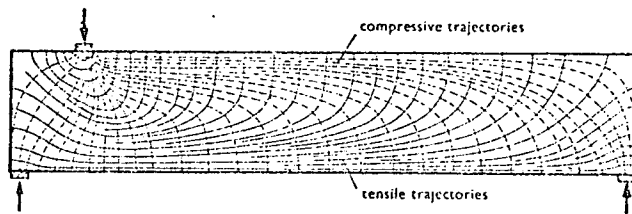
Fig. 6-11

ULTIMATE SLAB LOAD VS. LOAD IN BOTTOM WALL

6.5 FLOOR SLAB FAILURE

6.5.1 Introduction

Slab specifications and design calculations are given in Appendix 6. The failures observed were shear failures in the portion of the slab enclosed by the walls and a tensile failure in the slab at the face of the wall. The following diagram of the principal stress trajectories will be a help in visualizing the discussed failures*.



6.5.2 Shear Failure Round the End Reinforcement

Test No. 1 - 1:2:9 mortar walls at 200 lbf/in² precompression.

The concrete sheared round the end reinforcement as the slab began to lever the two wall sections apart (figs 6.12 & 6.13). The precompressive load was 10 tons producing an average shear stress of 200 lbf/in² over the concrete cross-section.

The theoretical failure stress of the concrete in shear without taking the reinforcement into account is 140 lbf/in² (equation A6.12 and section A6.4). The reinforcement at the end might have been of some help in increasing the shear strength beyond this value.

To stop this occurring again the slab was extended beyond the wall in the remaining tests.

* from a publication by Franz and Hiedenhoff (14).

6.5.3 Shear Failure Across the Reinforcement

Test No. 10 - 1: $\frac{1}{2}$:3 mortar walls at 600 lbf/in² precompression.

An inclined crack developed in the portion of the slab enclosed by the walls (fig 6.6). Horizontal cracks developed in the joints between the walls and the slab, the slab therefore resisting a precompressive load of 30 tons causing an average shearing stress of 410 lbf/in².

The calculated shear stress causing diagonal cracking is 315 lbf/in² (section A6.3.3). Stresses beyond this will not cause failure, the ultimate load going up to four times the cracking load.

Johnson (19) mentions that at small values of span/depth, the principal tensile stress at the neutral axis may be high enough for the diagonal crack to form before yielding of the tension reinforcement. The proportion of longitudinal reinforcement at the critical cross-section then has little influence on the cracking load, which is governed only by the dimensions of the cross-section and the strength of concrete.

If the slab had not been carried through the wall, the failure would have occurred round the end reinforcement.

6.5.4 Tensile Failure

Test No. 3 - 1:2:9 mortar walls at 400 lbf/in² precompression.

Failure was caused by tensile cracking, the tension steel yielding and the concrete hinging about the compression steel (fig 6.14). The recorded failure moment was 52 000 lbf in/ft.

The calculated value is 45 000 lbf in/ft (section A6.5). In a slab without compression steel the calculated ultimate moment would be approximately 33 000 lbf in/ft .

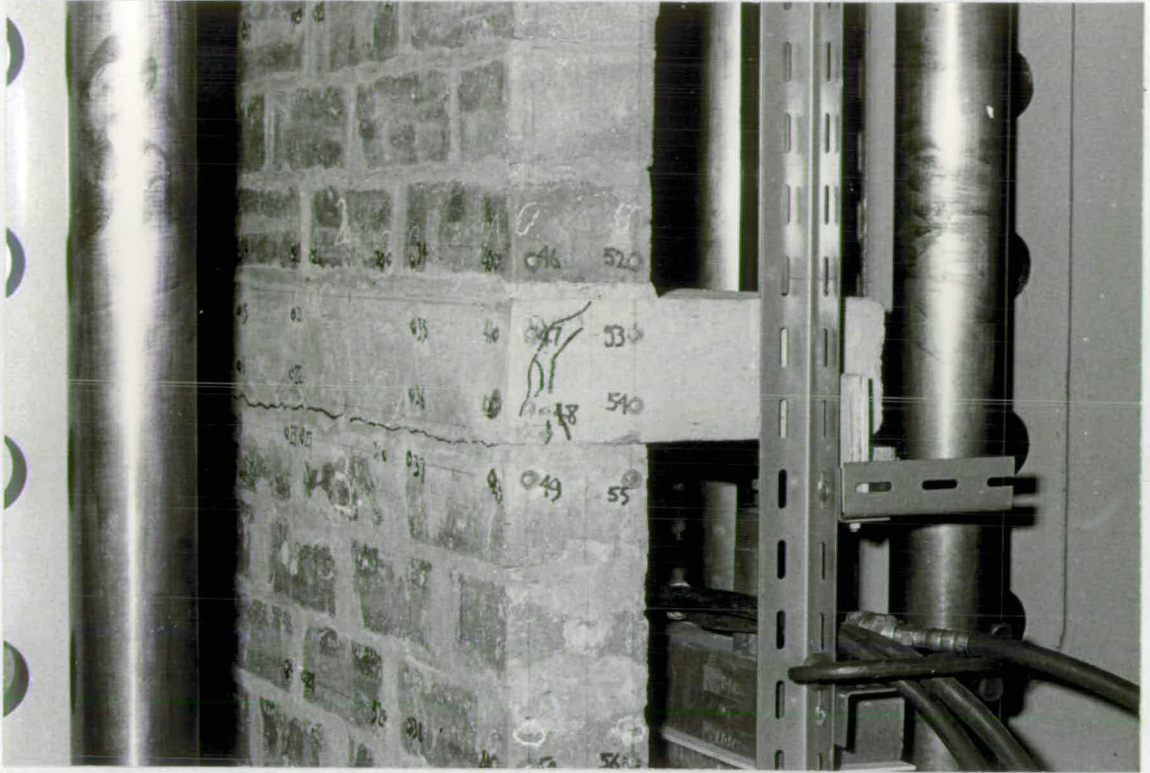


Figure 6.12 - Shear Failure in the Slab Round the End Reinforcement.
Test No. 1 .

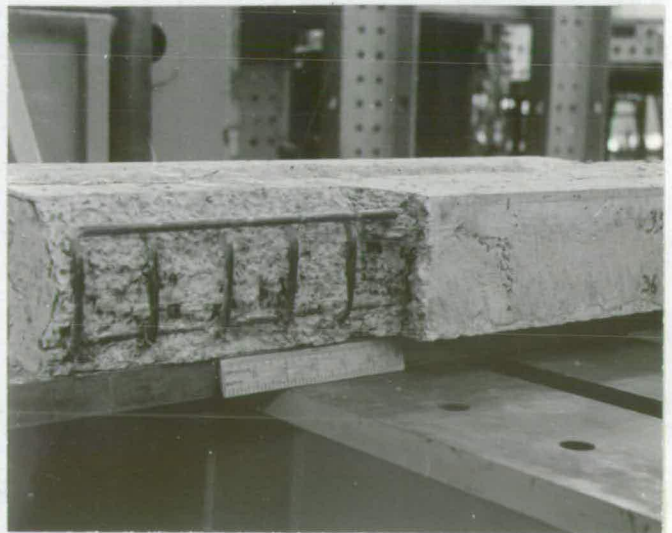


Figure 6.13 - View of the End Reinforcement in
the Slab after the Damaged Concrete
was Removed - Test No. 1 .

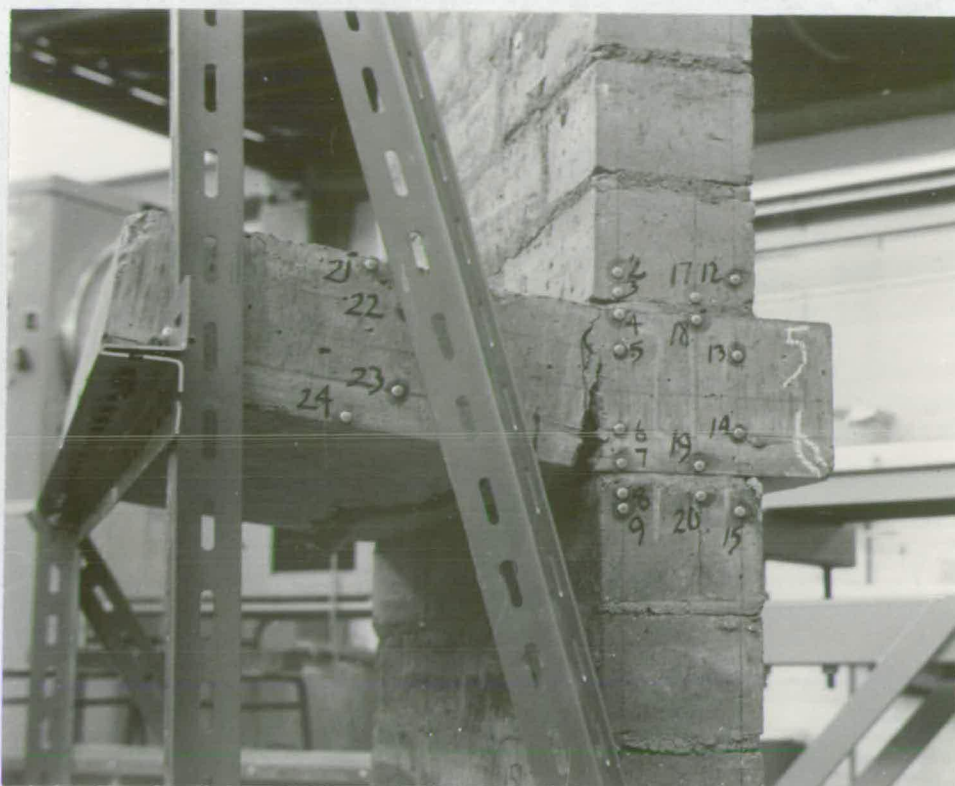


Figure 6.14 - Two Views of Tensile Failure in the Slab at the Face of the Wall - Test No. 3 .

6.6 CONCLUSIONS

1. After tensile cracking in a wall-floor slab connection, the bottom wall resists a greater proportion of the total applied moment because the slab reaction is displaced from the centre line of the wall.
2. With the wall stresses allowed by the British Code of Practice on Brickwork (8), failure at the wall-floor slab junction is usually confined to :
 1. equilibrium failure - the end of the floor levers the walls apart at constant moment causing horizontal cracks and local crushing of the joint with the weaker mortars.
 2. tensile failure of the floor slab at the inner face of the wall.
 3. shear failure round the end reinforcement or a diagonal crack across the reinforcement.
3. An explanation is given for the failure of short single leaf walls with no tensile strength under axial load and moment. If the wall has central gaps in the mortar joint, the predicted ultimate moment based on axial loading tests is much increased. The maximum moment such a wall can resist occurs when the precompression is half the ultimate axial stress.
4. The load reduction factors for eccentricity in the proposed revision of the British Code of Practice on Structural Brickwork (9) greatly underestimates the strength of the walls in the test models. As the factors are based on a solid wall this may partly explain the difference. Even so, the factors are too high at low eccentricities and should be reduced to a level obtained for a solid wall and an experimental stress-strain curve.

CHAPTER 7 - FLOOR SLAB - WALL INTERACTION IN A FULL SCALE BUILDING

7.1 INTRODUCTION

A full-scale, five storey brickwork building (figs 7.1 & 7.2) was built in a disused quarry to investigate its properties under lateral loading (33).

An investigation into the behaviour of the floor slabs at their junction with an outside wall is presented in this chapter. Two questions led to this investigation. Is there increasing deflection and end rotation of the floor slabs in the higher storey levels? What moment is transmitted by the floor slab to the outside wall?

A floor section supported on three of its sides (marked A in figure 7.2) was uniformly loaded. This was repeated for each floor level in turn. The free edge was instrumented to give vertical slab deflection and rotation at its junction with the outside wall. Strain was measured in the walls surrounding the loaded slab.

A simplified theoretical analysis is presented for the behaviour of the junction of the wall and the floor slab near to the free edge of the floor.

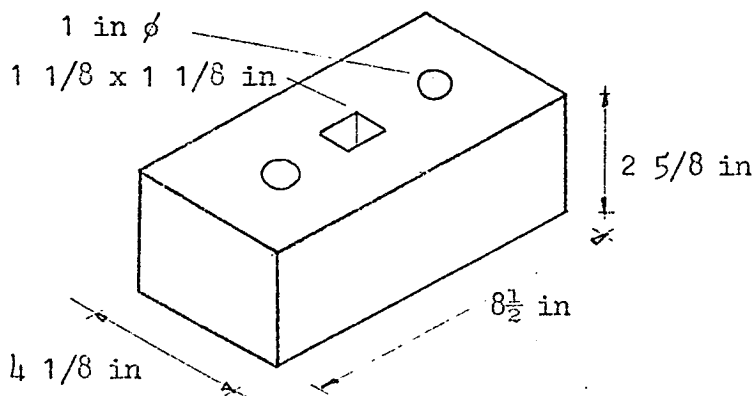
This investigation was a preliminary one. Further tests are in progress on a full-scale, five storey cavity wall structure built in the same quarry.

In this structure the walls and slabs are supported on two opposite sides only, making a theoretical analysis relatively easier.

7.2 MATERIALS

7.2.1 Brick

Perforated, wire cut bricks were used : 2 5/8 inch Coatham Stob Common Bricks. The average compressive strength of 10 bricks is 5020 lbf/in². (Tested in accordance with CP 3921 (10)).



7.2.2 Mortar

The mortar was a 1:¼:3 cement:lime:sand mix by volume. For proportioning of the lime and sand, batching boxes were used, their volumes in proportion to that of a bag of cement.

Cement - rapid-hardening Portland cement

Lime - hydrated white lime

Sand - a common building sand

The average compressive strength of 4 inch mortar cubes at 28 days was (tested in accordance with the BCRA Model Specification (5)) :

2000 lbf/in² - laboratory cured

1730 lbf/in² - site cured in air

7.2.3 Concrete

A 1:2:4 cement:fine aggregate:coarse aggregate mix by volume was used. The bottom two inches of the floor slab were precast while the top three inches were in-situ ready mixed concrete. For the in-situ concrete :

Cement - Ordinary Portland cement

Coarse Aggregate - ¾ in and ⅜ in maximum size

The average compressive strength of 4 inch laboratory cured concrete cubes at 28 days was 3165 lbf/in².

7.2.4 Brickwork

Prisms, six bricks high, were tested between plywood sheets to obtain their compressive strength and their stress-strain relationship. The average compressive strength of the brickwork at 28 days was 2450 lbf/in² (site cured in air).

The average compressive modulus was 1.2×10^6 lbf/in² - range from 0.9 to 1.7×10^6 lbf/in² (this excludes the 5th storey results where most prisms were damaged).

7.2.5 Floor Slabs

The floor slabs are composed of 2 inch precast 'Omnia Wide Slabs' with a 3 inch in-situ concrete topping (fig 7.3). The result is similar to an in-situ slab while there is also a saving of shuttering and time. The 2 inch precast sections do not bear onto the walls, therefore a good bond is obtained with the in-situ concrete. Mesh reinforcement (¼ in

square twisted bars at 8 in c/c) was provided in the bottom of the precast slab while similar reinforcement was provided in the top of the slab above the supports. The slab was designed to take a live load of 40 lbf/ft².

The modulus of elasticity to be used for the floor slabs presented some problems. Only two concrete cylinders were tested for their compressive modulus and these gave erratic results. The value used to obtain the theoretical slab deflections was taken to be 3×10^6 lbf/in². This is based on an empirical formula suggested by the American Concrete Institute (1).

$$E = 33 \sqrt{w^3 f'_c}$$

where f'_c = the concrete cylinder strength
 = $0.8^* \times 3165$ lbf/in²

w = the concrete density
 = 150 lbf/ft³ (value obtained from site cubes).

Poisson's ratio taken as 0.15 .

As a result of this uncertainty an extra floor slab was cast for the cavity wall structure mentioned in the introduction. An experimental value of the elastic modulus will be obtained from it and compared to the value obtained from cylinder and cube results.

*from reference 25, page 397 or reference 19, page 29 .

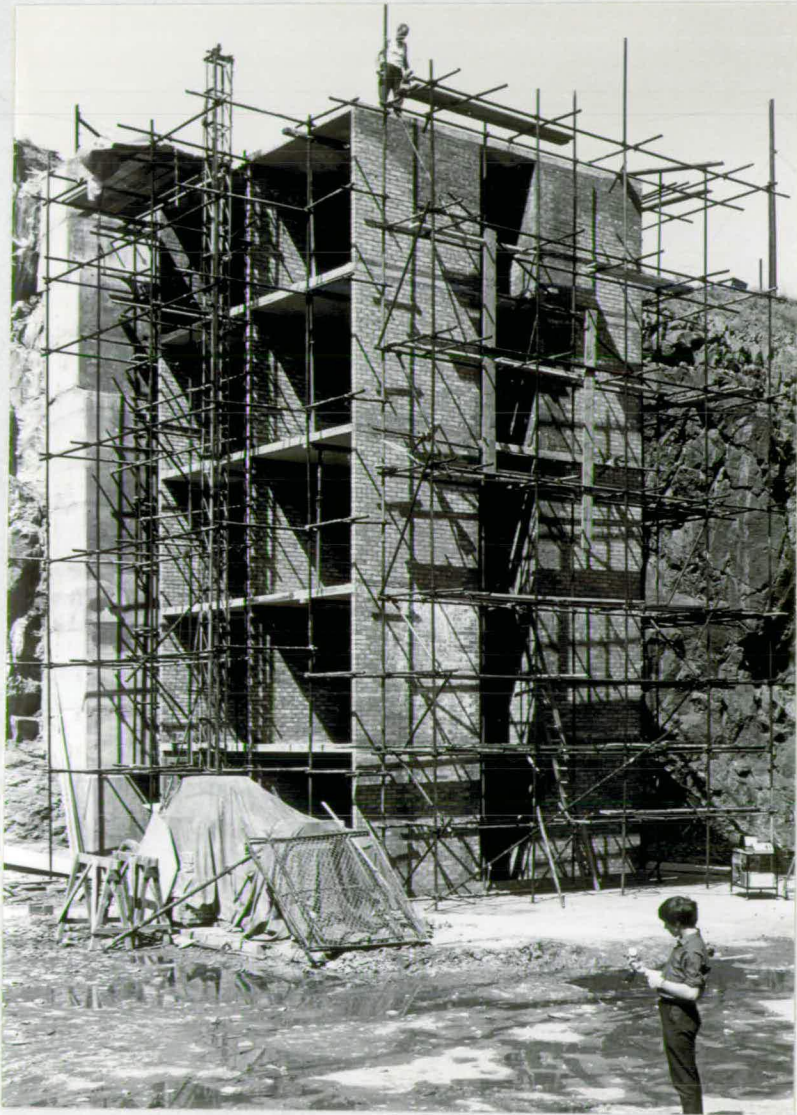


Figure 7.1 - View of the Five Storey Building

QUARRY
FACE

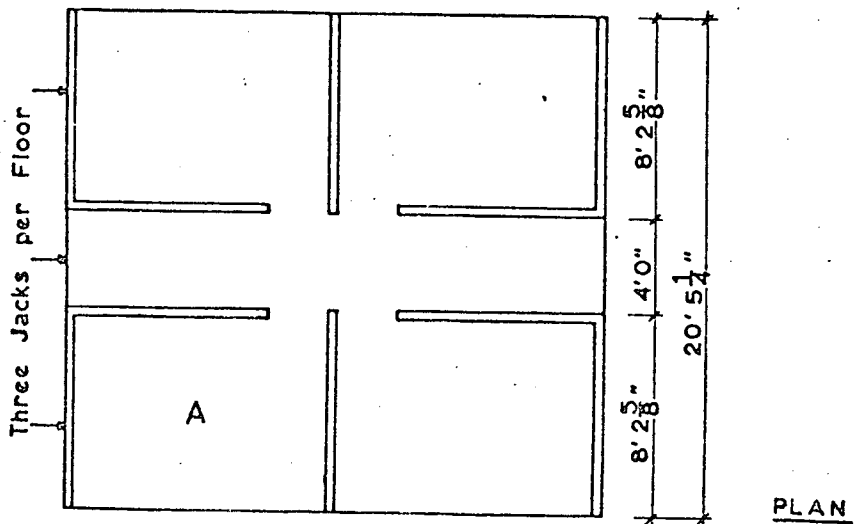
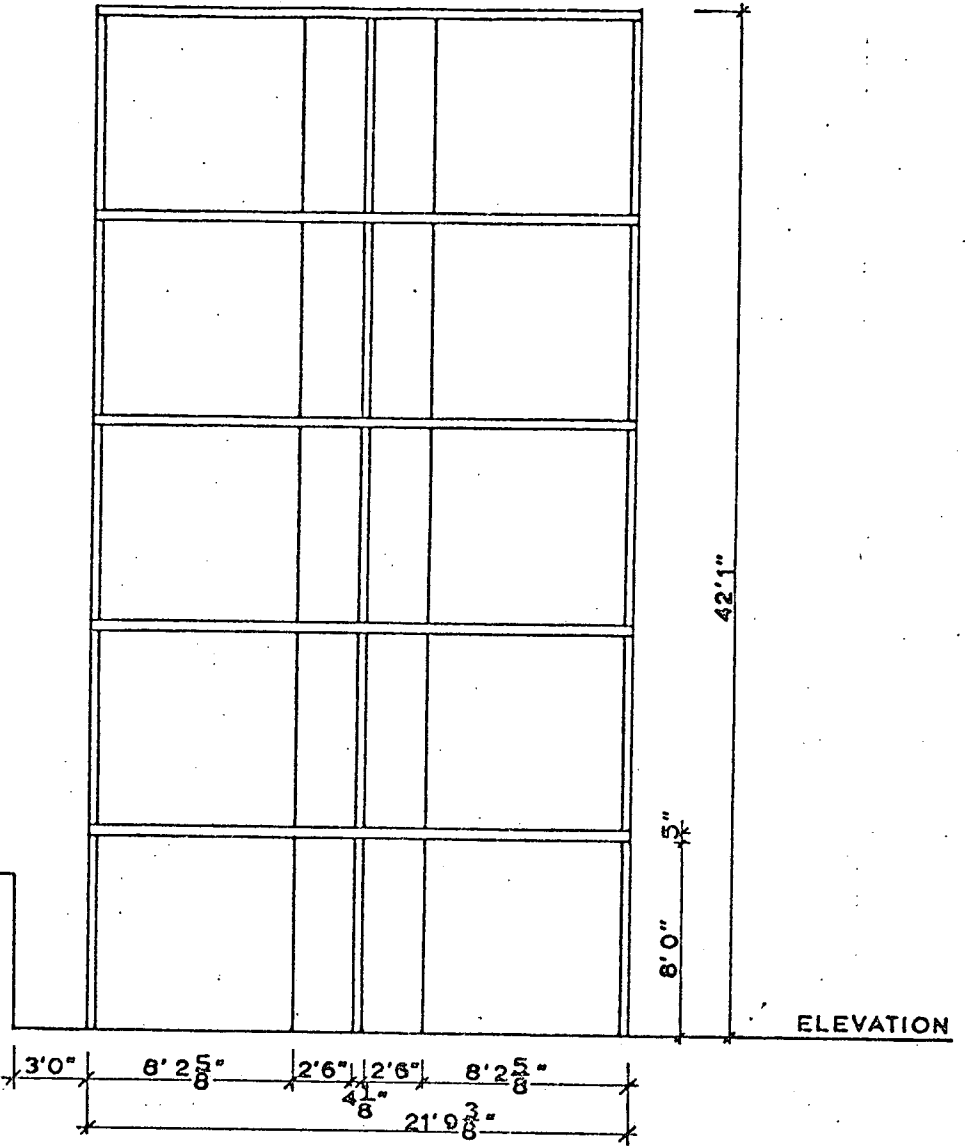
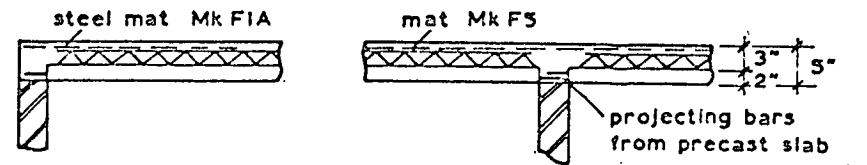
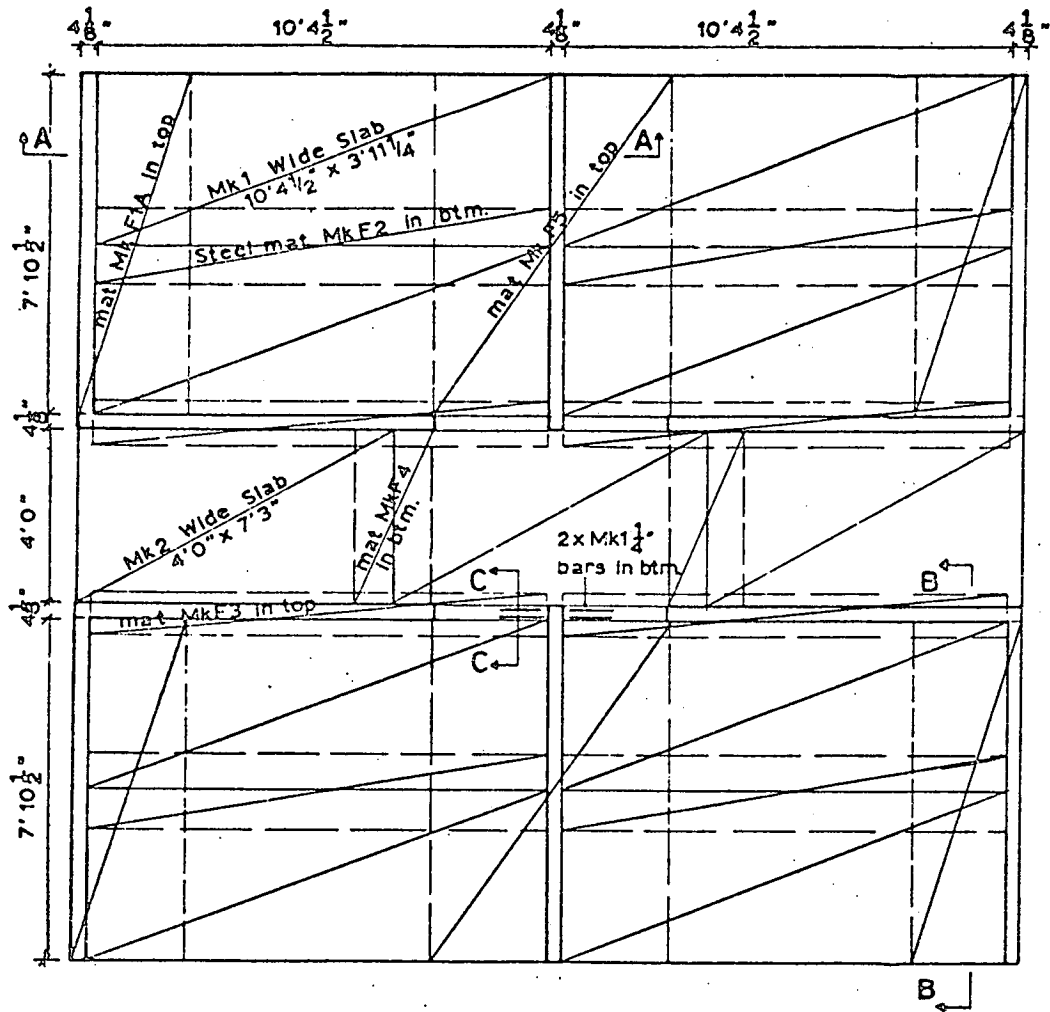
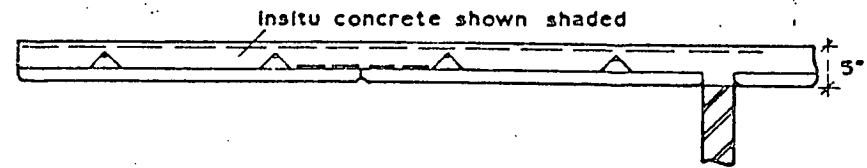


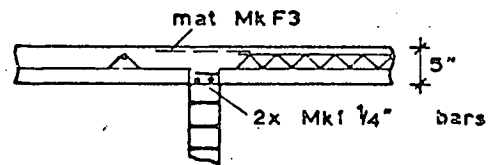
Figure 7.2 - Plan and Elevation of the Building



SECTION AA



SECTION BB



SECTION CC

Figure 7.3 - Layout of the Precast Slabs and Reinforcement in the In-Situ Concrete

7.3 PRECAUTIONS AND TECHNIQUE IN OUTDOOR TESTING

Testing a full scale structure in the open presents difficulties not encountered in the laboratory. To obtain reasonable results several points must be considered.

Plan observations so values can be confirmed. This is done for slab rotation which is measured by dial gauges and a clinometer. Strains in the wall and slab deflection give indirect confirmation.

With limited experienced personnel, there must be economy in observations to ensure reliable results. Recording of results must also be simplified. Printed forms were provided for gauge and clinometer readings while strain gauge readings were recorded on a portable tape recorder. Consistent numbering of gauge points is important - later analysis of results is then much easier. The same numbering is used on each floor, strain gauge points on opposite sides of a wall having the same initial number.

All gauge points were measured after the floor was unloaded. The results could then be compared to the initial reading as a check on accuracy. Again, to improve accuracy it is best to repeat the tests - this was done in a few cases.

Atmospheric effects are important. If possible, tests should be conducted on dry, overcast, calm days. This ensures a steady temperature and little wind. Wind affects the dial gauge supporting frames while sun causes temperature variations, thermal expansion of the walls ($\approx 6 \times 10^{-6}/^{\circ}\text{C}$) masking some of the small strains due to slab load and also affecting the dial gauge supporting frames.

Some good reviews on experimental technique are given by Rocha (29) and a RILEM symposium on the Observation of Structures (28).

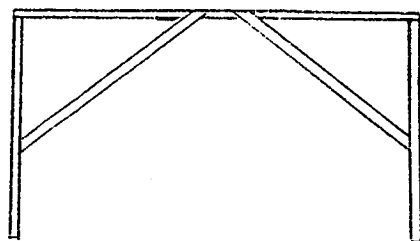
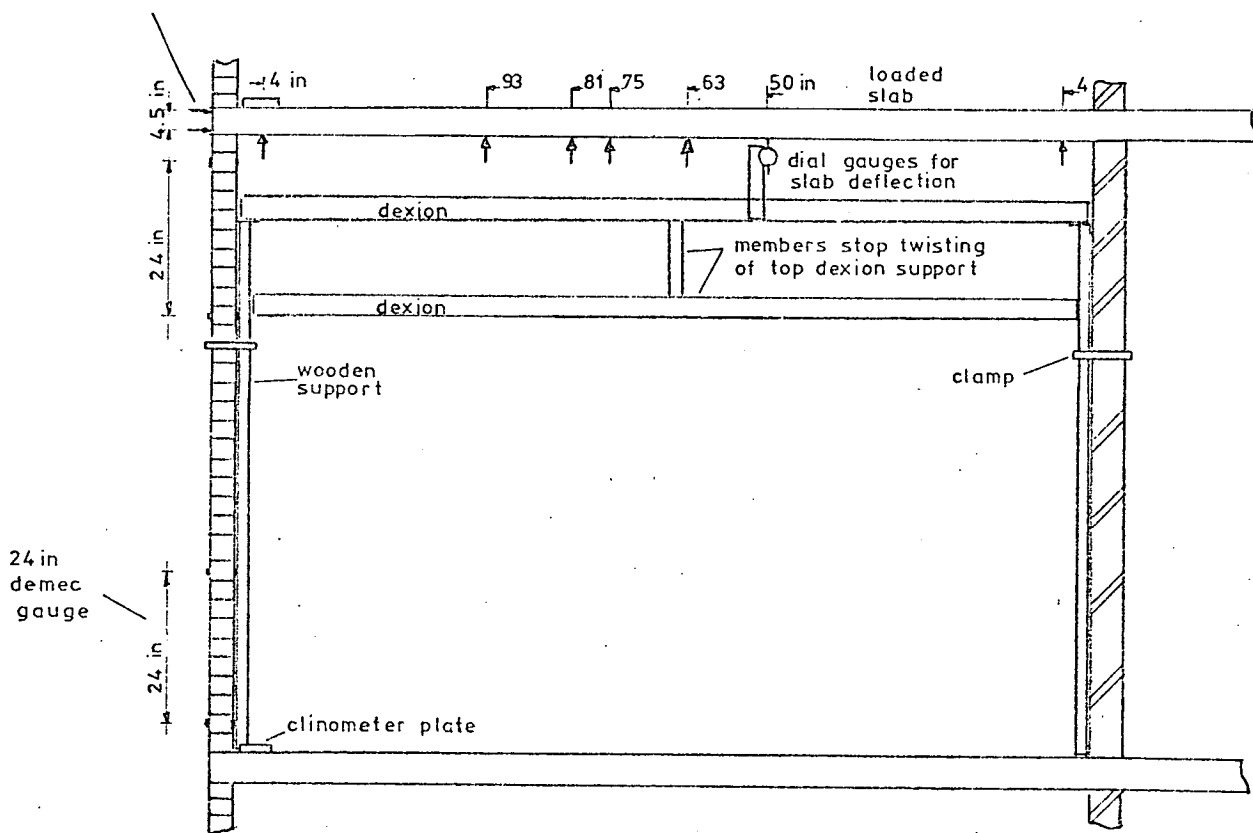
The floor slabs were loaded with bricks (fig 7.4) - the same bricks as those used for the walls. These were available in quantity and easy to handle. The floors were divided into sixteen rectangles by chalk lines. Into each of these rectangles was placed 19 + 19 bricks equivalent to loadings of 20 and 40 lbf/ft². For most tests ten bricks were weighed as a check on slab load. Differences in weight were small and mainly caused by water absorption. Bricks were kept under cover when not in use. Newman (26) gives details on slab loading tests.

7.4 SLAB LOADING TESTS

7.4.1 Experimental Measurements

The position of the gauges is best illustrated by the following diagram :

dial gauges measuring slab rotation supported by dexion fixed to quarry face



alternative dial gauge support system but is affected more by temperature

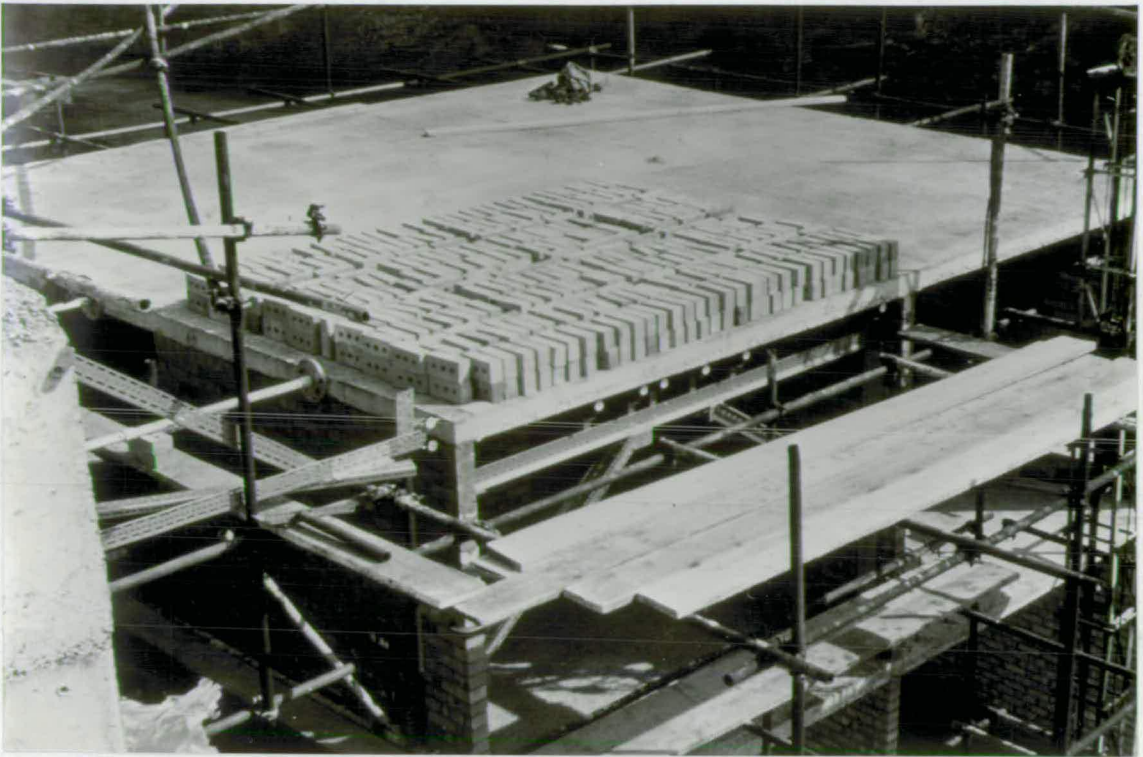


Figure 7.4 - The 5th Floor Loaded to 40 lbf/ft^2

7.4.2 Experimental Procedure

Initial gauge readings were recorded. The floor slab was then loaded to 20 lbf/ft^2 . This took about 20 minutes as the bricks were brought up in a wheelbarrow by a diesel powered hoist. The dial gauge and clinometer readings were recorded. Next the slab load was increased to 40 lbf/ft^2 and the gauges read in the following order : dial gauges, demec readings, clinometer and finally the dial gauges again. This took 30 to 40 minutes. The slab was then unloaded and all the gauges read again. An average test was four hours long.

7.4.3 Experimental Results

1. Slab Rotation at the Joint

Experimental results for slab rotation from both the dial gauges and the clinometer are shown in Table 7.1 .

2. Slab Deflection

The deflection along the free edge of the floor slab under a uniform load of 40 lbf/ft^2 is shown in figure 7.5 .

3. Wall Strains Near the Wall-Slab Junction

The bending strain distribution along the walls, above and below the floor slab, is shown in figure 7.6 . The axial strains are not presented as they are small as well as showing considerable scatter.

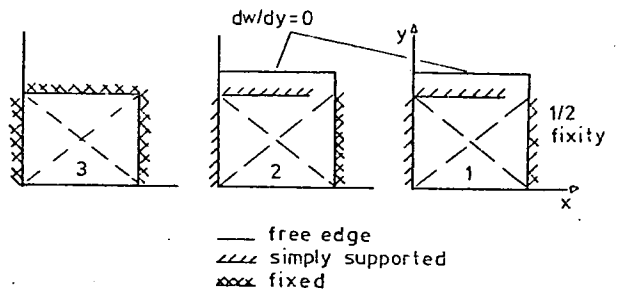
TABLE 7.1 - ROTATION OF THE FLOOR AT ITS JUNCTION WITH AN OUTSIDE BRICK WALL

Floor Slab Load ▽ No.	Experimental Values mrad					
	20 lbf/ft^2		40 lbf/ft^2		0 lbf/ft^2	
	Clino.	Dial Gauge	Clino.	Dial Gauge	Clino.	Dial Gauge
1	0.13	0.16	0.30	0.40	0.07	0.11
2	0.23	0.13	-	0.33	(-.27)	0.22
3	0.10	0.13	0.23	0.24	-0.07	-0.07
	0.13	0.07	0.28	0.22	0	-0.07
4	0.15	0.18	0.40	0.36	-0.02	0.07
	0.17	0.13	0.28	0.29	0	0.07
5	0.27	0.24	0.36	-	0	(-.47)
	-	0.27	-	0.47	-	0.09

Notes :

1. Values in brackets - change in angle from 40 to 0 lbf/ft^2 load.
2. Two sets of readings are the results of two tests.
3. Clinometer resolution : $\approx 0.03 \text{ mrad}$ (7 sec)
Dial Gauge resolution : $\approx 0.02 \text{ mrad}$ (5 sec)

* + Results
 Uniform Load
 40 lb/ft²



Rotation at outside wall:
 $\phi_1 = 0.42 \text{ mrad}$ $\phi_2 = 0.335 \text{ mrad}$ $\phi_3 = 0 \text{ mrad}$

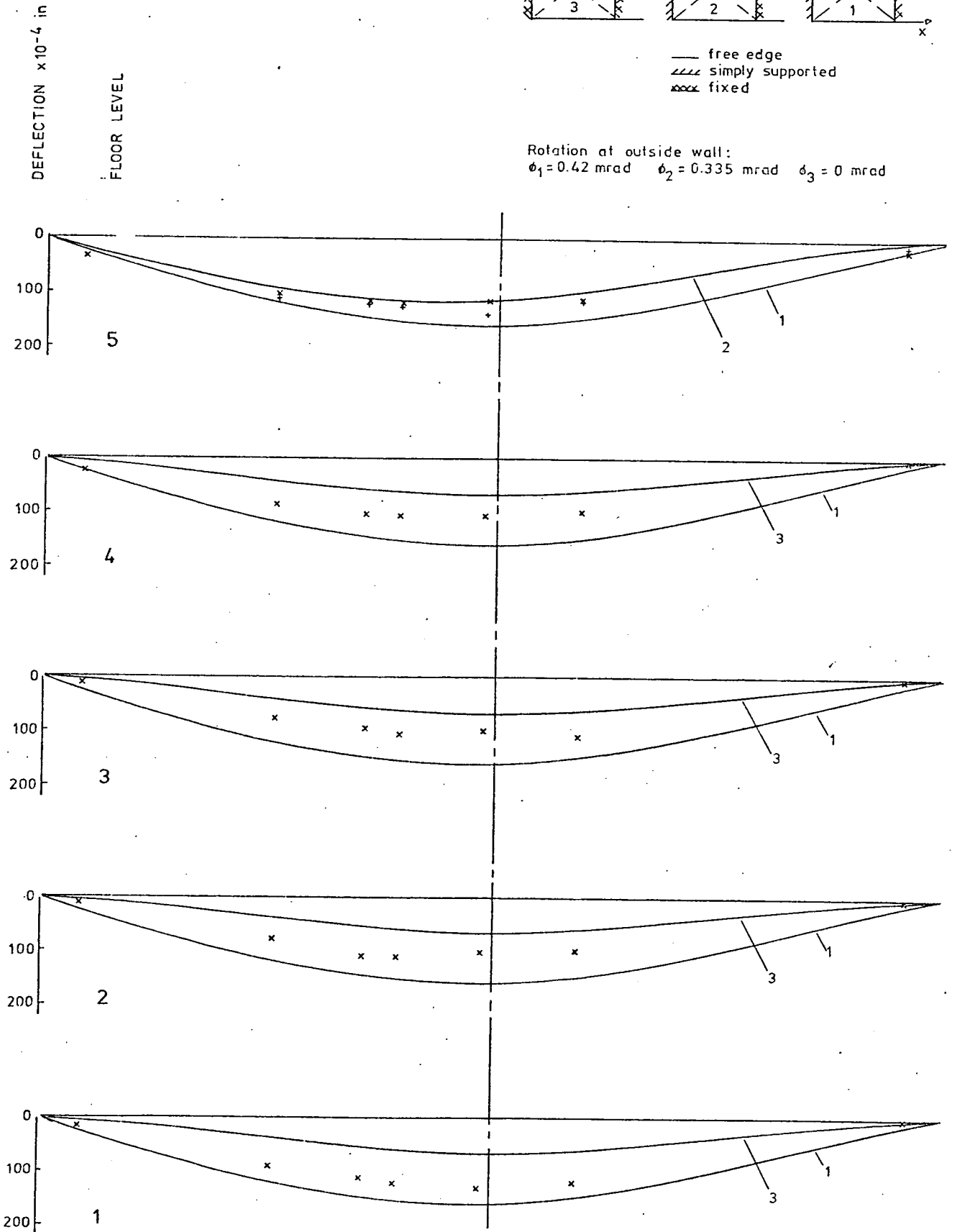


Fig. 7.5 DEFLECTION OF THE FREE EDGE OF THE FLOOR

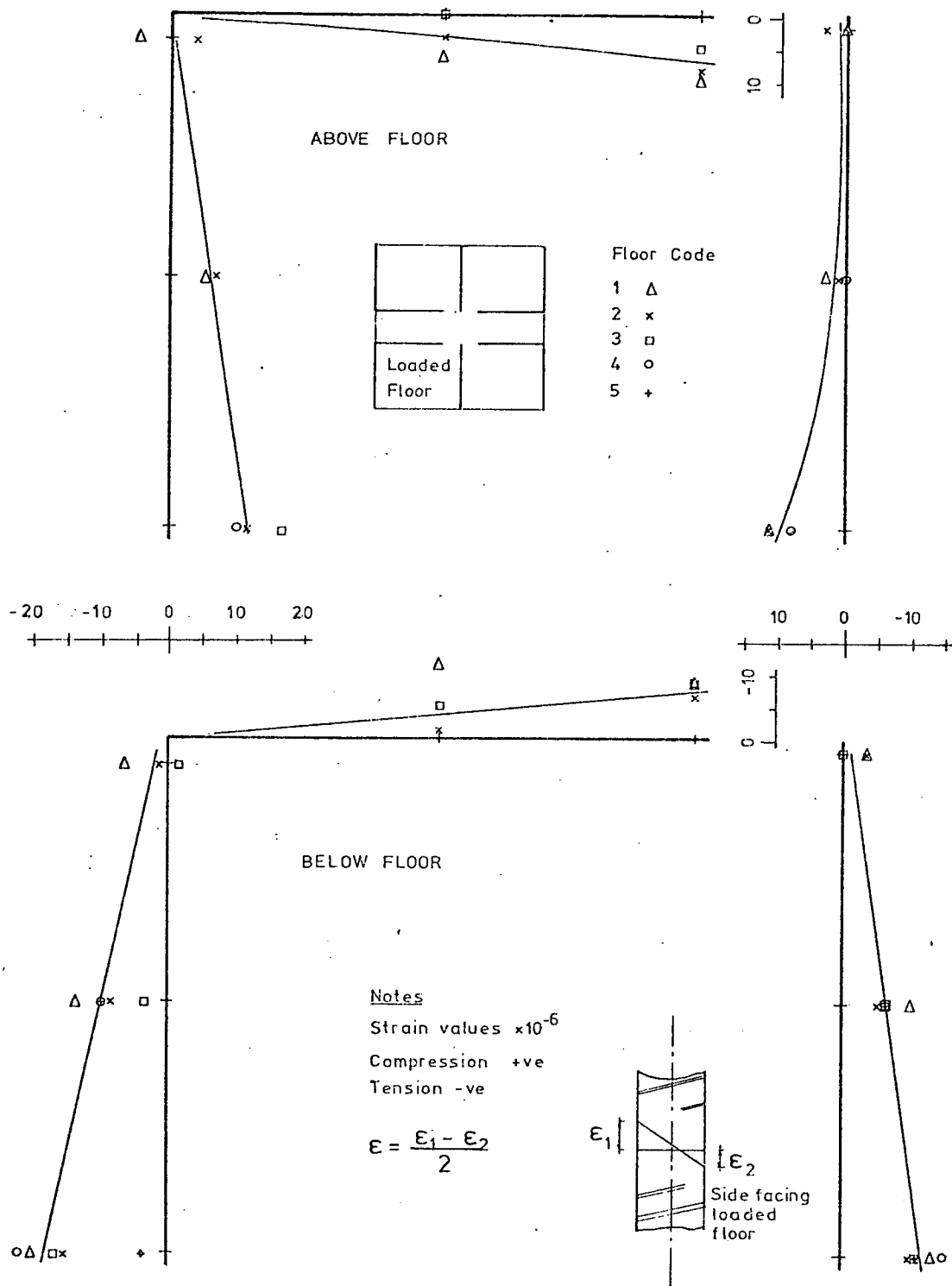


Fig. 7.6 FLEXURAL STRAINS IN WALLS SURROUNDING LOADED FLOOR

7.5 ANALYSIS OF RESULTS

7.5.1 Introduction

The analysis is meant for walls and slabs spanning in one direction but has been adapted to explain the trend of the experimental results along the free edge of the slab where its behaviour tends most to a one way system. More needs to be known about wall behaviour before a more complex analysis is used.

The effect of axial load on the lateral deflection can be neglected as the loads are low and the wall is restrained at one end.

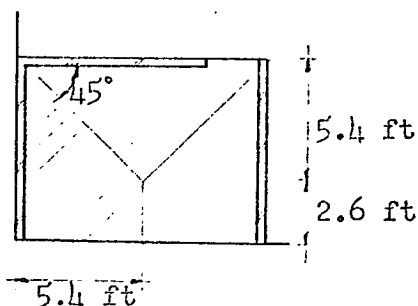
The outside walls are assumed to have the same properties above and below the slab, thus before tensile cracking occurs, half the slab restraining moment is taken by each wall.

The analysis is divided into the following sections :

1. An estimate of the average dead load stresses in the outside walls.
2. End moment - rotation relationship for the walls.
3. End moment - rotation relationship for the slabs together with the deflection of the slabs.
4. Combining relations (2) and (3) to give the equilibrium position for the wall and slab.
5. Evaluating the moments applied to the wall together with the resulting strains in the wall.

7.5.2 Precompression

The precompression was estimated on the basis of the following sketch. It assumes uniform support conditions for the slab which in practice is not the case but a more accurate analysis is not warranted.



1. Weight of Brickwork

The weight of brickwork is taken to be 320 lbf/ft run of 8 ft high wall. The stress at the bottom of a wall due to its own weight = 6.5 lbf/in².

2. Weight of Floor Slabs

Dead load = 62.5 lbf/ft²

Live Load = 40 lbf/ft² (one floor at a time).

Average stress over wall due to slab dead load = 4.5 lbf/in².

Average stress over wall due to slab live load = 3 lbf/in².

3. Average Stress in the Outside Walls Due to Dead Load

Floor	Stress (lbf/in ²)	Above Slab	Below Slab
1		44	49
2		33	38
3		22	27
4		11	16
5		0	5

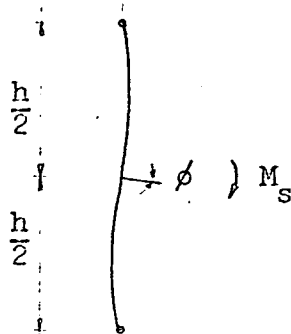
7.5.3 Rotation of the Walls at the Junction with the Slab

1. End Moment-Rotation Relationship

The initial portion of the wall moment-rotation relationship will be linear. As tensile cracking develops at the joint, the relationship becomes non-linear tending to a limiting equilibrium moment.

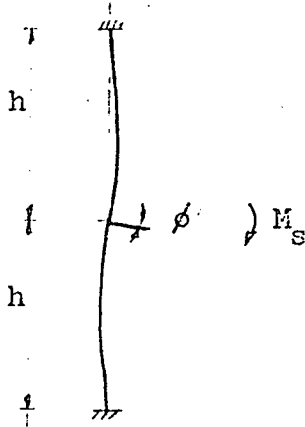
For wall rotation the previous loading history must be taken into account as the moment-rotation relationship is not linear throughout its whole range. Thus dead load must be considered. It is uniformly applied to all the floor slabs while the live load is applied to only one slab at a time.

The slab dead load will induce an approximately equal moment in the top and bottom walls of a joint. The slab supports were not removed before the next storey was built. For dead load the following deflection pattern is assumed :



$$\begin{aligned} \phi/M_s &= h/12EI \\ &= 97 \text{ nrad/lbf in/ft} \end{aligned}$$

For live load another pattern is assumed :



$$\begin{aligned}\phi/M_s &= h/8EI \\ &= 145 \text{ nrad/lbf in/ft}\end{aligned}$$

where :

M_s = slab restraining moment

$E = 1.2 \times 10^6 \text{ lbf/in}^2$

$I = 69 \text{ in}^4$

$h = 96 \text{ in}$

ϕ = wall rotation at junction with the slab

2. Moment Causing Tensile Cracking at the Joint

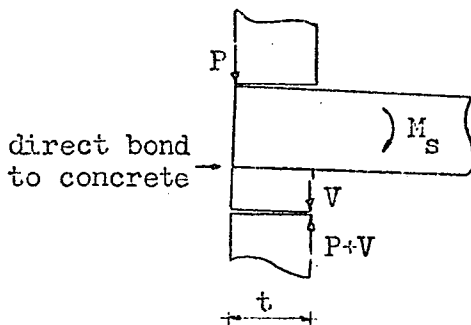
If there is an 1 inch gap in the mortar joint (width of perforations and mortar furrowing) cracking will be delayed*.

The ratio of mortar joint gap to wall thickness, a/t , becomes 0.24 giving from figure 4.9 an eccentricity ratio, $e/t = 0.22$, the eccentricity necessary to start tensile cracks for a material with no tensile strength. Thus tensile cracking starts when $e = 0.9 \text{ in}$ as opposed to $e = 0.7 \text{ in}$ for a solid section. It is the point at which the moment-rotation relationship becomes non-linear.

The cracking moment is given by $2 \sigma_b t (0.22t)$ where σ is the dead load stress.

3. Ultimate Equilibrium Moment

The stresses in the walls are low and thus it is possible for the equilibrium moment to be reached. The limiting equilibrium moment is reached when the eccentricity equals half the wall width.



Slab restraining moment = Pt

Moment in upper wall = $Pt/2$

Moment in lower wall = $(P+V)t/2$

*This is an assumption but is inserted to show its effect on the calculation procedure. Its effect on the compressive modulus is small.

These equilibrium moments are based on a constant precompression. But for this building, uplift at the joint can cause considerable increases in precompression (18) causing an increase in the limiting equilibrium moment.

The equilibrium moment is the upper limit for the moment-rotation curve - the rotation keeps increasing at constant moment. In terms of the dead load stress the limiting moment is given by $(\sigma_{bt})t$.

The moment-rotation relationships are plotted in figure 7.7. The non-linear part is an estimate.

7.5.4 Rotation and Deflection of the Floor Slab

1. Floor Slab Deflection and Rotation

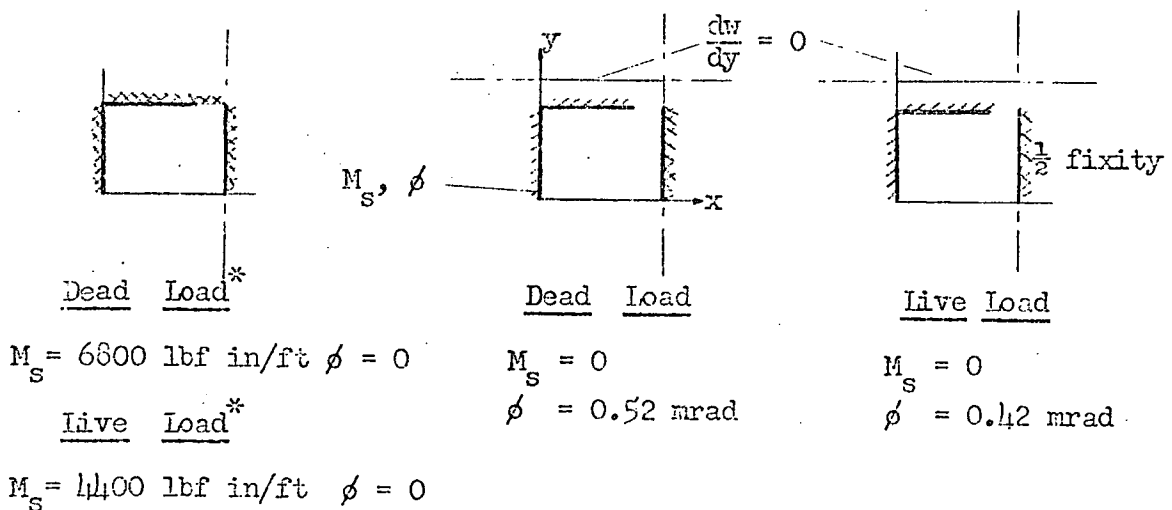
The floor slab deflection and end rotation were analysed using a computer program. Initially a finite difference technique was used and later a standard finite element program (see Appendix 7).

This was tried for various boundary conditions - combinations of fixed and simple supports. The deflections for the free edge are shown in figure 7.4.

2. Moment-Rotation Relationships

Consider the junction of the slab with the outside wall. The end rotation and end restraining moment can vary between two limits :

1. Fully fixed - maximum moment with no rotation.
2. Simply supported - no restraining moment with maximum rotation.



* Fixing moments from Theory of Plates & Shells by Timoshenko & Woinowsky-Krieger (36).

The limits are plotted on the graph in figure 7.6 and a straight line drawn between them. This assumes a linear variation which is reasonable as long as no cracking occurs at the other boundaries of the slab and the slab has a constant stiffness within the load range taken.

7.5.5 Interaction of the Floor and the Wall

1. Slab Restraining Moment and End Rotation

The slab restraining moment and end rotation are given by the intersection of the wall and slab moment-rotation curves.

This is initially found for the slab dead load and then for the slab dead load plus live load. The difference gives the moment and rotation due to live load. If the wall moment-rotation curves were linear these values could be found directly taking only the live load into account. The wall curves are different for dead and live load, the latter having a smaller slope.

The method used here is a graphical form of moment distribution which is easier to work with when the moment-rotation relationships become non-linear.

The slab restraining moments and end rotations are given in Table 7.2 .

2. Moment Applied to the Walls

The moments applied to the walls at their junction with the floor slab are given in Table 7.3 . The slab moment is distributed equally between the walls above and below. If tensile cracks occur in the joint with the bottom wall, the wall will have to resist an additional moment from an eccentrically applied slab load. Section 6.2.3 explains the procedure for calculating this additional moment.

Before cracking occurs, the ratio of slab restraining moment to slab load is approximately 11 inches which coincides with the ratio in the test models.

3. Strains in the Wall

Table 7.4 shows the bending strains for the outside wall towards the free edge of the slab at the level where the experimental strain measurements were made. The assumed moment distribution is also shown.

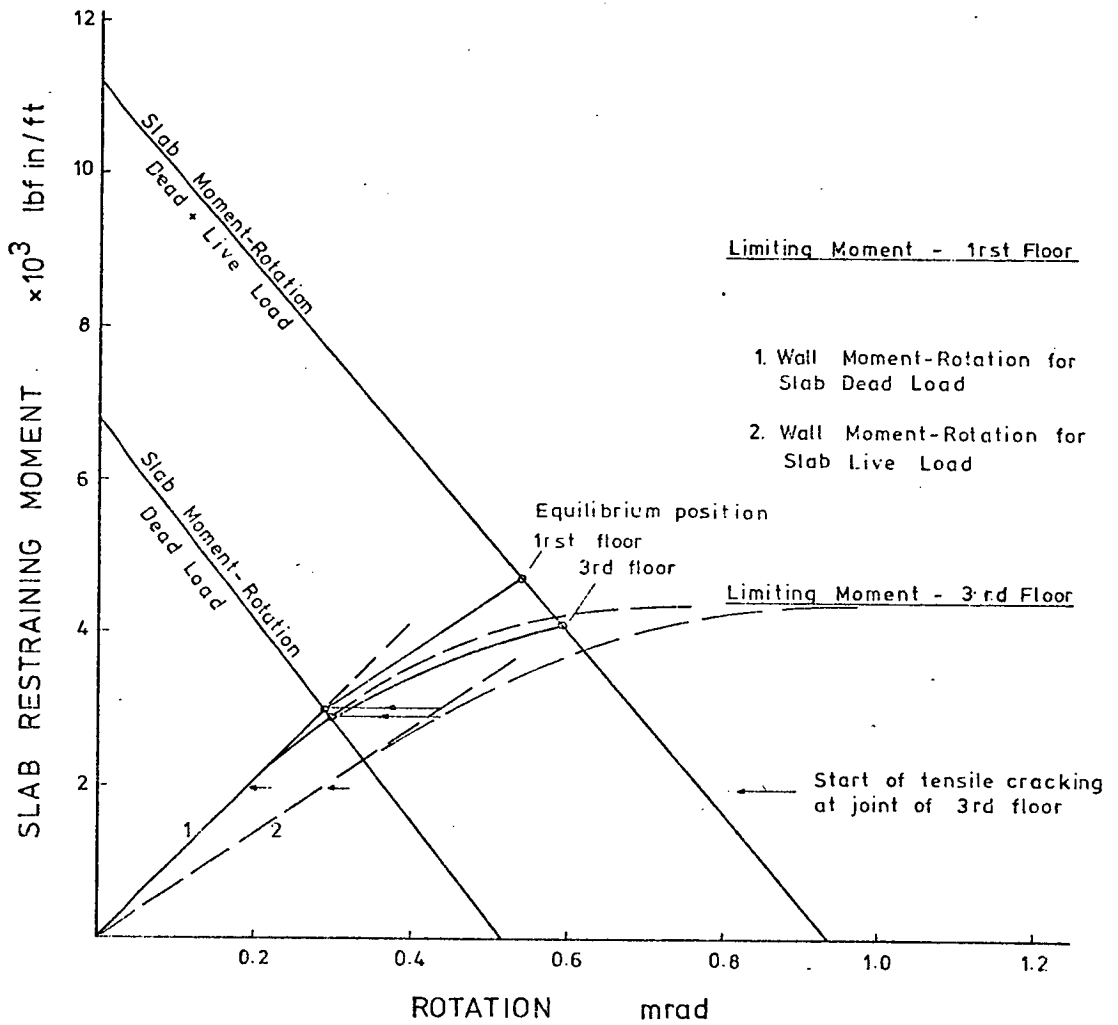


Figure 7.7 - End Moment-Rotation Curves for Floor and Wall

TABLE 7.2 - FLOOR RESTRAINING MOMENT AND END ROTATION

Floor	Dead Load		Live Load		Live+Dead Load	
	Moment	Rotation	Moment	Rotation	Moment	Rotation
	lbf in	mrad	lbf in	mrad	lbf in	mrad
1	3000 (44)	0.29	1700 (39)	0.25	4700	0.54
3	2900 (43)	0.30	1200 (27)	0.29	4100	0.59
5	0	0.52	0	0.42	0	0.94

Note : Values in brackets are percentage of full fixity (no wall rotation).

TABLE 7.3 - MOMENTS APPLIED TO THE OUTSIDE WALLS

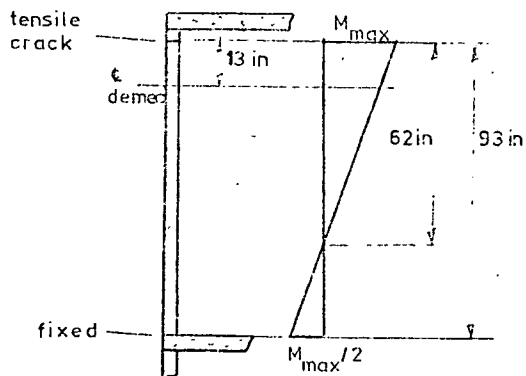
Floor	Wall	Moment lbf in/ft					
		Dead Load		Live Load		Live+Dead Load	
		Eccentric Slab Load	1/2 Slab Moment	Eccentric Slab Load	1/2 Slab Moment	Eccentric Slab Load	1/2 Slab Moment
1	Upper	-	1500	-	850	-	2350
	Lower	0	1500	0	850	0	2350
3	Upper	-	1450	-	600	-	2050
	Lower	120	1450	535	600	655	2050
5	Lower	460	0	300	0	760	0

TABLE 7.4 - STRAINS IN THE WALLS DUE TO LIVE LOAD

Floor	1		3		5
Wall	Upper	Lower	Upper	Lower	Lower
Bending Strain $\times 10^{-6}$	+15	+15	+10	+20	+6

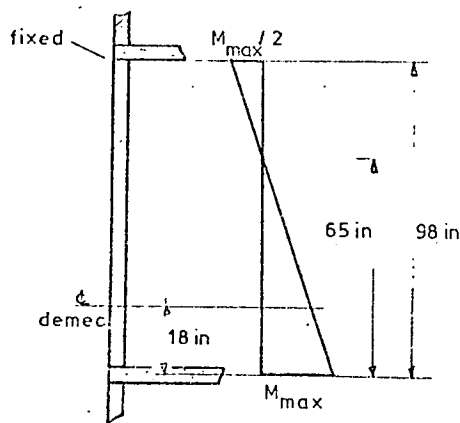
Notes : Bending strains given by $\pm M/EZ$ where $E = 1.2 \times 10^6$ lbf/in²
 Strains at demec level. $Z = 34$ in³.
 Assumed Moment Distribution :

Top Floor



$$M_{demec} = 0.79M_{max}$$

Other Floors



$$M_{demec} = 0.72M_{max}$$

7.6 DISCUSSION

This chapter measures the behaviour of the joint under working loads in a full-scale structure. Because joint behaviour under working loads was investigated outside the laboratory, the small deformations due to slab forces are difficult to measure accurately. In the model joint tests there were higher loads and deformations under laboratory conditions.

The slab deflections causing the largest gauge readings gave the best results, the residual deflection on unloading being comparatively small (approximately 7%).

The slab end rotations show larger variations but this is mainly due to the smaller deformations measured - errors become more important. The difference between two gauge readings was no more than about 20 divisions (0.002 in).

With strain measurements, only the difference of the strains on opposite sides of the wall, equivalent to bending strain, gave good enough readings to show a general trend. The sum of the strains, equivalent to the axial strain, gave too large a scatter (compression +ve, tension -ve).

This shows the care and accuracy needed to obtain good results.

The theory predicts the general trend of the results with slab deflections falling within the limits of the theoretical calculations - these are based on the assumption that the correct section properties have been used.

The slab rotations for the first four floors are approximately in the same range, experimental scatter making it difficult to detect any differences. The roof slab definitely showed larger end rotations but less so with slab deflection. There are also bending strains in the walls caused by the slab, the theory showing that the slab restraining moments are approximately 30% of the full fixing moment. The maximum calculated restraining moment (including dead and live load) is 4700 lbf in/ft. This would cause a tensile stress of approximately 100 lbf/in^2 in the slab. But the concrete can take an estimated tensile stress of 500 lbf/in^2 (1)*, thus no cracking would occur in practice but nevertheless some nominal top reinforcement should be provided. The slab centre span moment will also be reduced.

* $7.5 \sqrt{f'_c}$ to $12 \sqrt{f'_c}$ (375 to 600 lbf/in²) where $f'_c = 0.8 \times 3100 \text{ lbf/in}^2$

Changes in precompression do not seem to alter the slab rotations nor the wall bending strains. This confirms the results obtained from the model joint tests.

When cracking occurs, the precompression will have an effect but while theoretically the third and fourth floors are expected to develop cracks, the experimental results do not definitely show this. The roof slab definitely cracked at the joint (one course down from the slab) to at least half way along the outside wall. The end brick of the top course at the free edge was in fact fully separated from the brick below due to faulty erection of edge shuttering used for placing the roof slab.

These tests have been a good lesson in experimental technique outdoors and have shown it is possible to obtain reasonable results under working loads.

7.7 CONCLUSIONS

1. If there are no tensile cracks in the joint, the precompression does not affect the slab restraining moment. This is confirmed by the model joint tests.
2. The slab restraining moment can be quite considerable - up to an estimated 30% of full fixity in these tests. Top reinforcement should be provided although the tensile strength of the concrete was not exceeded.
3. Tensile cracking occurs in joints with very low precompressions. This occurred in the roof slab. Although no moment is transferred from the slab, the slab load is applied eccentrically.
4. With low loads, the possible failures are confined to cracking at the joint with possible tensile cracks in the slab at its junction with the wall.

CHAPTER 8 - GENERAL CONCLUSIONS AND SUGGESTIONS FOR FURTHER RESEARCH

8.1 GENERAL CONCLUSIONS

A knowledge of the behaviour of the joint, wall and floor is needed to find the moment distribution between the floors and walls. The wall and the wall-slab joint have been investigated for a concrete slab bearing fully into a single leaf brick wall.

1. Stress-Strain Relationship of the Wall Under Axial Load

The stronger the wall the more linear the stress-strain curve at low stresses - walls with increasing mortar strength. Over the precompressive stresses used in this thesis the 1: $\frac{1}{4}$:3 mortar wall has a linear curve while the 1:1:6 and 1:2:9 mortar walls become non-linear in this range (reducing modulus with increasing stress).

On unloading a different stress-strain path is observed of increased modulus, and a permanent strain occurs at zero stress. The permanent strain and the ratio of unloading to loading modulus (at the point of maximum stress) increase with decreasing brickwork strength and with increasing stress levels. On reloading there is a more linear stress-strain curve (except at very low stresses) up to the point of the maximum previously attained stress - the curve may be considered to be equivalent to the initial tangent modulus.

The experimental compression modulus based on a solid cross-section is underestimated if there are central gaps in the mortar joint.

2. Flexural Behaviour of the Wall due to Floor Loading

No Tensile Cracks

The flexural behaviour of the wall is related to its stress-strain relationship. A non-linear stress-strain curve (reducing modulus) causes increased rotations with increasing stress levels while an unloading curve with a higher modulus decreases the rotation.

Central gaps in the mortar joint must be taken into account if the stress-strain relationship is found experimentally. Otherwise the calculated compression modulus will be underestimated.

A linear theory is proposed taking into account a central gap in the mortar joint and an unloading modulus different from the loading modulus. This can be used with accuracy with the $1:\frac{1}{4}:3$ mortar brickwork.

The experimental moment-rotation curves of the slab at the joint all have an initial approximately linear portion. The initial slope of this curve decreases with decrease in brickwork strength. The linear theory overestimates the experimental initial slope. Reasons for this could be variations in assumed properties and local deformation at the joint. Assuming a solid section and a single compression modulus will underestimate the experimental slope.

The linear theory also predicts the moments and load applied to the wall by the floor slab, the best accuracy being obtained with the $1:\frac{1}{4}:3$ mortar walls.

The experimental moment-rotation curves for a given mortar wall have approximately the same initial slope for the three different, constant precompressions applied to the wall. Thus if there are no tensile cracks precompression has little effect on slab rotation. An exception to this may occur when the precompressive stress causes a reduction in the wall tangent compression modulus allowing increased slab rotation.

Tensile Cracks

In a solid, linearly elastic, rectangular wall, tension will occur when the load eccentricity exceeds one-sixth of the wall thickness. A non-linear stress-strain curve (reducing modulus) and/or residual strain at zero stress will decrease the eccentricity necessary to cause tension while a central gap in the mortar joint will increase the eccentricity.

Horizontal tensile cracking occurs in the mortar joints as these are usually weaker in tension than the bricks. The cracking reduces the slope of the moment-rotation curve of the slab, the slope becoming zero when a limiting eccentricity approaching half the wall thickness is reached or when failure occurs in the wall or slab. The maximum eccentricity is limited by local deformation and failure at the joint. In the test models the limit ranged from $e/t = 0.42$ to 0.45 . Over the cracking range an increase in wall precompression will reduce the floor slab rotation at the joint.

With tensile cracking in a wall-floor slab connection, the bottom wall resists an additional moment because the slab reaction is displaced from the centre line of the wall. Failure in a wall therefore usually occurs in the wall below the slab.

3. Moment Distribution

When no tensile cracking occurs, the moment distribution may be calculated using standard methods but the flexural properties discussed in the previous section must be taken into account.

In the tests on the full scale structure the slab restraining moment was quite considerable - up to an estimated 30% of the moment allowing no slab rotation (full fixity). Top reinforcement may be necessary although in this case the tensile strength of the concrete was not exceeded.

With tensile cracking, the joint behaviour becomes non-linear. For tensile cracking in the wall at the joint, an approximate graphical method has been proposed and used to explain results from the full scale structure.

Tensile cracking in the wall makes analysis complex. A theoretical solution to this for a solid, linearly elastic wall has been given by Sahlin (30,32).

4. Ultimate Strength of the Joint

With wall stresses in practice, failure at the wall-floor junction is usually confined to :

1. Tensile cracking at the joint leading to equilibrium failure or shear failure round the end reinforcement of the floor slab or a diagonal crack across the reinforcement.
2. Tensile cracking of the floor slab at its junction with the wall.

Wall failure occurs at higher wall precompressions. If the central gaps in the mortar joint are neglected, the predicted ultimate moment based on the axial stress-strain relationship is considerably underestimated. With central gaps, the maximum moment a wall can resist occurs when the precompression is half the ultimate axial stress.

The load reduction factors for eccentric load in the proposed revision of the British Code on Brickwork (9) greatly underestimates the strength of the walls in the test models at higher eccentricities. The code relationship is similar to that for a solid wall with a non-linear stress-strain relationship. Even though the factors may be far too low at high eccentricities, they are too high at low eccentricities.

8.2 SUGGESTIONS FOR FURTHER RESEARCH

The work in this thesis has shown there is a need to investigate some aspects in more detail. Two such aspects are :

1. The stress-strain properties of brickwork under axial and flexural loading (including cycled loading).

The ultimate strength of brickwork under flexural load. Are there other reasons apart from gaps in the mortar joint for the increased flexural strength ? Are these gaps significant in nine inch brickwork ? The use of solid bricks with no frogs and perforated bricks may answer these questions.

2. Further tests on wall-floor interaction models similar to those in this thesis but with more accurately defined end conditions - hinged ends together with lateral restraint at floor level. The investigation should consider tests on differing joints, cycled loading and a theoretical curve for the non-linear part of the slab moment-rotation curve. The tests should concentrate on $1:\frac{1}{4}:3$ mortar brickwork which gives the most consistent results.

REFERENCES

1. ACI COMMITTEE 435. Deflections of reinforced concrete flexural members. ACI Journal, Vol 63, June 1966, 637-674.
2. ANGERVO K and PUTKONEN A I. Erweiterung der theorie der biegun g eines pfeilers ohne zugfestigkeit und ihre anwendung zur berechnung von rahmentragwerken mit unbewehrten stielen. (Extension of the theory of a pillar without tensile strength and its application to the calculation of frame structures). Publication 34, The State Institute for Technical Research, Helsinki, 1957.
3. BASE G D. Further notes on the demec, a demountable mechanical strain gauge for concrete structures. Magazine of Concrete Research, Vol 7, No 19, March 1955, 35-38.
4. BRADSHAW R E and THOMAS K. Modern developments in structural brickwork. Technical Note No 3, Vol. 2, Clay Products Technical Bureau, London, 1968.
5. BRITISH CERAMIC RESEARCH ASSOCIATION. Model Specification for load-bearing brickwork. Special Publication 56, BCRA, 1967.
6. BUILDING RESEARCH STATION. Strength of brickwork, blockwork and concrete walls. Digest 61, 2nd Series, BRS, Watford, 1965.
7. BRITISH STANDARDS INSTITUTION. Hot rolled steel bars and hard drawn mild steel wire for the reinforcement of concrete, BS 785: Part 1. BSI, London, 1967.
8. BRITISH STANDARDS INSTITUTION. Structural recommendations for loadbearing walls, CP 111. BSI, London, 1964.
9. BRITISH STANDARDS INSTITUTION. Draft British standard code of practice for structural recommendations for walls constructed of brickwork, blockwork or masonry (revision of CP 111:1964). No 70/1556, BSI, London, 1970.
10. BRITISH STANDARDS INSTITUTION. Specification for bricks and blocks of fired brickearth, clay or shale, CP3921. BSI, London, 1965.

11. CARLSEN B E. On the bearing capacity of joints between precast slabs and brick walls. CIB International Symposium on Bearing Walls, Warsaw, 1969.
12. CENTRE SCIENTIFIQUE ET TECHNIQUE DU BATIMENT. Méthodes de calcul des murs. Cahiers du CSTB, No 571, Paris, June 1964.
13. CLARK L E, GERSTLE K H and TULIN L G. Effect of strain gradient on the stress-strain curve of mortar and concrete. ACI Journal, Vol 64, No 9, September 1967, 580-586.
14. FRANZ G and NIEDENHOFF H. The reinforcement of brackets and short deep beams. Translation No 114, Cement and Concrete Association, London, 1964. (Beton- und Stahlbeton, Vol 58, No 5, May 1963, 112-120).
15. GOEL J -J. Program GC-21 (Finite element analysis of plates). IBM System/360, Share 360D - 16.2.022.
16. HALLER P. The physics of the fired brick, Part one : Strength properties. LC 929, Building Research Station, Watford, 1960.
17. HALLER P. Load capacity of brick masonry. Designing, Engineering and Constructing with Masonry Products (International Conference - Texas - 1967), editor, F B Johnson. Gulf Publishing Company, Houston, 1969, 129-149.
18. HENDRY A W, SINHA B P and MAURENBRECHER A H P. Full-scale tests on the lateral strength of brick cavity walls with precompression. Paper presented at the Fourth Symposium on Load-Bearing Brickwork, British Ceramic Society, November 1971.
19. JOHNSON R P. Structural Concrete. McGraw-Hill Co Ltd, London, 1967.
20. KHOO C L and HENDRY A W. Triaxial compression of brickwork mortar. Technical Note 172, British Ceramic Research Association, 1971.
21. LOGCHER R D, CONNOR Jr J J and FERRANTE A J. ICES STRUDL II - The structural design language. Engineering User's Manual, Research Report R68-92, Dept. of Civil Engineering, MIT, Massachusetts, 1969.

22. MAURENBRECHER A H P and HENDRY A W. Aspects of the strength and fixity of the joint between a brick wall and a floor slab. SIBMAC Proceedings (Second International Brick Masonry Conference, 1970), editors - H W H West and K H Speed. British Ceramic Research Association, 1971, 186-190.
23. MORICE P B and BASE G D. The design and use of a demountable mechanical strain gauge for concrete structures. Magazine of Concrete Research, Vol 5, No 13, August 1953, 37-42.
24. NATIONAL INSTITUTE FOR MATERIALS TESTING. Bestämning av plastiseringsmoment och vinkeländring i knutpunkten mellan murverk och bjälklag. (Tests on the deformation and strength of joints between concrete slabs and masonry walls). Intyg. U64-3778, Statens Provningsanstalt, Stockholm, 1966.
25. NEVILLE A M. Properties of Concrete. Pitman & Sons Ltd, London, 1963. (Paperback edition - 1968).
26. NEWMAN A J. Measuring appliances and methods used in field testing. Civil Engineering Reference Book - Editor, J Comrie. Vol 1, 2nd Edition, Butterworth & Co Ltd, London, 1961, 485-495.
27. DE PAIVA H A R and SIESS C P. Strength and behaviour of deep beams in shear. Proceedings American Society of Civil Engineers, Vol 91, ST5, October 1965, 19-41.
28. RILEM. Symposium on the Observation of Structures. RILEM, Lisbon, 1955.
29. ROCHA M. In situ strain and stress measurements. Stress Analysis - Editors, O C Zienkiewicz and G S Holister. John Wiley & Sons Ltd, 1965, 425-461.
30. SAHLIN S. Structural interaction of walls and floor slabs. National Swedish Council for Building Research, Report 35, Stockholm, 1959.
31. SAHLIN S. Interaction of brick masonry walls and concrete slabs. Designing, Engineering and Constructing with Masonry Products (International Conference - Texas - 1967), editor, F B Johnson. Gulf Publishing Company, Houston, 1969, 266-277.

32. SAHLIN S. Structural Masonry. Prentice-Hall, New Jersey, 1971.
33. SINHA B P, MAURENBRECHER A H P and HENDRY A W. Model and full-scale tests on a five-storey cross-wall structure under lateral loading. SIBMAC Proceedings (Second International Brick Masonry Conference, 1970), editors - H W H West and K H Speed. British Ceramic Research Association, 1971, 201-208.
34. STRUCTURAL CLAY PRODUCTS RESEARCH FOUNDATION. Small scale specimen testing. Progress Report No 1, Structural Clay Products Institute, Geneva, Illinois, October 1964.
35. STRUCTURAL CLAY PRODUCTS INSTITUTE. Recommended Practice for Engineered Brick Masonry. SCPI, Virginia, 1969.
36. TIMOSHENKO S P and WOINOWSKY-KRIEGER S. Theory of Plates and Shells. 2nd Edition, McGraw-Hill, New York, 1959. (student edition).
37. TIMOSHENKO S P. Strength of Materials - Part II: Advanced. 3rd Edition, Van Nostrand Reinhold Co, New York, 1956.
38. TYLER R G. Developments in the measurement of strain and stress in concrete bridge structures. Report LR 189, Road Research Laboratory, Crowthorne, 1968.
39. WATSTEIN D and JOHNSON P V. Experimental determination of eccentricity of floor loads applied to a bearing wall. Building Science Series 14, National Bureau of Standards, Washington DC, 1968.
40. WINTER G, URQUHART L C, O'ROURKE C E and NILSON A H. Design of Concrete Structures. 7th Edition, McGraw-Hill, New York, 1964.
41. YOKEL F Y, MATHEY R G and DIKKERS R D. Compressive strength of slender concrete masonry walls. Building Science Series 33, National Bureau of Standards, Washington DC, 1970.
42. YOKEL F Y, MATHEY R G and DIKKERS R D. Strength of masonry walls under compressive and transverse loads. Building Science Series 34, National Bureau of Standards, Washington DC, 1971.

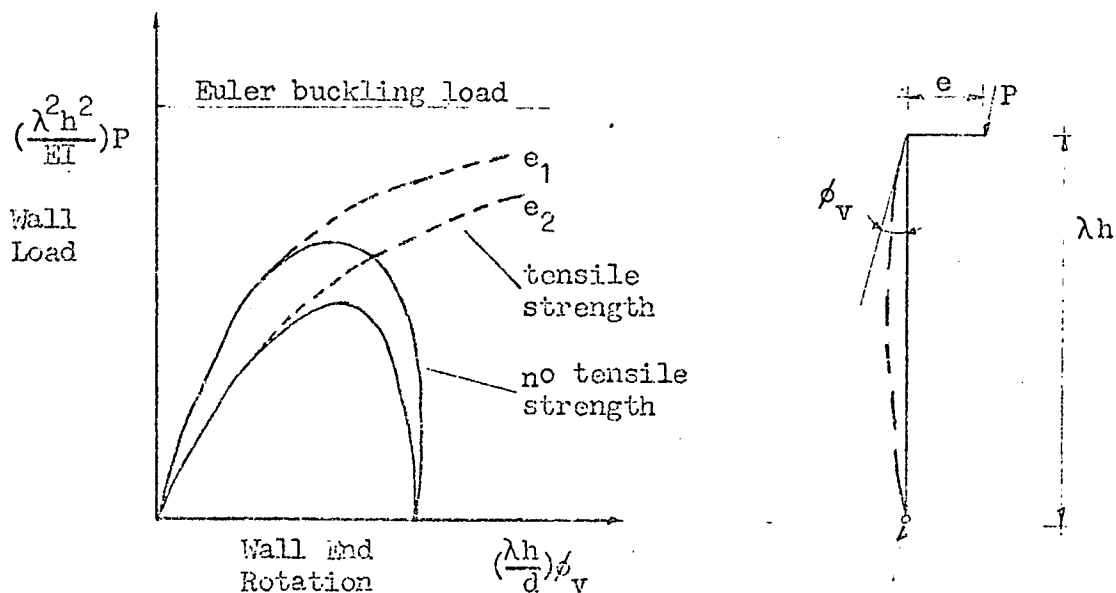
APPENDIX 1A1.1 REVIEW - SAHLIN (30,31,32)A1.1.1 Introduction

A review of Sahlin's work is presented with comments. Notation is Sahlin's.

His work is the only extensive treatise on the subject of joint behaviour in brickwork. His experimental work on brickwork covers wall-slab joints where the slab bears half way into a 10 inch (two brick) thick wall.

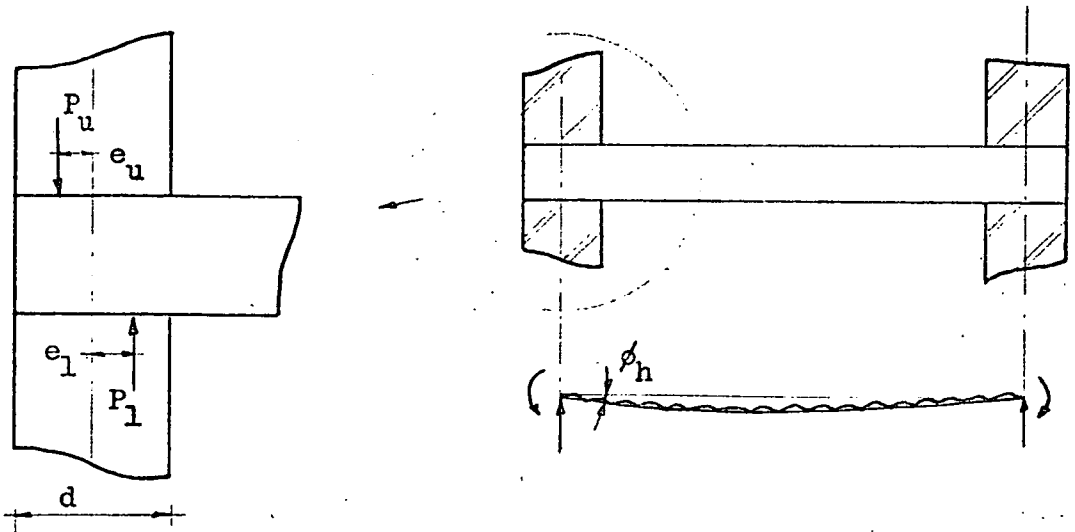
A1.1.2 Theory1. Wall Behaviour

Sahlin has further extended the theory for the behaviour of linearly elastic, solid walls with no tensile strength including the effect of axial load on lateral deflection. This gives the relationship between wall end rotations, ϕ_v , and the magnitude and eccentricity of the applied load.



2. Floor Slab Behaviour

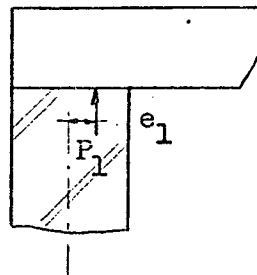
A simple analysis is proposed for slab end rotation for the following case :



The slab end rotation, ϕ_h , is equal to the simply supported rotation minus the rotation due to a restraining end moment = $P_u e_u + P_l e_l$.

Assuming $e_u \approx e_l = e$, the restraining moment becomes $e(P_u + P_l)$.

In the analysis an error occurs when the roof slab is considered. There $P_u = 0$, allowing the slab to rotate freely but the analysis gives an end restraining moment = $P_l e_l$ which can only occur if tensile stresses are allowed. At low eccentricities before tensile stresses occur there is no end restraining moment either.



3. Joint Behaviour

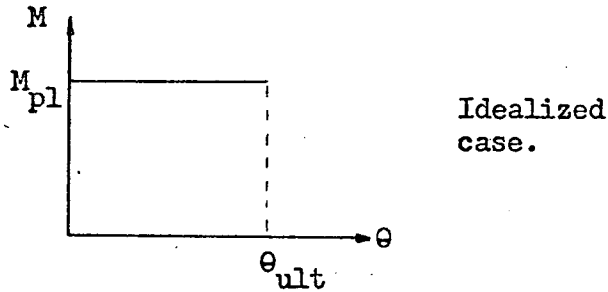
Next Sahlin considers the joint between the wall and the slab. If the joint is rigid, the wall rotation equals the slab rotation, $\phi_v = \phi_h$. For a wall resisting no tensile stresses this relationship is valid throughout the cracking range (assuming no failure, local crushing and deformation). If the wall can resist tensile stresses except at the joint then a difference of rotation may occur dependent on the rigidity of the walls and slab. If local failure occurs at the joint but not in the rest of the wall then it is possible for the load to increase while the slab restraining moment is constant - 'plastification'. This latter case is considered by Sahlin.

The relation $\phi_v = \phi_h$ is true up to a limiting slab restraining moment, M_{pl} , after which there is a divergence between the two rotations given by θ , the 'joint rotation'.

$$\theta = \phi_h - \phi_v$$

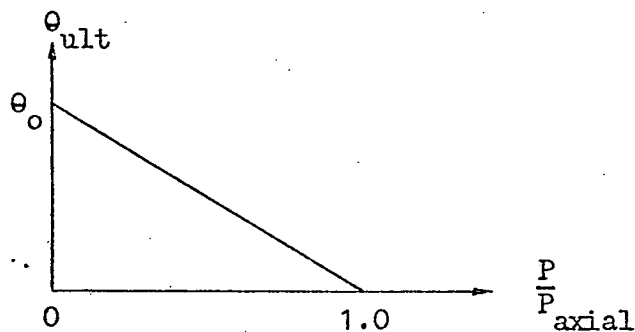
$$\theta = 0 \text{ for } M < M_{pl}$$

Thereafter joint rotation increases at approximately constant moment, M_{pl} .



Joint rotation is primarily due to failure at the joint and partly due to local deformation. Care must be taken in evaluating joint rotation when tensile cracking occurs at eccentricities greater than $d/6$.

The limiting moment, M_{pl} , and the ultimate joint rotation, θ_{ult} , were measured experimentally in a series of full-scale model tests - both statically determinate and indeterminate. From these results a relationship between θ_{ult} and the wall failure load, P , was proposed :



This is a very approximate relationship there being a large scatter of results. A centrally loaded wall close to failure will tolerate little disturbance due to joint rotation. A more exact wording would be slab rotation - it is not necessary for joint rotation to occur at higher

loads especially for a slab carried through the wall. For slabs bearing half way into the wall the assumptions are more correct as initial failure is due to vertical splitting of the wall above the edge of the slab which may allow some joint rotation before final failure.

4. Failure of the Wall and Joint

Using the experimental results the theory can be used to predict failure loads. Four cases are considered :

$$1. \quad \theta = 0 \quad (\phi_v = \phi_h) \quad 0 \leq M \leq M_{pl} \quad \sigma_{edge} = \sigma_{ult \text{ axial}}$$

Failure occurs when the ultimate edge stress is reached before the limiting slab restraining moment is attained.

$$2. \quad 0 < \theta < \theta_{ult} \quad M = M_{pl} \quad \sigma_{edge} = \sigma_{ult \text{ axial}}$$

Failure occurs when the ultimate edge stress is reached after the limiting slab restraining moment is attained.

$$3. \quad 0 < \theta = \theta_{ult} \quad M = M_{pl} \quad \sigma_{edge} < \sigma_{ult \text{ axial}}$$

Failure occurs when the limiting joint rotation is reached.

$$3b. \quad 0 < \theta = \theta_{ult} \quad M < M_{pl}$$

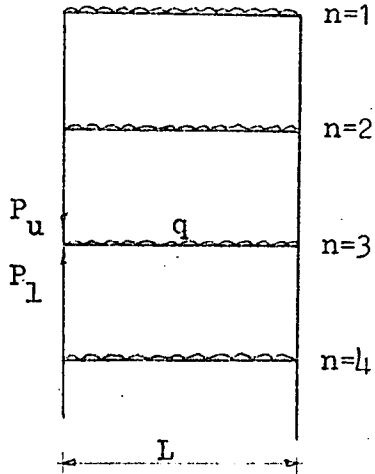
For cases where there is not a pronounced yield point - gradual yielding at the joint. The maximum load is governed by the maximum permissible rotation $\theta_{ult} = \theta_o (1 - P/P_{axial})$.

Equations for solving these cases are tabulated in reference 32.

A1.1.3 Experimental

1. Test Procedure

The following type of structure was considered :



$$P_u = (n-1)\frac{qL}{2} + (n-1)G_{wall}$$

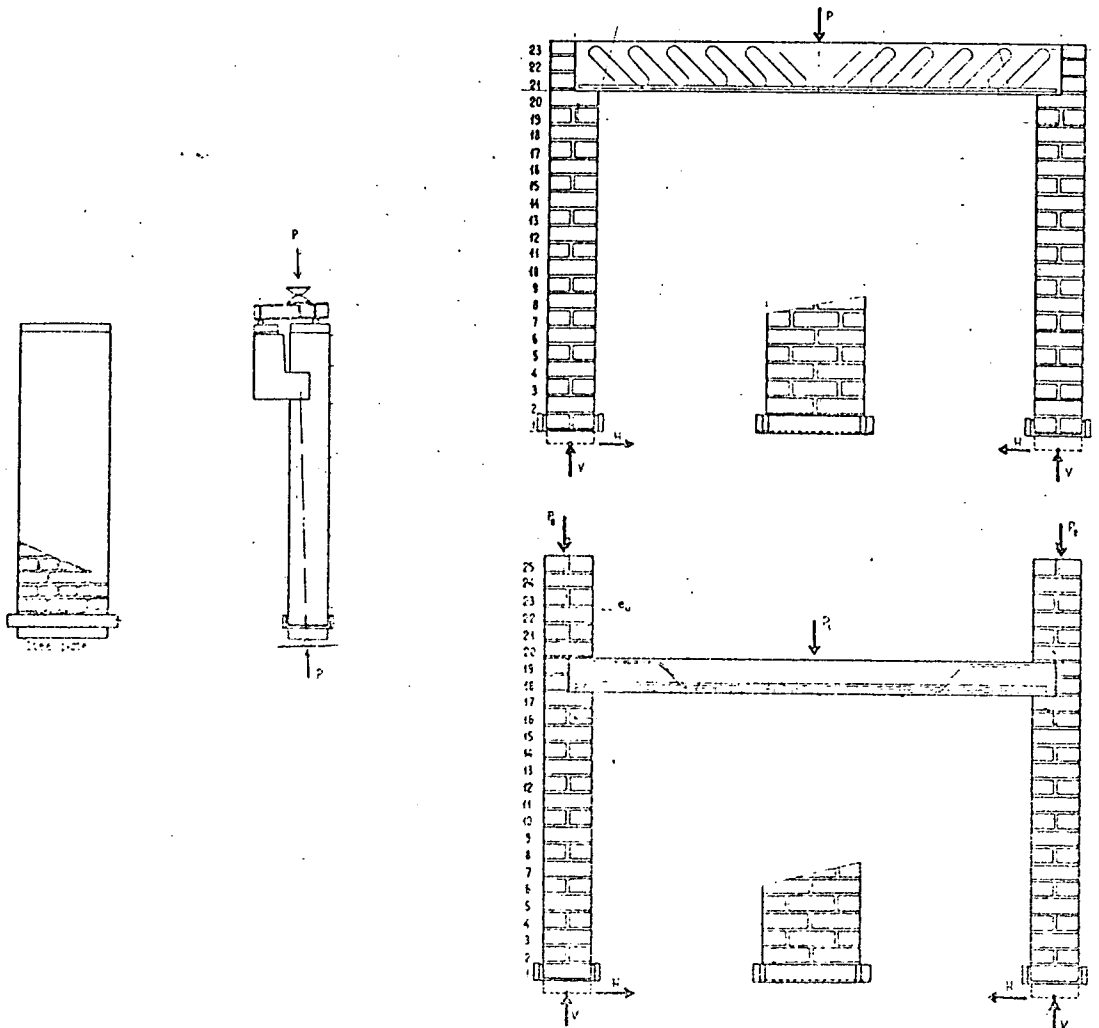
$$P_1 = \frac{qL}{2} + P_u$$

q = slab load/unit area

G = wall load/unit length

n = storey level numbered from the top.

The wall-slab interaction models tested were :



During each test a constant load ratio, P_u/P_1 , was maintained, representing a joint in the structure sketched on the previous page in which all floors are simultaneously loaded. The storey level considered depends on the ratio of the loads, P_u/P_1 . The loads were increased from zero to failure in the same proportion. For a statically determinate test this means a constant wall load eccentricity at the joint with an increasing precompressive and slab load, enabling an investigation into the relative rotation between the slab and the wall due to 'plastification' - thus the effects of tensile cracking are minimized, or nil if the eccentricity is less than $d/6$ (this eccentricity is assumed to cause zero stress on one side of the wall). This test procedure is different from that used in the test models in this thesis where the eccentricity increases with a constant precompressive load - the latter procedure is also, in effect, used in Sahlin's tests on roof joints where the precompressive load may be considered to be constant and equal to zero while the eccentricity of the load on the wall below the slab initially tends to increase.

For the statically indeterminate tests the eccentricity reduces as higher loads are reached. This is caused by failure and local deformation at the joint, limiting the maximum moment even though axial loads still increase while also limiting the maximum eccentricity (for roof slabs).

2. Material Properties and Construction Procedure

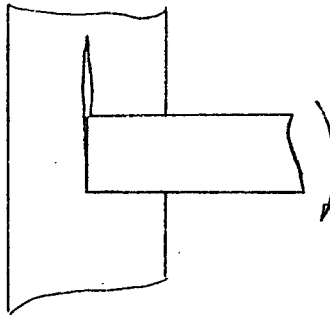
The compressive strength of the concrete slabs, the brickwork, brick and mortar is :

Brick	3800 lbf/in ²	(tested according to the Swedish code)
Mortar	28 day strength of cylinders :	
	120 lbf/in ²	1:5 lime:sand by weight
	240 lbf/in ²	2:1:15 lime:cement:sand by weight
Brickwork	600 lbf/in ²	1:5 mortar mix
	1000 lbf/in ²	2:1:15 mortar mix
Concrete	Six inch cube strength - statically indeterminate models :	
	4630 lbf/in ²	

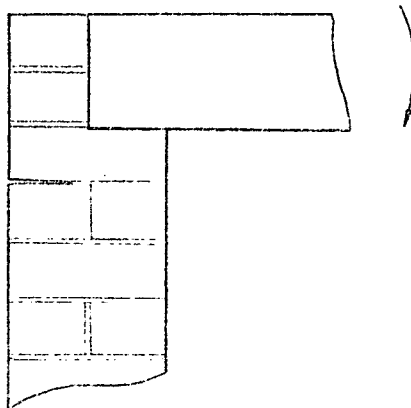
Mortar joint thickness was an average of 0.5 inch. The floor slabs were cast in-situ producing an excellent bond with the adjacent brickwork. One test shows brick failure before bond failure.

3. Measurements

The angle of rotation of the wall and of the slab were measured, the difference giving the angle of rotation of the joint. For slabs bearing into a wall, the joint was satisfactory ($\theta = 0$) up to a limiting moment, M_{pl} , which caused splitting in the wall above the slab. The increase in joint rotation is then very large while the moment is fairly constant or decreases. There is an uncertainty in the angle of joint rotation because of inaccuracies in wall rotation obtained from deflection measurements on the outside face.

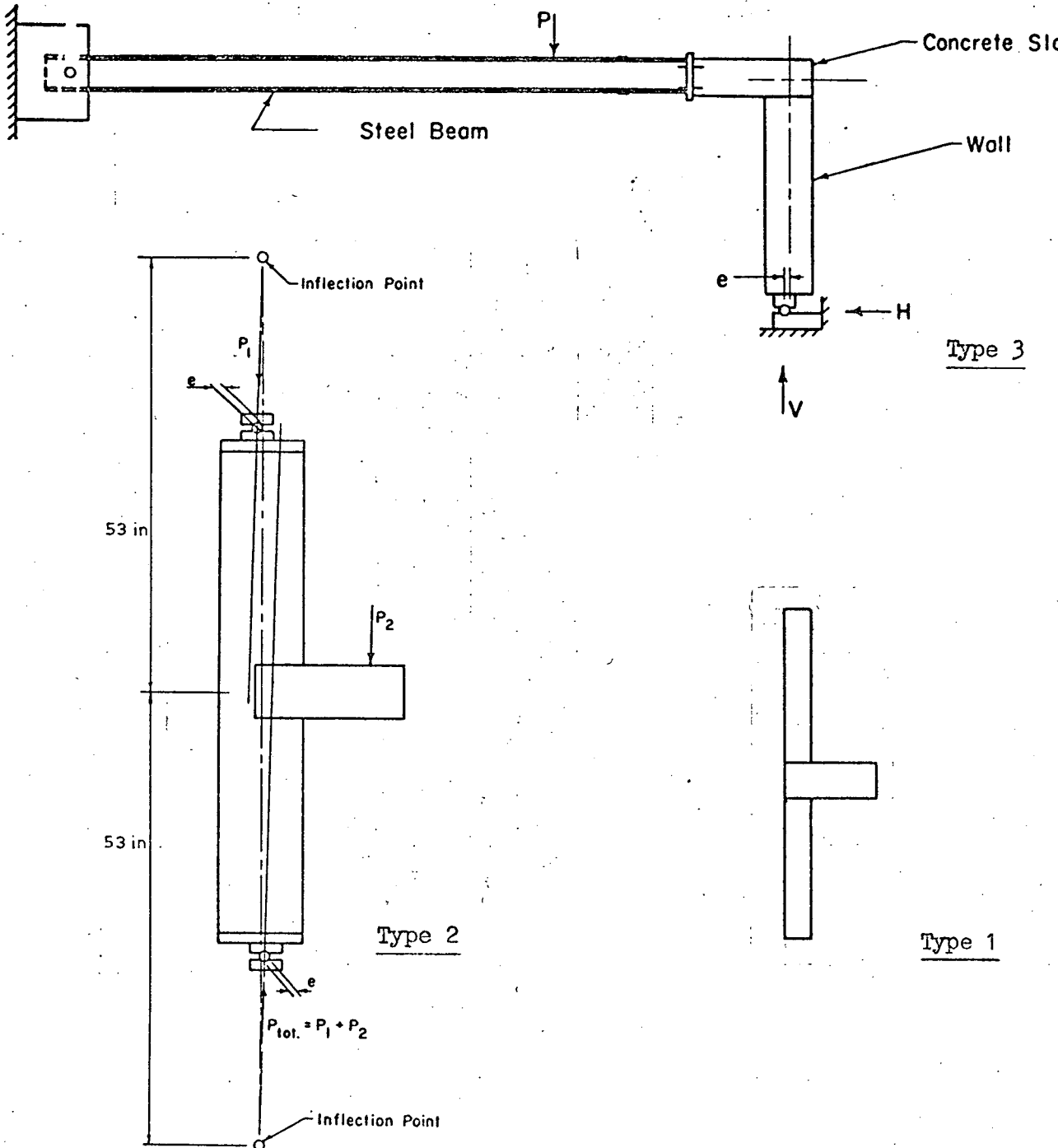


For a slab bearing onto a wall (roof joint) there is an important difference with the other tests. Tensile cracking starts at an early stage, a crack predominating in the first mortar joint below the slab. Joint rotation occurs at low loads increasing with increasing load. Here the moment-rotation idealized diagram is not followed. Joint rotation is predominately due to tensile cracking with increased difference at higher loads when local crushing may occur.



A1.2 REVIEW - NATIONAL INSTITUTE FOR MATERIALS TESTING (24)

The work is experimental and has been reviewed by Sahlin (31,32).
Brickwork and blockwork models of the following type were tested :



The tests measured joint rotation, the limiting moment, M_{pl} , and the ultimate failure loads.

Model types 1 and 2 differ in some respects from a statically indeterminate model at failure. The slab moment is directly proportional to slab load thus any reduction in slab moment after the limiting 'plastic' moment, M_{pl} , is reached means a reduction in slab load and therefore a reduction in the load on the wall above the slab (one control for both loads). The average stress at failure then is less than the stress when M_{pl} is reached. In addition there is no lateral restraint at slab level. Results for model 1 are not accurate due to lateral deflection partly initiated by tensile cracking (see section 6.3.2). For type 2 the eccentricity of the load at slab level does not cause tension, the walls are thicker and the slab does not bear completely into the wall thus the lack of restraint is not so important.

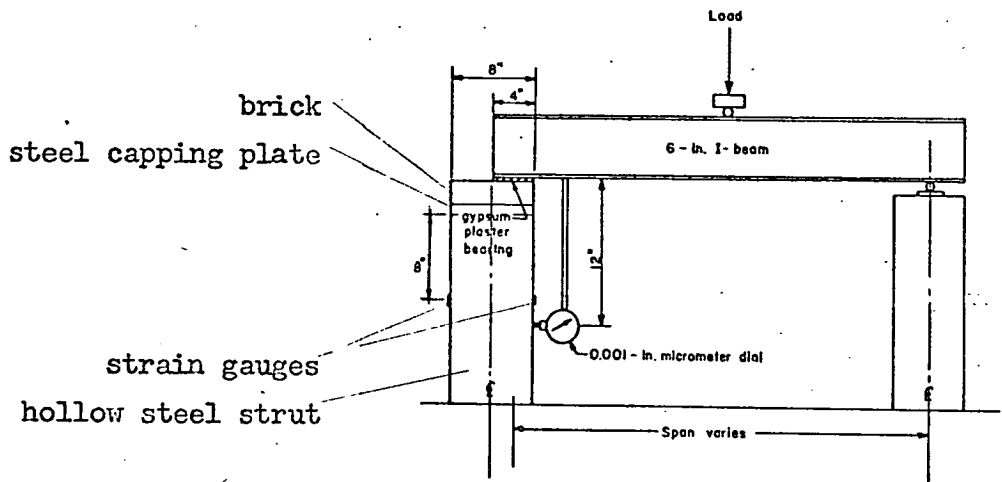
1. Material Properties

The compressive strength of the concrete, the bricks, the blocks, the brickwork, the blockwork and the mortar is :

Bricks	4250 lbf/in ²			
Concrete Blocks	450 - 810 lbf/in ²			
Mortar	1800 lbf/in ²	Class B	1:1.85:15	lime:cement:sand by weight
	850 lbf/in ²	Class C	1:1:15	lime:cement:sand by weight
Concrete	5700 lbf/in ²	6 inch cube at 28 days. Slabs cast in-situ.		
Brickwork	1060 - 1680 lbf/in ²			
Blockwork	310 - 630 lbf/in ²			

A1.3 REVIEW - WATSTEIN and JOHNSON (39)

Watstein and Johnson have conducted some preliminary tests on the eccentricity of the floor load for attic type joints (see diagram).



An interesting point is their method of finding the eccentricity of the floor load. As the wall they use a hollow steel strut to which are attached electrical resistance strain gauges. The eccentricity is then found by measuring the strain on opposite faces of the strut.

The results are preliminary and only simulate localized behaviour at the wall-floor joint. The floor is simulated by a steel joist bedded onto a brick which in turn is glued to the top of the steel strut.

For an unbonded plaster joint (plaster confined between polyethylene sheets) with increasing floor load, the eccentricity increased from $e/t = 0.35$ to a limiting value of 0.43 for the range tested.

For a bonded plaster joint the eccentricity decreased from $e/t = 0.32$ to a value of 0.24. This result is surprising - a higher initial eccentricity is expected for small floor rotations if the bond was unbroken, the bond imposing a restraining moment on the floor. When tensile cracking occurred the eccentricity should drop to a similar level obtained in the unbonded case (see section 6.3.3).

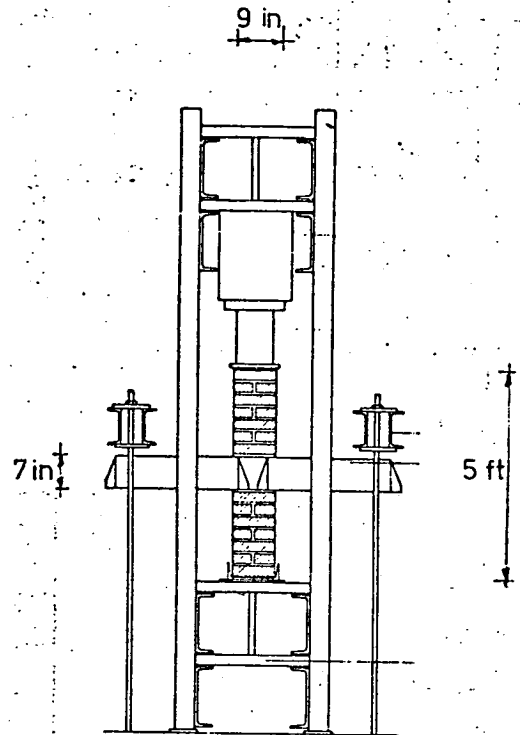
Tests using a rubber packing reduced eccentricity, the floor reaction tending towards the centre of the floor bearing length for the initial floor loads and slowly increasing with increasing load and floor rotation.

A1.4 REVIEW - CARLSEN (11)

Carlsen tested a small number of joints between a precast concrete floor slab and a brickwall.

Axial compressive strength
of brickwork = 980 lbf/in^2

Width of model = 4 ft



The reference only gives very brief details about the experimental work and results.

Precast concrete slabs were placed into position as shown in the sketch. The gap between the slabs was filled with concrete and then a further section of brickwork built onto the joint.

The purpose of the investigation : The effect of the length of bearing of the slabs on the bearing capacity of the joint and the ultimate slab restraining moment. The effect of slab moment on the ultimate strength of the wall.

The conclusions : The bearing capacity of the wall is not affected by the bearing length of the slabs. The slabs are clamped in position. A reduction in bearing length reduces the ultimate slab moment.

From the information given it is not clear if both slabs were loaded although this seems likely - for all the loading cases there was little difference in the ultimate strength of the wall.

A1.5 REVIEW - MAURENBRECHER and HENDRY (22)

Maurenbrecher and Hendry have published experimental results given in this thesis covering the following two aspects :

1. Relationship between the slab rotation and the moment exerted by the slab at the joint for varied precompressions in the brick wall.
2. The ultimate strength of the joint.

The publication assumes a simplified analysis for ultimate equilibrium failure (section 6.2.2) and an incorrect ultimate moment for a joint test with a 1:2:9 mortar mix and a precompression of 200 lbf/in² (too low a result because of faulty load cell wiring).

APPENDIX 2

A2.1 EXPERIMENTAL EQUIPMENT

A2.1.1 The Demec Gauge

The demec gauge is a demountable mechanical strain gauge (3, 23). Its main components are an invar main beam with two conical locating points, one fixed and the other pivoted on a knife edge. This pivoting movement is transmitted to a dial gauge (graduated in 10^{-4} in). The gauge requires only very small temperature corrections during use. An invar reference bar is provided as a check and is also useful as a guide to the general condition of the gauge. Reference bar readings are usually taken before and after a test.

A setting out bar is provided to give the correct gauge length when gluing the stainless steel discs onto the test structure. The discs are $\frac{1}{4}$ inch in diameter with a 0.04 inch hole into which the conical gauge points are located. The surface of the test structure should be smooth, dry and clean. The position of the discs is marked out by pencil lines, then a thin layer of Durofix is spread over the marked positions and allowed to dry. A second layer is applied to two points at a time and the discs pressed onto the two positions and kept in place by the setting out bar for approximately one minute to allow initial setting of the glue. Several hours (preferably 24) should elapse between fixing the discs and using them. An alternative to Durofix is sealing wax. Each locating disc is backed with a dab of sealing wax. One disc of a pair is then held in position by a small screwdriver and a soldering iron applied, melting the wax. When the wax has rehardened, the other disc is held in position with the setting out bar and similarly stuck on. Discs stuck in this way can be used immediately. Wax is more successful than Durofix on damp surfaces.

When measuring strain with the Demec gauge just enough pressure should be applied to the gauge to provide good contact. The reading is repeated to improve accuracy. The gauge is always held in the same way for a particular position. When measuring vertically the fixed point should be in the lower disc. Throughout a test only one person should take readings for a particular measuring point. With experience accuracy improves.

Specifications :

Manufactured by W H Mayes & Son Ltd .

Gauge lengths obtainable - 2 to 80 inches.

Price range - gauge, setting out bar and invar reference bar - £57 to £128 . Stainless steel discs - 112 @ £1.75 .

Calibrated by the Cement & Concrete Association :

2 inch gauge	-	2.48×10^{-5}	strain per division
8 " "	-	1.01×10^{-5}	" " "
12 " "	-	6.6×10^{-6}	" " "
24 " "	-	3.33×10^{-6}	" " "

A2.1.2 Vibrating Strain Gauge

Gauge :

Tyler Recoverable Surface Mounting (38).

Manufactured by Gage Technique at approx. £11 each .

Lengths used : 2.5 in and 5.5 in .

Gauge factors : 0.54×10^{-9} for the 2.5 inch gauge
 3.0×10^{-9} for the 5.5 inch gauge

Plucking voltage : 24 volts for the 5.5 inch gauge while 60 or 120 volts was necessary to obtain stable readings in the 2.5 inch gauge.

Accuracy : 1.5 to 3×10^{-6} strain for equipment reading to 1 Hz .

Measurement of Frequency :

A portable digital strain measuring instrument, Model PSM, measures the period over 100 or 1000 cycles.

Manufactured by Deakin Instrumentation at approx. £600 .

Mounting of Gauges :

Brackets were fixed onto the test specimen (fig 3.7) using a Cataloy paste. To make sure the brackets were in the same plane and the correct distance apart they were bolted to a steel plate which kept the brackets in position while the paste hardened. The plate was then removed and the gauge put in its place.

A2.1.3 Dial Gauge

Specifications : Baty Dial gauge costing approx. £8 .

1 division = 0.0001 in

Range 0.2 in or 0.5 in

A2.1.1 Clinometer

Inclinometer Model M1 manufactured by WH Mayes & Son Ltd .

Description :

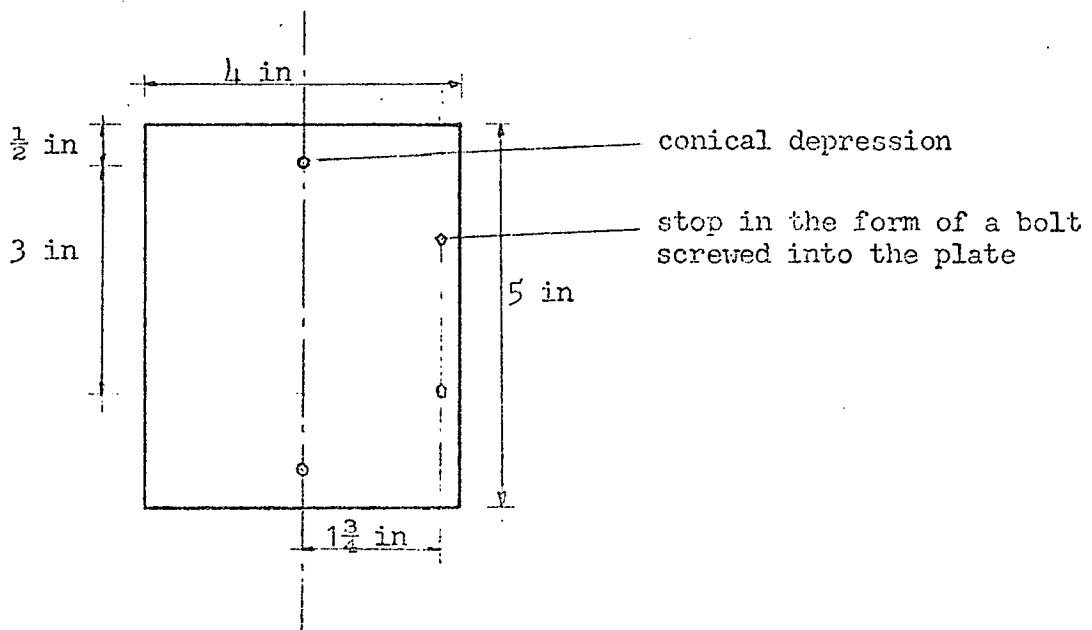
The instrument is based on an engineering sine bar with 3 inch centres. A micrometer thimble (graduated in 0.0001 inch/division) is fitted to obtain the vertical displacement. A bubble spirit level (sensitivity 1 division = 1 minute) is fitted to provide a datum zero. The clinometer is supported by three hemispheres.

Measurements :

The accuracy of the measurements are dependent on two main factors :

The first and main difficulty is in estimating the central position of the bubble - it depends on the direction from which the level is viewed. Thus the level should be viewed from the same position. To overcome this problem in future an optical system should be attached which makes the ends of the bubble coincide.

The second difficulty is ensuring the clinometer is in the same position every time a reading is taken at a particular point. Flat steel plates were used as bases (see sketch). The clinometer was positioned by a cone shaped depression and a stop. The clinometer position could be reversed to further improve accuracy. The plates needed painting to prevent rust. In future completely flat plates would be best, the clinometer held in position by stops only. For outdoor use the plate should also be resistant to rust.



A2.1.5 Load Cells

Load was measured using 3 ton Davey United Toroidal Load Cells with a self-aligning loading cap. They have an output of 13 mV at 3 tons with a 10 V DC stabilised power supply.

A2.1.6 Digital Voltmeter

The output from the load cells was measured by a Dynamco Digital Voltmeter.

Resolution : $50\mu\text{V}$ and a later model (DM 2022) $10\mu\text{V}$.

APPENDIX 3

A3.1 EFFECT OF GAUGE LENGTH ON THE MEASUREMENT OF VERTICAL STRAINS

A3.1.1 Choice of Gauge Length

The gauge length over which the strain is measured affects the accuracy of the strain. The length should be large in comparison to the components of the material making up the structure and large enough to give deformations the strain gauge can measure. The gauge length is restricted by the condition that strains over the gauge length should either be constant or vary linearly. Rocha (29) discusses the choice of gauge and gauge length.

Gauge lengths should be short enough to accurately represent the strain (no sudden variations within the gauge length). Full scale models and structures have the advantage of having gradual strain variations over larger gauge lengths - larger than in small scale models thus the choice of gauge and gauge length is not unduly restricted by this factor.

Brickwork is a composite material thereby affecting the choice of gauge length. Figure A3.1 illustrates the variation in the measured brickwork modulus with gauge length and position for a brick to mortar modular ratio of 5 - approximately equivalent to a 1:2:9 mortar wall (the vertical dimensions of the brick and mortar are $2 \frac{7}{8}$ inch and $\frac{3}{8}$ inch respectively). The possible values of modulus calculated from measured strains are given by the area enclosed by the two limiting curves.

When using demec gauges the demec discs are usually positioned on the brick thus the variation in modulus is given by either of the two limiting curves, the area in between becoming significant when a fraction of a mortar joint is enclosed in the gauge length.

In the experimental work in this thesis gauge lengths are kept in consistent positions. When strains between different experiments are compared these will have been measured in similar positions on the brickwork. This removes some of the restrictions on gauge length. Quoted moduli will usually be that obtained from an 8 inch gauge length covering two mortar joints and thus not the moduli equivalent to one brick and one mortar joint.

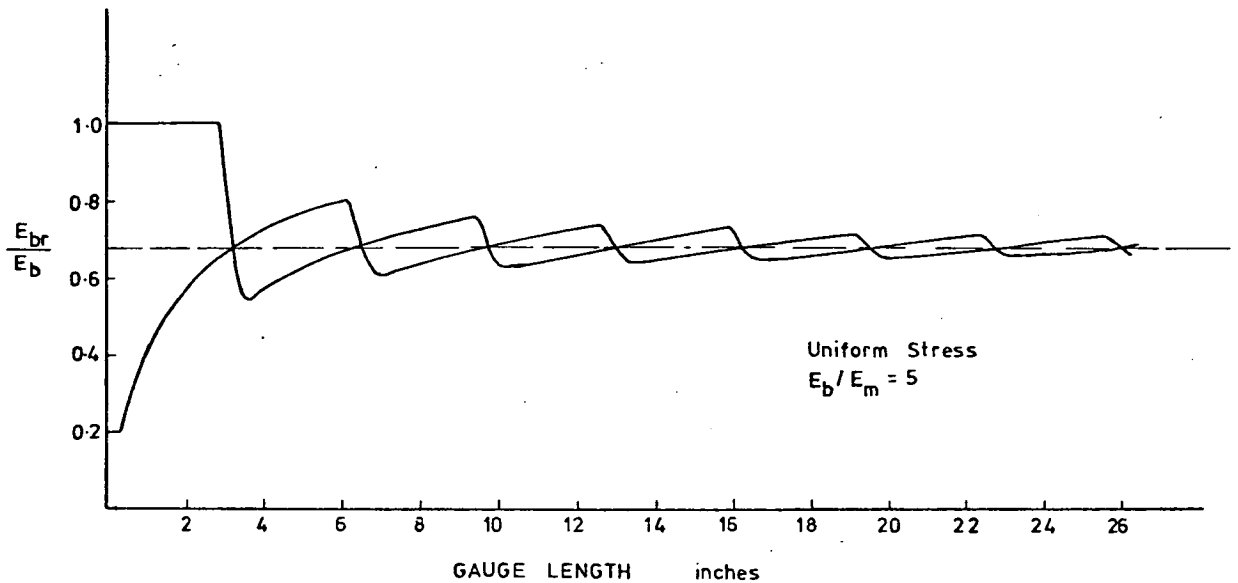


Fig. A3.1 Variation of the Brickwork Compression Modulus with the Size and the Position of the Gauge Length

A3.1.2 Relationship between the Gauge Length and the Brickwork Modulus

Notation : E_s = brickwork modulus over the gauge length considered
 E_b = brick modulus
 E_m = mortar modulus
 $\epsilon_b = \sigma/E_b$ = strain in brick
 $\epsilon_m = \sigma/E_m$ = strain in mortar
 ϵ_{br} = average strain over gauge length, l_{br}
 l_{br} = gauge length
 l_m = thickness of mortar joint
 n = number of mortar joints covered by gauge length
 V_b = proportion of brick in gauge length
 $V_m = 1 - V_b$ = proportion of mortar in gauge length
 σ = vertical stress

The brick and mortar are in parallel. The vertical stress is thus the same in both materials. In a vertical gauge length, l_{br} , covering both brick and mortar, the proportion of brick covered is :

$$V_b = (l_{br} - nl_m)/l_{br} \quad \text{--- (A3.1)}$$

The average strain over the gauge length becomes :

$$\epsilon_{br} = \frac{V_b l_{br} \epsilon_b + V_m l_{br} \epsilon_m}{l_{br}} \quad \text{--- (A3.2)}$$

The compression modulus becomes :

$$E_s = \sigma / \epsilon_{br} = \frac{E_b}{V_b + (E_b / E_m)(1 - V_b)} \quad \text{--- (A3.3)}$$

This expression assumes that the brick and mortar moduli changes, due to their interaction at the interfaces, are negligible. Alternatively the moduli can be taken as those occurring in the composite state.

Vertical strain measurements were usually carried out with gauge lengths of 2 and 8 inches. The corresponding values of V_b are (assuming a 3/8 inch mortar joint) :

8 inch gauge length	across two mortar joints	$V_b = 0.91$
	across three " "	$V_b = 0.86$
2 inch gauge length	across one " "	$V_b = 0.81$

A gauge length crossing the equivalent of one mortar joint and one brick has a value of $V_b = 0.88$ (3 1/4 inch gauge length). Large gauge lengths will tend to this value.

A3.2 EFFECT OF A GAP IN THE MORTAR JOINT - FINITE ELEMENT ANALYSIS

A3.2.1 Finite Element Program

A standard program provided by IBM is used - STRUDL, The Structural Design Language (21). Its finite element capability applied to two dimensional problems is quite extensive, allowing a choice of many different types of element. The element chosen was rectangular with four nodes giving eight degrees of freedom - Type PSR. The displacement function is of the form :

$$u(v) = a + bx + cy + dxy$$

where a, b, c and d are constants.

Each element is given values of elastic modulus and Poisson's ratio (isotropic). The program allows plane stress or plane strain - the former is used.

The program was run on an IBM 360/50 computer.

A3.2.2 Analysis

The finite element program was used to investigate the effect on vertical strains of gaps in the mortar joints of a single leaf brick wall.

Two types of wall section were analysed :

1. Three courses of single leaf brickwork under uniform load. The structure is symmetrical, therefore half the section is considered (fig A3.2).
2. Four courses of single leaf brickwork under uniform and eccentric load. The effect of eccentric loads on the vertical strains was investigated (fig A3.3).

The results from both analyses are shown in Table A3.1 . In addition the principal strain distribution is shown for the case $E_m/E_b = 1$ (fig A3.4).

Elements covering the gap in the mortar joint were given an elastic modulus of 1 lbf/in², effectively removing them from the structure.

To improve accuracy in the wall section with three courses, the applied loads at the top can be readjusted and the program re-run according to the results obtained from an intermediate mortar joint in the first run.

TABLE A3.1 - RESULTS OF THE FINITE ELEMENT ANALYSIS

Input				Output				Simple Theory				
$\frac{E_m}{E_b}$	E_b	E_m	a	E_b	E_m	E_{exp}	ϵ	E_s	I	ϵ	a_e	$\frac{E_{exp}}{E_s}$
1	2	2	0	2	2	2	434	2	70	442	0	1
0.3	2	0.6	0	1.98	0.61	1.57	553	1.57	70	563	0	1
1	1.96	1.96	2.62	0.92	1.38	0.96	508	1.96	60.5	521	2.11	0.49
0.21	2.4	0.5	2.62	0.95	0.25	0.71	637	1.66	57	653	2.36	0.43
1	2.4	2.4	1.92	1.58	2.08	1.63	376	2.4	67.6	381	1.32	0.68
1	2.4	2.4	1.06	2.08	2.33	2.11	-	2.4	70	-	0.36	0.88

Notes :

Units : $E \times 10^6$ lbf/in² ; a inches ; I in⁴ ; $\epsilon \pm 10^{-6}$

ϵ - flexural strain due to applied moment.

a_e & E_s obtained from equations 3.1 & 3.2 respectively

$I = b(t^3 - a_e^3)/12$ (here $b = 12$ in)

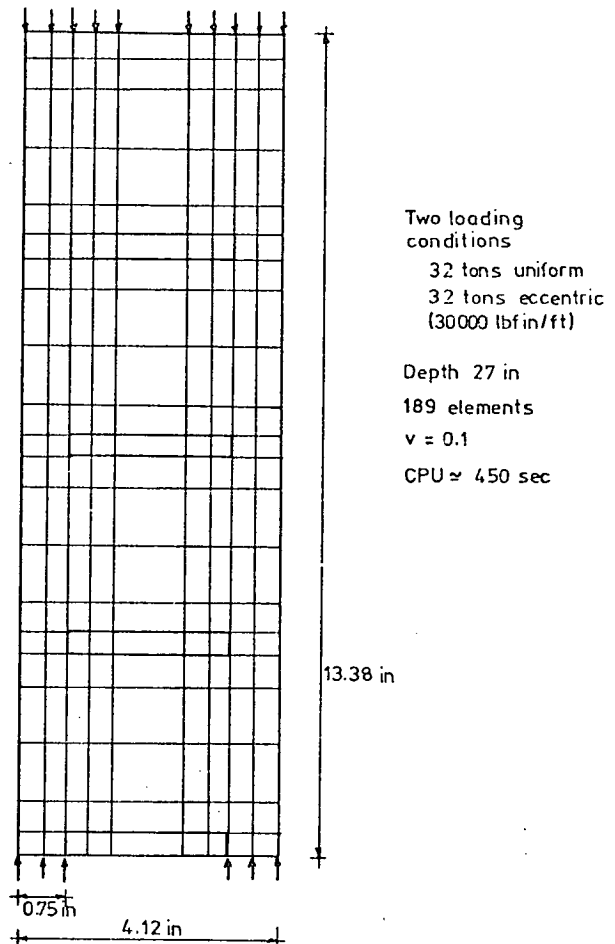
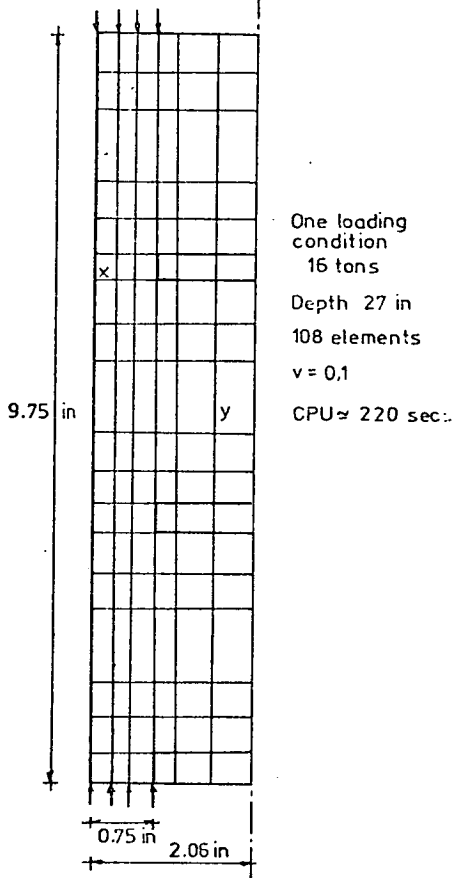


Fig. A3.2 Three Courses of Brickwork Divided into Elements

Fig. A3.3 Four Courses of Brickwork Divided into Elements

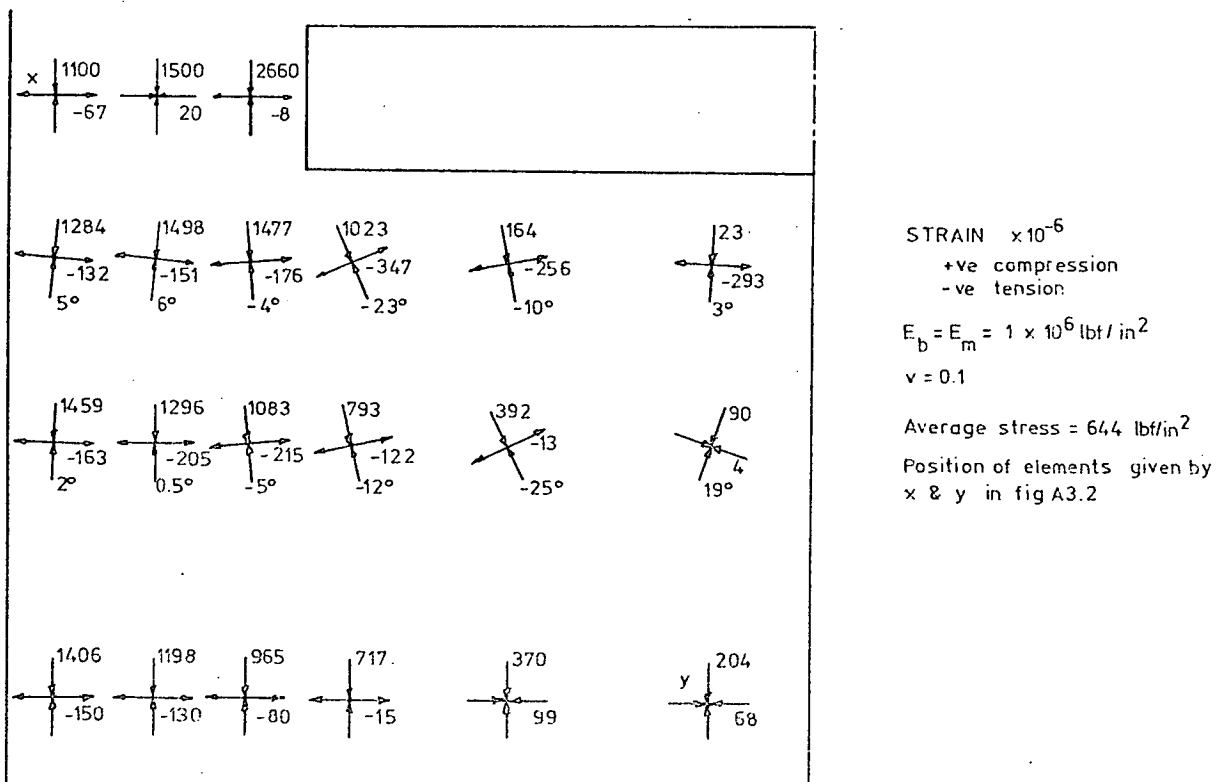


Fig. A3.4 Principal Strain Distribution

APPENDIX 4 - LINEAR STRESS-STRAIN THEORY

A4.1 INTRODUCTION

The effect of the following is considered :

1. Linear stress-strain
2. Differing loading and unloading modulus
3. A central gap in the wall

Notation :

- ϵ_c = compressive strain +ve
 ϵ_t = tensile strain +ve
 v = distance to the neutral axis from the side under tensile strain.
 A_c = area under the compressive stress curve +ve
 A_t = area under the tensile stress curve +ve
 σ_c = compressive stress +ve
 σ_t = tensile stress +ve
 t = thickness of wall
 E_s = compressive modulus (loading)
 kE_s = tensile modulus (unloading)
 a_e = width of central gap
 b = width of wall

Assumptions :

Plane sections remain plane.

Note :

The term tensile strain is used for convenience. The strains used in the calculations are measured bending strains taken about a set precompressive datum. Thus tensile strain is the unloading strain and does not become a true tensile strain until the initial compressive strain is overcome.

Al.2 CENTRAL GAP IN WALL $a_e/t \leq 1 - 2v/t$

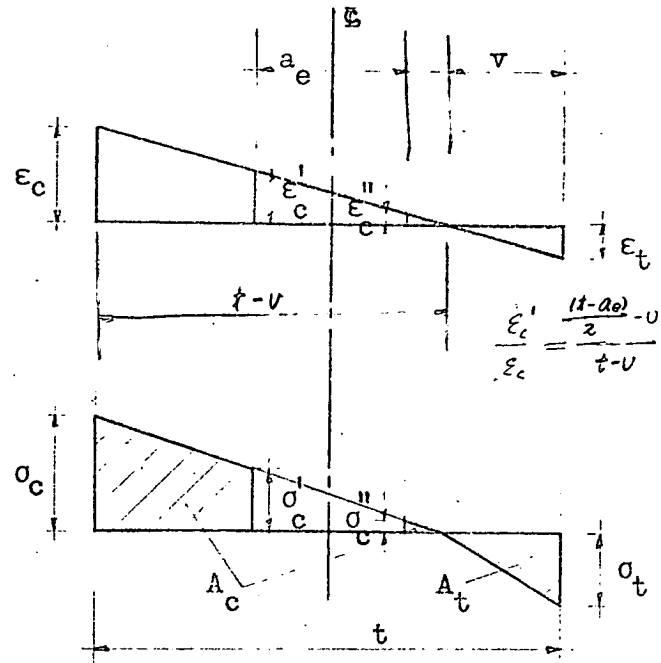
$$v/t = \epsilon_t / (\epsilon_c + \epsilon_t)$$

$$\epsilon_c^I = \frac{\epsilon_c (t - 2v + a_e)}{2(t - v)}$$

$$\epsilon_c^{II} = \frac{\epsilon_c (t - 2v - a_e)}{2(t - v)}$$

$$A_c = \frac{(\sigma_c^I + \sigma_c^{II})(t - a_e)b}{4} + \frac{\sigma_c^{II}(t - a_e - 2v)b}{4}$$

$$A_t = \frac{1}{2} \sigma_t vb$$



Al.2.1 Moment

Taking moments about the centre line of the wall :

$$M = \frac{\sigma_c^I (t - a_e)(t + 2a_e)b}{24} + \frac{\sigma_c^{II} (t - a_e)(2t + a_e)b}{24} + \frac{\sigma_c^{II} (t - a_e - 2v)(t + 2a_e - 2v)b}{24} + \frac{\sigma_t (3t - 2v)vb}{12} \quad \text{--- (Al.1)}$$

In terms of the compressive strain :

$$M = \frac{E_s bt^2 \epsilon_c}{12(1 - v/t)} \left[\left(1 - \frac{a_e^3}{t^3}\right) + \frac{v^2}{t^2} \left(3 - \frac{2v}{t}\right)(k - 1) \right] \quad \text{--- (Al.2)}$$

$$\text{If } k = 1 \quad M = \frac{\epsilon_c + \epsilon_t}{2} \frac{E_s}{Z} \quad \text{--- (Al.3)}$$

$$\text{where } Z = \frac{b(t^3 - a_e^3)}{6t}$$

$$\text{If } a_e = 0 \quad M = \frac{E_s bt^2 \epsilon_c}{12(1 - v/t)} \left[1 + \frac{v^2}{t^2} \left(3 - \frac{2v}{t}\right)(k - 1) \right] \quad \text{--- (Al.4)}$$

$$\text{If } a_e = 0 \quad k = 1 \quad M = \frac{\epsilon_c + \epsilon_t}{2} \frac{E_s}{Z} \quad \text{--- (Al.5)}$$

$$\text{where } Z = bt^2/6$$

A4.2.2 Increasing Axial Load

Letting the increasing axial load = ΔP

$$\Delta P = A_c - A_t$$

In terms of the compressive strain :

$$\Delta P = \frac{E_s b t (1 - a_e/t) \epsilon_c}{2(1 - v/t)} \left[\left(1 - \frac{2v}{t}\right) - \frac{(v/t)^2 (k - 1)}{(1 - a_e/t)} \right] \quad \text{--- (A4.6)}$$

A4.2.3 No Increase in Axial Load

$$A_c = A_t$$

In terms of strain :

$$\epsilon_c = \epsilon_t \frac{k - a_e/t}{1 - a_e/t} \quad \text{--- (A4.7)}$$

$$\text{If } k = 1 \quad \epsilon_c = \epsilon_t$$

$$\text{If } a_e = 0 \quad \epsilon_c = \sqrt{k} \epsilon_t$$

In terms of v :

$$\left(\frac{v}{t}\right)^2 \left(\frac{k - 1}{2(1 - a_e/t)}\right) - \frac{v}{t} + 0.5 = 0 \quad \text{--- (A4.8)}$$

$$\text{If } k = 1 \quad v/t = 0.5$$

$$\text{If } a_e = 0 \quad v/t = 1/(1 + \sqrt{k})$$

A4.3 CENTRAL GAP IN WALL

$$a_e/t \geq 1 - 2v/t$$

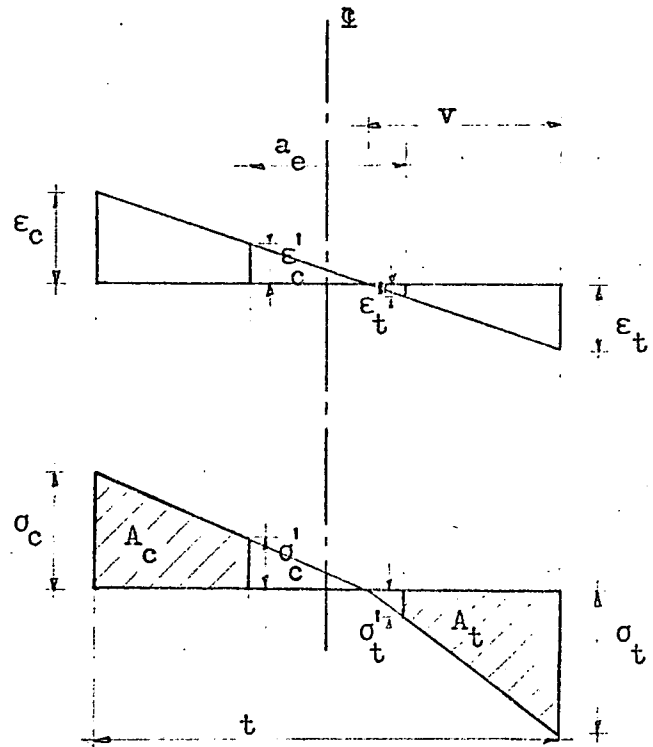
$$v/t = \epsilon_t / (\epsilon_c + \epsilon_t)$$

$$\epsilon_c' = \frac{\epsilon_c (t - 2v + a_e)}{2(t - v)}$$

$$\epsilon_t' = \frac{\epsilon_t (2v - t + a_e)}{2v}$$

$$A_c = \frac{\sigma_c + \sigma_c' (t - a_e)b}{2}$$

$$A_t = \frac{\sigma_t + \sigma_t' (t - a_e)b}{2}$$

A4.3.1 Moment

Taking moments about the centre line of the wall :

$$M = \frac{b(t - a_e)}{24} \left[(\sigma_c' + \sigma_t')(t + 2a_e) + (\sigma_c + \sigma_t)(2t + a_e) \right] \quad \text{--- (A4.9)}$$

In terms of compressive strain :

$$M = \frac{E_s b t^2 \epsilon_c}{48(1 - v/t)} \left[\left\{ (5 - k) - 2(k + 1) \left(\frac{a_e}{t} \right)^3 \right\} + 3(k - 1) \left(\frac{2v}{t} \left(1 - \frac{a_e}{t} \right) + \frac{a_e^2}{t^2} \right) \right] \quad \text{--- (A4.10)}$$

If $k = 1$ See equation A4.3

If $a_e = 0$ Not valid unless $k = 1$. See equation A4.4

If $k = 1$
 $a_e = 0$ See equation A4.5

A4.3.2 Increasing Axial Load

Let the increase in axial load = ΔP

$$\Delta P = A_c - A_t$$

In terms of the compressive strain :

$$\Delta P = \frac{E_s (1 - a_e/t) b t \epsilon_c}{8(1 - v/t)} \left[2(1 - 2v/t) + (1 + a_e/t) - k \{ 4v/t - (1 - a_e/t) \} \right] \quad \text{--- (A4.11)}$$

A4.3.3 No Increase in Axial Load

$$A_c = A_t$$

In terms of v :

$$v/t = \frac{(1 + a_e/t)(1 - k)}{4(1 + k)} + 0.5 \quad \text{--- (A4.12)}$$

In terms of k :

$$k = \frac{1 + a_e/t + 4(0.5 - v/t)}{1 + a_e/t - 4(0.5 - v/t)} \quad \text{--- (A4.13)}$$

A4.4 MOMENT AND AXIAL LOAD PREDICTED FROM STRAINS

A4.4.1 Effect of a_e and k on the Moment Predicted from Strains

When experimental strains are used to predict the moment, the magnitude of this moment will depend on the chosen values of effective gap and the unloading to loading modulus ratio.

Figure 4.5 shows the variation. It is based on the following equations :

1. Solid Section

Using equation A4.5
$$M = \frac{E_s \epsilon_c b t^2}{6} \quad \text{--- (A4.14)}$$

$$\begin{aligned} \text{where } k &= 1 \\ a_e &= 0 \\ \epsilon_c &= \epsilon_t \end{aligned}$$

2. Section with Gap $a_e/t \geq 1 - 2v/t$

Using equation A4.10 and writing it in terms of E_{exp} where

$$E_{\text{exp}} = (1 - a_e/t) E_s$$

$$M = \frac{\epsilon_c t^2 b E_{\text{exp}}}{48(1 - v/t)(1 - a_e/t)} \left[\text{as equation A4.10} \right] \quad \text{--- (A4.15)}$$

Dividing equation A4.15 by its value when $k=1$ and $a_e=0$ gives

$$M/M_{k=1, a_e=0} = \frac{1}{8(1 - v/t)(1 - a_e/t)} \left[\text{as equation 4.10} \right] \quad \text{--- (A4.16)}$$

3. Section with a Gap $a_e/t \leq 1 - 2v/t$

Using equation A4.2 and writing it in terms of E_{exp} gives

$$M = \frac{\epsilon_c b t^2 E_{\text{exp}}}{12(1 - v/t)(1 - a_e/t)} \left[\left(1 - \frac{a_e^3}{t^3}\right) + \frac{v^2}{t^2} \left(3 - \frac{2v}{t}\right)(k - 1) \right] \quad \text{--- (A4.17)}$$

Dividing equation A4.17 by its value when $k = 1$ and $a_e = 0$ gives

$$M/M_{k=1, a_e=0} = \frac{1}{2(1 - v/t)(1 - a_e/t)} \left[\text{as equation A4.17} \right] \quad \text{--- (A4.18)}$$

4. Relationship between v/t and k

The relationship between v/t and k is given by equations A4.8 and A4.12 .

A4.4.2 Effect of a_e and k on the Axial Load Predicted from Strains

If the axial load increase is predicted from experimental strains, the magnitude of this predicted load will depend on the chosen values of k and a_e .

Figure 4.7 shows the effect of k and a_e on axial load. This graph is based on equations A4.6 and A4.11 which give :

$$\Delta P = - R E_{\text{exp}} b t \epsilon_c \Delta k \quad \text{--- (A4.19)}$$

where R is given by :

$$a_e/t \geq 1 - 2v/t \quad R = \frac{4v/t + a_e/t - 1}{8(1 - v/t)} \quad \text{--- (A4.20)}$$

$$a_e/t \leq 1 - 2v/t \quad R = \frac{(v/t)^2}{2(1 - v/t)(1 - a_e/t)} \quad \text{--- (A4.21)}$$

A4.5 STRESS DISTRIBUTION DUE TO ECCENTRIC LOADING IN A SOLID, LINEARLY ELASTIC WALL WITH NO TENSILE STRENGTH

Consider a wall under two differing loading arrangements :

1. An increasing moment applied to a wall under a constant precompression (constant axial load and an increasing moment).
2. An increasing moment applied to a wall with an initial precompression which increases in proportion to the moment.

Figures A4.1 and A4.2 illustrate and explain the two cases. The following points should be noted :

1. Before tensile cracking occurs, the strain planes in both cases have the same slope for the same moment. With constant precompression all planes pass through a common point situated on the centre line of the wall at a level equivalent to the constant precompression. With increasing precompression (increasing in direct proportion to the applied moment) all planes also pass through a common point at a level equivalent to the initial precompression but offset from the centre line of the wall (this offset depends on the ratio of the increasing precompressive force to the increasing moment).
2. The diagrams are drawn to the same scale thus giving an idea of the relative magnitudes of the stresses with increasing moment for the particular loading condition.

A4.6 MOMENT CAUSING TENSION IN THE WALL

In the test models, tension occurs when the bending tensile strain exceeds the precompressive strain. In terms of stresses this occurs when

$$\frac{P}{A} = \frac{My}{I} \quad \text{--- (A4.22)}$$

1. A Solid, Rectangular Section

$M = Pe$; $\bar{y} = t/2$; $I = bt^3/12$; $A = bt$ - with these values equation A4.22 gives

$$e = t/6 \quad \text{--- (A4.23)}$$

the eccentricity beyond which tension occurs.

2. A Rectangular Section with a Central Gap

$M = Pe$; $\bar{y} = t/2$; $I = b(t^3 - a_e^3)/12$; $A = b(t - a_e)$ - with these values equation A4.22 gives

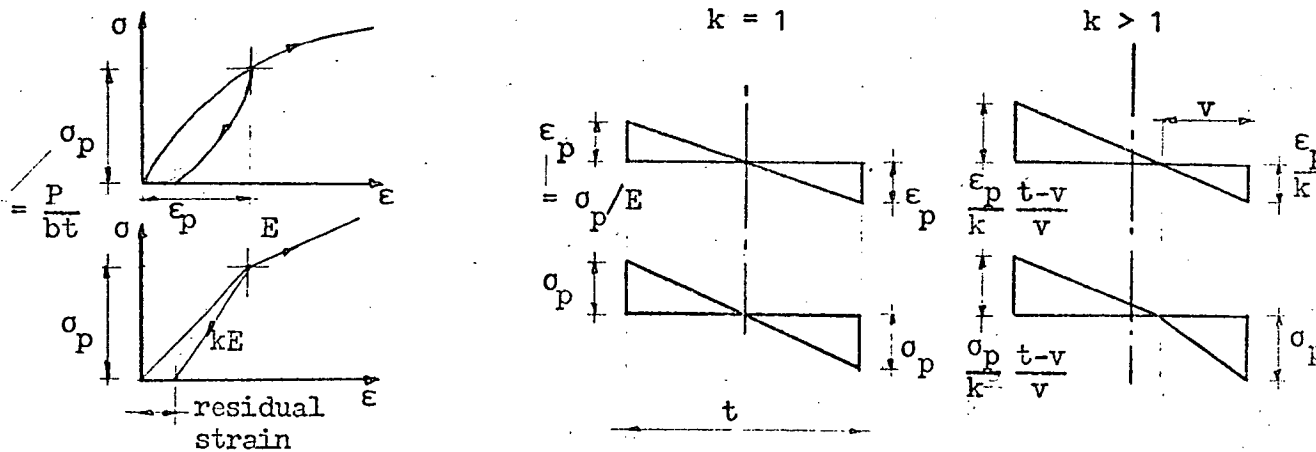
$$e = (t + a_e + \frac{a_e^2}{t^2})/6 \quad \text{--- (A4.24)}$$

larger eccentricities causing tension.

Equation A4.24 is illustrated graphically in terms of e/t and a_e/t (fig 4.9).

3. A Rectangular, Solid Section with a 'Tensile' Modulus larger than the Compressive Modulus ($k > 1$)

An unloading stress-strain curve different from the loading curve becomes significant for 1:1:6 and 1:2:9 mortar brickwork. The eccentricity causing tension depends on the loading stress-strain curve for the side under increasing compression and on the residual strain at zero stress for the opposite side (here a linear unloading modulus depends on the residual strain). Both are represented by a linear curve as shown in the following sketch. Typical stress and strain planes are also shown.



4. A Rectangular Section with a Central Gap and $k > 1$

Considering a similar stress-strain curve as sketched in the previous section the case is considered where $a_e/t \geq 1 - 2v/t$.

Equation A4.15 in terms of the tensile strain becomes :

$$M = \frac{\epsilon_t b t^2 E \exp}{48(v/t)(1 - a_e/t)} \left[\left\{ (5 - k) - 2(k + 1) \left(\frac{a_e}{t} \right)^3 \right\} + 3(k - 1) \left(\frac{2v}{t} \left(1 - \frac{a_e}{t} \right) + \frac{a_e^2}{t^2} \right) \right] \quad \text{--- (A4.25)}$$

$$\text{where } \epsilon_t = \epsilon_c \frac{v/t}{1 - v/t}$$

$$\text{For no tension } \epsilon_t < \frac{P}{btkE_{\text{exp}}}$$

Substituting this into equation A4.25 :

$$\frac{M}{P} = e = \frac{t}{48k(v/t)(1 - a_e/t)} \quad \left[\text{as equation A4.25} \right] \quad \text{--- (A4.26)}$$

If $k = 1$ Equation A4.24 is obtained.

$$\text{If } k > 1 \quad \frac{e}{t} = \frac{1}{6k} \frac{1 - v/t}{v/t} \frac{M}{M_{k=1, a_e=0}} \quad \text{--- (A4.27)}$$

the latter term of the equation is given by equation A4.16 or figure 4.5 .

A similar procedure is used for the case $a_e/t \leq 1 - 2v/t$.

The effect of k on the eccentricity causing zero stress on one side of the wall is shown in figure 4.9 for $k = 2$.

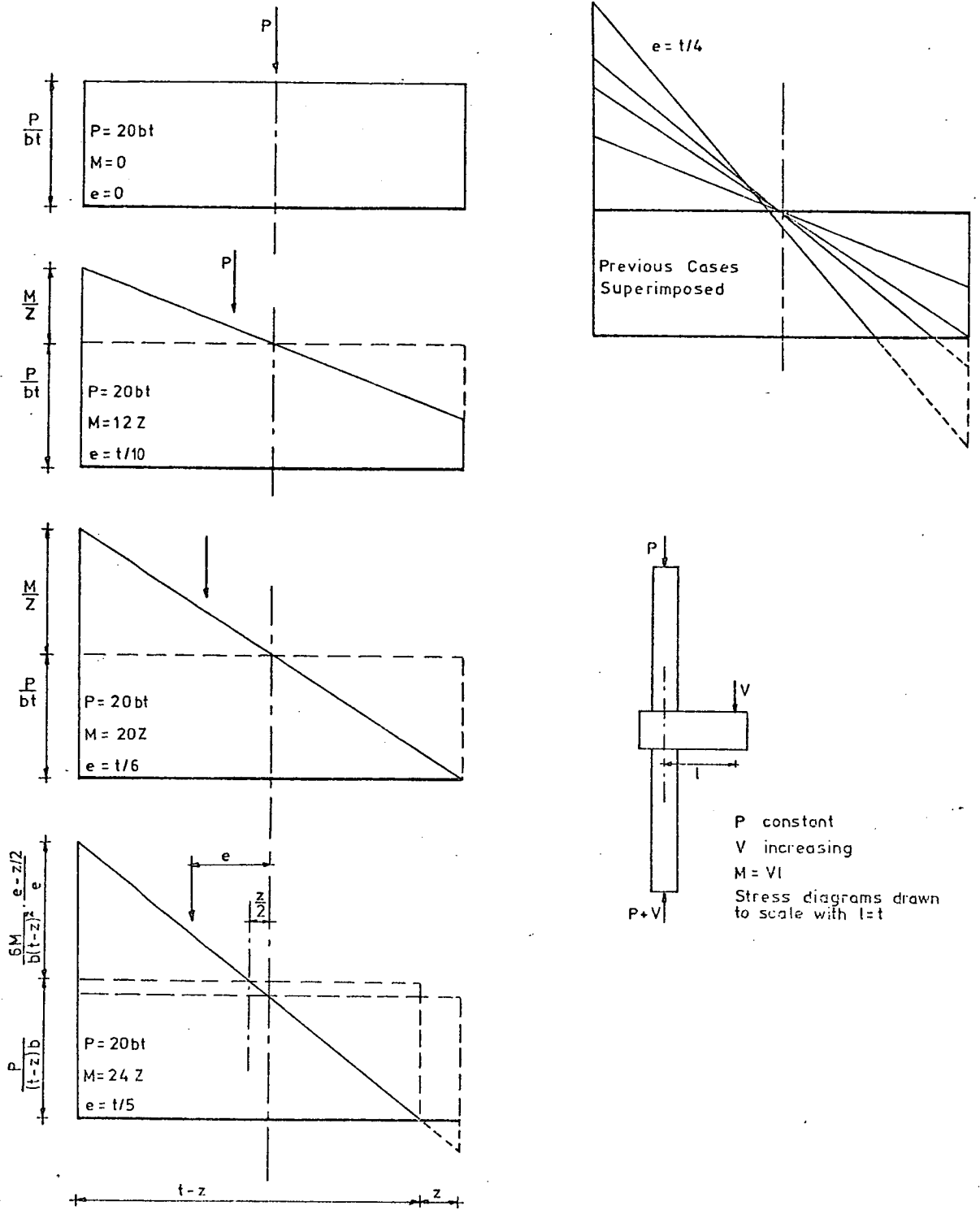
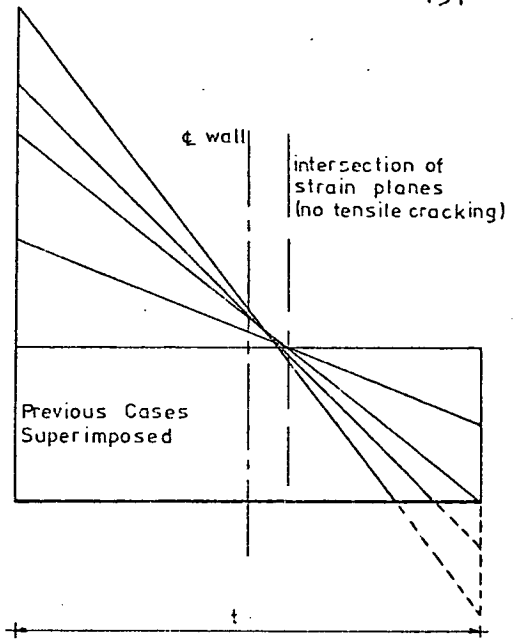
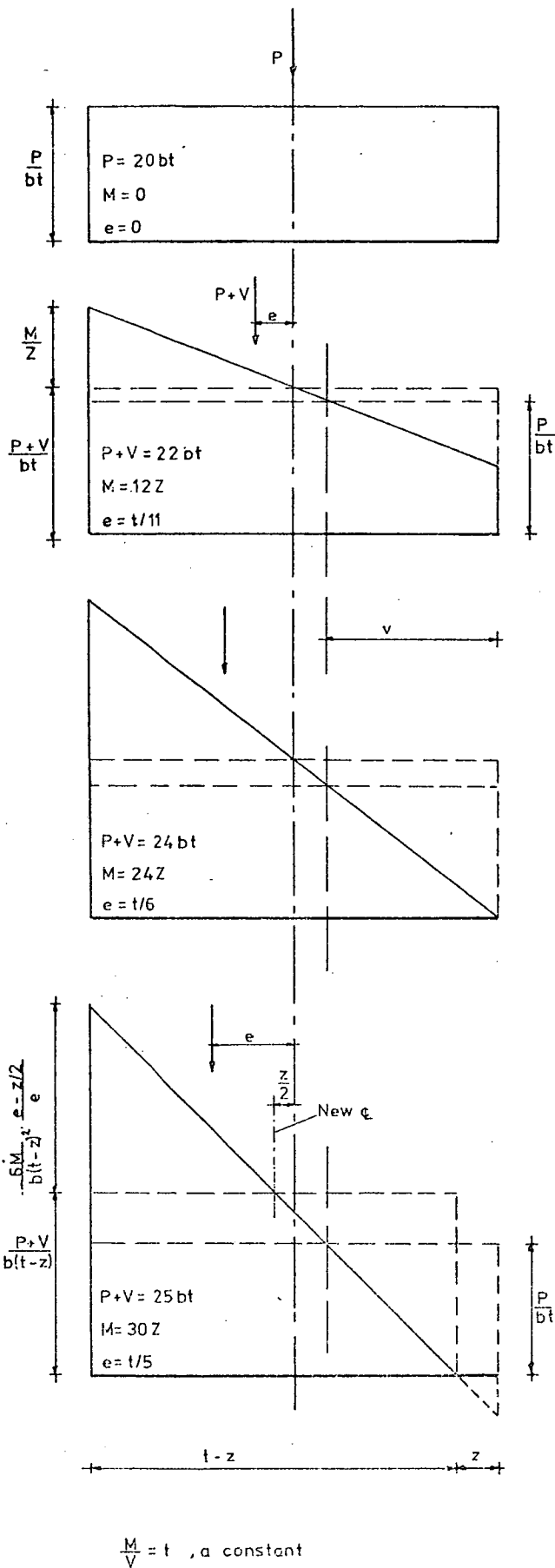


Fig. A4.1

Case 1 - MOMENT WITH CONSTANT PRECOMPRESSION



NOTES

UNCRACKED SECTION

Maximum & Minimum Stresses

$$\sigma = \frac{P+V}{bt} + \frac{M}{Z}$$

where $Z = bt^2/6$

Load Eccentricity

$$e = M/(P+V)$$

CRACKED SECTION

Maximum & Minimum Stresses

$$\sigma_{\max} = \frac{1_1(P+V)}{3bt(1 - 2e/t)}$$

$$\sigma_{\min} = 0$$

Section Properties

Effective depth = $t - z$

Effective eccentricity about centre of effective depth = $e - z/2$

Effective eccentricity = $(t - z)/6$

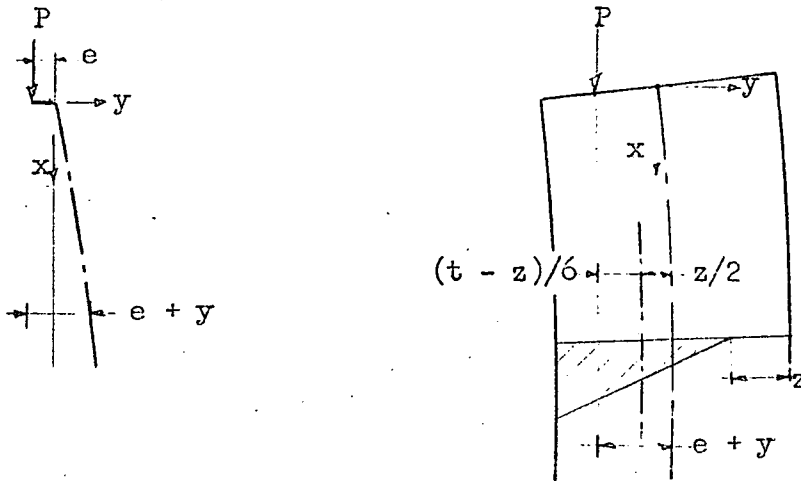
Equating two previous expressions gives $z = 3(e - t/6)$

Area under stress diagram = $\frac{1}{2} \max b(t - z) = P+V$

Giving $\sigma_{\max} = \frac{2(P+V)}{b(t - z)}$

Fig. A4.2

Case 2 - MOMENT WITH INCREASING PRECOMPRESSION

APPENDIX 5A5.1 EQUATIONS GOVERNING THE BEHAVIOUR OF A SOLID, LINEARLY ELASTIC WALL WITH NO TENSILE STRENGTHA5.1.1 Wall with No Tensile Cracks

$$EI \frac{d^2 y}{dx^2} + P(e + y) = 0 \quad \text{--- (A5.1)}$$

where e = the eccentricity of load P

If the effect of axial load on lateral deflections is neglected equation A5.1 becomes :

$$EI \frac{d^2 y}{dx^2} + Pe = 0 \quad \text{--- (A5.2)}$$

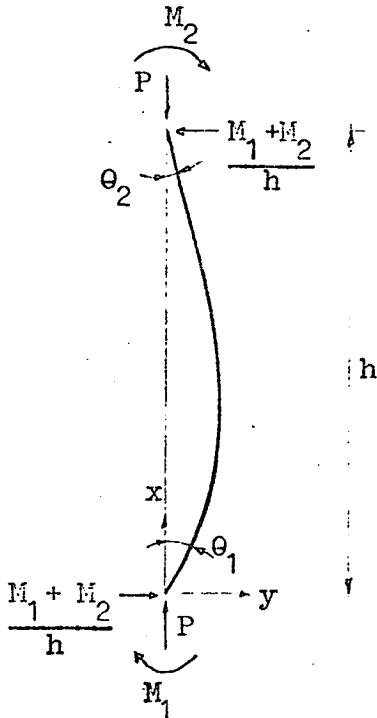
A5.1.2 Wall with Tensile Cracks

$$EI \left(\frac{t - z}{t} \right)^3 \frac{d^2 y}{dx^2} + P \left(\frac{t - z}{6} \right) = 0 \quad \text{--- (A5.3)}$$

where $z = 3(e + y - \frac{t}{6})$

If the effect of axial load on lateral deflections is neglected equation A5.3 is still used but z becomes $3(e - t/6)$.

A5.2 EQUATIONS FOR WALL DEFLECTION AND ROTATION



A5.2.1 Wall with No Tensile Cracks

From equation A5.1 the lateral deflection and end rotation become :

$$y = -\frac{M_1}{P} \cos qx + \frac{1}{P \sin qh} (M_1 \cos qh + M_2) \sin qx - \frac{(M_1 + M_2)x}{Ph} + \frac{M_1}{P} \quad \text{--- (A5.4)}$$

where $q^2 = P/EI$

$$\theta_1 = \frac{M_1 h}{3EI} \left(3 \left(\frac{1}{2u \tan 2u} - \frac{1}{(2u)^2} \right) - \frac{M_2 h}{6EI} \left(\frac{1}{(2u)^2} - \frac{1}{2u \sin 2u} \right) \right) \quad \text{--- (A5.5)*}$$

where $u^2 = Ph^2/4EI$

If the effect of axial load is neglected, equation A5.2 gives :

$$y = \frac{1}{EI} \left(\frac{M_1 + M_2}{6h} x^3 - \frac{M_1 x^2}{2} + \frac{(2M_1 - M_2)hx}{6} \right) \quad \text{--- (A5.6)}$$

$$\theta_1 = \frac{h}{EI} \left(\frac{2M_1 - M_2}{6} \right) \quad \text{--- (A5.7)}$$

$$\theta_2 = \frac{h}{EI} \left(\frac{2M_2 - M_1}{6} \right) \quad \text{--- (A5.8)}$$

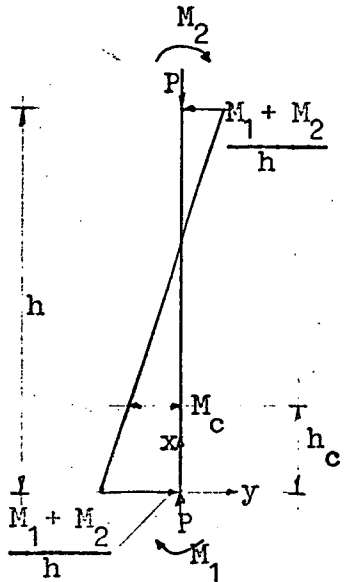
* see Timoshenko (Reference 37, Chapter 2)

A5.2.2 Wall with Tensile Cracks

The effect of axial load on lateral deflections and end rotations is taken into account by Sahlin (30, 32) and Angervo & Putkonen (2).

Equations A5.2 and A5.3 are used in the following analysis in which the effect of axial load is neglected.

Two portions of the wall have to be considered - a length where the eccentricity is greater than $t/6$ thus causing cracking and a length in which there is no tensile cracking.



$$0 \leq x \leq h_c$$

$$\frac{d^2 y}{dx^2} = \frac{-2P}{9Eb \left(\frac{t}{2} - \frac{1}{P}(M_1 - (M_1 + M_2)\frac{x}{h}) \right)^2}$$

$$h_c \leq x \leq h$$

$$\frac{d^2 y}{dx^2} = -\frac{1}{EI} \left(M_1 - (M_1 + M_2)\frac{x}{h} \right)$$

$$\frac{h_c}{h} = \frac{M_1 - M_c}{M_1 + M_2}$$

It is assumed that M_2 will never be large enough to cause tensile cracking in the top section of the wall. The resulting equations for deflection and rotation contain many terms and only one of main interest is given - the value of θ_1 .

$$\theta_1 = \frac{k}{EI} \left(\frac{1}{t/2 - M_1/P} + A \right) \quad \text{--- (A5.9)}$$

where $k = 2P^2 h I / 9b(M_1 + M_2)$

$$r = h_c/h$$

$$A = \frac{M_1 h}{3k} (1 - r)^3 - \frac{M_1 h}{6k} (1 - 3r^2 + 2r^3) - \frac{P}{M_1 + M_2} \log_e \left(\frac{t}{2} - \frac{M_1}{P} \left(1 - \frac{M_1 + M_2}{M_1} r \right) \right) - (1 - r) \frac{1}{\frac{t}{2} - \frac{1}{P}(M_1 - (M_1 + M_2)r)}$$

For the case where $M_2 = 0$, equation A5.9 becomes :

$$\theta_1 = \frac{M_1 h}{3EIc} \quad \text{--- (A5.10)}$$

$$\text{where } \frac{1}{c} = \left(\frac{1}{6e/t}\right)^3 + \frac{1}{18(e/t)^2} \left(\frac{1}{0.5 - e/t} - \frac{1}{2e/t} - \frac{1}{e/t} \log \frac{1}{1.5 - 3e/t}\right)$$

$$e = M_1/P$$

The relationship between c and e/t is illustrated graphically in figure A5.1*.

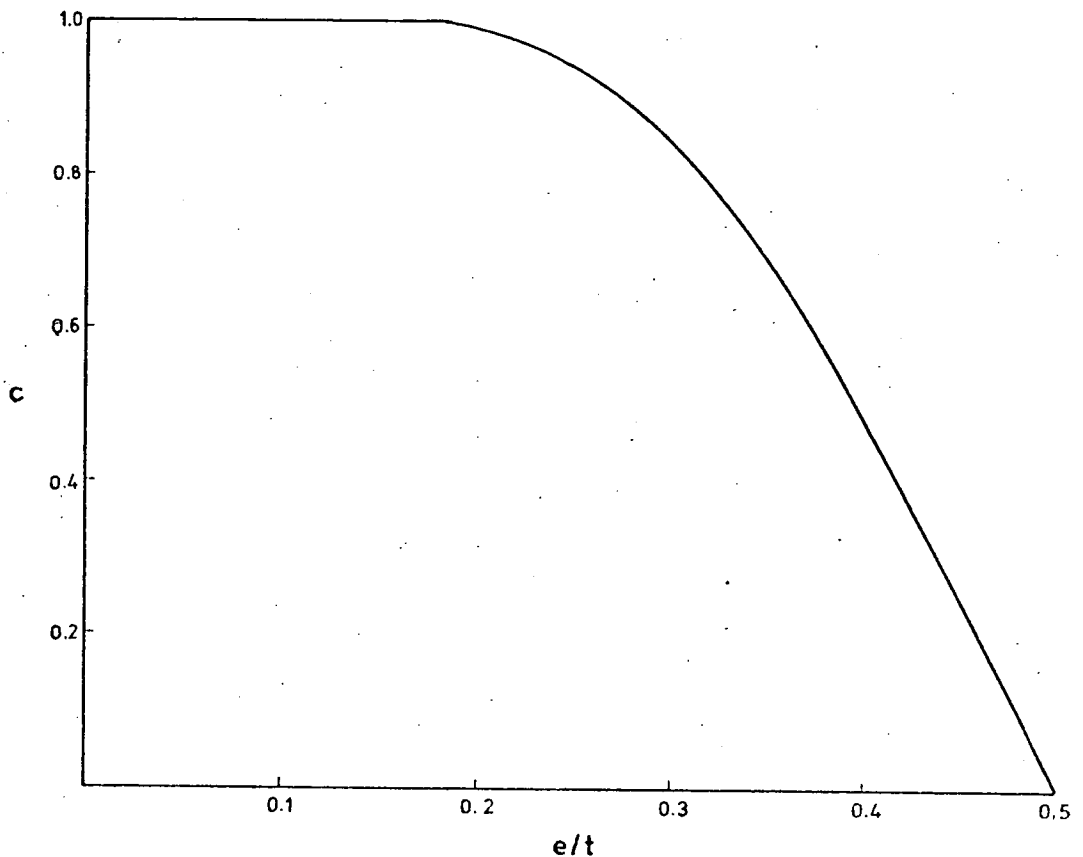


Figure A5.1 The Relationship Between c and e/t

*Also presented graphically by Sahlin (30, 32) based on work by H. Nylander - Undersökning av bärkraften hos murade cementstensväggar (Investigation of the Load-Carrying Capacity of Cement Block Masonry Walls), Betong, Häfte 3, Stockholm, 1944.

APPENDIX 6A6.1 THE AXIAL LOAD - MOMENT INTERACTION DIAGRAMA6.1.1 Linear Stress-Strain

The walls are assumed to fail when a limiting stress is reached. The failure stresses are taken from values obtained in walls axially loaded to failure :

1790 lbf/in² for a 1:¼:3 mortar brickwork.

1340 lbf/in² for a 1:1:6 mortar brickwork.

1000 lbf/in² for a 1:2:9 mortar brickwork.

1. Solid Cross-section

To obtain the maximum stress, equations based on those in figure A4.2 are used.

$$\text{No tensile cracks : } \sigma = \frac{Q}{bt} + \frac{M}{Z} \quad \text{--- (A6.1)}$$

$$\text{Tensile cracks : } \sigma = \frac{4}{3bt(1 - \frac{2M}{Qt})} \quad \text{--- (A6.2)}$$

where Q = axial load on the wall.

2. Cross-section with a Central Gap

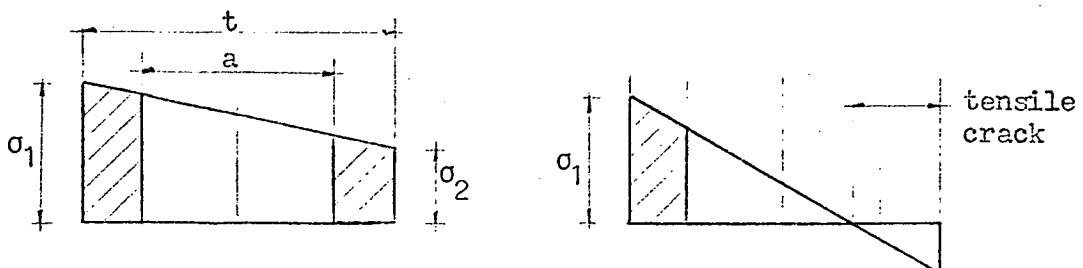
The mortar joint is taken to be the critical section, thus the actual gap in the joint is considered - 2.62 in, the width of the frog in the brick (see sketch).

$$\text{No tensile cracks : } M = (\sigma_1 - \sigma_2) \frac{I}{t} \quad \text{--- (A6.3)}$$

$$Q = b(t-a)(\sigma_1 - \sigma_2)/2 \quad \text{--- (A6.4)}$$

where $I = b(t^3 - a^3)/12$

With tensile cracks : The moment and axial load are calculated directly from the stress distribution over the cross-section of the wall.



A6.1.2 Experimental Stress-Strain

The stress-strain diagram obtained from an axially loaded wall is used to predict the stresses in an eccentrically loaded wall. Failure is assumed to occur when a limiting strain is reached. Using this strain as a fixed point various strain planes can be drawn and the corresponding axial force and moment for each plane can be calculated by dividing the cross-section up into parallel sections with the stress variation linear over each section (see sketch).

The limiting strains have been estimated from the maximum observed strains in the test models (Table A6.1). The strains used in the calculations are :

- 3000 x 10⁻⁶ for the 1:¼:3 mortar brickwork.
- 4000 x 10⁻⁶ for the 1:1:6 mortar brickwork.
- 5000 x 10⁻⁶ for the 1:2:9 mortar brickwork.

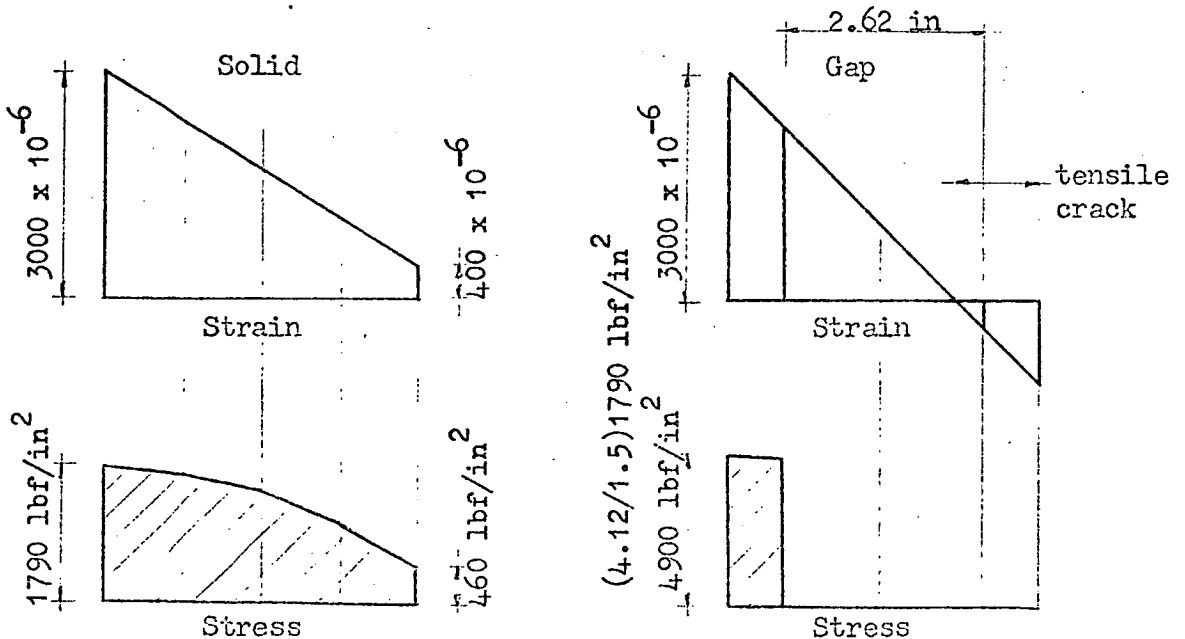
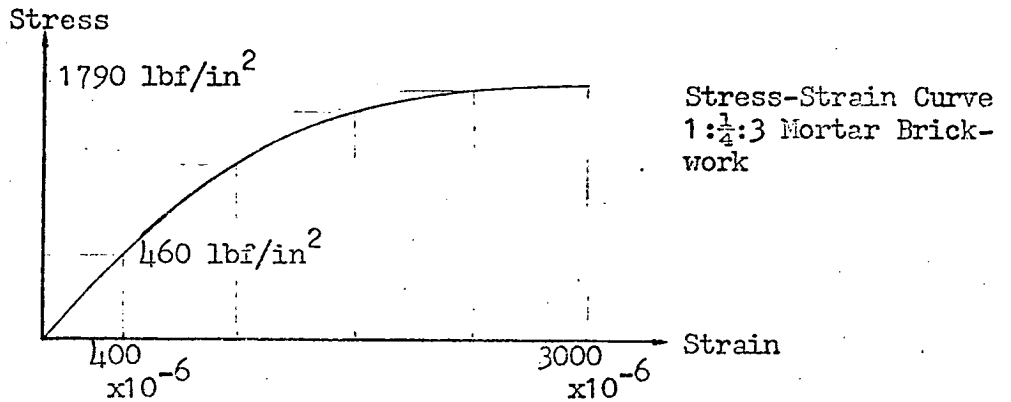


TABLE A6.1 - MAXIMUM RECORDED COMPRESSIVE STRAIN

Wall No.	Strain			Moment		Stress	
	Flexural	Axial	Sum	Strain	Ultimate	Strain	Ultimate
		$\times 10^{-6}$		$\times 10^3$ lbf in/ft		lbf/in^2	
<u>1:2:9 Mortar</u>							
WS12	4424 ¹	919	5343	77 ²	82	400 ³	-
WS4	3439	1762	5201	66	76	600	-
W1	-	2400	2400	-	-	845	1005
W5	-	2485	2485	-	-	1005	1185
<u>1:1:6 Mortar</u>							
WS5	2459	773	3232	77	85	400	-
WS7	2964	939	3903	88	99	600	-
W3	-	1782	1782	-	-	905	1150
W7	-	2630	2630	-	-	1185	1340
<u>1:1/4:3 Mortar</u>							
WS9	1616	454	2070	88	93	400	-
WS10	2121	788	2909	132	137	600	-
W6	-	1590	1590	-	-	1180	1420
W6	-	2360	2360	-	-	1380	1420
W4	-	2285	2285	-	-	1720	1790

Notes :

For wall properties see Table 3.1 .

WS = wall-slab test model ; W = wall loaded axially to failure

1. Flexural strains are measured in the more heavily loaded wall section and includes strain due to slab load.
2. Flexural strain measured at this moment.
3. Axial strain measured at this stress.

A6.2 RELATION BETWEEN ULTIMATE MOMENT AND PRECOMPRESSION IN THE JOINT TEST MODELS

Using the axial load - moment interaction curves, a curve can be drawn relating ultimate moment to precompression for the test models (fig 6.11).

The more heavily loaded wall fails. From the axial load - moment interaction curve, the ultimate moment is known for a given axial load (in this case P+V). If there are no tensile cracks at failure, the other wall is assumed to take the same moment. If there are tensile cracks, the more heavily loaded wall takes a greater proportion of the moment. Relationships for the latter case are obtained from figure 6.1 using a linear approximation.

Relationships for three gap width ratios are given below :

$$a/t = 0.45 \quad \frac{M_2}{gM_s} = 0.128 \frac{gM_s}{Pt} + 0.444 \quad \text{--- (A6.5)}$$

$$V^2 - (3.12(P+V) + 0.726M_2)V + 0.726(P+V)M_2 = 0 \quad \text{--- (A6.6)}$$

$$(e/t)_{\text{tension}} = 0.22$$

$$a/t = 0.64 \quad \frac{M_2}{gM_s} = 0.154 \frac{gM_s}{Pt} + 0.41 \quad \text{--- (A6.7)}$$

$$V^2 - (8.57(P+V) + 2.16M_2)V + 2.16(P+V)M_2 = 0 \quad \text{--- (A6.8)}$$

$$(e/t)_{\text{tension}} = 0.29$$

$$a/t = 0 \quad \frac{M_2}{gM_s} = 0.103 \frac{gM_s}{Pt} + 0.475 \quad \text{--- (A6.9)}$$

$$V^2 - (2.04(P+V) + 0.443M_2)V + 0.443(P+V)M_2 = 0 \quad \text{--- (A6.10)}$$

$$(e/t)_{\text{tension}} = 0.12$$

where $M_2/gM_s \geq 0.5$; if less $M_2 = gM_s/2$; $(e/t)_{\text{tension}}$ based on an experimental stress-strain curve.

Using these equations, V may be found for a given value of P+V and M_2 (the moment in the more heavily loaded wall section). Knowing V, the slab moment, M_s , and the precompression, P, are found. The curves plotted in a dimensionless form are the same for the three types of mortar tested.

A6.3 DESIGN OF THE SIX INCH SLAB

A6.3.1 Specifications

1. Design Loads

The maximum precompressive force, P , applied to the wall is 30 tons. The maximum possible jacking load, V , then becomes 16.2 tons ($0.54P$). The maximum shear force is either 16.2 tons or 30 tons as the slab levers the two wall sections apart:

2. Concrete and Steel Strength

Concrete :

A 1:2:4 mix by volume.

The 4 inch cube strength at 28 days = 5300 lbf/in^2 (average of 3 cubes).

The equivalent cylinder strength is approximately $0.9(5300) = 4750 \text{ lbf/in}^2$ (25).

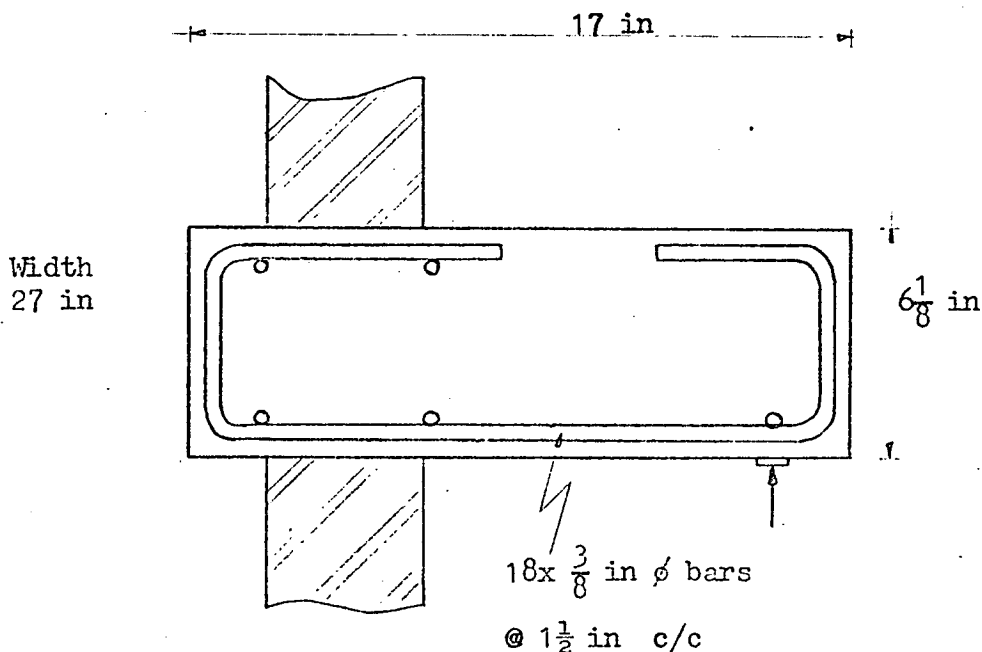
Steel :

Plain mild steel bars were used.

Yield stress* = $36\,000 \text{ lbf/in}^2$

Ultimate stress = $63\,000 \text{ lbf/in}^2$

3. Dimensions and Reinforcement



* Values from reference 7 used. They compare well with experimental values.

A6.3.2 Ultimate Moment

If the ultimate moment is reached the slab will fail by yielding of the tension reinforcement ($p < p_b$). Using equations from a textbook by Winter, Urquhart, O'Rourke and Nilson (40), the ultimate moment is given by :

$$M_u' = Tz = A_s f_y d_1 \left(1 - \frac{\beta f_y}{\alpha f_c'} p\right) \quad \text{--- (A6.11)}$$

$$= 365 \text{ 000 lbf in}$$

This is larger than the maximum design moment = 326 000 lbf in .

Notation to equation A6.11 :

$$d_1 = 5.4 \text{ in}$$

$$A_s = 2 \text{ in (18 x 3/8 in dia. bars)}$$

$$p = A_s / b d_1 = 0.0137$$

$$f_c' = 4750 \text{ lbf/in}^2$$

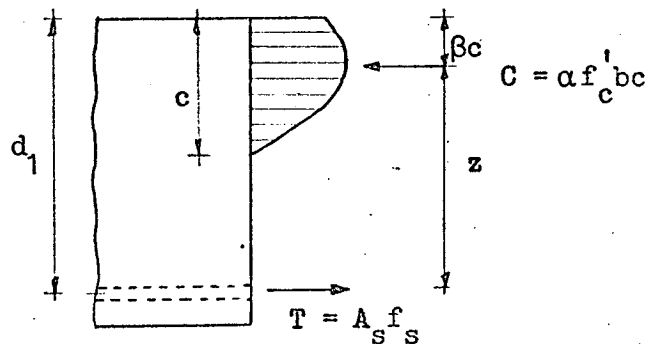
$$f_y = 36 \text{ 000 lbf/in}^2$$

$$\alpha = 0.69^*$$

$$\beta = 0.406$$

$$\alpha = f_{av} / f_c'$$

$$C = f_{av} bc$$



A6.3.3 Ultimate Shear

de Paiva and Siess (27) have shown that deep beams can support a considerable additional load beyond diagonal cracking for shear span to depth ratios, $a/d_1 <$ approximately 3. They give an equation which predicts the inclined cracking load due to diagonal tension :

$$v_{cr} = 2.14 \sqrt{f_c'} + 4600 p V d_1 / M \quad \text{--- (A6.12)}$$

*For values of $f_c' \leq 4000 \text{ lbf/in}^2$ α and β are constant (0.72 & 0.425).
 α decreases by 0.04 for every 1000 lbf/in^2 above 5000 lbf/in^2 .
 β decreases by 0.025 for every 1000 lbf/in^2 above 5000 lbf/in^2 .

where v_{cr} = average shear stress
 $V_{cr} = v_{cr} b d_1$
 M = moment at section considered
 V = shear at section considered

The critical section is assumed at the middle of the shear span (for short beams the crack is initiated at the middle).

For a 9 inch shear span of the slab ($a/d_1 = 1.7$), $v_{cr} = 221 \text{ lbf/in}^2$ or a shear force of 14.4 tons. This underestimated the maximum possible load but should that load have been reached final failure would not have occurred.

For a 4 inch shear span (if levering of walls occurred) ($a/d_1 = 0.74$), $v_{cr} = 315 \text{ lbf/in}^2$ or a shear force of 20.5 tons. Thus if lifting of the walls occurred during a test with a 30 ton precompressive load, diagonal cracking will occur. This will not cause failure, the ultimate load reaching up to four times more than the cracking load.

A6.3.4 Bond

The minimum length necessary to develop, by bond, a given bar force, $A_s f_s$, is given by (40) :

$$L_d = A_s f_s / u_u' \Sigma_o \quad \text{--- (A6.13)}$$

$$= 8 \text{ in}$$

where f_s = stress in steel at point of maximum moment
 $= 26\,000 \text{ lbf/in}^2$

Σ_o = sum of bar perimeters
 $= 21.2 \text{ in}$

u_u' = bond stress for plain steel bars
 $= 300 \text{ lbf/in}^2 \text{ (40)}$

Adequate bond length is provided.

A6.4 SLAB FOR TEST MODEL NO. 1

1:2:9 mortar walls at 200 lbf/in^2 precompression.

A6.4.1 Slab Properties

Concrete Strength : 3×4 inch cubes at 30 days = 4650 lbf/in^2

Size : $4 \times 11 \times 27$ in

Reinforcement : $13 \times \frac{1}{4}$ in diameter bars at 2 in c/c .

A6.5 SLAB FOR TEST MODEL NO. 3

1:2:9 mortar walls at 400 lbf/in² precompression.

A6.5.1 Slab Properties

Concrete Strength : 4x 4 inch cubes at 28 days = 6160 lbf/in²

Size : 4 x 17 x 27 in

Reinforcement : 13x $\frac{1}{4}$ in diameter bars at 2 in c/c .

$$\begin{aligned} f_y &= 36\,000 \text{ lbf/in}^2 & ; & & f_{su} &= 55\,500 \text{ lbf/in}^2 & * \\ A_{st} &= 0.64 \text{ in}^2 & ; & & p &= 0.007 \\ d_1 &= 3.4 \text{ in} & ; & & \alpha &= 0.66 & ; & \beta &= 0.386 \end{aligned}$$

A6.5.2 Ultimate Moment

From equation A6.11, the ultimate moment is :

$$M_u = 76\,000 \text{ lbf in}$$

At that moment the slab would fail by the yielding of the tension reinforcement. In this case there was compression steel in the top of the slab (same amount as the tension steel) - this would retard failure of the concrete in compression and the slab would be able to take more moment allowing the steel stress to reach its ultimate tensile capacity (although together with large crack widths).

Increase due to top reinforcement :

$$\begin{aligned} M_u &= A_s f_{su} (d_1 - d_1') & \text{--- (A6.14)} \\ &= 100\,000 \text{ lbf in} \end{aligned}$$

where d_1' is the distance from the surface of the slab to the centroid of the compression reinforcement = 0.6 in .

At this moment the slab would hinge about the compression steel and rotate at constant moment.

* experimental value

APPENDIX 7A7.1 Finite Element Analysis of the Floor Slab Deflection

A standard program provided by IBM is used - GC 21 (Analysis of a plate in bending) (15). It was run on an IBM 360/50 computer. The finite element approximation of the slab using rectangular elements is shown in figure A7.1 .

The program allows the calculation of the displacements, internal moments and reactions of a plate of any shape in bending. The plate can be supported in any possible way and loaded by any external force.*

The plate can be of constant or variable thickness. It can be simply supported or clamped on separate points or along segments of a straight line. The values of the displacement at some points can also be imposed; this possibility is used in the analysis of the subsidence of a support. The external forces are formed by distributed vertical loads, concentrated loads and concentrated moments applied to the boundary. Several load cases can be processed in the same run.

The mathematical model of Kirchhoff is used; in this model, the unknown is the vertical displacement of the middle plane of the plate. The numerical calculation is then performed by the finite element method. The curved boundary is treated as polygonal lines; the plate is divided into triangular or rectangular elements; both types can be used together in a same computation.

Rectangular and triangular elements (with four and three nodes respectively) are used with six parameters to each node. The deflection, w , along the sides of an element is a polynomial of the fifth degree and the normal derivative, dw/dn , is a cubic polynomial. The elements satisfy the displacement compatibility (both deflection and slopes are continuous across element boundaries).

* This paragraph and the following two are obtained from section I of the instruction manual (15).

A7.2 Finite Difference Analysis of the Floor Slab Deflection

Before the finite element program was available a finite difference technique was used to obtain the slab deflection*. A set of 42 simultaneous equations obtained from the 16 inch grid representing the floor slab were solved by a program written in Fortran IV on an IBM 360/50 computer (fig A7.1). The program incorporated a standard matrix subroutine, SIMQ, which solves $AX=B$ by Gaussian elimination (X & B are single column matrices).

Theory

The basic equation to be satisfied is :

$$\delta^4 w / \delta x^4 + 2\delta^4 w / \delta x^2 \delta y^2 + \delta^4 w / \delta y^4 = q/D \quad \text{--- (A7.1)}$$

$$\text{where } D = Et^3/12(1 - \nu^2)$$

q = load/unit area

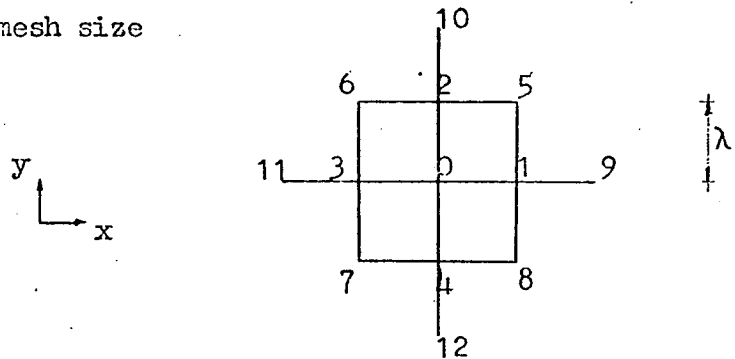
t = thickness of the slab

ν = Poisson's ratio

The finite difference approximation is :

$$20w_0 - 8\sum w_1 + 2\sum w_5 + \sum w_9 = \lambda^4 q_0/D \quad \text{--- (A7.2)}$$

where λ = mesh size



The boundary conditions are given by (perpendicular to x direction) :

$$\text{Fully fixed boundary} : \delta w / \delta x = 0 \quad \text{--- (A7.3)}$$

$$\text{Simple support} : \delta^2 w / \delta x^2 = 0 \quad \text{--- (A7.4)}$$

* see, for example, Timoshenko & Woinowsky-Krieger, Theory of Plates and Shells, p. 361, (36).

Free edge (two conditions) :

$$\delta^2 w / \delta x^2 + \nu \delta^2 w / \delta y^2 = 0 \quad \text{--- (A7.5)}$$

$$\delta^3 w / \delta x^3 + (2 - \nu) \delta^3 w / \delta x \delta y^2 = 0 \quad \text{--- (A7.6)}$$

Finite difference approximations :

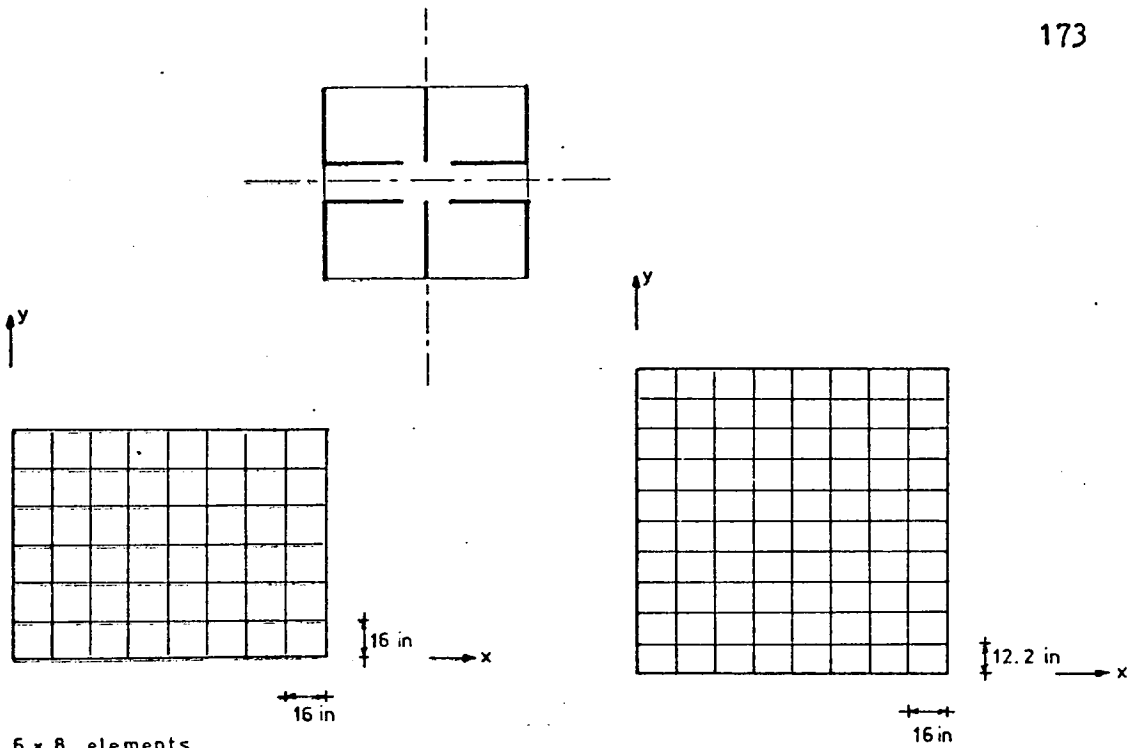
$$(\delta w / \delta x)_0 = \frac{w_1 - w_3}{2\lambda} \quad \text{--- (A7.7)}$$

$$(\delta^2 w / \delta x^2)_0 = \frac{w_1 + w_3 - 2w_0}{\lambda^2} \quad \text{--- (A7.8)}$$

$$(\delta^2 w / \delta y^2)_0 = \frac{w_2 + w_4 - 2w_0}{\lambda^2} \quad \text{--- (A7.9)}$$

$$(\delta^3 w / \delta x^3)_0 = \frac{w_9 - w_{11} - 2w_1 + 2w_3}{2\lambda^3} \quad \text{--- (A7.10)}$$

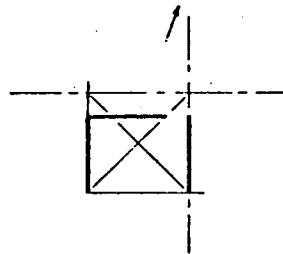
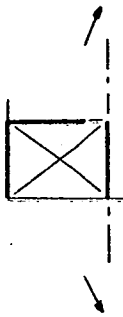
$$(\delta^3 w / \delta x \delta y^2)_0 = \frac{w_5 + w_8 - w_6 - w_7 - 2w_1 + 2w_3}{2\lambda^3} \quad \text{--- (A7.11)}$$



6 x 8 elements
CPU time \approx 260 sec

FINITE ELEMENT

10 x 8 elements
CPU time \approx 400 - 500 sec



FINITE DIFFERENCE

Slab divided into a 6 x 8 grid
CPU time \approx 20 sec

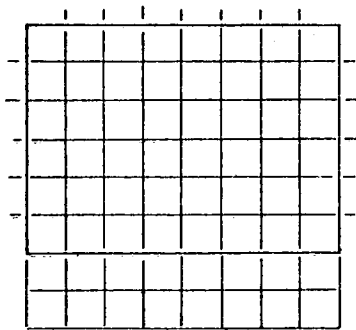


Fig. A7.1 FINITE ELEMENT AND FINITE DIFFERENCE MODELS OF THE FLOOR SLAB